MODELLING DRIVING BEHAVIOUR AT MOTORWAY WEAVING SECTIONS

Andyka Kusuma

Submitted in accordance with the requirements for the degree of

Philosophy of Doctoral Degree

The University of Leeds

Institute for Transport Studies

September 2015

The candidate confirms that the work submitted is his own and that appropriate credit has been given where reference has been made to the work of others.

This copy has been supplied on the understanding that it is copyright material and that no quotation from the thesis may be published without proper acknowledgement.

Acknowledgement

Abstract

This research focuses on the understanding of driving behaviour in motorway weaving sections, particularly the lane-changing and acceleration behaviours which are significant factors in characterising the operations of weaving section.

Drivers' lane-changing behaviour is a series interdependent decisions according to a particular lane-changing plan (latent). An intensive interaction with neighbouring traffic increases the lane-changing complexity in weaving section. The drivers' choices in weaving section can be significantly affected by the actions of the neighbourhood drivers and moving as a group (i.e. platoon and weaving). Furthermore, the intensity of lane-changing has significant impact on the acceleration behaviour in weaving section traffic which may response differently from the stimulus (i.e. leave a space for pre-emptive lane-changing).

An analysis of detailed trajectory data collected from moderately congested traffic flow of a typical weaving section in the M1 motorway, UK (J 42-43). The data reveals that a substantial proportion (23.4%) of the lane-changing at weaving section exhibits such group behaviour (i.e. platoon and weaving). The current study extends the state-of-the-art latent plan lane-changing model which account explicitly the various mechanisms. The model constitutes that the driver is most likely performing a pre-emptive lane-changing at the beginning of weaving section and moving toward kerbside (left direction). Moreover, the driver aggresiveness affects significantly on weaving and least on platoon lane-changing.

The proposed acceleration model allows the car-following behaviour (acceleration/deceleration) corresponds with both stimulus (positive/negative relative speed). The model is conditional on gap threshold and reaction time distributions (probabilistic model) capturing the heterogeneity across drivers. most of traffic response differently from the stimulus condtions where 43.5% falls in deceleration with positive relative speed.

All the parameters in each model are estimated jointly using Maximum Likelihood Estimation technique and reveal significant differences. The results show promising contribution towards improving the fidelity of microscopic traffic performance analysis.

Table of Contents

List of Figures

List of Tables

Declaration

Some parts of the works in this thesis have been presented in the following conferences

1. Title　　　　: Gap Acceptance Behaviour in Motorway Weaving Sections

　　Authors　　: Andyka Kusuma, Ronghui Liu, Francis Montgomery

　　Publication : Eastern Asia Society for Transportation Studies, 2013, Vol. 9 pp. 51-59

　　Presented　: 10th Eastern Asia Society for Transportation Studies Conferences, EASTS 2013, Taipei, Taiwan.

2. Title　　　　: Analysis of the Driving Behaviour at Weaving Section Using Multiple Traffic Surveillance Data

　　Authors　　: Andyka Kusuma, Ronghui Liu, Charisma Choudhury, Francis Montgomery

　　Publication : Transport Research Procedia, 2014, Vol. 3 pp. 51-59

　　Presented　: 17th Meeting of the EURO Working Group on Transportation, EWGT 2014, Sevilla, Spain.

3. Title　　　　: Lane-changing characteristics at weaving section

　　Authors　　: Andyka Kusuma, Ronghui Liu, Charisma Choudhury, Francis Montgomery

　　Presented　: 94th Transportation Research Board Annual (2015), Washington, USA.

4. Title　　　　: Modelling the effect of lane changing mechanisms in a weaving section

　　Authors　　: Andyka Kusuma, Ronghui Liu, Charisma Choudhury

　　Presented　: 95th Transportation Research Board Annual (2016), Washington, USA.

List of Abbreviations and Notations

$a_n(t)$: Acceleration of vehicle n at time t

$a_n^{cf}(t)$: Acceleration of vehicle n under car-following regime at time t

$a_n^{ff}(t)$: Acceleration of vehicle n under free-flow regime at time t

$a_n^{cf,g}(t)$: Acceleration g of vehicle n under car-following regime at time t

$a_n^{cf,g,st}(t)$: Car-following g of vehicle n under car-following regime associated with stimulus st at time t (m/sec^2)

$a_n^{cf,acc,+}(t)$: Car-following acceleration of vehicle n associated with positive st at time t

$a_n^{cf,acc,-}(t)$: Car-following acceleration of vehicle n associated with negative st at time t

$a_n^{cf,dec,+}(t)$: Car-following deceleration of vehicle n associated with positive st at time t

$a_n^{cf,dec,-}(t)$: Car-following deceleration of vehicle n associated with negative st at time t

$a_n^{ff}(t)$: Acceleration of vehicle n under free-flow regime at time t

$a_n^g(t)$: Acceleration of vehicle n at time t (m/sec^2)

$a_{n-1}^g(t)$: Acceleration of vehicle $n-1$ at time t (m/sec^2)

AIC   : Akaike Information Criterion

ARTEMIS   : Analysis of Road Traffic and Evaluation by Micro simulation

ATMS   : Advanced Traffic Management System

ATIS   : Advance Traveller Information

b_n : Most severe breaking which the driver is able to undertake.

$\hat{b}$: An estimated of breaking rate by the driver of vehicle n

CALTRANS : California Transportation

cf : Car following regime

CORSIM   : Corridor traffic simulation model

d_0 : Distance from t_0 to the nearest point outside the span of N points to be considered in fitting the curve.

d^{cr} : Critical distance from MLC location which is associated with a particular message sign (i.e. last message for exit sign)

$d_n^{exit}(t)$: Remaining distance to the mandatory lane changing point of driver n driver at time (t), ∞ if no mandatory lane changing is required.

dec_n : Deceleration of vehicle n

dec'_{n+1} : Deceleration of preceding vehicle $n+1$ speed at time t

d_n^{min} : Minimum deceleration of vehicle n

dec_{n+1}^{lag} : The target lane lag vehicle decelerates

dec_{safe} : The critical acceleration threshold

$d_n^{MLC}(t)$: Remaining distance to the mandatory lane changing point of the nth driver at time (t), ∞ if no mandatory lane changing is required.

$\Delta d_n(t)$: Relative distance / Space gap between the subject and front vehicle at time t

DLC   : Discretionary lane-changing

DMRB   : Design Manual for Road and Bridges

DRACULA : Dynamic Route Assignment Combining User

DTP   : Decision-Theoretic-Planning (DTP)

$f\left(a_n^{cf,g,st}(t)|\tau_n\right)$: Function car-following distribution g of vehicle n associated with stimulus st and reaction time τ at time t

$f(t,\beta^{loc})$: Function of fitted location of the observed vehicle at the time (t) by the local regression

$f(\vartheta_n)$: A distribution of individual-specific random term

ff : free flow regime

$g \in \{accelerate(acc), decelerate(dec)\}$

$G_n(t - \tau_n)$: Available gap event for vehicle n at the observed time $(t - \tau_n)$ (sec)

G_n^* : The threshold value of the available gaps at time t (sec)

$G^{*,min}$: Minimum (lower boundary) of the gap threshold (sec)

$G^{*,max}$: Maximum value (upper boundary) of the gap threshold (sec)

G^{cur} : Gap to front vehicle at current lane

$G_n^{cr,j}(t)$: Critical gap j of driver n at time t

$G_n^{cr,j,l,m}(t)$: Critical gap j at target lane l of driver n for lane changing mechanism m at time t

$G_n^{cr,j,l'}(t)$: Critical gap j at the direction of target lane l' of driver n at time t

$G_n^{cr,lead,l,s}(t)$: Individual lead critical gap at target lane l of driver n at time t

$G_n^{cr,lead,l,p}(t)$: Platoon lead critical gap at target lane l of driver n at time t

$G_n^{cr,lead,l,w}(t)$: Weaving lead critical gap at target lane l of driver n at time t

$G_n^{cr,lag,l}(t)$: Lag critical gap at target lane l of driver n at time t

G^{lead} : Gap to lead vehicle at target lane

G^{lag} : Gap to lag at target lane

$G_n^{lead,l'}(t)$: Available lead gap at target lane l' for driver n at time t.

$G_n^{lead,l,m}$: Available lead gap at target lane l with mechanism m for driver n

$G_n^{lag,l,m}$: Available lag at target lane l with mechanism m for driver n

$G_n^{lag,l'}(t)$: Available lag gap at target lane l' for driver n at time t.

$G_n^{max',j}$: Upper bound of j gap acceptance at the target lane

$G_n^{min',j}$: Lower bound of j gap acceptance at the target lane

$G_n^j(t)$: Available gaps j at time t

G^{min} : Minimum accepted gap at the target lane

$G_n^{min,j}$: Minimum accepted gap j at the target lane of vehicle n

$\overline{G_n'}^j$: Average accepted gap j of vehicle n

HALOGEN : Highway Agency Logging Environment

HCM   : Highway Capacity Manual

h_n^* : The estimated threshold value of the available gap (sec)/ The threshold value of the available headway (sec)

$h_n(t - \tau_n)$: Time headway at time $(t - \tau_n)$

$h^{*,min}, h^{*,max}$: Minimum and maximum value of the headway threshold (sec) respectively

$\boldsymbol{h_n(t)}$ **:** Available headway towards the front vehicle at the observed time (t) (sec)

HMM : Hidden Markov Model

IDM   : Intelligent Driver Model

INTRAS   : Integrated Traffic Simulation

$I_n^l(t)$: EMU of individual n action associated with plan l at time t

$j \in \{lead, lag\}$

k : Traffic density of the road section

$k_n(t - \xi\tau_n)$: Ahead traffic density at time $(t - \xi\tau_n)$

$k_n(\text{t})$: Number of vehicle in front of vehicle n at time t

$l\{1, 2, 3, \ldots, L\}$: Number of lanes

$l_n(t)$: Changing lane toward lane l in direction l'

$lc_n(t)$: Accepting available gaps at the direction of lane l

l' $\in \{left, right\}$ depends on the orientation of target lane l with respect to the current lane.

$l'_n(t)$: {left, current (cur), right}

$loc(t)$: Observed vehicle location at the observed time

$\widehat{loc(t)}$: The estimated vehicle location

loc_n : Observed vehicle n location

loc^{max} : The end point of the observation

loc^{min} : The starting point of the observation

$length_{n-1}$: Length of the front vehicle

$L(\beta^*)$: Final likelihood value

$L(0)$: Initial likelihood value

L_B : Base length. The distance between the respective gore areas at the on- and off-ramps

L_L : Long length. The distance between physical barriers marking the ends of merging and diverging gore areas

LL : Log likelihood

L_{max} : The maximum length of weaving section (based on the short length definition)

L_{min} : The minimum length of weaving section (based on the short length definition)

L_n : Number of available lane/choice/classes set of individual n

L_s : Short length. The distance between the end points of any barrier markings (solid white lines) that prohibit or discourage lane-changing $L_s = 0.77 \, x \, L_B$

LOC : Column vector of the N position observations used to estimate a trajectory function

m_n : Intermediate plan choice set/lane changing mechanism of individual n

m' : Number of available intermediate plan choice set of individual n

$M(.)$: Memory function which represents the current driver behaviour based on series of the previous information

MAE : Mean Absolute Error

MDP : Markov Decision Proces

MIDAS : Motorway Incident Detection and Automatic Signalling

MITSIM : Microscopic Traffic Simulator

MLC : Mandatory lane-changing

MLE : Maximum Likelihood Estimation

MOBIL : Minimising Overall Breaking Induced by Lane-changing

NGSIM : Next Generation Simulation

NNT : Neural Network Technique

$N(0,1)$: normally distributed with mean 0 and standard deviation 1

$No.LC$: Number of lane changing required from the current lane toward desired target lane.

N_{wl} : Number of lanes for weaving manoeuvre.

$Occ_n^l(t)$: Lane l occupancy level of driver n at time (t) (percentage (%))

p : Platoon lane changing mechanism

$P(l_n)$: Probability of individual n for choosing plan l

$P(l_n(t)|\vartheta_n)$: Probability of individual n for choosing the specific target lane l at time t

$P(l'_n(t)|\vartheta_n)$: Probability of driver n choosing the specific target lane l' at time t

$P(lc_n^m|l_n, m_n)$: Probability of individual n for choosing plan l conditional on plan choice l and intermediate plan choice m.

$P(lc_n(t)|l_n(t), m_n(t), \vartheta_n)$: The probability of accepting available gaps at the direction of lane l at time t conditional on individual specific random term ϑ_n

$P(lc_n(t)|l'_n(t), \vartheta_n)$: Probability of gap acceptance with conditional on lane direction individual specific error term

$P(LC_n)$: Probability of individual n for choosing movement LC associated with intermediate plan m and action lc

$P(LC_n(t)|\vartheta_n)$: Probability of individual n of choosing movement LC at time t with conditional on driver characteristics ϑ

$P(LC_n^{l'}(t)|\vartheta_n)$: Probability of lane change in direction l' at time t with conditional on driver characteristics ϑ

$P(LC_n^{MLC})$: Probability of vehicle n starts MLC manoeuvre

s : Solo lane-changing mechanism

$(\dot{s})$: State in MDP

$S[.]$: Function of sensitivity car-following acceleration at time t

SITRAS : Simulation of Intelligent Transport System

st : The condition of stimulus

t, T : Observation time period for each vehicle.

t' : Time length between consecutive calculation of speed and position

T_n : Number of observed time period for each nth driver $(1, 2, 3, ..., T_n)$

TASAS : Traffic Accident Surveillance and Analysis System

Q : Number of traffic flow

(u) : The time function (u) between the observed location and the interested point.

$u(t_0, t)$: Normalised measure of the time difference between t_0 and t

$U_n(t)$: Utility of lane change of driver n at specific time t

$U_n^l(t)$: Target lane l of driver n at time t

$\widehat{U}_n^l(t)$: Systematic part of the utility of target lane l of driver n at time t

VISSIM : **V**erkehr **I**n **S**tädten – **SIM**ulations modell

$V_n(t)$: Vehicle n speed at time t

$V_{n+1}(t)$: Preceding vehicle $n+1$ speed at time t

$V_n(t - \tau_n)$: Speed of vehicle n at time $t - \tau_n$

$V_n^{DS}(t - \tau_n)$: Desired speed of driver n at time $(t - \tau_n)$

$[V_n^{DS}(t - \tau_n) - V_n(t - \tau_n)]$: Function of stimulus driver n at time $(t - \tau_n)$

VR : Volume ratio (Volume of weaving/Total traffic in the segment)

$V_n^{max}(t + t')$: Maximum safe speed for vehicle n with respect to the preceding vehicle at time $(t + t')$

$\overline{V}_n^l(t)$: Average speed at lane l of driver n at time (t) (m/sec)

$\overline{V}_{TMS}$: Aggregated time-mean speed

$\overline{V}_{SMS}$: Aggregated space-mean speed

$\Delta V_n(t - \tau_n)$: The relative speed between the speed of front vehicle (V_{n-1}) and subject vehicle (V_n) at time $(t - \tau_n)$

$|\Delta V_n^+(t - \tau_n)|$: The absolute value of the relative positive speed between the speed of the front vehicle (V_{n-1}) and subject vehicle (V_n) at time $(t - \tau_n)$

$\Delta V_n^l(t)$: Relative speed between driver n with the leading vehicle l at lane l at time t

$\Delta V_n^{cl}(t)$: Relative speed between driver n and the front vehicle at current lane l at time t

$[\Delta V_n^+(t - \tau_n)]$: Stimulus, positive relative speed

$|\Delta V^+(t - \tau_n)|$: The absolute value of the relatively positive speed between the speed of the object vehicle (V_{n-1}) and subject vehicle (V_n) at time$(t - \tau_n)$.

$[\Delta V_n^-(t - \tau_n)]$: Stimulus, negative relative speed

$|\Delta V^-(t - \tau_n)|$: The absolute value of the negative relative speed between the speed of the object vehicle (V_{n-1}) and subject vehicle (V_n) at time $(t - \tau_n)$.

$[\Delta V_n^{st}(t - \tau_n)]$: Stimulus, a function of relative speed between the subject and front vehicle at time $(t - \tau_n)$. (m/sec)

w : Weaving lane changing mechanism

$(\dot{w}(u))$: Weight condition

$\dot{w}(t_0, t)$: Weight assigned to the observation at time t in fitting a curve centred at t_0

$\dot{W}$: [NxN] matrix with elements corresponding to weight of observations used for local regression

χ^2 : Chi-square test value

$X_n(t)$: Vector of explanatory variables associated with individual n at time

$X_n^{cf,acc}(t)$: Vector of explanatory car-following acceleration variables associated with the sensitivity of driver n at time t

$X_n^{cf,dec}(t)$: Vector of explanatory car-following deceleration variables associated with the sensitivity of driver n at time t

$X_n^{cf,g}(t)$: Vector of explanatory car-following g variables associated with the sensitivity of vehicle n at time t

$X_n^{cf,g}(t - \xi\tau_n)$: Vector of explanatory car-following g variables associated with driver n at time $t - \tau$

$X_n^{DS}(t - \tau_n)$: Vector of explanatory variables of desired speed of driver n driver at time $t - \tau_n$

$X_n^l(t)$: Vector of explanatory variables associaed with driver n for lane l at time t

$X_n^{lc,m}$: Vector of individual n attributes associated with action lc with intermediate m

$X_n^{j,l,m}(t)$: Vector of explanatory variables associated with driver n lane changing mechanism m and critical gap j

$X_n^j(t)$: Vector of explanatory variables associated with driver n at time t for critical gap j

$X_n^{j,l'}(t)$: Vector of explanatory variables associated with driver n at time t for critical gap j, target lane l' and lane changing mechanism m

$X_n^{l'}(t)$: Vector of explanatory variables associaed with driver n for lane l' at time t

X_i^{τ} : Explanatory variables of the reaction time distribution

α^l : Estimated parameters of individual specific random effect ϑ_n for lane l

$\alpha^{l'}$: Estimated parameters of individual specific random effect ϑ_n for direction l'

$\alpha^{j,m}$: Estimated parameters of individual specific random effect ϑ_n for critical gap j and lane changing mechanism m

β : Vector of estimated parameters

β^{cf} : Estimated parameters of car following

$\beta^{cf,high}$: High sensitivity value, if the gap to the front vehicle is relatively close

$\beta^{cf,low}$: Low sensitivity value. If the gap is relatively large

$\beta^{cf,V}$: Estimated sensitivity parameter for the subject vehicle speed

$\beta^{cf,\Delta d}$: Estimated sensitivity parameter for the relative distance between the subject and front vehicle

$\beta^{cf,g,k}$: Estimated sensitivity parameter for the traffic density for car-following g

β^{DS} : Estimated constant desired speed

β^{ff} : Estimated constant sensitivity

β^j : Vector of estimated parameters for critical gap j

β^l : Vector of estimated parameters associated with target lane l

$\beta^{l'}$: Vector of estimated parameters associated with target lane l'

$\beta^{j,l'}$: Vector of estimated parameters for critical gap j

$\beta^{j,m}$: Vector of estimated parameters for critical gap j and lane changing mechanism m

β^{loc} : Vector parameters of the estimated curve, and $\varepsilon(t)$ a normally distributed error term.

$\beta^{MLC}, \beta^{No.LC}, \beta^{k}$: Estimated parameters of MLC, Number of lane changing, and density respectively

β_i^{τ} : Specific constant parameter of reaction time

$\varepsilon_n(t)$: Random error term

$\varepsilon_n^{cf,g}$: Random error term associated with acceleration g for driver n at time t, ($\varepsilon_n^{cf,g}) \sim N(0, \sigma^{cf,g^2})$

$\varepsilon_n^{cf,acc,+}$: Random error term associated with car-following acceleration, conditional on positive ΔV for driver n at time t

$\varepsilon_n^{cf,acc,-}$: Random error term associated with car-following acceleration, conditional on negative ΔV for driver n at time t

$\varepsilon_n^{cf,dec,+}$: Random error term associated with car-following deceleration, conditional on positive ΔV for driver n at time t

$\varepsilon_n^{cf,dec,-}$: Random error term associated with car-following deceleration, conditional on positive ΔV for driver n at time t

$\varepsilon_n^{ff}(t)$: Random error term associated with car-following under free flow regime for driver n at time t

$\varepsilon_n^{cr}(t)$: Random error term associated with critical gap for driver n at time $\varepsilon_n^{cr}(t) \sim N(0, \sigma_\varepsilon^2)$

$\varepsilon_n^{j}(t)$: Random error term associated with critical gap j for driver n at time t, $\varepsilon_n^{j} \sim N(0, \sigma^{j^2})$

$\varepsilon_n^{l}(t)$: Random term associated with the utility of the target lane l for driver n at specific time t

$\varepsilon_n^{l}(t)$: Random error term associated with target lane l for n^{th} driver at time t

$\varepsilon_n^{j}(t)$: Random error term associated with critical gap j for driver n at time t

$\varepsilon_n^{j,l,m}(t)$: Random error term associated with critical gap j and lane changing mechanism m for n^{th} driver at time t, ($\varepsilon_n^{j,l,m}$)$\sim N(0, \sigma^{j,m^2})$

$\varepsilon_n^{cf,g,st}$: Random error term of car-following g associated with conditional st for driver n at time t ($\varepsilon_n^{cf,g,st}$)$\sim N(0, \sigma^{cf,g,st^2})$

$\varepsilon_n^{cf,acc,+}$: Random error term of car-following acceleration associated with positive ΔV for driver n at time t

$\varepsilon_n^{cf,acc,-}$: Random error term of car-following acceleration associated with negative stimulus ΔV for driver n at time t

$\varepsilon_n^{cf,dec,+}$: Random error term of car-following deceleration associated with positive ΔV for driver n at time t

$\varepsilon_n^{cf,dec,-}$: Random error term of car-following deceleration associated with negative ΔV for driver n at time t

ξ $\epsilon[0,1]$, a parameter for sensitivity lag

μ_h, σ_h : Mean and standard deviation of the non-truncated headway distribution

μ_τ, σ_τ : Mean of the $ln(\tau_n)$ distribution and standard deviation of the $ln(\tau_n)$ distribution

τ_n : Reaction time of vehicle n

τ^{max} : Upper bound of the reaction time distribution

τ^{min} : Lower bound of the reaction time distribution

ϑ_n : Individual specific random error term to account for unobserved driver characteristics, assumed to follow normal distribution $\vartheta_n \sim N(0,1)$

θ : Span size or degree of smoothing

σ_{SMS}^2 : Variance of the space mean speed

$\sigma^{cf,g,\Delta V'}$: Standard deviation of car-following distribution g of vehicle n associated with $\Delta V'$

$\sigma^{cf,acc,+}$: Standard deviation of acceleration car-following distribution of vehicle n associated with relative positive speed

$\sigma^{cf,acc,-}$: Standard deviation of acceleration car-following distribution of vehicle n associated with relative negative speed

$\sigma^{cf,dec,+}$: Standard deviation of deceleration car-following distribution of vehicle n associated with relative positive speed

$\sigma^{cf,g,st}$: Standard deviation of car-following distribution g of vehicle n associated with stimulus st

σ^{ff} : Standard deviation of free flow distribution of vehicle n

σ^{ff^2} : Variance of free-flow error terms

$\bar{\rho}^2$: Adjusted rho-bar

$\phi[.]$: Probability distribution functions of a standard normal distribution random variable

$\Phi[.]$: Cumulative distribution functions of a standard normal distribution random variable

$\delta[g_n(t)]$: 1 if the driver accelerates; 0 otherwise.

$\delta[\Delta V_n^{st}(t - \tau_n)]$: 1 if the relative speed is positive, 0 otherwise.

$\delta_n^{left}(t)$: 1 if driver changes to the left lane at time t; 0 otherwise

$\delta_n^{cur}(t)$: 1 if driver changes to the current lane at time t; 0 otherwise

$\delta_n^{right}(t)$: 1 if driver changes to the right lane at time t; 0 otherwise

$\delta_n^k(t)$: Dummy variable with value 1 if final target l is k ($k = 0,1,2$) lanes away from current position

Chapter 1   Introduction

1.1 Background

Driving in a weaving section is challenging, because the driver has to adjust his/her path and maintain the safest gap towards the neighbourhood vehicle in a relatively short-length of road section. The operation at a weaving section is characterised by the complexity of traffic interaction (complex traffic interaction) during the lane-changing movement and acceleration behaviour (Sarvi et al., 2011). Indeed, these characteristics are slightly different from the basic section of motorway network. The high intensity of lane-changing movement in weaving movement leads drivers to interact and adjust their speed to maintain their driving in a safe manner. While aggressive movement may contribute to traffic disruption and accident risk, Golob et al (2004) found that 23.9% of the accidents in weaving section involve a sideswipe collision. These concerns require researchers and engineers to work hand in hand in developing an analysis tool which can capture driver characteristics in a weaving section.

Over the last decade, weaving section traffic has become an important topic in highway transport research area. The recent update of Highway Capacity Manual (HCM) has an improved analysis algorithm for a typical weaving section traffic performance which incorporates the geometric information as a critical factor in the operation of weaving section (HCM, 2010). However, the algorithm has difficulties in identifying the operational problem precisely and providing a unique optimum solution for improving the traffic performance. Implementing a long run traffic survey and various potential solutions directly into the traffic are some of the other approaches, which require the traffic engineer to identify the main problem directly in a typical weaving section. However, these approaches are prohibitively expensive and inefficient.

Microscopic simulation tools, therefore, are extensively used in the traffic research area for evaluating alternative strategies for transport planning and operation in recent times,

such as: MITSIM (Yang and Koutsopoulos, 1996), CORSIM (Halati et al., 1998), DRACULA (Liu, 2007), and VISSIM (PTV, 2011). It replicates real traffic conditions and it is an efficient way to analyse different scenarios, in particular motorway network i.e. weaving section. This approach analyses the complexity of traffic interaction explicitly through a detailed individual driver behaviour. Driving behaviour models, which include lane-changing model, acceleration model, and route choice model, form the core of these simulation tools. The lane-changing model describes the lateral movement of vehicle that incorporates target lane selection and gap acceptance while the acceleration model represents a response of stimulus and driver sensitivity in maintaining a safe gap toward the front vehicle. The behaviour models are also very important for safety studies and air quality analysis.

Both lane-changing and acceleration behaviours of individual drivers are affected by several factors including the characteristics of the observation area, the subject vehicle, and neighbouring traffic condition. The relative speed explains the interaction between the subject and object vehicles explicitly. It has a direct impact on both individual lane-changing and acceleration decision together with type of vehicle and position. Having a good knowledge of the network (i.e. curvature, speed limit, and location of slip road) and individual driver capability also influence the strategies and tactics in individual driver decision. In fact, driver decision varies depending on traffic condition.

The lane-changing characteristics in weaving section may differ from the other parts of the motorway network. The action of neighbouring traffic may significantly affect the lane-changing strategy in the weaving section, where the traffic is required to adjust their lanes in a relatively short length of the road. Moreover, it is common that the lane-changing vehicle in this section moves in a group due to the limitation of the length of the road. For instance, if the current lane front vehicle changes lanes in the same direction, the subject vehicle may be inclined to move as a platoon and accepts smaller gaps to complete the lane-changing manoeuvre. Similarly, the acceptable gap of weaving lane-changing may differ as opposed to the isolated/solo lane changing strategies. These issues have not been addressed in the existing lane-changing model. Most existing lane changing studies are focused on isolated lane-changing (i.e. Toledo et al. 2007, 2005; Choudhury, 2007). Those studies omit the various lane-changing strategies, which are significant components in the weaving section lane-changing decision-making process in particular.

The weaving section traffic has to adjust their speed preparing for a pre-emptive lane changing and leave a safe gap toward the current lane front vehicle. The acceleration behaviour in this section, therefore, is slightly different from the basic section of motorway sections. For example, if the subject vehicle faces adjacent lane merging vehicle, the movement requires acting differently from the stimulus though the current lane front vehicle moves faster than the subject vehicle that decelerates and leaves the gap for the adjacent lead vehicle to merge. However, the current acceleration models represent the acceleration decision as strictly correlated with the stimulus condition (i.e. Ahmed, 1999; Subramanian, 1996; Toledo, 2003). Those models neglect the impact of different stimulus conditions in the acceleration behaviour that frequently appear in the weaving section traffic.

There has been extensive research on improving driving behaviour models emphasising on more complex traffic condition such as weaving traffic, which very often are the sources of traffic bottlenecks. A fidelity in characterising the individual driver behaviour (i.e. lane-changing and acceleration behaviour) improves the applicability of the microscopic traffic simulation in responding to the variation of traffic scenarios in a particular facility such as weaving section, and the analysis of scenarios which may not be presented in the current real traffic conditions (Alexiadis et al., 2004).

Current Ph.D. research, therefore, proposes a novel state-of-the-art in lane-changing and acceleration models. The proposed lane-changing model incorporates various lane-changing strategies that are relevant with the front/lead vehicle movement and car-following behaviour in each relative speed conditions. The individual driver may prefer different lane-changing strategies (i.e. isolated/solo, platoon, and weaving) corresponding to the front/lead vehicle movement. This study considers those lane-changing strategies in the gap acceptance model which is the second level (action) of the proposed lane-changing modelling framework. Note that the gap acceptance model in this thesis incorporates both the accepted and rejected gaps. Meanwhile, the proposed acceleration model approach lessens the relationship between acceleration behaviour and stimulus. This study allows different responses (acceleration and deceleration on each positive and negative stimulus. Those concerns in the proposed lane changing and acceleration models shall improve the driving behaviour models performance.

Both the proposed modelling frame work assist the engineer/practitioners in understanding the nature of driving behaviour particularly in weaving section. This leads the highway engineer to come up with safer weaving section designs which

minimise the conflict and accident risk due to an intensive merging and diverging movements in the weaving section. A well designs of engineering interventions assists the engineers to distribute properly both the movements along the section (for example; lane-marking redesign, speed policy, application of ramp metering, and geometric improvement).

1.2 Research Objectives

The main objective of this research is to improve the state-of-the-art and proposed a lane-changing and acceleration behaviours modelling frameworks in a weaving section, which is one of the critical sections in multilane motorway networks. Both models are estimated to be based on the same set of individual vehicle trajectory dataset.

The current study investigates the effects of group behaviour in further details and proposes a lane-changing modelling framework which explicitly incorporates various impact of the group behaviour as part of individual lane-changing mechanism (i.e. isolated/solo, platoon and weaving movement). This issue becomes critical in a weaving section, where the traffic has to adjust its lanes in a particular length of the road. The decision-making process of lane changing is a result of the target lane choice and gap acceptance of individual driver. This process is a hidden (latent) plan while it is only possible to observe the individual driver decision either changes lane or maintain at the current lane. This research is therefore developing a lane-changing model that incorporates the impact of various lane changing mechanisms in the decision-making process. It is worth noting that the proposed modelling framework considers both accepted or rejected lane-changing conditions

This study aims to imitate the acceleration behaviours in the car-following regime and free-flow regime. The proposed model relaxes the car-following regime stimulus in the previous studies by allowing the acceleration behaviour to relate with each stimulus. This framework provides an opportunity for capturing a wider range of acceleration behaviours associated with different types of stimulus.

An empirical analysis of traffic surveillance data summarises the weaving section characteristics including speed, acceleration, gap acceptance, lane-changing location and direction, and lane-changing strategy. The use of loop detector of Motorway Incident Detection and Automatic Signalling (MIDAS) (DMRB, 1994) provides an aggregate data of speed, traffic flow and lane occupancy while the extracted vehicle

trajectory dataset represents all vehicle movements inside the observation area. The study applies both datasets to estimate the lane-changing and acceleration models.

1.3 Research Methodology

The proposed research initially requires the description of aims and objectives to provide research direction in modelling. A significant number of literature reviews supported the background for the modelling development both lane changing and acceleration models.

This study extends the general framework of latent plan model that incorporates the phenomena of group behaviour as intermediate plan (lane changing mechanisms). Consequently, the proposed lane-changing decision-making process framework follows a schematic procedure, namely: target lane, intermediate plan, and gap acceptance respectively. The decision-making process is latent (unobserved) while the observation can only capture the turning movement corresponding with the intermediate plan (lane-changing strategies). A driver, who tends to change lane, has to accept both gaps with lead vehicle and lag vehicle at the target lane simultaneously or he/she has to stay at the current lane. There are three types of lane-changing strategies: isolated/solo, platoon, and weaving. Platoon lane changing appears when the front vehicle at the current lane performs a lane changing during the same period, while the observed vehicle will be involved in weaving when the vehicle swaps lanes with the neighbouring vehicle. The driver involves in solo lane changing, if he/she changes lane individually as the front/lead vehicle maintains at their current lane. Several attributes are involved and explain the driver's decision, such as vehicle attributes, traffic attributes, individual characteristics, and previous decision effect. Individual characteristics in this model is captured by the level of aggressiveness, which varies among individuals.

The acceleration model is a function of driver sensitivity component (driver attributes) and stimulus as a linear function of relative speed between the front vehicle and the observed vehicle. The sensitivity may have a positive or negative value. This study that applies gap threshold, classifies the acceleration into two regimes: car-following regime and a free flow regime, while reaction time represents the driver aggressiveness in responding to the stimulus. This study suggests that the distribution of both values follow the lognormal distribution with truncation on both sides. In fact, it is similar with the observed gap acceptance distribution profile while the application of lognormal

distribution in gap distribution implies that a high proportion of traffic accepts short reaction time. Furthermore, the proposed acceleration model extends the car-following regime conditions by allowing different acceleration behaviours (acceleration and deceleration) in each stimulus conditions (relative positive speed and negative relative speed). Given this assumption, the model has four decisions in the car-following regime: acceleration with the relative positive speed, acceleration with negative relative speed, deceleration with positive relative speed, and deceleration with negative relative speed. This assumption relaxes the limitation of the previous studies and provides an opportunity to observe various car-following behaviours especially in the weaving sections where some traffic may act differently from the stimulus.

The study uses two types of surveillance data: traffic video recording and MIDAS. The traffic video records all the vehicle movement at the observed weaving section area. However, it requires an extraction process to gather the individual vehicle trajectory data by means of vehicle trajectory extractor application developed by Lee et al. (2008). The extracted trajectory data should be fitted /smoothed to minimise the unusual oscillations in the speed and acceleration profiles. All analysis is based on the fitted vehicle trajectory data. Meanwhile, MIDAS is based on loop detector data, which provides aggregated traffic characteristics such as speed, lane occupancy, and types of vehicle. It is necessary to validate the traffic video recording with MIDAS data to ensure the quality of trajectory data. The fitted and validated data will be used in the estimation process to explain the individual driver characteristics in both lane-changing and car-following behaviours.

The traffic movement analysis shows that the traffic at the observation area is moderately congested with level of service C based on HCM 2010 algorithm (see. Appendix-A). A significant capacity drop occurs when the weaving ratio is moderate or high (Wang et al., 2014). Detailed analysis of the trajectory dataset illustrates that both front and lead vehicles movement on the current and target lanes affects the lane changing tactical. There are three different lane-changing strategies in this study namely: individual/solo (76.6%), platoon (10.7%), and weaving (12.7%). Meanwhile, the cooperative lane-changing strategy is likely to appear during congested traffic flow which is beyond of the scope of this work.

Both the lane-changing and acceleration models are estimated separately using the same set of data source. Meanwhile, all the parameters of each model are estimated jointly

under the likelihood estimation procedure. The estimation process in this study is performed in R programming application developed by R Development Core Team (2010). In the microscopic model algorithm, the parameters of lane-changing and acceleration models vary depend on the weaving section geometric and driving behaviours which are presented in the vehicle trajectory dataset. Adopting the proposed modelling framework, this study suggests to re-estimate the modelling parameter due to the transferability of the proposed modelling framework for different trajectory dataset. The thesis validates modelling results with the observed trajectory dataset and pervious researches findings.

1.4 Thesis Outline

The remaining of this thesis is systematised as follows:

Chapter 2 contains a literature review of related studies in this research area including the weaving section characteristics, lane changing model and car-following model. This chapter provides a background and supporting details for the modelling developments in the following chapters.

Chapter 3 presents a general framework and the estimation procedure for the proposed latent plan decision-making process. This proposed model provides a flexibility to incorporate intermediate plan during the decision-making process.

Chapter 4 elaborates the application of the proposed latent plan model in the lane-changing movement. The proposed model integrates several lane changing strategies in weaving section (i.e. individual, platoon and weaving) into the modelling framework as an intermediate plan. This component is observed at the time when the vehicle executes lane-changing movement.

Chapter 5 discusses the proposed acceleration model that lessens the relationship between acceleration decision (response) and relative speed (stimulus). This relaxation provides flexibility in capturing various decisions in car-following regime. Furthermore, this chapter presents as well the estimation procedures of the proposed modelling.

Chapter 6 describes the data collection process, data extraction and management process and data analysis. The data collection process section discusses the selection of site and detailed application of both data sources at the observation area: the traffic surveillance camera and particular MIDAS loop detectors. Meanwhile, the data extraction and management include the vehicle trajectory extraction process, fitting method of the

vehicle trajectory data and validation process of the fitted trajectory with MIDAS loop detectors data. The data analysis section presents the traffic characteristics analysis based on both data sources including speed, acceleration, lane utilisation and traffic proportion. Moreover, analysing the vehicle trajectory data provides more detailed individual vehicle movement characteristics such as relative speed, gap acceptance, lane changing strategies and location.

Chapter 7 presents the estimation processes and results of the proposed lane-changing and acceleration models. A comparison of both lane-changing and acceleration models resulted in discounted models performed in terms of the goodness-of-fit including: Adjusted Rho-bar, Chi-square test and Akaike Information Criterion (AIC). Furthermore, this chapter validates the current result with the observed dataset and previous studies result.

Chapter 8 summarises all works in this research, discusses the limitation of the studies, and identifies the opportunities and direction for further researches in the driving behaviour research area in weaving section traffic.

Chapter 2   Literature Review

This chapter presents a review of both weaving section characteristics and driving behaviour models. In terms of traffic, weaving section has a slight different characteristic in comparison to other multilane facilities. The traffic in weaving section has to adjust its position in the relatively short length of the weaving section. This specific characteristic affects the driving behaviour which focuses on two aspects: (1) lateral movement or lane-changing movement; (2) acceleration movement. This section discusses several relevant existing studies with the proposed study including the characteristics of weaving section, lane-changing behaviour and acceleration behaviour.

2.1 Weaving Section

2.1.1   Geometry

A weaving facility is defined as a section of motorway connecting a pair of closely spaced junctions. In the UK, DMRB (DMRB, 2006) defines the distance of weaving section as between 100-3,000m with respect to designed speed and hourly traffic volume. Meanwhile, HCM specifies the length of weaving section is between 150-762m (500-2,500ft) which is slightly shorter compared to DMRB definition.

Design Manual for Roads and Bridges

DMRB (2006) defines that the weaving section length is a distance between the ends of the merging taper to the beginning of the diverging taper as shown in **Figure 2.1**.
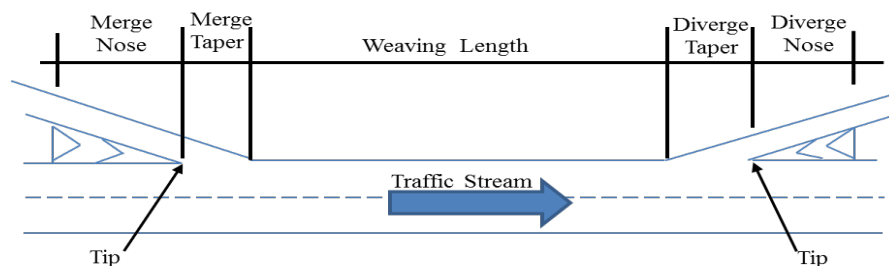
Figure 2.1 The UK weaving segment layout (DMRB, 2006)

They state the length of weaving section as a distance between the ends of merging taper and the beginning of the diverging taper. Meanwhile, the desirable length of motorway weaving section is between 2,000-3,000 m. They found that there is no weaving interaction if the section is longer than 3,000 m (DMRB, 2006). However, there is a difficulty for the road traffic authorities to fulfil the minimum desirable weaving section length due to spatial limitation issues. This condition has stimulated the highway engineers and designers to come out with a minimum length of weaving section as shown in **Figure 2.2**.
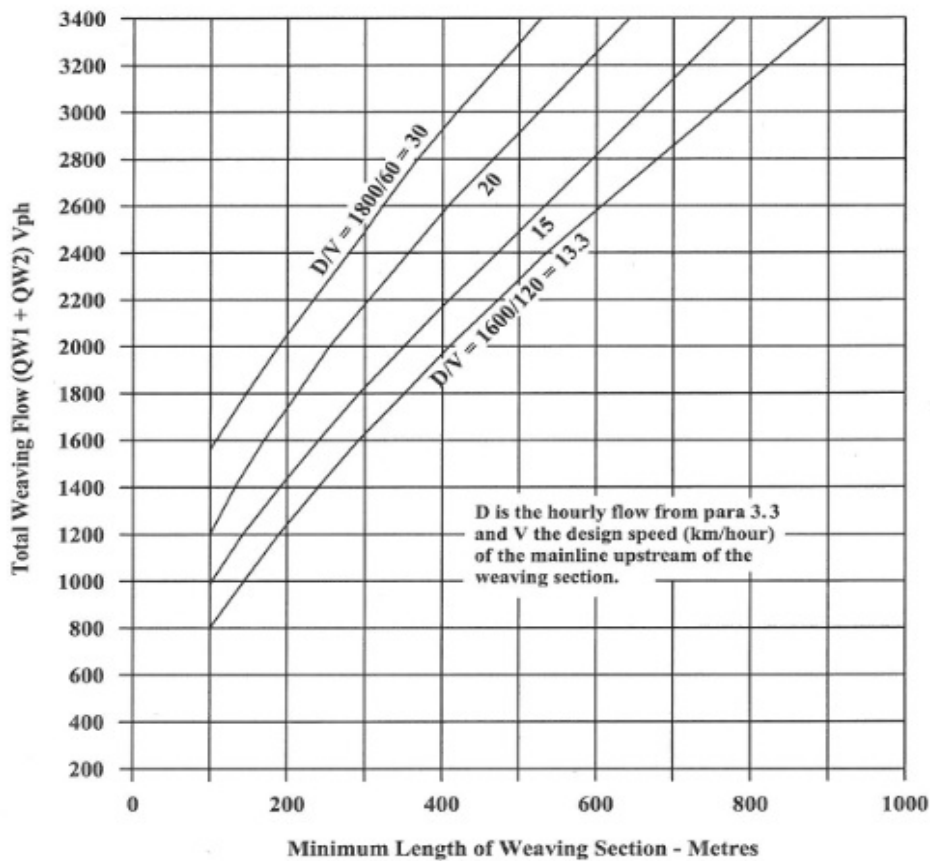
Figure 2.2 Weaving Length Diagram (DMRB, 2006)

DMRB (2006) defines several types of weaving section in the UK as shown in **Figure 2.3**. The classification of the weaving section in the UK is totally based on the appearance of auxiliary lane, lane gain and lane drop:
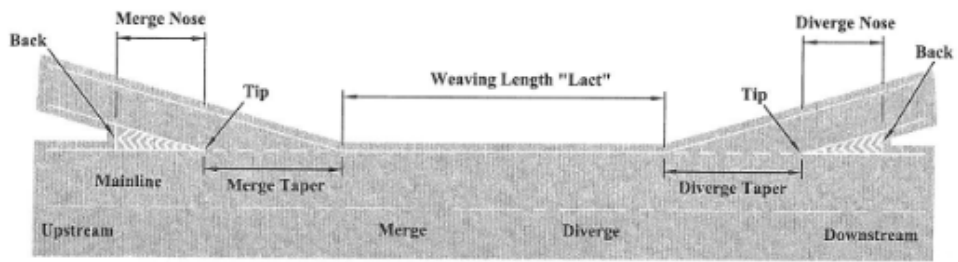
(a) Basic weaving section layout
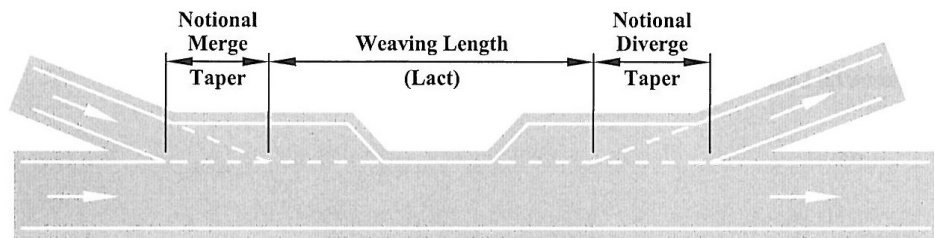
(b) Parallel merge/diverge as for Taper Merge/Diverge by notional layout

d = 100m for design speeds of 120/100 kph
d = 50m for design speeds of 85 kph and below
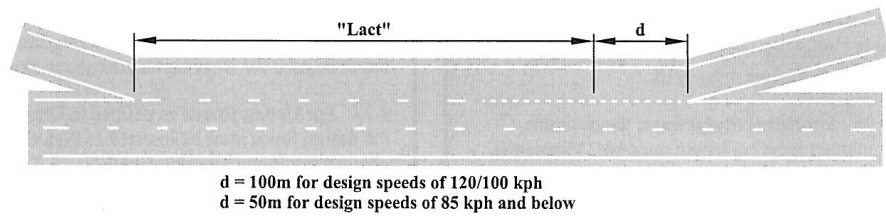
(c) Lane gain or lane drop

(d) Lane gain only

d = 100m for design speeds of 120/100 kph
d = 50m for design speeds of 85 kph and below
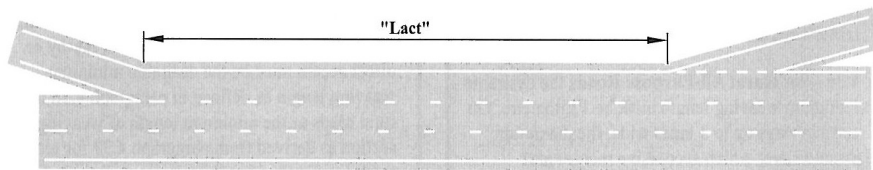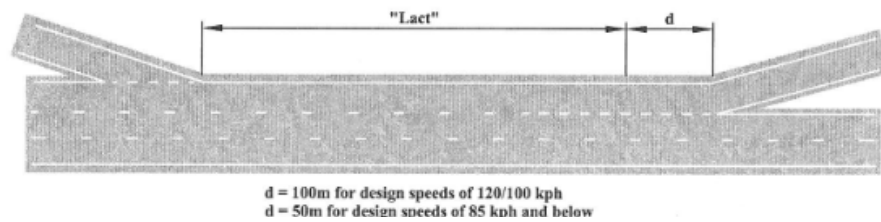
(e) Lane drop only

Figure 2.3 Type of weaving sections according to DMRB (DMRB, 2006)

Highway Capacity Manual

In comparison to the DMRB, HCM (2010) has different terms and approach for the weaving section length. The length in HCM is expressed as the distance (feet) between the merge and diverge that form the weaving section. Furthermore, they divide the weaving section length into two parts namely the short length and base length (see **Figure 2.4**).
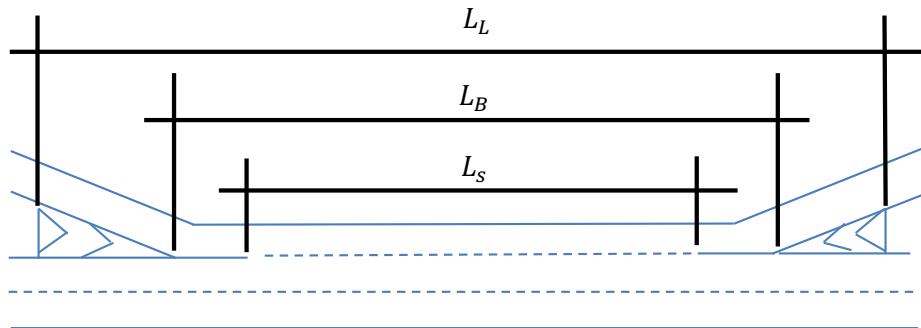
Figure 2.4 US weaving section layout (HCM, 2010)

Where;

L_L : Long length. The distance between physical barriers marking the ends of merging and diverging gore areas.

L_B : Base length. The distance between the respective gore areas at the on- and off-ramps.

L_S : Short length. The distance between the end points of any barrier markings (solid white lines) that prohibit or discourage lane-changing $L_S = 0.77 \; x \; L_B$

It is the fact that there is also a situation where $L_S = L_B$, when there is no solid marking on the pavement. Those two parameters are based on the field measurement.

In HCM 2010, the characteristics of weaving section vary depend on three parameters, namely volume ratio between weaving and non-weaving traffic, the estimated maximum length of weaving section (L_{max}), and the short length (L_S). L_{max} and L_S justify whether the observed location is analysed as a weaving section or two separate junctions. There are two conditions in these regards; when the value of L_S is less than the L_{max} value ($L_S < L_{max}$), the observed location is analysed as weaving section. When L_S is greater than or equal to the maximum ($L_S \geq L_{max}$), the observed location is analysed as two separate junctions. The estimated maximum length of weaving section can be expressed as follows:

$$L_{max} = [5{,}728(1 + VR)^{1.6}] - [1{,}566N_{wl}] \qquad (2.1)$$

Where;

L_{max} : The maximum length of weaving section (based on the short length definition) (ft)

VR : Volume ratio (Volume of weaving/Total traffic in the segment)

N_{wl} : Number of lanes for weaving manoeuvre.

Considering the algorithm, it may be the case that the analysis approaches vary over the observation period due to the traffic characteristics. For example, a particular weaving section can operate as two separate junctions due to a low number of weaving traffic while it acts as a weaving section, concerning the increased weaving traffic. This approach is slightly different compared to previous HCM 2000 version, where the weaving section characteristics are determined on basis of the observed weaving section length.

Moreover, the new version of HCM (2010) classifies the weaving section based on the ramp location as follows:

• One-sided weaving section is the one where weaving manoeuvres do not require more than two lane changes to be successfully completed.

• Two-sided weaving section is the one where at least one weaving manoeuvre requires three or more lane changes to be successfully completed or in which a single-lane on-ramp is closely followed by a single-lane off-ramp on the motorway's opposite side.

These classifications are different in comparison to HCM 2000 version which classifies the weaving section based on the minimum number of lane-changing required. There are three types of weaving section in HCM 2000 namely type A (1 lane-changing), type B (2 lanes changing), and type C (more than 2 lanes changing). **Table 2.1** summarises the type of weaving sections both in HCM 2000 and 2010.

Table 2.1 Types of section based on HCM

HCM 2000	Configuration	HCM 2010	Configuration
	Type A		One-Sided Weaving Section
Major Weave with Lane Balance at Exit Gore		One-Sided Ramp Weave	
		One-Sided Major Weave	
	Type B		Two-Sided Weaving Section
Lane Balance at Exit Gore		Weaving Section with Single-Lane Ramps	
	Type C		Weaving Section with Three Lane Changes
Merge at Entry Gore			
Merge at Entry Gore and Lane Balance at Exit Gore			

A summary of weaving section characteristics in DMRB and HCM is presented in **Table 2.2** which incorporates the minimum lane changing for merging and diverging from the weaving section and the availability of weaving section.

Table 2.2 Summary of weaving section characteristics in DMRB and HCM

Source	Type	Min. Lane Changing		Auxiliary Lane
		Merging	Diverging	
DMRB (2006)	Basic weaving section	1	1	No
	Parallel merge and diverge	1	1	Partial
	Lane gain/lane drop	1	1	Yes
	Lane gain only	None	1	No
	Lane drop	1	None	No
HCM (2010)	One-sided ramp	1	1	Yes
	One-sided ramp with major weave	1	1	No
	Two-sided with single-lane ramp	None	2	Yes
	Two-sided with three lane-change	1	1	No

2.1.2 Capacity analysis

Weaving section capacity is defined as the maximum number that is able to pass the weaving section during a specific period of time, under prevailing road, environment, traffic and traffic control conditions (HCM, 2000). Several factors affect the weaving section capacity including number of lanes, the proportion of weaving and non-weaving traffic, traffic composition, driver characteristic and geometric configuration (Shoraka and Puan, 2010).

The capacity and operational of weaving section has been an important issue since mid-1980's. HCM 1985 initiated the analyse of weaving performance which relied on the average operating speed of both weaving and non-weaving traffic (Leisch and Leisch, 1984). The proposed algorithm provides unrealistic speed result, which is slightly lower compared to the observed speed, in various sections. Cassidy et al. (1989) compared

contradictorily eight major freeway weaving sections and found that the weaving speeds are not as sensitive to geometric factors as previously believed. Furthermore, Stewart et al. (1996) simulated the HCM 1994 weaving section analysis algorithm using the INTEGRATION (Van Aerde, 1994). They found that the number of lanes on weaving capacity affects the traffic performance significantly compared to the length. However, the empirical lane capacity model/value for the estimation of weaving section capacity is unavailable in the study.

Roess and Ulerio (2000) raised several issues in HCM 1997 weaving section analysis algorithm such as; under-predicted speeds of weaving and non-weaving vehicle, unsystematic calibration algorithm, and missing real model for capacity of weaving section. They, therefore, proposed the weaving section capacity as a function of the combination of weaving movement (freeway-to-ramp, and ramp-to-freeway) and non-weaving (freeway-to-freeway and ramp-to-ramp) flows, length, width and weaving section geometry. Although this algorithm is adopted in HCM 2000, there is no closed-form solution for capturing the interaction among those listed variables. Trial and error procedures are performed in estimating the traffic performance for given value of volume ratio (VR), length of weaving section (*L*) and type of weaving section.

By focusing on the capacity analysis of weaving section type A and B to which it is associated, Lertworawanich and Elefteriadou (2001, 2003) defined the weaving section capacity as a function of maximum traffic flow, volume ratio (VR) between the rap and main traffic and number of lane changing. Later, Lertworawanich and Elefteriadou (2007) proposed an algorithm of weaving section capacity analysis for typical weaving sections. This study finds that the weaving section length and gap acceptance affect the weaving section capacity significantly. In addition, longer length weaving section provides more opportunity for the weaving vehicle to change lane, which resulted in increased capacity. In fact, this model neglects individual lane choice effect and variation of gap acceptance of individual that affects the possible number of lane changing in the weaving section.

Awad (2004) adopted Neural Network Technique (NNT) algorithm to estimate the weaving section capacity. The NNT algorithm is similar to the architecture of the human brain and neurons systems which consists of three layers; input, hidden and output layer. All nodes are interconnected across layers. Although the complexity is increased, the NNT modelling framework work properly in type B and C only. The algorithm of NNT, however, is difficult to be interpreted as the correlation between the layers is presented inconsistently. For example: some factors in the input layer may not be included to the following layers.

By improving the HCM 2000 algorithm, Roess et al. (2008) and Roess and Ulerio (2009) formulated the weaving section level of service as a relationship of the average speed (weaving and non-weaving traffic) and overall density. They represented this relationship as a single function rather than varying on the basis of weaving section specification. Later, HCM (2010) adopts this approach in their algorithm, which requires detail information on the geometric information (e.g., number of lanes and weave length) and the total hourly volume rates and the HCM weaving volume to total volume ratio (VR). Although the algorithm gives different outcomes of predicted density and level of, Bloomberg (2011) found that the outcomes of both HCM 2000 and HCM 2010 have similar pattern including:

- The density decreases with the increased of weaving section length,
- The density increases with the weaving volume,
- A sharp reduction appears when the observed section classification changes from weaving to basic

The new algorithm of weaving section analysis in HCM 2010 will be subsequently presented in Appendix-A later on.

Meanwhile, Skabardonis and Mauch (2015) identified the limitation in HCM 2010 analysis method that predicts the capacity in moderate traffic flow properly. The algorithm underrated the traffic density and overrated the congested traffic and uncongested traffic condition respectively. Those conditions hold the weaving section to be in D level of utility.

Various specification of analysis algorithm has been introduced in analysing the weaving section capacity and traffic performance. Nevertheless, they find difficulty in identifying the optimum model and the impact of each observed variables that contribute in the operational of weaving section due to lack of real traffic data. Neglecting the variation of individual driver characteristics may mislead the model or result in improper traffic analysis which is clearly seen in all version of Highway Capacity Manual including the recent HCM 2010. In fact, the proposed empirical algorithms are strictly fitted for particular traffic condition only. This condition affects the decision of the traffic engineers equipped with incorrect counter measurement programme or solution to improve the weaving section traffic performance. A significant number of researchers are therefore considering this opportunity to analyse the weaving section traffic characteristics by using a high-level of data details (microscopic level), which contribute to the weaving section performance. The reviews of the weaving section traffic characteristics are presented in the following section.

2.1.3   Traffic characteristics

Weaving traffic involves two or more streams of traffic travelling in the same direction crossing each other along or change lane in a relatively short section between an on- and off-ramp without any assistance from traffic control. As mentioned earlier, the weaving section length in the UK is between 2,000 – 3,000 m (DMRB, 2006) while it is slightly shorter in US, which is between 150 – 762 m (HCM, 2000).

According to Cassidy (1990), the term of conflict area in this study is defined as a location where most traffic disruption appears between the auxiliary lanes and curb side of the main traffic along the weaving section. **Figure 2.5** illustrates the schematic of weaving section conflict area.
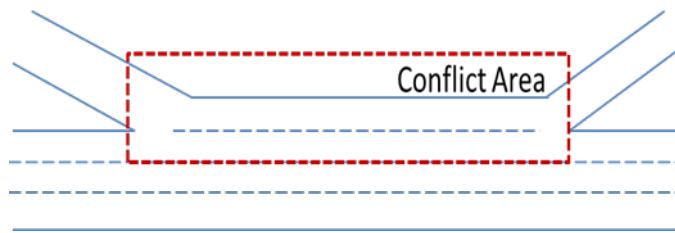
Figure 2.5 Weaving section conflict area

Due to the movement complexity, weaving section accidents are more likely to involve changing-lanes vehicles, because the requirement for either merging or diverging vehicles, or both, to execute a lane change is a defining feature of weaving sections. Therefore, it is necessary to include the safety aspect consideration in the weaving section design. This ensures the vehicle to move safely through the weaving section. Golob et al. (2004) analysed the accident characteristics at weaving section by using the Traffic Accident Surveillance and Analysis System (TASAS) in year 1998. The study focused on three major types of freeway accidents: rear-end, sideswipe and hit an object. 36.8% of accidents in weaving section occur in the middle lanes of weaving sections where 23.2% of accidents is classified as sideswipes accident due to a high proportion of lane-changing traffic. The analysis shows that weaving section of type A has the lowest accident risk compared to type B and C. Meanwhile, type B has the most severe accident risk as the minor on ramp traffic has to merge and diverge from the main traffic in particular length. Most of the accidents in type C weaving section occurs during the congested traffic associated with slowing and stopping traffic. (see **Table 2.1** for the HCM 2000 weaving section designs).

Wang et al. (1993) proposed a microscopic traffic simulation INTRAS (integrated traffic simulation) and empirical observation to analyse the impact of individual movements on the capacity of the weaving section. The study defined that the weaving

section traffic performance is significantly affected by the total flows and lane-changing activity in associated with the availability gaps in the traffic streams. The simulation constitutes the first 250ft (76.2m) of weaving section as the critical zone due to a high proportion lane-changing movement in that area. In fact, this work focuses only on the lane-changing movement between the auxiliary lane and kerbside lane, while they ignore the lane-changing movement in the other lanes.

Lane changing in a weaving section is more challenging to be performed compared to other motorway or urban road facilities. Al-Kaisy et al. (1999) simulated an empirical dataset of weaving section traffic, which was developed by Cassidy (1990), using an INTEGRATION microscopic traffic simulation (Van Aerde, 1994). This application allows tracking the individual vehicle movement. They identified that the traffic tend to change lane at the first attempt as they reach the end of merge gore particularly in the congested traffic, while the moderate traffic shifts the lane-changing movement towards the downstream. Although it has similar pattern, this distribution pattern of the estimated and observed lane-changing location fits properly only in the congested traffic while the estimated lane-changing location is overrated or underrated in other traffic condition. There is an unclear explanation regarding the difference in the result between the predicted and observed lane-changing location. Moreover, an empirical modelling explaining the lane-changing movement is unavailable in the study.

By analysing the NGSIM vehicle trajectory data set, Bham (2006) identified the lane-changing movement characteristics in weaving section. An intensive lane changing occurs in the first 91 m (300ft) of the weaving section where 76% of the lane-changing traffic change lane in this particular area. The intensive lane-changing between the kerbside and auxiliary lanes makes the traffic on those lanes to be more vulnerable due to higher possibility of conflicting point compared to the other lane-changing movement. The study result is relatively similar to Wang et al. (1993) as both studies identifies the upstream area of weaving section as a point due to high lane-changing proportion in the area.

Skabardonis and Kim (2010) subsequently adopted the Caltrans Highway Design Manual (CALTRANS, 2007). They confirm the previous research finding showing that the kerbside and auxiliary lane as the critical zone, particularly in upstream traffic (i.e. Wang et al., 1993; Bham, 2006; Wang et al., 2014) . Moreover, a high concentration diverging manoeuvre in the upstream triggers a bottleneck condition especially when the on-ramp traffic flow is relatively small compared to main lanes traffic. In contrast, the increased of on-ramp traffic flow reduces the attraction of the auxiliary lane. This condition ends the bottleneck condition and distributes the lane-changing movement toward the downstream of the weaving section. In that case, both number of lane-

changing and spatial distribution affect the released of bottleneck in weaving section significantly. Despite the dataset of microscopic-level details, this study focuses only the aggregate analysis in macroscopic level and without any consideration in the impact of traffic interaction.

Al-Jameel (2011, 2013) studied the UK motorway weaving traffic characteristics by combining two types of data: Motorway Incident Detection and Automated Signalling (MIDAS) and vehicle trajectory data. The application of HCM 2000 algorithm in this study reports several significant driving characteristics in the UK weaving sections:

- The weaving section effective length equals to the whole length weaving section if the section is less than 300m; while the effective length equals 200m, if the weaving section is greater than 300m.
- A high proportion of traffic segregates them from the main traffic at the first 250m due to prepare lane changing. Based on two observations, above 85% of traffic segregates from the traffic at the first 250m.
- 70% of the bottleneck location occurs over the first 250 m of the weaving section and as a result, a bottleneck builds up 70m from the on-ramp. The bottleneck effect starts while the VR equal to 0.27. This is slightly lower compared to HCM 2000 finding which is 0.35.
- More details on merging and diverging traffic show that 80% of merging points is in the first 100m while the diverging movement in this area is 90%.
- The proportion of weaving driver, who accepts the first available gaps, is higher than the corresponding percentage of drivers in isolated merging section.

This study works in microscopic level of detailed which allows to identify the traffic characteristics in the UK typical weaving sections. However, this study focuses on empirical analysis of both traffic surveillance data methods (MIDAS loop detector, and vehicle trajectory data). It omits the impact of traffic interactions that affect the driving behaviour in weaving section significantly.

Meanwhile, Knoop et al. (2012) studied the characteristics of discretionary lane-changing movement, in the merging and diverging area in two different motorway section, namely A270 (Eindhoven, Netherlands) and M42 (Birmingham, UK). The traffic video trajectory data were extracted from A270 (Eindhoven, Netherlands), while the loop detector data were collected from M42 (Birmingham, UK). Both observation areas are classified as two separate junctions instead of single weaving section due to large distance between the entry- and off- slip road. In this case, the lane changing towards the kerb lane is slightly higher than toward the median lane which is most likely occurred in the downstream traffic. This finding demonstrates that weaving section

length has significant impact on the driving behaviour, lane-changing movement in particular.

The complexity of the weaving section movement appears also during the acceleration-deceleration behaviour. Sarvi et al. (2011) presented the complexity of interaction and identified the acceleration-deceleration behaviour on the congested freeway weaving section. A vehicle trajectory dataset of two weaving sections in Hakozaki (Tokyo, Japan) and Southbank (Melbourne, Australia) have been extracted. The relative speed and spacing headway captured the relationship between the observed vehicle and the neighbouring traffic at the current and target lane. By extending the non-linear GM model Gazis et al. (1959), the estimation indicated that the acceleration behaviour of the weaving traffic is slightly different from the non-lane changing traffic. Various reaction time values have been tested while the estimation resulted in 0.72 sec as the optimum value. Nevertheless, the study focuses on the acceleration behaviour rather than the lane-changing movement in weaving section itself. The lane-choice during the movement is inexplicitly explained in the model.

Similarly, Wan et al. (2014) modelled the vehicle interactions during merging in a congested weaving section where the cooperation behaviour takes the important role during the lane-changing process. This study represents the interaction in the response-stimuli and car-following theory as they believe that it captures the interaction between the observed and neighbouring traffic (Putative leader and Putative lag) simultaneously during the lane-changing movement. Furthermore, the use of car-following visual information algorithm allows this study to capture the dynamic acceleration-deceleration behaviour during the lane-changing process. A set of NGSIM data of five lanes weaving section used in the estimation implying that the lateral separation between the observed vehicle and target lane traffic cannot be omitted in the lane-changing process. The cooperation (yield) behaviour of the putative leader and lag appears in the lane-changing process during the congested traffic.

The literature in weaving section research area shows that moving in the section is more challenging compared to the other part of a motorway network. In this case, the traffic has to adjust their movement in a relatively short length of the section without any assistance from traffic management instruments. There are several contributing factors in the weaving section traffic performance including; the road geometric characteristics (i.e. number of lanes, length of the sections), and the driving behaviour (i.e. lane changing, acceleration and gap acceptance behaviours). The literature reveals that studying a microscopic level of detail would provide better knowledge in understanding the nature of the driving behaviour in weaving section. Several microscopic studies in weaving section demonstrate that the kerbside lane and auxiliary lane are critical

conflict areas due to high proportion of lane changing traffic in upstream traffic. This traffic characteristic requires individual driver to interact and respond to the change of downstream traffic condition including the lane-changing movement, acceleration behaviour. The listed microscopic studies in weaving section traffic focus on aggregate individual characteristics of both lane changing and acceleration behaviours in weaving section. The variation of individual driver characteristics during their movement in weaving section has not been incorporated into the model. Following Section 2.2 and 2.3 will provide and discuss the existing lane changing and car-following model which formwork for the modelling development later on.

2.2 Lane Changing Models

Over the past decades, the number of studies in the lane-changing model has contributed significantly to the development of micro simulation. **Figure 2.6** illustrates a schematic lane-changing movement, where the subject vehicle changes lane to the right direction.

Modelling the lane-changing movement is particularly complex, since the model has to capture both decision of target lane and gap acceptance behaviour. The lane-changing model can be generally classified into three modelling approaches: models made on basis of lane-changing rules, game theory based approach on the interactive behaviour, and discrete choice models of lane-changing choices.
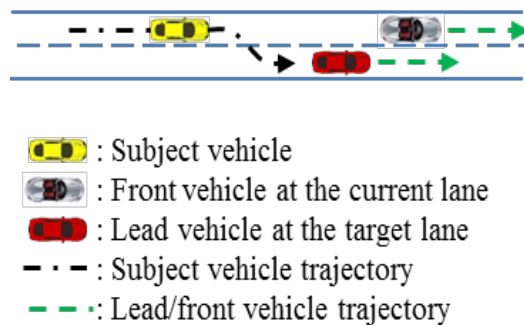
Figure 2.6 Schematic lane-changing movement

2.2.1 Rule-based lane changing models

Gipps' model

Gipps (1986) was among the first who develop a lane-changing modelling framework based on a rule-based approach that captured the safety, necessity and desirability of the lane changing movement. Moreover, the study identifies several objectives of lane changing:

- Safe target lane gap: The driver changes lane if the gap at target lane is acceptable in order to minimise the collision risk.
- Avoiding of permanent obstruction: The driver executes the lane-changing while approaching the obstruction (i.e. on street parking on curb side lane)
- The existence of transit lanes: A non-transit vehicle will change lane in avoiding to enter the transit lanes.
- Driver's intention for turning movement: The driver aggressiveness is increased when approaches the mandatory lane-changing point
- Facing the heavy vehicle: Moving behind the heavy vehicle is less preferable due to their lower speed.
- Increasing speed: Changing the lane may provide an opportunity for the vehicle to gain a speed advantage.

Based on those reasons, the lane-changing characteristics can be classified into two groups:

- Mandatory lane-changing (MLC): If the driver must change lane in order to maintain the drivers' path plan (i.e. merging, diverging, avoiding of permanent obstruction)
- Discretionary lane-changing (DLC): If the lane-changing driver aims to improve driving environment (i.e. increased, speed, avoiding the heavy vehicle)

The lane-changing model in his study is designed in in correspond with Gipps' car following model (Gipps, 1981), which is presented in car-following model section. This model considers the driver breaking rate limit as a significant factor while calculating the lane-changing vehicle safe speed. The model is consequently written as follows:

$$V_n^{max}(t + t')$$

$$= b_n t' + \left[b_n^2 t'^2 - b_n \left(\begin{matrix} 2\{loc_{n-1}(t) - length_{n-1} - loc_n(t)\} \\ -V_n^{max}(t)t' - V_{n-1}^{max}(t)^2/\hat{b} \end{matrix} \right) \right]^{1/2} \qquad (2.2)$$

Where;

$V_n^{max}(t + t')$: Maximum safe speed for vehicle n with respect to the preceding vehicle at time $(t + t')$

b_n : Most severe breaking which the driver is able to undertake

t' : Time length between consecutive calculation of speed and position

$loc_n(t)$: Observed vehicle location at the time t

$length_{n-1}$: Length of the front vehicle

$\hat{b}$: An estimated of breaking rate by the driver of vehicle n

The study assumed that the lane-changing process follows a decision tree with a series of lane-changing condition. At the lowest level of the decision tree, the driver faces a binary choice; to change or not change the lane. However, the lane-changing model has several limitations: the goal of the lane-changing movement is determined deterministically, the model presumed that individual driver decision in an identic traffic condition is homogeneity rather than non-homogeneity. Note that each driver still has different preference in facing an identic condition. The lane-changing is a model that strictly based on function of speed where the parameters are not estimated formally.

Wei's Heuristic lane-changing model

Wei et al. (2000) developed a heuristic lane-changing model by identifying the individual vehicle movement characteristics. They incorporated a pre-emptive lane-changing scenario and identified gap acceptance as a critical factor in the lane changing process. The lane-changing appears if the vehicle accepts all the available gaps: (1) gap to lead vehicle at target lane G^{lead}, (2) gap to lag at target lane G^{lag}, and (3) gap to front vehicle at current lane G^{cur}. The gaps are compared to a specific gaps threshold, which is based on the vehicle trajectory dataset. If one of the gaps is smaller than the threshold, the driver rejects to execute the movement and maintain it at current lane while seeking for the next gap. Instead of MLC and DLC, this study incorporated pre-emptive lane changing if the driver pretends to execute the DLC only if the speed advantages and disadvantages threshold are greater than the threshold. Moreover, the study demonstrates that the vehicle speed affects the lane-changing duration significantly. If the speed is slower than 10mph (16.1kph), the lane-changing vehicle requires 2.3-2.5 sec to complete the movement. In this case a faster vehicle than 10mph requires longer period between 3.0 and 7.5 sec. This modelling framework fits with the urban street network with six or more lanes.

Although a microscopic level dataset (i.e. vehicle trajectory data) is used in the current study, the research focuses partially on the gap acceptance behaviour as part of the lane-changing model. It neglects the objective of lane-changing movement. Similar to Gipps' model, the model ignores the traffic interaction and presumes that the drivers are homogeneous as the responds of different driver with same traffic condition are identic.

Application of the rule-based lane-changing model in microsimulation

Several number of micro-simulation tools adopt the rule-based lane-changing approach (i.e. Hidas, 2002; Kesting et al., 2007; Liu, 2010; Zhang et al., 1998). This section discusses briefly the modelling framework of those existing micro simulations.

Zhang et al. (1998) adopted the rule-based algorithm in the multi regime microscopic traffic simulation (MRS). Similar with the existing rule-based algorithm, the simulation classifies the lane-changing characteristics into two categories; MLC and DLC. In such rule-based model, the critical gap, acceleration and deceleration behaviour have significant roles during the lane-changing process. Moreover, the model demonstrates that MLC critical gap is decreased as the vehicle approaches the MLC point. The simulation is able to replicate the acceleration behaviour during the lane changing. Note that the traffic has to adjust their acceleration in order to find a safest gap for executing the lane-changing movement. Several lane-changing strategies are incorporated in this micro simulation:

- Without changing in acceleration: The vehicle accepts the adjacent gap directly.

- Require acceleration / deceleration: If the vehicle fails to meet one of the gaps at the target lane.

- The movement of both target lane lead and lag vehicles: There is an occurrence when both target lane lead and lag vehicle adjust their speed in order to leave space for the subject vehicle to merge.

- An immediate stop of subject vehicle: It commonly occurs when the subject vehicle fails to execute MLC as he/she reaches the final point of MLC.

This algorithm is transformed into CORSIM structure that which codes under the visual c++. The simulation demonstrated that the appearance of MLC affects the performance of weaving section significantly. By incorporating various components of driving behaviour (i.e. lane-changing, gap acceptance, acceleration behaviour) the detail of the road infrastructure can improve the simulation outcome significantly in representing the real traffic condition. However, the study encounters a difficulty to validate the result due to the limitation on the real-world data set. None of empirical driving behaviours model is presented in the study.

Hidas (2002) developed Simulation of Intelligent Transport System (SITRAS). This simulation is structured on basis of a multi-agent simulation system where all vehicles are modelled as an autonomous agent. The multi-agent based approach is able to replicate the complexity of traffic interaction between the vehicles. The driver has to

react and decide based on his/her best knowledge due to the surrounding traffic movements. SITRAS has four lane-changing modules:

- Route building

- Vehicle generation

- Route selection: based on individual driver characteristics

- Vehicle progression: relates to the proposed driving behaviour theory (car-following and lane-changing theory)

The simulation identifies the lane-changing movement with a small gap acceptance as a potential disturbance in the target lane. This modelling framework applies in a basic motorway section and fit well under the uncongested traffic flow. Meanwhile, the courtesy lane-changing tactical has insignificant impact in those type of traffic. Moreover, the model concentrates more in the acceleration behaviour adopting Gipps' (1986) model rather than the lane-changing itself. The target lane-choice is included implicitly in the modelling framework, despite the unavailable empirical lane-changing model. Similar to Zhang et al., (1998), the study finds difficulty to validate the simulation outcome due to the real traffic data absence. Later, he developed Analysis of Road Traffic and Evaluation by Micro simulation (ARTEMiS) by using the game-theory approach, which incorporates the courtesy/cooperative lane-changing strategy. The details of the game-theory will be presented in the following section.

Similar to Hidas (2002), Kesting et al. (2007) identified the lane-changing characteristics based on the car-following driver behaviour. They introduced Minimising Overall Breaking Induced by Lane-changing (MOBIL) algorithm for a wide class of car-following behaviour. The algorithm defined that the target lane attractiveness and risk depend on the vehicle acceleration. Moreover, the model includes the general safety and incentive criteria for the overtaking manoeuvre. The safety criterion in this study relates with the gap at the target lane gap, which based on the movement of target lane lag vehicle. In addition, the target lane lag vehicle shall decelerate less $\left(dec_{n+1}^{lag}\right)$ than the critical acceleration threshold (dec^{safe}).

The condition can be written as follows:

$$dec_{n+1}^{lag} \geq dec^{safe} \tag{2.3}$$

This study applies MOBIL's safety criteria into Intelligent Driver Model (IDM) which is developed by Treiber et al. (2000). Furthermore, the study introduces the driver heterogeneity based on the types of vehicle, namely slow vehicle ($V_n = 80\ km/h$) and fast vehicle ($V_n = 120\ km/h$). The politeness parameter in his study assists the

simulation to characterise the lane-changing rate degree of both drivers aggressiveness (or politeness) factor and lane changing location are found to affect lane changing rate, with lane-changing increases significantly around the mandatory lane-changing location (i.e. at the end of a link or at an off-ramp). However, the modelling of politeness factor is non-existent in the works. Moreover, other simulation parameters including the acceleration threshold and maximum safe distance are deterministic rather varying during the lane-changing process.

Liu (2010) defined a lane-changing decision-making process into three phases: (1) the aim of lane changing, (2) target lane selection, (3) executing the lane changing if the target lane gap is acceptable. By adopting Gipps' rule-based lane-changing classification, this study further described MLC as situations where a turning vehicle having to get into the correct lane which allows that particular junction turnings, or a bus needing to get into/out of a bus layby. Meanwhile, DLC movement included advanced lane changing in anticipation of junction turns further downstream. The lane changing occurs if both lead and lag gaps are acceptable. The driver in MLC regimes becomes more aggressive by accepting smaller gap as he/she approaches the end point of MLC movement. Please note that the vehicle in DLC movement occurs if the available gap at target lane is larger than a minimum safety gap G^{min}:

$$G^{min}(t) = V_n(t)\tau_n + \frac{V_n^2(t)}{2dec_n} - \frac{V_{n+1}^2(t)}{2dec'_{n+1}} + d_n^{min} \qquad (2.4)$$

Where;

$G^{min}(t)$: Minimum accepted gap at the target lane at time t

$V_n(t)$: Vehicle n speed at time t

$V_{n+1}(t)$: Preceding vehicle n+1 speed at time t

τ_n : Reaction time of vehicle n

dec_n : Deceleration of vehicle n

dec'_{n+1} : Deceleration of preceding vehicle n+1 speed at time t

d_n^{min} : Minimum deceleration of vehicle n

The algorithm is simulated in Dynamic Route Assignment Combining User Lear and Micro simulation (DRACULA), developed by the University of Leeds (Liu et al., 1995). In spite of incorporating the gap acceptance, the goal of lane changing in DRACULA

is deterministic in associated with a particular observed traffic condition. The structure of model omits the variation of individual driver (heterogeneity) characteristics (i.e. driver aggressiveness) that affects the lane-changing decision as discussed in Kesting et al. (2007). This condition, indeed, misleads the outcome or analysis of lane-changing model.

To summarise the discussion on rule-based approach, it is clear that most of them have limitations: (1) limited goals/tactical on lane changing are included, (2) ignoring the interaction between the traffic. The goals in the rule-based are deterministic and predefined for particular traffic condition. The main challenge of rule-based is to identify the exact goal of lane-changing movement, as the decision is a result of several possible goals that can be hidden from the observation. Traffic interaction during the lane-changing movement is inevitable. Note that the individual driver decision varies in associated with the traffic condition rather than homogeneous. Lane choice is a critical component in lane-changing movement that does not describe and incorporated appropriately in the rule-based algorithm. Imprecision in determining the goal and identifying the goal in the rule-based model leads to unrealistic outcome and modelling interpretation.

2.2.2 Game theory models

Kita (1999) introduced a "game theory" approach where lane changing is modelled as a two drivers, non-zero-sum, non-cooperative game. This modelling framework simplifies the traffic interaction explicitly by classifying the influence of neighbouring traffic (direct and indirect) instead of incorporating a large number of the influence of neighbouring traffic as explanatory variables. The rule of the game depends on the lateral vehicle movement, for example: (1) subject vehicle tends to merge (merge or pass), (2) target lane lag vehicle maintain to drive at target lane (giveaway or not). This strategy affects structure the pay-off matrix. By using a bimatrix game, the algorithm allows unique equilibrium solution of mixed strategy, which relates to both probabilities of merging (subject vehicle) and giveaway (target lane lag vehicle). The game is represented as the utility function of the pay-off based on several available gaps (i.e. gap to lead vehicle, gap to the collision, etc.), the aim is to take the safest action. This model incorporates the time to collusion that expresses the accident risk (time to collusion) while the speed in the modelling is constant. Moreover, the parameters are estimated by a maximum likelihood estimation procedure. This framework is simple and straightforward in representing the interaction between the subject vehicle and the neighbouring traffic during the lane-changing movement. The availability of real data traffic in this study allows the simulation outcome of proposed modelling framework to be validated. However, the structure does not consider the individual driver lane-choice

and the heterogeneity of individual driver decision, which is important component in lane-changing modelling framework.

Wang et al. (2005a) and Wang (2006) extended the game theory that incorporated the decision-making process during the lane-changing movement. In this case, the driver manages his/her speed (accelerate or decelerate) in according to maximise the chance of available gaps by considering either the nearside traffic and remaining distance to the MLC movement. Thus, this model has five sub-models: acceleration model, gap-selection model, gap-acceptance model, merge model and cooperation model, that represents both cooperative lane changing behaviour and courtesy yielding. The cooperative behaviour of traffic that allows the lag vehicle to create gaps and facilitate the merging movement, affects the traffic performance of merging during the congested period significantly. The probability of this type of movement is drawn randomly from a binomial distribution. While the courtesy yielding occurs if the target lag vehicle decelerates and allow the subject vehicle to merge at the target lane. Similarly with cooperative lane changing, the decision distribution in courtesy yield follows a binomial distribution corresponds to the specification of the range of target lane lag gap (G^{lag}); $G^{min} < G^{lag} < G^{max}$.

The simulation demonstrates that the vehicle in both cooperative and courtesy lane changing tactical are forced to accept the first gap. The proportion of taking the first gap is decreased while the acceleration lane length is longer than 100m. In addition, the drivers prefer to delay the movement and accept the following gap. The model finds that gap selection, acceleration and deceleration behaviour, and cooperative lane-changing model are significant components in order to mimic the dynamic interaction during gap creation and lane changing behaviour lane changing movement. The study explains the lane changing characteristics in more details compared to the previous game theory model. Introducing various lane changing tactical and the availability of real data traffic improve the reliability of the model. Instead of estimating from real traffic data, all parameters in this study are based on the various study rather than estimated directly from the real traffic data. This simplification can mislead the simulation outcome considering that the parameters may be inappropriate for the real traffic condition.

Hidas (2005) developed Analysis of Road Traffic and Evaluation by Microsimulation (ARTEMiS) by extending the application of game theory approach. The lane changing in ARTEMiS is classified into three groups based on relative gaps between leader and follower as follows:

- Typical lane changing: The vehicle moves immediately through the target lane (left or right) as a result of an evaluation on the target lane traffic condition. The

subject changes lane in relatively free traffic without interfering the traffic at the target lane.

- Courtesy lane changing: This type of lane changing is related to forced lane-changing movement. The driver of high priority courtesies with both target lane lead and lag vehicle when calling for a space to merge into the target lane. An indication of the courtesy lane changing appears if the gap at target lane is constant or narrower before the lane-changing movement. The gap will be subsequently increased as the subject vehicle joins the target gap traffic

- Cooperative lane changing: This type is contradicted to the forced lane changing. The traffic in target lane increases to provide a gap for the subject vehicle to merge. The gap will be subsequently narrower after the movement.

Moreover, ARTEMiS identified that the cooperative lane-changing phenomena appears under the congested traffic flow both in the freeway section and signalised urban section. This framework has explicitly relaxes the inefficiency and unreliability on simulating the complexity traffic interaction particularly in congested traffic flow that appears in SITRAS (Hidas, 2002).

Liu et al. (2007) improved the game theory approach by assuming that the vehicle aims to maintain the driving conditions. They sets aside the assumption of constant variable speed proposed by Kita (1999). Furthermore, the study includes the minimum safety gap and remaining distance to MLC point as one of the attributes in the players' payoff function. The game strategy allows the subject vehicle either to merge or pass and seek for the next available target lane gap, while target lag vehicle strategy is either to maintain or giveaway by decelerating the vehicle. The pay-off function demonstrates that the aggressiveness of subject vehicle increases if the target lag vehicle chooses not to giveaway. This characteristic is significantly shown by increased acceleration behaviour. A pre-emptive deceleration movement allows the target lag vehicle to move in comfortable deceleration rate. The non-linear programming is performed in the estimation to minimise the total deviation between observation and predicted merging choice. This study finds that the target lane lag vehicle tends to maintain and minimise speed variation, while the subject vehicle merges towards the target lane in relative short period of time to minimise the potential disruption in the target lane (i.e. delay, uncomfortable deceleration and incident). Similar to Kita (1999), the framework simplifies the lane-changing movement into two-players game between lead and lag vehicles while the rest neighbouring traffic are not taken into consideration. This assumption is unrealistic in the real traffic condition where the vehicle has to interact with the neighbouring traffic, particularly with the target lane lead and lag vehicles during the lane-changing process.

Those listed game theory models discuss the ability well in representing the interaction between the subject vehicle and the target lane traffic, especially the target lane lag vehicle. The vehicles in this model are assumed to cooperate and manage their movement by accelerating or decelerating situated on several parameters i.e. speed, breaking ability, and gap acceptance. The microscopic simulations demonstrated that the cooperation and courtesy lane-changing strategies likely to occur during the congested traffic flow. Although it will simplify the traffic interaction, there is a limitation in representing the interaction between subject and neighbouring traffic. This modelling framework simplifies the lane-changing movement as a two-player game between the subject and lag vehicles and ignores the impact of target lane lead vehicle movement that leads to unrealistic modelling result. The lane choice and variations of individual driver decision are incorporated in this game-theory modelling specification.

2.2.3 Discrete choice models

MITSIM' lane-changing model

Yang and Koutsopoulos (1996) introduced the random utility approach in the context of lane changing. They applied this approach in Microscopic Traffic Simulation (MITSIM) that establishes laboratory environment for testing and evaluating designs of Advanced Traffic Management System (ATMS) and Advanced Traveller Information (ATIS). Adopting Gipps' model, MITSIM structures the lane-changing movement into three phases: (1) defining the need and type of lane changing, (2) defining the target lane choice, and (3) observing and accepting the target lane gaps to change lane. This study classifies the lane changing into two types:

- Mandatory Lane-changing (MLC): When the vehicle that changed lane as a reaction of avoiding lane closure in responding to the Variable Message Sign (VMS), has merged or diverged from main lane traffic. The probability of the driver involved in MLC at the distance from MLC location (d^{MLC}) is written as follows:

$$P(LC_n^{MLC}) = \begin{cases} exp\left[\dfrac{d_n^{MLC} - d'}{\beta^{MLC} + \beta^{No.LC}No.LC + \beta^k.k}\right], & d^{MLC} > d^{cr} \\ 1 \quad, & d^{MLC} \leq d^{cr} \end{cases} \qquad (2.5)$$

Where;

$P(LC_n^{MLC})$: Probability of vehicle n starts MLC manoeuvre

d_n^{MLC} : Remaining distance to the mandatory lane-changing point of driver n at time (t), ∞ if no mandatory lane changing is required.

d^{cr} : Critical distance from MLC location which is associated to particular message sign (i.e. last message for exit sign).

$No.LC$: Number of lane changing required from the current lane toward the desired target lane.

k : Traffic density of the road section.

$\beta^{MLC}, \beta^{No.LC}, \beta^{k}$: Estimated parameters of MLC, Number of lane changing, and density respectively

Once the vehicle is classified as MLC, this status will remain attributed to the vehicle until the lane changing occurs or it moves into the downstream link.

- Discretionary Lane-changing (DLC) occurs if the subject vehicles aim to improve their driving environment (i.e. increasing speed, overtake slow traffic). This type of movement depends significantly on the traffic condition at both target lane and current lane. Impatience and speed indifference factors affect the driver decision in DLC movement significantly. Note that the driver uses those two factors to find the safest lane-changing speed, that allows the vehicle to merge smoothly and create less disruption at the target lane traffic.

The target lane choice is related to several criteria including lane-changing regulation, lane use privilege, lane connection, signal state and incident, prevailing traffic conditions, driver's desired speed, and maximum speed on the lane. The driver will then observe the available gap at the target lane in order to execute the lane changing movement.

Minimum acceptable gap of the DLC movement is given as follows:

$$G_n^{min,j} = \overline{G_n'}^{j} + \varepsilon_n^j \qquad\qquad j\{lead, lag\} \quad (2.6)$$

Where;

$G_n^{min,j}$: Minimum accepted gap j at the target lane of vehicle n

$\overline{G_n'}^{j}$: Average accepted gap j of vehicle n

ε_n^j : Random error term of gap j

Meanwhile, the gap acceptance for MLC is decreased in according to the vehicle remaining distance to MLC location (d^{MLC}). The driver in MLC is assumed to be more aggressive by accepting smaller gaps as he/she approaches the MLC location. MLC gap acceptance model is subsequently written as follows:

$$G_n^{min,j}$$

$$= \begin{cases} G^{max^{'},j} & loc_n \geq loc^{max} \\ G^{min^{'},j} + \left(G^{max^{'},j} - G^{min^{'},j}\right)\dfrac{(loc_n - loc^{min})}{(loc^{max} - loc^{min})} & loc^{min} < loc_n < loc^{max} \\ G^{min^{'},j} & loc_n \leq loc^{min} \end{cases} \quad (2.7)$$

Where;

$G_n^{max',j}$: Upper bound of j gap acceptance at the target lane

$G_n^{min',j}$: Lower bound of j gap acceptance at the target lane

loc_n : Observed vehicle n location

loc^{max} : The end point of the observation

loc^{min} : The starting point of the observation

MITSIM lane-changing model provides greater flexibility in capturing the traffic interaction compared to the rule-based and game-theory approaches. The lane changing decision in this method is assumed to be affected by several factors such as driver impatient factor, relative speed, and appearance of the heavy vehicle. However, the modelling framework is not well developed as none of lane choice and gap acceptance parameters are estimated in this stage.

Dynamic discrete-choice model

Ahmed et al. (1999) performed an extensive work on modelling lane change decisions with discrete choice modelling approach. Similar with Yang and Koutsopoulos (1996), lane changing is shaped as a result of the two-step process: (1) lane selection and (2) gap acceptance. The model captures the decision of lane changing as a probability of target lane and gap acceptance function that are estimated based on MLE.

The decision-making process in this study is latent as the dataset can only capture the action of lane-changing movement. Note that the driver must accept both gaps (lead and lag) at the target lane in order to change lane. The lane-changing movement is classified into two groups MLC or DLC.
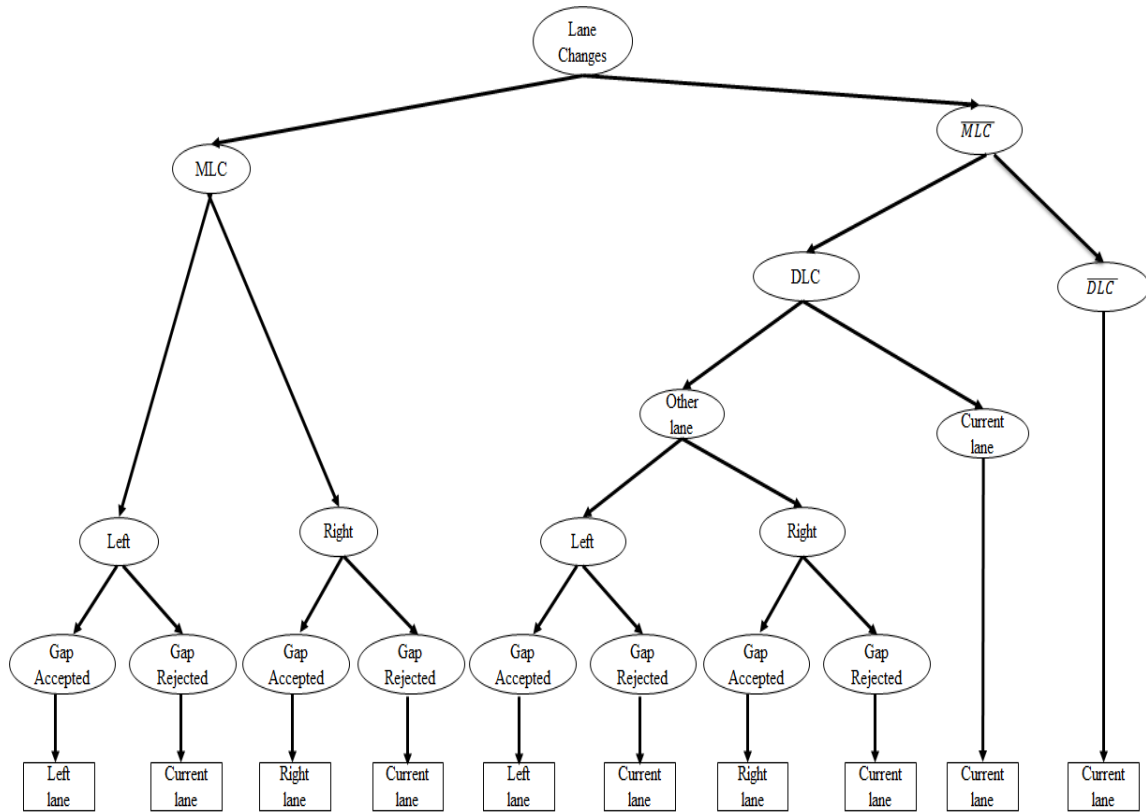
Figure 2.7 Lane-changing modelling structure (Ahmed, 1999)

Figure 2.7 demonstrates the lane-changing decision-making process in correspond with the type of lane changing. In this case, the MLC driver faces a binary condition whether to change lane or delay for the better lane-changing movement ($\overline{MLC}$). Several explanatory variables may affect MLC movement decision, such as remaining distance to MLC, the number of lane-changing required, the density of the target lane, etc. MLC condition does not apply to the lane-changing driver if he/she prefers not to respond or delay the movement ($\overline{MLC}$). Furthermore, the driver evaluates the current lane condition and the adjacent lane (left, right) in order to decide whether it requires DLC (change lane under discrete lane changing at the first attempt) or $\overline{DLC}$. The driver will most likely change lane towards the target lane that provides better driving environment for the driver. As discussed in Yang and Koutsopoulos (1996), impatience factor and speed indifference factor have significant impact on DLC decision. Once the driver defines the target lane, he/she observes and defines the safest gaps (lead and lag) for changing lane. If the gaps are rejected, the driver should stay at the current lane and seeks for the next available gaps.

The lane-changing decision is discrete based on time and correlated for each individual. The probability of the individual lane changing is a function of the lane utility where the random component of the function consists of two elements: individual-specific

random term (driver heterogeneity) and random term. The lane change utility can be written as follows:

$$U_n(t) = \beta.X_n(t) + \vartheta_n + \varepsilon_n(t) \qquad (2.8)$$

Where;

$U_n(t)$: Utility of lane change of driver n at specific time t

β : Vector of estimated parameters

$X_n(t)$: Vector of explanatory variables associated with n driver at time t

ϑ_n : Individual specific random error term to account for unobserved driver characteristics, assumed to follow normal distribution $\vartheta_n \sim N(0,1)$

$\varepsilon_n(t)$: Random error term

Meanwhile, Ahmed et al. (1996) applied probit model to formulate the gap acceptance model that captures the interaction between the subject vehicle and neighbourhood vehicles at the target lane. This approach is suggested by Daganzo, (1981), who was among the first to introduce the application of probit model in the gap acceptance model. The gap acceptance in this study incorporates driver heterogeneity that representing the individual driver characteristics over the observation period. The driver n accepts the available gaps j at time t $\left(G_n^j(t)\right)$ if it is larger than the critical gaps, which are the minimum unobservable gaps. Considering such assumption, the gap acceptance model can be written as follows:

$$G_n^{cr,j}(t) = \exp\left(X_n^j(t).\beta^j + \vartheta_n + \varepsilon_n^j(t)\right) \quad j \in \{lead, lag\} \ (2.9)$$

Where;

$G_n^{cr,j}(t)$: Critical gap j of driver n at time t

$X_n^j(t)$: Vector of explanatory variables associated with driver n at time t for critical gap j

β^j : Vector of estimated parameters for critical gap j

$\varepsilon_n^j(t)$: Random error term associated with critical gap j for driver n at time t, $\varepsilon_n^j \sim N(0, {\sigma^j}^2)$

The critical gap follows the lognormal distribution. The conditional probabilities of accepting the available gap can be written as follows:

$$P\left(G_n^j(t) \geq G_n^{cr,j}(t)|\vartheta_n\right)$$

$$= P\left[ln\left(G_n^j(t) \geq G_n^{cr,j}(t)|,\vartheta_n\right)\right]$$

$$= \Phi\left[\frac{ln\left(G_n^j(t)\right) - \left(X_n^j(t).\beta^j + \vartheta_n\right)}{\sigma^j}\right] \tag{2.10}$$

Where ;

Φ : Cumulative standard normal distribution

Then, the probability of lane-changing modelling framework in **Figure 2.7** can be written as follows:

$$P\left(LC_n^{l'}(t)|\vartheta_n\right) = [P(l_n(t)|lc_n(t), l_n'(t), MLC, \vartheta_n)][P(lc_n(t)|l_n'(t), MLC, \vartheta_n)] *$$

$$[P(l_n'(t)|MLC, \vartheta_n) + P(l_n(t)|lc_n(t), l_n'(t), DLC, \overline{MLC}, \vartheta_n)] *$$

$$[P(lc_n(t)|l_n'(t), DLC, \overline{MLC}, \vartheta_n)][P(l_n'(t)|DLC, \overline{MLC}, \vartheta_n)] *$$

$$[P(DLC|\overline{MLC}, \vartheta_n)][P(\overline{MLC}|, \vartheta_n)] \tag{2.11}$$

Where;

$P\left(LC_n^{l'}(t)|\vartheta_n\right)$: The probability of lane change in direction l' at time t

$l_n(t)$: Changing lane toward lane l in direction l'

$lc_n(t)$: Accepting available gaps at the direction of lane l

$l_n'(t)$ $\in$ {left, current (cur), right}

The unconditional of the lane-changing likelihood function is written by:

$$LC_n = \prod_{n=1}^{N} \int_{-\infty}^{\infty} \prod_{n=1}^{T_n} \left[P\left(LC_n^{left}(t)|\vartheta_n\right)\right]^{\delta_n^{left}(t)} \left[P\left(LC_n^{cur}(t)|\vartheta_n\right)\right]^{\delta_n^{cur}(t)} *$$

$$\left[P\left(LC_n^{right}(t)|\vartheta_n\right)\right]^{\delta_n^{right}(t)} f(\vartheta)\, d\vartheta \qquad (2.12)$$

Where;

$\delta_n^{left}(t)$: 1 if driver changes to the left lane at time t; 0 otherwise

$\delta_n^{cur}(t)$: 1 if driver changes to the current lane at time t; 0 otherwise

$\delta_n^{right}(t)$: 1 if driver changes to the right lane at time t; 0 otherwise

The heterogeneity attribute in the lane changing and gap acceptance models is particular probabilistic function rather than deterministic value as previously believed in Kesting et al. (2007). It represents the variation decision of individual in different traffic conditions during the observation as a conditional function of the lane-changing probability in Equation 2.12.

A significant finding in this research says that the distance to the intended turning point affects significant lane-changing decision particularly in the upstream traffic, while it is less significant on the behaviour at the beginning of the observed road stretch. The distance effect arises as the driver enters the middle section of the observed road stretch. Note that lane changes driver at this road section begins to adjust their speed in order to prepare lane changes or turning movement through the target lane. Moving towards the end of the observation, lane change driver has settled in the correct lane, and maintain their drive towards the intended turning point.

This modelling framework extends the rule-based framework explicitly where the lane-changing decision is described to be whether MLC or DLC. As discussed earlier in Section 2.2.1, it is exceptionally difficult to identify the lane-changing characteristic or goal precisely and directly from traffic observation. Note that the lane-changing decision is a result of several goals that may be hidden from the direct observation.

Integrated lane-changing model

Toledo (2003), therefore, suggested a joint model for lane choice and gap acceptance where the MLC and DLC lane changing conditions are integrated into a single framework. The proposed model captures trade-offs among the various concerns and avoids identifying MLC trigger situation. Furthermore, the modelling framework is able

to incorporate with dynamic changing of the traffic situation. In the real traffic, the driver requires evaluating and updating his/her short-term plan decision in at specific time step (i.e. 1sec) whether moving to lane l'; left, right or maintain at the current lane. An application of random utility choice approach assists to capture the interdependencies and correlation over all levels of decision-making process. The target lane choice model, therefore, can be defined as multinomial logit model with the conditional probability of choosing a specific lane as follows:

$$P(l'_n(t)|\vartheta_n) = \frac{exp(\beta^{l'}.X_n^{l'}(t) + \alpha^{l'}.\vartheta_n|\vartheta_n)}{\sum_l exp(\beta^{l'}.X_n^{l'}(t) + \alpha^{l'}.\vartheta_n|\vartheta_n)}$$

$$l' \in \{left, current, right\} \quad (2.13)$$

Where;

$P(l'_n(t)|\vartheta_n)$: Probability of driver n choosing the specific target lane l' at time t

$X_n^{l'}(t)$: Vector of explanatory variables associaed with driver n for lane l' at time t

$\beta^{l'}$: Vector of estimated parameters associated with target lane l'

ϑ_n : Individual specific random error term to account for unobserved driver characteristics, assumed to follow normal distribution $\vartheta_n \sim N(0,1)$

$\alpha^{l'}$: Estimated parameters of individual specific random term ϑ_n for lane l'

The driver observes and seeks the safest gaps (lead and lag) at the target lane for lane changing. Similar with the previous research prerequisites, the lane-changing movement occurs if the minimum acceptable gaps in the target lane is larger than the critical gaps (i.e. Ahmed, 1999; Hwang and Park, 2005). It is worth noting that the critical gap varies among the drivers due to driver preferences and traffic characteristics at both current and target lane.

The critical gaps of lane-changing model are written as follows:

$$G_n^{cr,j,l'}(t) = \exp\left(X_n^{j,l'}(t).\beta^{j,l'} + \alpha^j\vartheta_n + \varepsilon_n^{j,l'}(t)\right) \quad j \in \{lead, lag\} \quad (2.14)$$

Where;

$G_n^{cr,j,l'}(t)$: Critical gap j at the direction of target lane l' of driver n at time t

$X_n^{j,l'}(t)$: Vector of explanatory variables associated with driver n at time t for critical gap j, target lane l' and lane-changing mechanism m

$\beta^{j,l'}$: Vector of estimated parameters for critical gap j

α^j : Estimated parameters of individual specific random effect ϑ_n for critical gap j

$\varepsilon_n^{j,l'}(t)$: Random error term associated with critical gap j for driver n at time t, $\varepsilon_n^{j,l'} \sim N(0, \sigma^{j^2})$

The probability of gap acceptance with conditional on lane direction individual specific error term is written as follows:

$$P(lc_n(t)|l'_n(t), \vartheta_n)$$

$$= [P(accept\ lead\ gap|l'_n(t), \vartheta_n)][P(accept\ lag\ gap|l'_n(t), \vartheta_n)]$$

$$= \left[P\left(G_n^{lead,l'}(t) \geq G_n^{cr,lead,l'}(t)|l'_n(t), \vartheta_n\right)\right] *$$

$$\left[P\left(G_n^{lag,l'}(t) \geq G_n^{cr,lag,l'}(t)|l'_n(t), \vartheta_n\right)\right]$$

$$= \Phi\left[\frac{ln\left(G_n^{lead,l'}(t)\right) - \left(X_n^{lead,l'}(t).\beta^{lead,l'} + \alpha^{lead}\vartheta_n\right)}{\sigma^{lead}}\right] *$$

$$\Phi\left[\frac{ln\left(G_n^{lag,l'}(t)\right) - \left(X_n^{lag,l'}(t).\beta^{lag,l'} + \alpha^{lag}\vartheta_n\right)}{\sigma^{lag}}\right] \tag{2.15}$$

Where;

$P(lc_n(t)|l'_n(t), \vartheta_n)$: The probability of gap acceptance with conditional on lane direction individual specific error term

$G_n^{lead,l'}(t)$: Available lead gap at target lane l' for driver n at time t.

$G_n^{lag,l'}(t)$: Available lag gap at target lane l' for driver n at time t.

$\Phi[\cdot]$: Cumulative standard normal distribution

A Next Generation SIMulation (NGSIM) trajectory data that includes location and speed at specific discrete time, is used to estimate the modelling parameters collectively with acceleration model. Moreover, the modelling estimation demonstrates that path

plan variable assists this study in order to capture the group variables such as the distance between the current position and the intended turning point at the target lane. MITSIM demonstrates that the integrated lane-changing modelling framework improves the simulation ability while the congestion is built up and discharged. In fact, the target lane choice is beyond the scope of the model and this modelling framework, that it is not applicable in a general lane-changing context.

Explicit target lane choice model

Toledo et al. (2005) and Choudhury (2007) extended further the discrete-choice approach where the choice set of lanes is assumed to include all available lanes as opposed to adjacent lanes. The modelling structure removes the limitation on the target lane choice tactic that appears in the previous lane-changing models. The model framework presumes that the driver changes lane towards the target lane due to various factors and goals. Lane changing consists of two level decision-making processes: (1) target lane choice and (2) gap acceptance. Note that the process is presumed to be latent as it is unobserved in driver choice at the observation period.
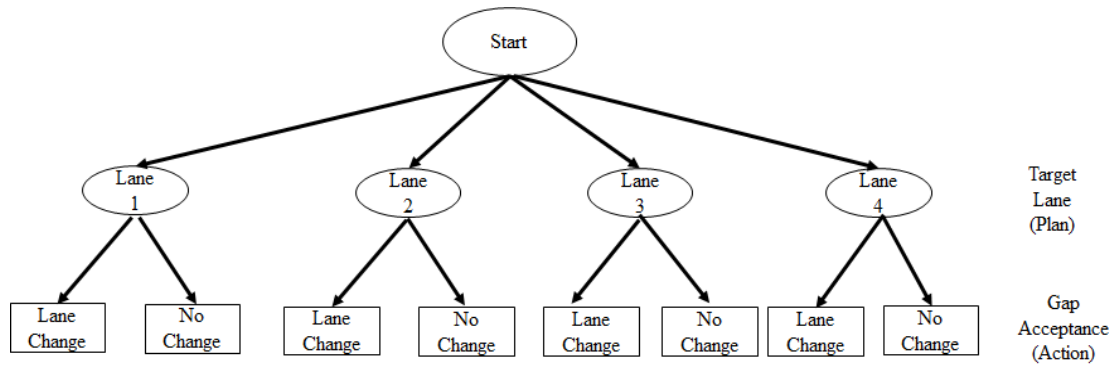
Figure 2.8 An explicit lane-changing modelling framework (Toledo et al., 2005)

The target lane choice model sets up all available lanes that are eligible for the driver. Given the illustration in **Figure 2.8** the utilities of target lane can be written as follows:

$$U_n^l(t) = \beta^l . X_n^l(t) + \alpha^l . \vartheta_n + \varepsilon_n^l(t) \qquad l \in \{1, 2, 3, \dots, L\} \quad (2.16)$$

Where;

$U_n^l(t)$: Target lane l utility of driver n at time t

$X_n^l(t)$: Vector of explanatory variables associated with driver n for lane l at time t

β^l : Vector of estimated parameters associated with target lane l

ϑ_n : Individual specific random error term to account for unobserved driver characteristics, assumed to follow normal distribution $\vartheta_n \sim N(0,1)$

α^l : Estimated parameters of individual specific random term ϑ_n for lane l

$\varepsilon_n^l(t)$: Random error term associated with target lane l for n^{th} driver at time t

L : Number of available lanes in the section

Assuming that the random error term ε_n^l is independent and identically distributed (IID). Note that the error term in multinomial logit follows Gumbel distribution corresponds to the difference of random variables which has logistic form. The probability of target lane choice of the multinomial logit model with conditional on the individual specific error term can be written as follows:

$$P(l_n(t)|\vartheta_n) = \frac{exp(\beta^l.X_n^l(t) + \alpha^l.\vartheta_n(t)|\vartheta_n)}{\sum_l exp(\beta^l.X_n^l(t) + \alpha^l.\vartheta_n|\vartheta_n)} \qquad l \in \{1,2,3,\ldots,L\} \quad (2.17)$$

Where;

$P(l_n(t)|\vartheta_n)$: Probability of driver n choosing the specific target lane l at time t

Same gap acceptance modelling and joint estimation procedure in Toledo (2003) is adopted in those researches. All the estimated parameters are based on the NGSIM trajectory dataset. The estimation suggests that the driver's decision in target lane choice is significantly affected by several explanatory variables; lane average speed, spacing, relative speed with the lead vehicle, number of lane change and path plan. In this case, the driver preference on changing lane is significantly decreased while approaching the MLC point. Meanwhile, the relative speed variable affects the decision of gap acceptance behaviour. Moreover, specifying the full set of available lanes in the target lane choice set will improve the goodness-of-fit as well as MITSIM' simulation results.

Furthermore, Choudhury (2007) extended the application of latent plan lane-changing modelling framework in the freeway merging that incorporates normal, courtesy and forced lane-changing tactical. The estimation indicates that the decision of merging is affected significantly by relative speed and the remaining distance to the end of merging point. In this case, the driver tends to involve in a forced lane changing by accepting smaller critical gap as he/she approaches the end of on-ramp. The study reports the cooperation tactic is likely to occur in congested traffic that is similar to the previous research findings in the game theory models as discussed in Section 2.2.2.

The application of discrete choice modelling in the lane-changing behaviour has been developed since the first appearance in late 90's. Toledo (2003) presented a significant improvement in this modelling framework by suggesting a single utility instead of varying based on the objective of lane-movement (DLC or MLC). This approach presumes the lane changing as the trade-offs between several attributes and avoids improper identification of the MLC cause. This assumption simplifies the structure of lane-changing model into two levels; (1) target lane choice and (2) gap acceptance. The discussion of gap acceptance model will be discussed in following sections. In fact, the decision-making process in target lane choice is latent (hidden) from the direct observation. It is only the action (gap acceptance) which can be observed directly from the trajectory dataset.

The latent plan framework, as one of a discrete choice modelling specification, provides flexibility in capturing the traffic interaction, lane-changing strategies and correlation among the individual decision during the lane-changing process. However, those listed models (i.e. Ahmed, 1999; Choudhury, 2007; Toledo, 2003; Toledo et al., 2005) focus explicitly in the isolated lane-changing movement. Meanwhile, those listed models omit the differences between individual and group lane changing which may affect significantly the weaving section performance.

2.2.4 Gap acceptance models

Gap acceptance is one of the significant components of the lane changing model together with the modelling specification, and lane changing tactic. Significant number of studies has been performed with various structures and assumptions since early 60's. Herman and Weiss (1961) presumed the gap acceptance by following the exponential distribution, while Drew et al. (1967) and Ashworth (1970) assumed lognormal and normal distributions respectively. In fact, those earliest studies were focused on the mean gap acceptance and ignored the gap acceptance resulted from series of gap acceptance decisions (rejected and accepted gaps). The decision-making characteristic is actually identical with the nature of panel data as each individual has more than one observation.

Daganzo (1981), is therefore proposed the probit model that includes the correlation among the series of time gap acceptance decisions of each individual at T-intersection. In this case, the mean minimum value of the gap acceptance model known as the critical gap is a random variable that is normally distributed across the population. The function of critical gap for the driver n at time t is expressed as follows:

$$G_n^{cr}(t) = G_n(t) + \varepsilon_n^{cr}(t) \tag{2.18}$$

Where;

$G_n^{cr}(t)$: Critical gap of driver n at time t

$G_n(t)$: Critical gap attribute of driver n at time t

$\varepsilon_n^{cr}(t)$: Random error term associated with critical gap for driver n at time, $\varepsilon_n^{cr}(t) \sim N(0, \sigma_\varepsilon^2)$

The error term in this case is presumed as the difference between the critical gap and the observed value. The estimation is performed under the maximum likelihood method. The probability density of the accepted/rejected gap should be then expressed as conditional probability on the unknown parameters. The study found that the typical driver rejects the first large gap due to the hesitation and subsequently much smaller gap.

By applying the same dataset, Mahmassani and Sheffi (1981) threated the gap acceptance dataset as cross-sectional instead of panel data as suggested by Daganzo (1981). The critical gap in this study is distributed normally. The mean critical gap is represented as function of explanatory variables that allows for incorporating the impact of various factor on the driver gap acceptance behaviour. In fact, this study introduced the function of rejection number that captures the driver impatience factor, as the attribute of proposed critical gap model. The study found that incorporating the impatient factor affects the driver decision significantly. Meanwhile, the estimation result denotes that the driver tends to be more aggressive (accepting smaller gap) as the delaying time is increased. However, the assumption of normal distribution in both studies performed by Daganzo (1981) and Mahmassani and Sheffi (1981) resulted in critical gap value of negative value that is unrealistic.

Ahmed (1999) extended the probit gap acceptance modelling framework to capture the lane-changing behaviour on the merging area. The gap varies among the driver and for each driver in different traffic condition. This variation is represented as an individual specific. As discussed earlier, the gap acceptance is the second level of lane-changing decision making process. The drivers, should agree the lane choice in the first instance before observing the acceptable gap and lag at the target lane. His study introduced the exponential form of critical gap that ensures the critical gap to be a non-negative value instead of normal distribution as used by previous studies. The heterogeneity in gap acceptance explains the variation of individual driver in accepting or rejecting gaps formulated as truncated probabilistic function. This approach has been used widely in the recent development of gap acceptance model by Toledo et al (2005), Farah et al

(2009), and Choudhury et al (2010). It should be noted that all those studies measured the gap on basis of distance.

Skabardonis (2002) used CORSIM algorithm to assess the operation of weaving sections. The capacity of this algorithm is defined to be associated with minimum headway of the acceleration behaviour, the critical gap for lane-changing movement and the vehicle characteristics. However, the models have limited attributes that representing the traffic interaction during the movement in weaving section. They model the lane-changing model based on speed function while the acceleration acts as sensitivity factor (level of aggressiveness). In this case, the sensitivity factor remains constant since the vehicle is generated. This assumption may not present the real-traffic condition appropriately where the individual driver sensitivity varies over the observation period.

Bham (2008) studied the characteristics of rejected gap (mean and median), and the largest rejected gap in a mandatory lane-changing behaviour on a multilane freeway facility during the congested and uncongested traffic. The study utilises NGSIM trajectory data set. The gap in this study is represented in time form, which is a function of the distance gaps and the follower's speed, instead of the distance gap-based that was previously used by Ahmed (1999), Choudhury (2007), and Toledo (2003). In this case, the vehicle observes sufficient time gap when executing the lane changing in safe manner. The statistical test of goodness-of-fit and Kologromov-Smirnov (KS) show that the distribution profile of gap acceptance fits properly with the lognormal and gamma distribution. Assuming the critical gap as a random variable in a stochastic method, the study uses the maximum likelihood estimation for estimating the lead and lag gaps in the target lane for the mandatory lane changing. The estimation results constitute that the critical lag is slightly greater than the critical gap in both congested and uncongested. Moreover, the merging drivers from the on-ramp traffic in both traffic conditions are found to be slightly more aggressive as they accept smaller gaps compared to the drivers changing lanes towards the off-ramp. In the merging context, the critical gaps are found to be significantly different in congested conditions when the driver is merging normally, expecting a courtesy yielding from the mainline driver or forcing in Choudhury et al. (2007). However, the models are developed for MLC conditions and do not involve any lane choice component. Yet, the proposed gap acceptance model deficiencies in attributes are explaining the gap acceptance decision.

Recently, Chu et al. (2015) observed the impact of cooperation behaviour and accident in the driver gap acceptance characteristics using a binary (accept or reject) logit model framework. In this case, the study classifies the lane-changing behaviour into three categories as follows:

- Chase-merging: if the observed driver passes the lead vehicle and executes the gap in front the lead vehicle

- Direct-merging: if the observed driver checks his/her position and accept the available gap at the target lane

- Yield-merging: if the vehicle delay and accept the gap behind the lag gap

The use of inverse time to collusion variable (TTC^{-1}) explains the accident risks. The lane-choice is based on a binary logit structure to accept or reject the movement. The maximum likelihood algorithm assists the estimation process based on a particular merging section at Nagoya urban expressway traffic data. The estimation illustrates that the lane changing in high traffic density has higher probability to occur in the chase merging, while the longer acceleration lane results in higher direct-merging tactic. Yield-merging occurs if the density in the target lane is relatively low (< 40 veh/km/lane). Nonetheless, this gap acceptance model focuses only on the gap with the target lane lead vehicle while the lag gap is ignored. The impacts of lane-choice, variation of individual driver and group behaviour are omitted in this model.

To summarise it, gap acceptance behaviour is affected significantly by the lane choice and strategies. Several studies have been conducted to identify the gap acceptance characteristics focussing on the distribution profile and the modelling specification. In general, the gap can be measured on basis of distance and time. Most of the recent gap acceptance model developments use critical gap terms to represent the mean value of gap acceptance which varies among the individual and traffic conditions instead of gap acceptance terms. The critical gap lies between the observed accepted gap and rejected gaps. The analysis of vehicle trajectory dataset in the recent development of gap acceptance suggests that distribution of gap acceptance to follow the lognormal distribution. This assumption denotes that most the driver in the population accepts smaller gap when performing the lane-changing movement and ensures the critical gap from the unexpected value (i.e. avoid the negative value of critical gap). The heterogeneity in the gap acceptance model represents the variation of individual driver decisions. The literature in the gap acceptance provides a strong groundwork for the proposed gap acceptance as part of lane-changing model in Chapter 4.

2.3 Car Following Models

Car-following model demonstrates the following driver reaction towards leader driver behaviour. After reviewing the existing car-following model framework, the model can be classified into two groups: car-following model and acceleration model.

Subject/observed vehicle
: Front vehicle at the current lane
: Lead vehicle at the target lane
: Subject vehicle trajectory
: Lead/front vehicle trajectory
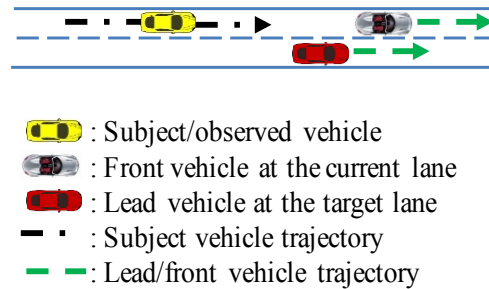
Figure 2.9 Schematic of car-following movement

Figure 2.9 demonstrates the car-following situation, where the subject vehicle satisfies and maintains the movement at the current lane.

2.3.1 Car Following Models

Pipes (1953) developed a mathematical analysis for modelling the car-following behaviour by using Laplace transformation procedure. The vehicle in this case is assumed to obey a postulate of California traffic codes saying that the subject vehicle requires a space with the lead vehicle by a length of car ($\pm$ 15 feet) for every 10 mil/hr of the subject vehicle speed. The study defines that the minimum safest time headway between the following and the leader vehicle is 1.02 sec. However, the finding has limitation since it is only applicable when the following vehicle obeys such code.

A massive work in car-following model has been done by General Motors' (GM) laboratory, Gazis et al. (1959) presented a car following behaviour as a response of sensitivity-stimulus framework. Considering the driver reaction time, the response can be written as follows:

$$Response_n(t) = [Sentivity_n\ (t)]\ [Stimulus_n\ (t - \tau_n)] \qquad (2.19)$$

Where;

τ_n : Driver n reaction time.

Driver reaction time represents the time lag between the appearance of stimuli and the individual driver response. The discussion of driver reaction time will be discussed in Section 2.3.3.

GM's first generation model presumes that the relative speed between the subject and front vehicle role as the stimulus component. Chandler et al. (1958) and Gazis et al. (1959) write the car-following model as follows:

$$a_n(t) = \beta^{cf}[\Delta V_n(t - \tau_n)] \tag{2.20}$$

Where;

$a_n(t)$: Acceleration of vehicle n at time t

β^{cf} : Estimated sensitivity parameters of car following

$\Delta V_n(t - \tau_n)$: The relative speed between the speed of leader vehicle (V_{n-1}) and subject vehicle (V_n) at time ($t - \tau_n$).

Both reaction time (τ_n) and sensitivity parameter (β^{cf}) are estimated on basis of the experimental data on the GM' test track. The observation requests the following (subject) vehicle to follow and maintain the safest gap with the front vehicle. Various combinations of τ_n and β^{cf} values are tested in the experimental design with assumption that the driver prefers a combination of those values with highest correlation. This estimation finds that the average values for both τ_n and β^{cf} are 1.55 sec and 0.37 sec^{-1} respectively.

Due to significant difference in the sensitivity parameters (0.17 to 0.74), the second generation proposed two states of sensitivity in correspond to the available gaps. The model applies a high sensitivity value($\beta^{cf,high}$), if the gap to the front vehicle is relatively close. If the gap is relatively large, the model employs the lower sensitivity value($\beta^{cf,low}$). Then, the acceleration model is given as follows:

$$a_n(t) = \begin{matrix} \beta^{cf,high} \\ or \\ \beta^{cf,low} \end{matrix} [\Delta V_n(t - \tau_n)] \tag{2.21}$$

However, there is difficulty to define the appropriate value of $\beta^{cf,high}$ and $\beta^{cf,low}$. It is also unrealistic while the acceleration behaviour considers only the relative speed component. In addition, the relative speed varies based on the relative distance as well. This limitation leads the next research to include the distance component as part of sensitivity terms. Gazis et al., (1959) proposed the third generation of GM model as follows:

$$a_n(t) = \frac{\beta^{cf}}{\Delta d_n(t)} \left[\Delta V_n(t - \tau_n) \right]$$

(2.22)

Where;

$\Delta d_n(t)$: Relative distance between the subject and front vehicle at time t

The experiments have been done in three different locations, namely GM track, Holland tunnel and Lincoln tunnel. The study reports that the sensitivity term is increased while the relative distance becomes smaller.

Table 2.3 Parameters for third generation of GM' model (Gazis et al., 1959)

Location	No. of driver	β^{cf} (mph)	τ (sec)
GM' test track	8	27.4	1.5
Holland tunnel	10	18.3	1.4
Lincoln tunnel	16	20.3	1.2

The fourth generation of GM' model incorporates the subject vehicle speed into the sensitivity component. Further improvement in the fifth generation has slightly changed the GM model into a non-linearity form. This model allows to capture different sensitivity terms for each sensitivity components that improves and generalises the sensitivity term. Gazis et al. (1961) formulated the fifth GM model as follows:

$$a_n(t) = \beta^{cf} \frac{[V_n(t - \tau_n)]^{\beta^{cf,V}}}{[\Delta d_n(t)]^{\beta^{cf,\Delta d}}} \left[\Delta V_n(t - \tau_n) \right]$$

(2.23)

Where;

$V_n(t - \tau_n)$: Speed of vehicle n at time $t - \tau_n$

$\beta^{cf,V}$: Estimated sensitivity parameter for the subject vehicle speed

$\beta^{cf,\Delta d}$: Estimated sensitivity parameter for the relative distance between the subject and front vehicle

The relative speed is stimulus of car-following behaviour while both the speed and headway/gap represent the individual driver sensitivity. However, the parameters estimation method is a result of trial and error method resulting in the non-optimum

model. All GM's modelling framework disregards the impact of the variations of individual driver car-following behaviour during the observation period.

In that case, Lee (1966) extended the GM model by incorporating the previous information on car-following behaviour for the current decision. The application of transform technique allows the modelling algorithm to represent the information as "memory function". The study presumes that the driver response depends on the series of previous relative speed. The formula is given as follows:

$$a_n^{cf}(t) = \int_0^t M(t - t')\Delta V_n(t')dt' \qquad (2.24)$$

Where;

$M(.)$: Memory function that represents the current driver behaviour based on series of the previous information.

However, the model disregards the driver sensitivity attribute which affects the individual driver decision. The study focuses only on the modelling development while the estimation of parameters in the proposed model are not presented. In that sense, it is difficult to validate the accuracy of the model.

Koshi et al. (1992) proposed a variation of GM model by incorporating two car following regime. Note that the car-following characteristics in both regime are slightly different. The modelling demonstrates that the driver awarness level in congested flow regime varies significantly in order to maintain both speed and gap toward the front vehicle. Note that less overtaking manoeuvre possibility is available in this regime, while driving in free-flow regime is capable to maintain the level of awarness. The modelling is based on the hypothetical mathematical equation associated with the observed traffic data. Conversely, there is no validation process or statistical test that proofs the validity of modelling framework.

Acceleration model

In early 1980's, a new paradigm in car-following model is proposed to incorporate the non car-following movement related to the development of micro simulation tools. Gipps (1981) proposed an acceleration model with several properties, namely ability to mimic the traffic behaviour, the parameters associated with specific driver characteristics and consistency during the estimation. The maximum acceleration is strictly constrained by two conditions: driver's desired speed and safest gap. The assumption is that the subject vehicle driver prefers the speed where he/she can safely

stop due to the lead vehicle movement. Hence, the new speed of subject vehicle is given by:

$$V_n(t + \tau)$$

$$= \min \{V_n(t) + 2.5 a_n \tau \left(1 - (V_n(t)/V^{DS})\right) \sqrt{(0.025 + (V_n(t)/V^{DS}))}, \qquad (2.25)$$

$$b_n \tau + \sqrt{\left(b_n^2 - b_n [2[loc_{n-1}(t) - length_{n-1} - loc_n(t)] - V_n(t)\tau - V_{n-1}(t)^2/\hat{b}]\right)}\}$$

Where;

$V_n(t)$: Driver n speed at time t

V^{DS} : Desired speed

b_n : Most severe breaking of individual driver n wishes to undertake

$\hat{b}$: Estimated the sever breaking of the object vehicle in front

$loc_n(t)$: observed of driver n location at time t (based on the front rear of the subject vehicle)

$length_{n-1}$: the length of the front vehicle

The model finds three key factors, which control the acceleration behaviour: desired speed distribution, driver reaction time, and ratio of mean breaking rate. Though the model parameters are not estimated thoroughly and the reaction time remain the same for all observed driver.

Yang and Koutsopoulos (1996) developed an acceleration model for MITSIM. The driver acceleration behaviour in associated with headway is classified into the following three regimes:

- Car-following: This regime calculates the vehicle acceleration resulted from its association with the front vehicle.

- Free-flowing regime: When the headway is larger than upper headway threshold $(h^{*,max})$. The vehicle moves on his desired speed.

- Emergency regime : When the headway is smaller than lower headway threshold $(h^{*,min})$. The vehicle decelerates to avoid an accident and increases the headway to the front vehicle.

However, their modelling framework ignores the driver reaction expectation for the stopped vehicle due to computational efficiency. The study estimates the parameter in based on generated traffic data rather than real traffic data.

Ahmed (1999) improved the acceleration model that omits the restriction on sensitivity and stimuli components. The driver sensitivity is a function of explanatory variables associated with car-following behaviour while the stimulus is a function or relative speed between the current lane front vehicle and the subject vehicle. The framework allows different modelling specification in correspond with car-following behaviour namely acceleration and deceleration. Adopting Subramanian (1996), the proposed model classifies the car-following into two different regimes: car-following (if the vehicle follows the leader), free-flow regime (if the vehicle would like to maintain the desired speed). The headway threshold (h^*), that is assumed to be constant for all drivers, is applied to differentiate between those two regimes. This condition is written as follows:

$$a_n(t) = \begin{cases} a_n^{cf}(t) & if\ h_n(t - \tau_n) < h_n^* \\ a_n^{ff}(t) & otherwise \end{cases} \tag{2.26}$$

Where;

$a_n^{cf}(t)$: Acceleration under car-following regime at time t

$a_n^{ff}(t)$: Acceleration under free-flow regime at time t

$h_n(t - \tau_n)$: Time headway at time $(t - \tau_n)$

h_n^* : Headway threshold for driver n

Furthermore, the car-following acceleration regime occurs if the relative speed is positive. When the relative speed is negative, the vehicle moves in the car-following deceleration regime. The general formulation of the car-following movement is given as follows:

$$a_n^{cf,g}(t) = S[X_n^{cf,g}(t)][\Delta V_n(t - \tau_n)] + \varepsilon_n^{cf,g} \qquad g \in \{acc, dec\} \tag{2.27}$$

Where;

$a_n^{cf,g}(t)$: Acceleration g under car-following regime of driver n at time t

$S[.]$: Function of sensitivity

$X_n^{cf,g}(t)$: Vector of explanatory car-following g variables associated with driver n at time t

$[\Delta V_n(t - \tau_n)]$: Stimulus, a function of relative speed $\Delta V_n(t - \tau_n)$

$\varepsilon_n^{cf,g}$: Random error term associated with acceleration g for driver n at time t, ($\varepsilon_n^{cf,g}$)~$N(0, \sigma^{cf,g^2})$

Extending the fifth generation GM' model, the sensitivity component in Ahmed (1999) incorporates the density. Then, it can be written:

$$S[X_n^{cf,g}(t - \xi\tau_n)] = \beta^{cf,g} \frac{[V_n(t)]^{\beta^{cf,g,V}}}{[\Delta d_n(t)]^{\beta^{cf,g,\Delta d}}} k_n(t)^{\beta^{cf,g,k}}$$ (2.28)

Where;

$\beta^{cf,g,k}$: Estimated sensitivity parameter for the traffic density for car-following g

While the driver moves under the free-flow regime, the acceleration formulation was given as follows:

$$a_n^{ff}(t) = \beta^{ff}[V_n^{DS}(t - \tau_n) - V_n(t - \tau_n)] + \varepsilon_n^{ff}$$ (2.29)

Where;

β^{ff} : Estimated parameters of car following under free-flow regime

$V_n^{DS}(t - \tau_n)$: Driver n desired speed

ε_n^{ff} : Random error term of acceleration under free-flow regime

The presumption is that the headway threshold (h^*) is distributed normally that truncated in both sides. Probability of the driver in the car-following is written by:

$P_n(car - following\ at\ time\ t)$

$$P(h_n(t) < h_n^*) = \begin{cases} 1 & h_n \leq h_{max}^* \\ 1 - \dfrac{\Phi\left(\dfrac{h_n(t) - \mu_h}{\sigma_h}\right) - \Phi\left(\dfrac{h_{min}^* - \mu_h}{\sigma_h}\right)}{\Phi\left(\dfrac{h_{max}^* - \mu_h}{\sigma_h}\right) - \Phi\left(\dfrac{h_{min}^* - \mu_h}{\sigma_h}\right)} & if\ h_{min}^* \leq h^* \leq h_{min}^* \\ 0 & Otherwise \end{cases}$$ (2.30)

The distribution function of the acceleration with a conditional of car-following regime and reaction time is given by:

$$f(a_n(t)|h^*, \tau_n) = \left[f\left(a_n^{cf}(t)|h^*, \tau_n\right)\right]\left[f\left(a_n^{ff}(t)|h^*, \tau_n\right)\right] \qquad (2.31)$$

Then, the unconditional likelihood function is formulated as follows:

CF_n

$$= \prod_{n=1}^{N} \int_0^{\tau_{max}} \int_{h_{min}^*}^{h_{max}^*} \left[\prod_{n=1}^{T_n} f\left(a_n^{cf}(t)|h^*, \tau_n\right).f\left(a_n^{ff}(t)|h^*, \tau_n\right)\right][f(h^*)][f(\tau_n)]dh^*d\tau_n \quad (2.32)$$

Both the headway threshold and reaction time distribution are random variables that follow a specific distribution. Those attributes represent the heterogeneity of the variations of individual driver decisions. All parameters in models are estimated jointly using maximum likelihood approach. However, the condition in car-following regime is strictly limited. It fits in a condition where a high proportion of traffic responses appropriately the types of stimulus. Note that the vehicle accelerates if the current lane front vehicle is faster than the subject vehicle, and decelerates if the current lane front vehicle is slower. Actually, the driver in real traffic may act differently towards the respond, for example: giving a priority for merging vehicle or preparing a lane-changing movement. The vehicle will decelerate even though the front vehicle is faster than his/her vehicle.

Toledo (2003) integrated the acceleration model with lane-changing model into a single driving behaviour modelling framework. In this case, the acceleration is the action component located at the lowest level of the decision-making process of the proposed model. The study classifies the acceleration into three different conditions:

- Stay-in-the-lane acceleration: If the driver satisfies with the current lane and does need lane-changing movement.

- Acceleration during lane changing: If the driver requires lane-changing movement towards the target lane.

- Target gap acceleration: This situation appears during the lane-changing process when the lane-changing driver rejects the adjacent gaps and stays at the current lane for seeking the following safest gaps.

By adopting Ahmed (1999) modelling framework and estimation procedure, this modelling framework incorporates the effect of the front vehicle as the stimulus of the car-following behaviour. This study applies two different car-following regimes for each type of conditions by specifying the headway threshold: constrained (if $h_n(t) < h^*$), and unconstrained (if $h_n(t) \geq h^*$). The estimation found that both headway and relative speed (sensitivity components) have significant effect in the driver decision in the target gap acceleration condition including the density as one of significant explanatory variables, to capture the downstream traffic condition effect on car-following behaviour. Meanwhile, the subject vehicle is less significant in deceleration movement.

The acceleration model is relatively more flexible compared to the basic car-following models such as GM's model. It allows various specifications, depending on the objective and traffic characteristics. A massive improvement of acceleration model was presented by Ahmed (1999). His study defines the acceleration behaviour as a respond of stimulus and individual driver sensitivity. The modelling framework classifies the acceleration into two regimes: car-following and free-flow regime based on a specific time threshold. The acceleration in the study is presumed to be the response of stimulus and driver sensitivity. In this case, the driver requires a particular time length to recognise, interpret and make a decision based on the neighbouring traffic condition. This time length is also known as driver reaction time that will be discussed in the following section. Both headway threshold and reaction time represent the heterogeneity of individual driver decision during the observation period as random variable. However, the conditional of acceleration behaviour is strictly limited in capturing the variation of car-following behaviours associated with each stimulus particularly in the car-following regime.

2.3.2 Extended car-following models

Wang's model

By adopting Gipps (1981), Wang et al. (2005b) developed a car-following which incorporates motorway traffic flow characteristic; traffic breakdown, hysteresis and shock wave propagation during the traffic congestion build up. The study focuses on the car-following during the traffic build up (i.e. from uncongested to congested traffic flow). In this case, three car-following regimes: alert (shorter reaction time and higher rate of acceleration and deceleration), close-following and non-alert (if the vehicle speed is higher than 50 km/h). As discussed in Dijker et al. (1998), the modelling algorithm in this study presumes that the shifting driving regime from a non-alert, to alert depends on the individual speeds during the process. This assumption considers

that the driver would be most likely under non-alert state during the traffic build and changing slightly towards the alert states as the congestion appears on the downstream traffic.

The micro simulation demonstrates that the reaction time, acceleration and deceleration behaviour varies with respect to the car-following regimes. Furthermore, the sensitivity analysis the driver reaction time affects the capacity and lane occupancy significantly while speed threshold for classifying the traffic condition in car-following (congested and uncongested) is less significant. However, all the parameters are based on previous research result rather than estimated directly from the observed vehicle trajectory data. The reaction time has totally same value for all individual drivers and traffic condition.

Time-gap based model

Zhang and Kim (2005) proposed a car-following for multiphase vehicular traffic flow. Instead of constant gap-time to the front vehicle, this approach applies a dynamic gap approach that works as gap-distance and traffic phase. Several modelling forms are represented in order to capture various car-following characteristic in different regimes: steady state condition, congested-uncongested traffic, transition region, acceleration-deceleration and free-flow. A simulation demonstrates the ability of the car-following model in capturing the capacity drop and traffic hysteresis. This study disregards the reaction time of individual drive. In fact, a rigorous framework of the parameters estimation is unavailable in this current work.

Tordeux et al. (2010) developed an adaptive time gap car-following model. The study consequently incorporates both time-gap and targeted safety as the component of speed function as part of the car-following model. There are two level of estimations in this model; (1) the target-gap (linear optimisation), and (2) modelling parameters (maximum likelihood). This study reported a significant different car-following characteristic between vehicle types and increased accident risk in correspond to the increased speed. Note that the heavy vehicle requires a larger gap compared to small vehicle. This model incorporates the reaction time as the function of speed between the subject and front vehicle and the number of vehicle in an interaction that is relatively difficult to examine directly from the observed traffic. Furthermore, the analysis of study focuses on gap-acceptance behaviour rather than the characteristics of car-following behaviour itself.

Visual angle car following model

Brackstone et al. (2002) introduced visual angle model which is a physiological or action point type models for the next vehicle decision to determine whether or not the

subject vehicle exceeds a specific angular velocity threshold. This approach considers the width of front vehicle in determining the safe headway between the subject and front vehicles (time to collusion). Similar to Tordeux et al. (2010), the study concentrates in defining the safest gap analysis instead of the car-following characteristics itself.

Al-obaedi and Yousif (2009) developed a car-following model based on visual angular velocity threshold by using the UK traffic characteristics. The threshold velocity is related to function of relative speed between the subject and front vehicles. This model integrates the reaction time as an attribute of visual angle parameter. The reaction decreases as the relative speed increased. Nevertheless, there is no rigorous framework for estimating the reaction time distribution. The study adopts the reaction time model by Hoffmann and Mortimer (1994).

Similar to the previous research, Yousif and Al-Obaedi (2011) implemented this visual angular approach in car-following model that captures two car-following conditions: small-small and small-heavy. This approach extends the acceleration model by incorporating the relative speed, headway and the front vehicle width as a consideration to maintain the safest car-following movement. The study presumes that the vehicle acceleration shall appear when the absolute angular velocity is higher than a particular threshold (negative angular velocity value) while deceleration has a positive angular velocity value. Although a large number of observations (4 million) were utilised in the study, the modelling estimation reports that the required spacing of those two scenarios is relatively similar. In other words, the drivers in the UK are less sensitive with the variation of front vehicle type as they accept similar gap.

Latent class model

Recently, Koutsopoulos and Farah (2012) introduced the latent plan modelling framework in the acceleration behaviour. This study focuses only on the car-following regime. The drivers face discrete situation with various type of choice; acceleration, decelerate and do nothing as a response of stimulus. The decision in acceleration behaviour, therefore, is presented as a probabilistic form and result of a function of explanatory variables (i.e. relative speed, gaps and speed). The acceleration framework, developed by Ahmed (1999), is adopted to represent the acceleration/deceleration mean value of the driver population. NGSim vehicle trajectory dataset is used in the estimation under the maximum likelihood approach. Although the result of proposed model is better than GM model, this model requires to be extended to the acceleration behaviour in other regimes. The modelling is relatively complex and employs a massive work particularly in the model specification.

A rigorous work from GM model in early 1960 has presented several series of car-following models that captured the acceleration and deceleration characteristics. However, this model has a limitation in observing the car-following behaviour in the other regimes (i.e. congested and uncongested, alert and non-alert) as we do believe that they are different. The acceleration/deceleration behaviour is characterised by several factors including the stimulus, sensitivity and reaction time. Various modelling specification have presented the importance of those attributes that can be defined as deterministic value or probability approach. Though, we do believe that individual driver reaction time of individual varies, depending on traffic condition. Following section discusses the driver reaction time.

2.3.3 Driver reaction time

Driver reaction time, by definition, represents a time lag between the appearance of stimulus and the response of the driver including the perception time and foot movement time (O'Flaherty, 1986). Note that this time length varies depending on several factors such as: space headway and visibility to the front object, and the driver preferences.

Gazis et al. (1960) studied the driver reaction time on the non-alerted traffic condition. This study observed the reaction time of 87 drivers when approaching a signalised intersection. In this case, the driver reaction time was a time lag between the appearance of amber light and brake light of the observed vehicle. The study reported that all vehicles have responded the stimulus within 61m (200ft) from the interaction with a reaction time median, mean and standard deviation 1.12, 1.14 and 0.32 sec., respectively.

Table 2.4 summarises the driver reaction time from different experiments. Note that the analysis is based on the real traffic observation. An empirical model of reaction time has yet developed in this study.

Table 2.4 Reaction time from experimental data (Seconds)

Researchers	No. of sample	Median	Mean	Std dev
Gazis et al. (1960)	87	1.12	1.14	0.32
Wortman and Matthias (1983)	837	1.14	1.30	0.6
Chang et al., (1985)	579	1.10	1.30	0.74
Sivak et al. (1982)	1,644	1.07	1.21	0.63

Analysing those previous studies, Taoka (1989) suggested that the distribution of reaction time fits with lognormal distribution due to the imbalance and unsymmetrical of distribution tail. The distribution is skewed to left side considering that a high proportion of traffic prefers short reaction time while less traffic accepts long reaction time. The range of the median is between 1.07 and 1.14 sec while the mean value is between 1.14 and 1.30 sec and the largest value of standard value is 0.74 sec.

Furthermore, Subramanian (1996) defined a driver reaction time as a result of the interaction between several human factors including age, gender, weather condition, weaving section geometry, vehicle characteristics and traffic condition. The reaction time distribution in this study was presumed to follow a lognormal distribution with a specific upper and lower value. This approach is well known as a truncated lognormal distribution. In this case, the driver reaction time distributes between 0 (τ_{min}) and 6 sec (τ_{min}) with the median, mean and standard deviation as 2.19, 2.29 and 1.42 sec respectively. Given the assumption, the driver reaction time distribution can be written as follows:

$$f(\tau_n) = \begin{cases} \dfrac{1}{\Phi\left(\dfrac{ln(\tau_n) - \mu_\tau}{\sigma_\tau}\right)\mu_\tau\sigma_\tau\sqrt{2\pi}} exp^{-\frac{1}{2}\left(\frac{ln(\tau_n)-\mu_\tau}{\sigma_\tau}\right)^2} & if\ \tau_{min} \leq \tau_n \leq \\ 0 & Otherwise \end{cases} \tag{2.33}$$

Where;

μ_τ : Mean of the $ln(\tau_n)$ distribution

σ_τ : Standard deviation of the $ln(\tau_n)$ distribution

Similarly, Ahmed (1999) defined the reaction time distribution as truncated lognormal distribution within 0 and 3 sec. The estimated median, mean and standard deviation of driver reaction are 1.31, 1.34 and 0.31 sec respectively. Meanwhile, Toledo (2003) found the reaction time distribution is between 0 and 6 sec where the mean, median and standard deviation values are 0.85, 1.10 and 1.00 sec respectively. Overall, it is worth noting that the variations of reaction time distribution parameters between those studies depend significantly on several factors including the modelling framework, data collection method and location, and the estimation process. The reaction time of individual driver varies depending on the traffic condition during the observation period. It is a conditional form that explains the heterogeneity of individual driver as regards the acceleration probability function.

2.4 Summary and Limitations of Existing Models

2.4.1 Summary

Weaving section is a unique multilane motorway facility, where two junctions are connected in relatively short distance. The traffic in weaving section is relatively more complex. In fact, two or more traffic streams that move in same direction, have to adjust their lane in relatively short distance without any traffic control assistance. The movement complexity raises the safety issue that shall be included into consideration during the design process.

Since early 1980, a significant number of studies have been performed in analysing the weaving section traffic performance and driving behaviours including the lane-changing and acceleration behaviours. Number of studies have been done and found several critical issues in weaving section performance such as; weaving section geometrics (i.e. weaving length, number of lanes, number of lane-changing), and traffic characteristics (i.e. volume ratio, density, speed). It is worth noting that this approach has limitation in representing the driving characteristic and interaction. Similar to other multilane facilities, the individual vehicle involves in lane changing and car-following movements in order to adjust and move towards their target lane. It is worth to note that an erroneous assumption in modelling framework (i.e. neglecting the impact of surrounding vehicle movement) will extend the modelling complexity. Indeed, this leads to an unrealistic result and interpretation.

2.4.2 Limitations of existing models

A large number of lane-changing and car-following (acceleration) models have been studied. The literature review reveals the strategy and tactic limitations on both existing models that have been discussed as follows:

Lane-changing

Most existing studies focus on the lane-changing issue as an isolated individual action ignores the impact on the surrounding traffic movement. In fact, the vehicle in weaving section has to change lane reasonably in different strategies and tactic in correspond to the front and lead vehicle movement. This issue in lane-changing behaviour, to our best knowledge, has not been explored in the previous studies. Furthermore, the impact of surrounding vehicle movement can be classified into two conditions:

- Impact of the front vehicle in the current lane: The subject vehicle movement is associated with platoon regime if the front vehicle moves towards the surrounding lane.

- Impact of the leading vehicle in the target lane: The subject vehicle movement is associated with weaving regime if he/she shifts the lane with the target lane leading vehicle

The literature review of lane-changing model reveals that decision-making process can be grouped into two levels including the lane-choice and gap acceptance model. The application of latent plan, which is one of discrete-choice model, provides flexibility in capturing the traffic interaction, lane-changing strategies and correlation among the individual decision during the lane-changing process. In that sense, it is acceptable to incorporate the impact of front and lead vehicle movement as an intermediate lane-changing plan. The details of decision-making framework will be presented in Chapter 3.

Acceleration

The existing acceleration model presumes that acceleration behaviour is highly correlated with the relative speed. Please note that the vehicle will accelerate if the front vehicle moves faster than subject vehicle (ΔV^+), and decelerate when the front vehicle is slower than the subject vehicle (ΔV^-). However, this ideal situation does not always occur in the real traffic situation where the traffic faces a disruption from the neighbourhood vehicle and has to prepare a pre-emptive lane-changing movement. Although the relative speed is positive, facing this situation suggests the subject vehicle to decelerate in order to provide a safest gap for the upcoming movement.

This study will consequently omit those limitations on the proposed modelling framework that will be discussed in Chapter 4 and 5. A successful story of implementing those assumptions will broaden the horizon to understand various characteristic, strategy and tactic in correspond with both individual and group lane-changing movement. Moreover, this will assist the transportation authority when designing road geometric and traffic management policies.

Chapter 3 Modelling Framework of Decision Making-Process

This chapter discusses a modelling framework of decision-making process with unobserved or latent component. A large number of studies have been presented in modelling a decision-making process with different approaches and assumptions. A brief discussion on existing models provides a background on extending the latent-plan modelling framework later in this chapter.

This chapter consists of five sections. Firstly, Section 3.1 discusses various approaches in existing planning behaviour models. Then, the following Section 3.2 presents detail information of the proposed latent plan modelling framework, and modelling specification. This proposed modelling framework incorporates the intermediate tactical, which will be the general structure of lane changing behaviour decision-making process in Section 3.3. A comparison with the other discrete choice modelling frameworks presents the advantage of latent plan model as shown in Section 3.4. Meanwhile, Section 3.5 summarises the discussion of the proposed modelling framework.

3.1 Planning Behaviour Models

Explaining the planning behaviour process is a complex task as it is a latent component that is hidden and cannot be captured directly from the observation. It is only the action of the individual, which can be obtained directly from the observation. Ajzen (1991) suggested that the individual behaviour varies depend on traffic condition. This variation on the individual behaviour appears as a result of interaction among several components including the intention to perform a particular behaviour. This complexity provides a great challenge for the researchers to develop analytical tools with different approach i.e. artificial intelligence.

Artificial Intelligence (AI) algorithm concerns in capturing an action of individual (agent) to achieve a particular plan. In general, AI specifies the planning behaviour problem as: current state of particular system, possible action of the system, and observe sequence of actions which transforms the system into a single action. Furthermore, this algorithm can incorporate and assess a plan in the choices set.

Feldman and Sproull (1977) introduced Decision-Theoretic-Planning (DTP) which transforms the decision of individual plan into a numerical utility model. The algorithm captures the trade-off and risk of individual plans rather than guaranteeing an appearance of particular action. This concept relaxes the limitation of classical AI theory. DTP involves as a problem solver tool to find the optimum plan to achieve a specific goal. In this case, the application of utility explores all the possible plans and suggests the plan with the highest utility. However, this study finds difficulty to find an optimum solution for DTP with a large number of plan choices due to estimation complexity. A suggestion on limitation may result on finding less optimal solution. Therefore, estimating an utility of a single plan choice is extremely expensive and time consuming since the number of outcomes is significantly large (Blythe, 1999). Instead of the utility approach, some other studies in artificial intelligence area adopt probabilistic approach (i.e. Shafer, 1987; Horvitz et al., 1988; Smets and Kennes, 1994) and conditional planning (i.e. Bertoli et al., 2006; Son and Baral, 2001).

Markov decision process (MDP) is an optimisation model of discrete-stage with a sequential decision-making process in a stochastic environment (White and White, 1989). The key characteristic of MDP: the current state condition has a significant impact on the transition probability, which captures the evolution of decision-making from the current to the following state. MDP conditional probability consists of two components: state ($\dot{s}$) and action ($\dot{a}$) components. Moreover, Rust (1994) adopted MDP algorithm to define the decision-making process conditional on the set of primitives (U, p, β). In fact, the utility function $U(\dot{s}, \dot{a})$ represents the individual's preference at particular time, $p(\dot{s}'|\dot{s}, \dot{a})$ denotes the transition MDP probability, and $\beta \epsilon (0, 1)$ is a weighted factor of the utility function to represents the individual confidence of the future condition. MDP algorithm has been applied in DTP choice model (i.e. Dean and Givan, 1997; Dean et al., 1993; Dearden and Boutilier, 1997; Precup et al., 1998) by incorporating reward component for individual for choosing a particular state.

Furthermore, Boutilier et al. (2000) applied dynamic programming to solve a DTP problem with a large number state spaces in a MDP framework. Note that the increased of state spaces grow exponentially in corresponds with the availability of plans. This research adopts the dynamic Bayesian network to proof the potential independence of

action's effect, regularities of an action in various states, and effect of reward component on the decision-making process.

Rabiner and Juang (1986) introduced Hidden Markov Model (HMM), which is a stochastic process with partially unobservable (latent) component. Moreover, the latent component can be captured through the other set of stochastic process with a sequence of observed symbols. A simple explanation of HMM is a coin toss; the observer, who has to close his/her eyes, flips a coin into the air and opens his/her eyes once the coin fall into the ground. The observer in this case does not know the process of the coin toss (i.e. how many does the coin flip), he/she knows only the outcome whether face or tail. Moreover, it is necessary in HMM to define a finite number of states, time step, probability distribution and the latent component, which are the challenge for the modellers. A large number of studies in different area applied HMM algorithm such as: speech recognition (i.e. Rabiner, 1989; Zhang and Levinson, 2004), food science (Eddy, 1996), and graphology (Yang et al., 1995). However, there is a limitation in capturing individual behaviour and choice in decision-making process as HMM focuses on a process without any involvement of choice modelling.

Overall, analysis of planning behaviour is a complex task due to the involvement of several hidden components, which affect the individual decision or response. A variation of the individual decision increases the complexity as well. The application of Markovian algorithm in the planning behaviour modelling relaxes those limitations. Although a large number of studies in planning behaviour adopt the algorithm in different assumption and approach, it has less focus on decision-making process aspect and ability to capture the variation of choice among the individual. However, The pieces of literature in Markov decision process provide a basic idea to perform the driving behaviour modelling, which will be presented in the following section.

3.2 Latent Plan Models

Choudhury (2007) presented a rigorous work on the latent plan modelling framework, in driving behaviour research area. The individual choice in this framework is made under discrete condition. Briefly, Discrete choice model, by definition, is the probability of individuals choosing a given option is a function of their socioeconomic characteristics and the relative attractiveness of the option. The basic assumption of the discrete choice model is each individual faces same set alternatives. However, they pick only one set of alternatives that give them the highest utility (Ortúzar and Willumsen, 2007; Train, 2009). The properties of discrete choice model are presented in Appendix-

B The general framework of latent plan model consist of two-levels: targeted plan and action. The plan choice in this framework is unobserved (latent) component. Meanwhile, the action is observed component, which reflects the plan choice at that time. The individual choices vary over a sequence of observations with a time step t' sec (i.e. 1sec).
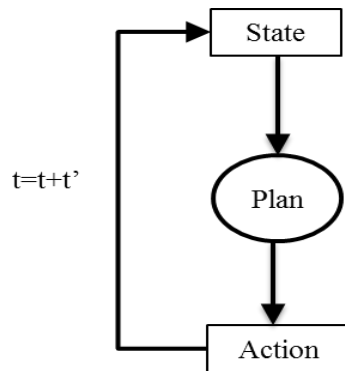
Figure 3.1 General framework of decision-making process

As discussed in Choudhury (2007), and Choudhury et al. (2010), the following list describes the latent plan model main features:

- Individuals choose among a particular plans (tactical/strategy). The choice subsequent relates with the preferred strategy or tactical. The modelling framework presumes the individual plan is latent while both intermediate strategy and the final action are observed.

- Both the plan and action choices are conditional on the preferred plan that fits with the utility maximisation theory. In this case, the correlation of each action represents the interdependencies of successive decisions.

- The individual choice depends on his/her preference for the available plan. Therefore, the utility of each individual varies in corresponding with the number of observation and the size of the choice set.

- The observable component of utility function captures the individual behaviour attributes while the heterogeneity is unobserved and varies among observed variable.

- The current plan in latent plan framework anticipates the future condition and may incorporate expected maximum utility (EMU) which captures the correlation of the decision among the chosen plan.

3.3 Latent Plan Modelling Framework

This PhD thesis extends the general latent plan modelling framework, which was developed by Choudhury (2007). The proposed latent plan modelling framework in this thesis incorporates the intermediate plan m as part of the action of individual n at time t with respect to the previous chosen plans, intermediate strategies and actions. This intuitive is significant issues on planning behaviour model as each individual may execute a plan in different strategies or plan Thus, the proposed latent plan models can be presented as shown in **Figure 3.2**.
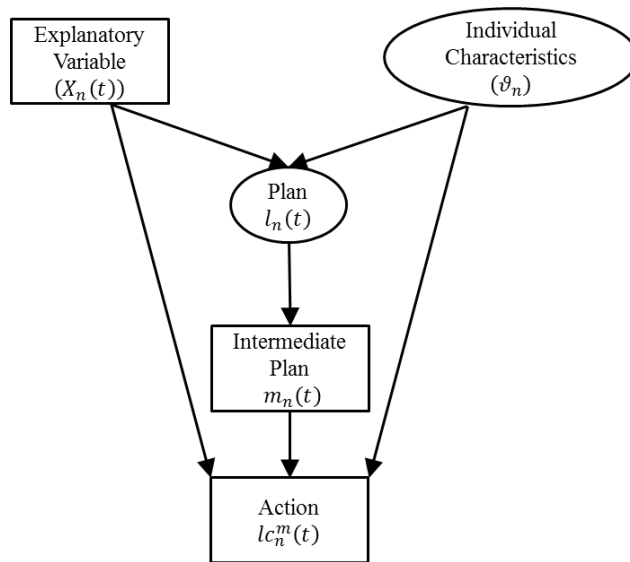
Figure 3.2 The Proposed latent plan modelling framework with intermediate plan

This extended latent plan framework represents the two level of the decision-making process: plan and action. The individual plan $(l_n(t))$ is latent while the decision in the action $(lc_n^m(t))$ conditional on the intermediate plan m is observable component from the dataset (i.e. trajectory data). It is worth noting that the individual plan $(l_n(t))$ and action plan $(lc_n(t))$ refer to the general latent plan modelling framework as discussed in Choudhury (2007). Meanwhile, the proposed latent plan modelling in this PhD thesis introduces the intermediate plan (m), which changes the lane plan modelling structure as shown in **Figure 3.2**.

Furthermore, both of individual n plan and action at any time t are significantly affected by the explanatory variables $(X_n(t))$ and individual-specific constant (ϑ_n). The explanatory variables $(X_n(t))$ are an observed component. In fact, the individual-specific constant (ϑ_n) captures the individual characteristics, which are latent and independent over time periods.

Figure 3.3 presents the proposed latent plan modelling framework which incorporates the intermediate plan. Similar with the general framework, the proposed framework consists of two decision levels: plan choice, and action conditional on the initial and intermediate plans. The available plan choices (l) in the upper level of modelling framework are the latent component. The selection of plan choice affects the intermediate plan and action in lower level of the structure. In that case, the variation of the individual choice set and corresponding utility depends significantly on the selected plan.
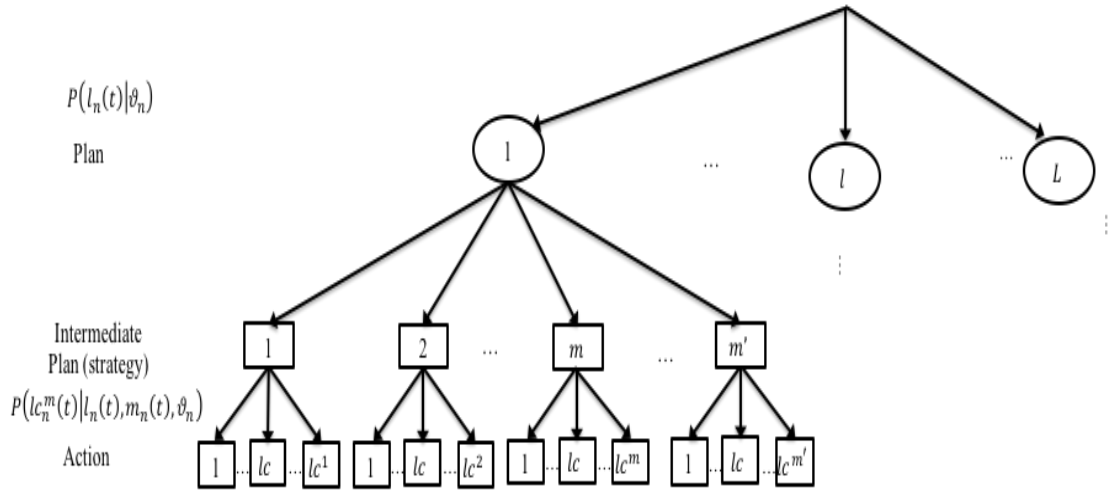
Figure 3.3 The proposed choice plan modelling framework

For example, the application of choice plan model in lane-changing movement classifies the decision-making process into two levels: target lane choice behaviour (plan) and gap acceptance (action) with conditional on lane-changing strategy. The individual n has to choose the available lane choice set while the action will take place directly after the individual agrees to the plan and strategy and if the gap at target lane is acceptable. Otherwise, the driver maintains at the current lane. The target lane choice is latent since it cannot be captured directly from the observation. It is only the lane-changing movement that can be observed. In the real traffic, the individuals have different preference on lane-changing strategy/tactical whether moving individually or as a group (i.e. platoon or weaving) though they move in the same plan and action. This strategy/tactical, which is observed together with the movement, is part of the intermediate plan of the lane-changing movement.

Several explanatory variables $\left(X_n(t)\right)$ explain the lane-changing behaviour such as lane attributes (i.e. average speed, density, distance), vehicle attributes (i.e. type of vehicle, speed) and available gaps at target lane. Meanwhile, the driving characteristics (ϑ_n) represent the driver aggressiveness, driver's knowledge of the particular path. This

attribute is latent which remain constant for the individual n. The extended latent plan model in lane-changing movement will be discussed more details in Chapter 4.

3.3.1 Probability of observed trajectory

The application of trajectory data captures series of all individual movement during over a particular path and time period with conditional on the previous plan and action, which is based on the proposed latent plan framework in **Figure 3.3**.
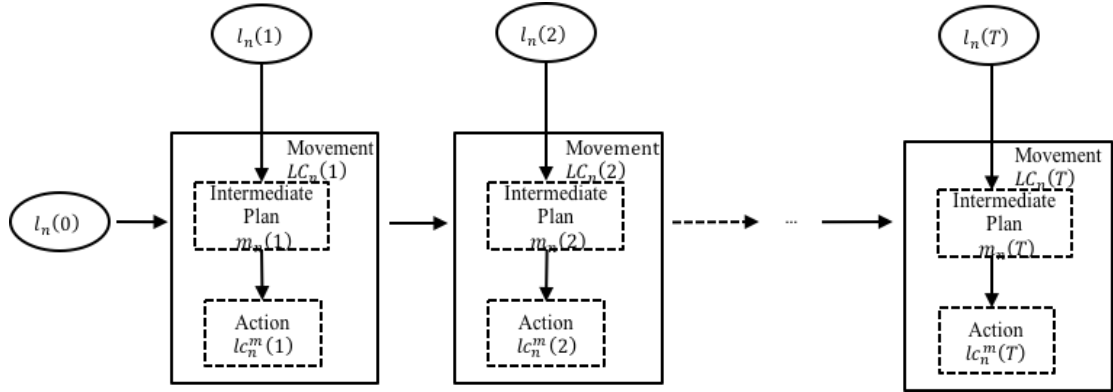
Figure 3.4 The development of individual n decision-making process in a latent-plan modelling framework.

Figure 3.4 illustrates the evolution of the individual n decision making process over the observation period. The upper level in the figure represents the advancement of the individual n plan starts from time t=0 $\left(l_n(0)\right)$ to the last plan at time T $\left(l_n(T)\right)$. Meanwhile, the individual n observed action in the lower level is affected by the chosen plan l at the same time period. It is worth noting that the action of individual n is conditional on a particular intermediate plan m and the movement lc itself.

Therefore, the probability of individual n of specific movement LC is a sum of all probabilities of the observed possible plans l for executing action lc conditional on intermediate strategy m with intermediate strategy/tactical m at particular time t. Then, the probability of movement can be written as follows:

$$P(LC_n(t)|\vartheta_n) = \sum_{l \in L} \sum_m [P(l_n(t)|\vartheta_n)][P(lc_n^m(t)|l_n(t), m_n(t), \vartheta_n)] \qquad (3.1)$$

Where;

$P(LC_n(t)|\vartheta_n)$: Probability of individual n of choosing movement LC at time t with conditional on driver characteristics ϑ

$P(l_n(t)|\vartheta_n)$: Probability of individual n for choosing plan l at time t with conditional on individual characteristics ϑ

$P(lc_n^m(t)|l_n(t), m_n(t), \vartheta_n)$: Probability for individual n of choosing m lc at time t with conditional on intermediate plan m and individual characteristics ϑ

L_n : Number of choice set of individual n

m_n : Intermediate plan choice set of individual n

T_n : Number of observed time period of individual n

Presuming the individual n plans, and actions are independent over a particular period. The joint probability of individual n involves in a decision-making process of the proposed latent plan modelling framework is given by:

$$P(LC_n(1), LC_n(2), \ldots, LC_n(T)|\vartheta_n)$$

$$= \prod_{n=1}^{T_n} \sum_l \sum_m [P(l_n(t)|\vartheta_n)][P(lc_n(t)|l_n(t), m_n(t), \vartheta_n)] \tag{3.2}$$

Note that the sequence length in Equation 3.2 is total length T of the observation for the individual n when executes action LC at time t. Therefore, the joint probability function of individual n is a product of summation of probabilities for choosing particular plan, and action. The probability of choosing specific plan is conditional on individual characteristics while the probability of choosing specific action is conditional on plan choice l, intermediate plan m and individual characteristics ϑ. Giving the description, the unconditional probabilities of a sequence of decision of the individual can be expressed by:

$$P\big(LC_n(1), LC_n(2), \ldots, LC_n(T)\big)$$

$$= \int_v [P(LC_n(1), LC_n(2), \ldots, LC_n(T)|\vartheta_n)]\ f(\vartheta_n)\ dv \tag{3.3}$$

Where;

$f(\vartheta_n)$: A distribution of individual-specific random term

3.3.2 Latent plan modelling specification

The probability of individual plan and action of the proposed latent plan modelling framework are estimated based on the utility maximisation approach. This estimation algorithm is used in the previous research i.e. Choudhury (2007), Choudhury et al. (2010), and Choudhury and Ben-Akiva (2013) . More detail of modelling specification will be discussed below.

Plan choice

This research assesses the plan choice based on the utility maximisation and may incorporate the EMU (Expected Maximum Utility). The utility of latent plan choice consists of three components including the explanatory variables, individual-specific, and a random error term. Assuming that the individual n choose a plan, which provides the highest utility in corresponds with his/her preferences. The utility of individual n of determining plan l at time t is written by:

$$U_n^l(t) = U\left(X_n^l(t), I_n^l(t), \vartheta_n, \varepsilon_n^l(t)\right)$$

$$I_n^l(t) = E\left(max\left(U_n^{l,1,m}(t), U_n^{l,2,m}(t), \ldots, U_n^{l,lc,m}(t), \ldots, U_n^{l,lc,m}(T)\right)\right) \qquad (3.4)$$

Where;

$U_n^l(t)$: Utility of plan l of individual n at specific time t

$X_n^l(t)$: Attributes of individual n plan l at time t

$I_n^l(t)$: EMU of individual n action associated with plan l at time t

$U_n^{l,lc,m}(t)$: Utility of action lc with intermediate plan m in corresponds with particular plan l at time t

ϑ_n : Individual-specific random effect

$\varepsilon_n^l(t)$: Random utility component associated with the plan l for individual n at time t

Action choice

As discussed earlier, the individual n action choice sets depend on the driver decision on the plan (upper level) and the observed intermediate plan. The utility of action choice set varies associated with the availability of choice sets for the selecting plan. The individual n chooses the action choice with highest utility value. The action choice utility can be derived as follows:

$$U_n^{l,lc,m}(t) = U\left(X_n^{l,lc,m}(t), \vartheta_n, \varepsilon_n^{l,lc,m}(t)\right) \tag{3.5}$$

Where;

$X_n^{l,lc,m}(t)$: Attributes of individual n plan l and action lc with intermediate m at time t

ϑ_n : Individual-specific random effect

$\varepsilon_n^{l,lc,m}(t)$: Random utility component associated with the plan l, action lc and intermediate plan m for individual n at time t.

In this case, the conditional probabilities of individual n for choosing plan l $\left(P(l_n(t)|\vartheta_n)\right)$ and action lc with intermediate plan m $\left(P(lc_n^m(t)|l_n(t), m_n(t), \vartheta_n)\right)$ are based on both utilities of plan choice $\left(U_n^l(t)\right)$ and action choice respectively $\left(U_n^{l,lc,m}(t)\right)$. The probability specification itself is subject to the assumption of the random error terms distribution. Meanwhile, the current study presumes the distribution of both random terms as IID (Independently, Identically, extreme value Distributed). This assumption leads the proposed choice model as logit model.

3.4 A comparison of latent plan with other discrete choice models

The general framework of latent plan model has similarity structure hierarchical nested logit (HL) model, which was developed by McFadden (1978). This algorithm is one of the discrete choice models, which allows a correlation among the group of the choice set. Vovsha and Bekhor (1998) introduced a cross-nested logit (CNL) model. This approach is a generalisation of two levels hierarchical logit with a correlation of among the choice set with a different degree of the choice set. The Recent development of CNL choice probabilities was performed by Papola (2004) .
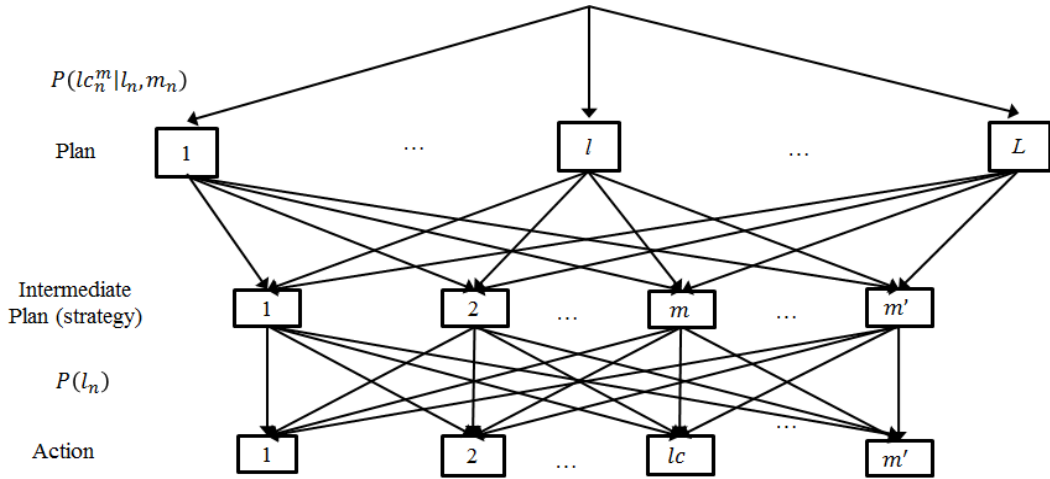
Figure 3.5 Cross-nested logit (CNL) logit model with intermediate plan

The probability of individual for choosing an action at the lower level of given CNL framework is written as follows:

$$P(LC_n) = \sum_{l=1}^{L} [P(l_n)][P(lc_n^m | l_n, m_n)] \qquad (3.6)$$

Where;

$P(l_n)$: Probability of individual n for choosing plan l

$P(lc_n^m | l_n, m_n)$: Probability of individual n for choosing plan l conditional on plan choice l and intermediate plan choice m.

$P(LC_n)$: Probability of individual n for choosing movement LC associated with intermediate plan m and action lc

L : Number of available choice set of individual n

m' : Number of available intermediate plan choice set of individual n

The probability of choosing a particular movement LC of individual n in CNL is the summation of all joint probabilities of the action choice over both available plans and intermediate plans (tactical). Note that the utility of lower level in CNL is independent from the upper level. Therefore, the utility of the action lc associated with intermediate plan m at lower level for plan l can be formulated as follows:

$$U_n^{LC,l} = U\left(X_n^{lc,m}, X_n, \varepsilon_n^{l,lc,m}\right) \qquad (3.7)$$

Where;

$X_n^{lc,m}$: Vector of individual n attributes associated with action lc with intermediate m

X_n : Vector of explanatory variables associated with individual n

$\varepsilon_n^{l,lc,m}$: Random error term component

Given the utility component, the action choice of individual n in CNL neglects the impact of the plan choice at an upper level. A large number of choices in CNL framework raise an estimation issue as the complexity is increased. In this case, all the choices in CNL are observable factors. This assumption is less, where some part of decision-making process in driving behaviour model is latent (i.e. individual characteristic). In comparison, the discussion of the hidden plan earlier implies that the ability of latent plan model relaxes those issues of CNL.

The recent development of latent class model (LCM) has similarity with the latent plan model. The LCM presumes that individual behaviour depends on the observed attributes and individual characteristics, which varies among the latent attributes (Greene and Hensher, 2003). It is worth noting that the number of observation and choice set for all individual may vary for each individual. Therefore, the LCM is written by:

$$P(LC_n) = \sum_{l=1}^{L} [P(l_n)][P(lc_n^m | l_n, m_n)] \tag{3.8}$$

Where;

$P(l_n)$: Probability of individual n for choosing class plan l

$P(lc_n^m | l_n, m_n)$: Probability of individual n for choosing specific-choice lc conditional on class-plan l and class-intermediate plan m.

L : Number of classes

The heterogeneity in tastes across individual varies among the available classes (Hess and Ben-Akiva, 2011). The utility of particular class choice, therefore, can be expressed as follows:

$$U_n^{l,LC} = U\left(l, X_n^{lc,m}, X_n, \varepsilon_n^{l,lc,m}\right) \tag{3.9}$$

Where;

$X_n^{lc,m}$: Vector of attributes of action lc conditional on intermediate m

X_n : Vector of attributes of individual n

In addition, the class-plan in LCM is affected only by the individual characteristics. This assumption leads the utility of class-plan to be written as follows:

$$U_n^l = U(X_n, \varepsilon_n^l) \tag{3.10}$$

However, the LCM has the limitation in permitting different restriction of specification both in the models and class specific choices probabilities. The specification of classes in LCM is strictly observed from the dataset. This situation gives difficulty the LCM to cope with the situation changes during the observation. In contrast, the latent plan model relaxes that limitation as the framework provides flexibility in capturing the unobserved component, which may change time by time.

3.5 Summary

This section presents the proposed latent plan modelling framework, which extends the general latent plan modelling framework by incorporating the intermediate plan. It is worth noting that all individuals in this framework involve in two levels of decision-making process: plan choice (upper level), and action choice (lower level). Introducing an intermediate plan in this study provides an opportunity to capture various strategies or tactical of individual when executing an action. The action choice at any instance depends on the plan choice and the intermediate plan at the same time. In this case, the plan choice is unobserved/latent while the intermediate plan and action are observed. The plan choice of individual is affected by plan attributes and individual-specific component, which is independent for a subsequent of plan choice. The individuals choose a plan with the highest utility value.

The latent plan has the similar framework with two discrete choice models, which are cross-nested logit model and latent class model. However, those approaches have various limitations in capturing the individual behaviour such as flexibility in dealing with changes, the large number of choices, and hidden component (i.e. individual characteristics). The appearance of latent plan relaxes those limitations and provides better interpretation of the decision-making process especially in driving behaviour research area where some of the components are latent.

Chapter 4   Lane Changing Model

This chapter discusses the lane changing modelling framework in weaving section which is part of multilane motorway facility. The lane changing process consists of two phases; (1) target lane choice, (2) gap acceptance. The target lane choice modelling structure allows flexibility depend on both geometric configuration (i.e. number of lane changing required, the existence of special lane, and length of the section) and traffic attributes (i.e. speed, and density). Meanwhile, the current study extends the state-of-the-art lane-changing model by introducing a different type of lane changing mechanisms (individual, platoon and weaving) as part of the gap acceptance model. The proposed lane-changing model is based on a moderate traffic flow.

The rest of this section is systematised as follows: Section 4.1 provides the background of the lane-changing model. A brief discussion on a potential lane changing mechanisms in weaving section is presented in Section 4.2. Section 4.3 will discuss the proposed lane changing modelling framework which includes both the target lane and gap acceptance model with respect to the type of lane changing mechanisms. Furthermore, this section discusses briefly the modelling attributes (such traffic, surrounding vehicle attribute and path-plan). Furthermore, the likelihood function of the proposed model is presented in Section 4.4 Note that both the target lane and gap acceptance model are estimated jointly. Section 4.5 summarises the discussion on the lane-changing modelling framework.

4.1 Background

Lane-changing (LC) behaviour is complex since two opposing directions of lane changes occur simultaneously in such traffic streams particularly. In the weaving section, lane changing is significant factors in characterising the operational of weaving section as the traffic involves a complex interaction at a particular short length of road section (Skabardonis, 2002). DMRB (2006) recommended that the distance of weaving

section is between 2,000m – 3,000m. The lane change traffic occurs while the through drivers make frequent overtaking manoeuvres as well to pass merging or diverging vehicles (which tend to be slower) or make pre-emptive lane changes to help an incoming driver to merge with the mainstream traffic.

The lane changing intensity, of the merging (and diverging) traffic crossing to join the mainline carriageway (and to the exit lane, respectively), presents special operational problems, congestion and incident (HCM, 2010; Jin, 2010; Liu and Hyman, 2012; Toledo and Katz, 2009). This behaviour in weaving section creates common points of bottleneck particularly in the upstream traffic due to a high proportion of lane-changing movement occurs in this area (i.e. Al-Jameel, 2013; Bham, 2006; Skabardonis and Kim, 2010; Wang et al., 1993).

Similar with other multilane facilities, the driver in weaving section performs a lane changing in order to perceive better driving environment (i.e. overtaking, merging and diverging). It is worth noting that the lane changing movement is a result of two level decision-making processes:

1) Target lane choice (plan): the decision in this level is latent that avoids direct observation from the examination (i.e. traffic video recording)

2) Gap acceptance and lane change execution (action): this is an observable decision making process that provides gap acceptance information in the target lane direction.

Moreover, the target lane choice implies the vehicle lane-changing direction with respect to the subject vehicle current lane. The driver has to accept both gaps at the adjacent lane correspond with the lane changing direction. In fact, it is unlikely that lane change is executed at the first attempt. The driver might observe and reject several gaps before turning his/her lane rather than accepting the first available gaps (lead and lag). In the weaving section, it is common that some of proportion lane changing driver perceives a pressure to move in a group movement including platoon or weaving due to a limitation of section length. The pressure is increased with the remaining distance toward the exit of weaving section.

Driving rules and speed limit, which varies among countries, affects significantly the motorway lane utilisation. In the UK motorway networks, highway agency defines the speed limit for the small vehicle as 110 km/h (70 mi/h) while HGV speed limit is 100 km/h (60 mi/h). The vehicle tends to change lane when there is a perceived need such as improving the speed and overtaking the front vehicle. Yousif et al. (2013) analysed

the lane distribution at a particular UK motorway section within 1,000m from the merge and diverge area by utilising Motorway Incident Detection and Automatic Signalling (MIDAS). The study developed a regression function and found that most of traffic (60%) concentrates moving on the lower speed lanes (kerbside lanes) under a free-flow (uncongested) traffic condition. Furthermore, this study reported that the appearance of HGV in slow lane affects the lane distribution significantly especially during the congested traffic conditions.

A substantial development on lane-changing modelling framework during the last decades provides flexibility in capturing lane-changing characteristics in various traffic scenarios and tactics. However, most of lane-changing models focus on the isolated/solo lane-changing movement (i.e. Toledo et al., 2005; Choudhury, 2007) and ignore the impact of group behaviour in their modelling structures. Disregarding the impact of the neighbouring traffic in modelling framework can lead to unrealistic traffic characteristics, especially in weaving sections where there is a significant presence of group behaviours and the effects of lane changing mechanisms are more dominant. The current study addresses this research gap, extending the state-of-the-art random utility-based models and explicitly captures the lane changing mechanisms depending on the the lead/front vehicle movement.

4.2 Lane Changing Mechanisms in Weaving Section

Weaving sections are subjected to a complex of lane-changing movements. Contrary to basic motorway sections, where a driver selects a target lane and finds a suitable gap to change lanes, in weaving sections, drivers' choices can be significantly affected by the actions of the neighbouring drivers. For instance, if the leader vehicle is changing lanes in the same direction, the subject driver may be inclined to move as a platoon and accept smaller lead gaps to complete the lane change manoeuvre. Similarly, the acceptable gaps may be different if there is a weaving manoeuvre as opposed to an isolated lane change. The current research extends the state-of-the-art lane changing models by explicitly incorporating the type of lane change (individual/solo, platoon and weaving) in the modelling framework.

HCM (2000) defines the platoon as a group of vehicles from the same traffic stream travelling together. Meanwhile, weaving is the crossing of two or more traffic streams in same traffic direction in a particular road length without any assistance of traffic control devices. The front vehicle in the current lane in the same traffic stream with the subject vehicle is termed as the front vehicle. While the target lane lead vehicle is termed

as the lead vehicle. **Figure 4.1** illustrates variations of lane changing mechanisms in a five lane weaving section namely solo, platoon and weaving lane changing mechanisms.

(a) Solo
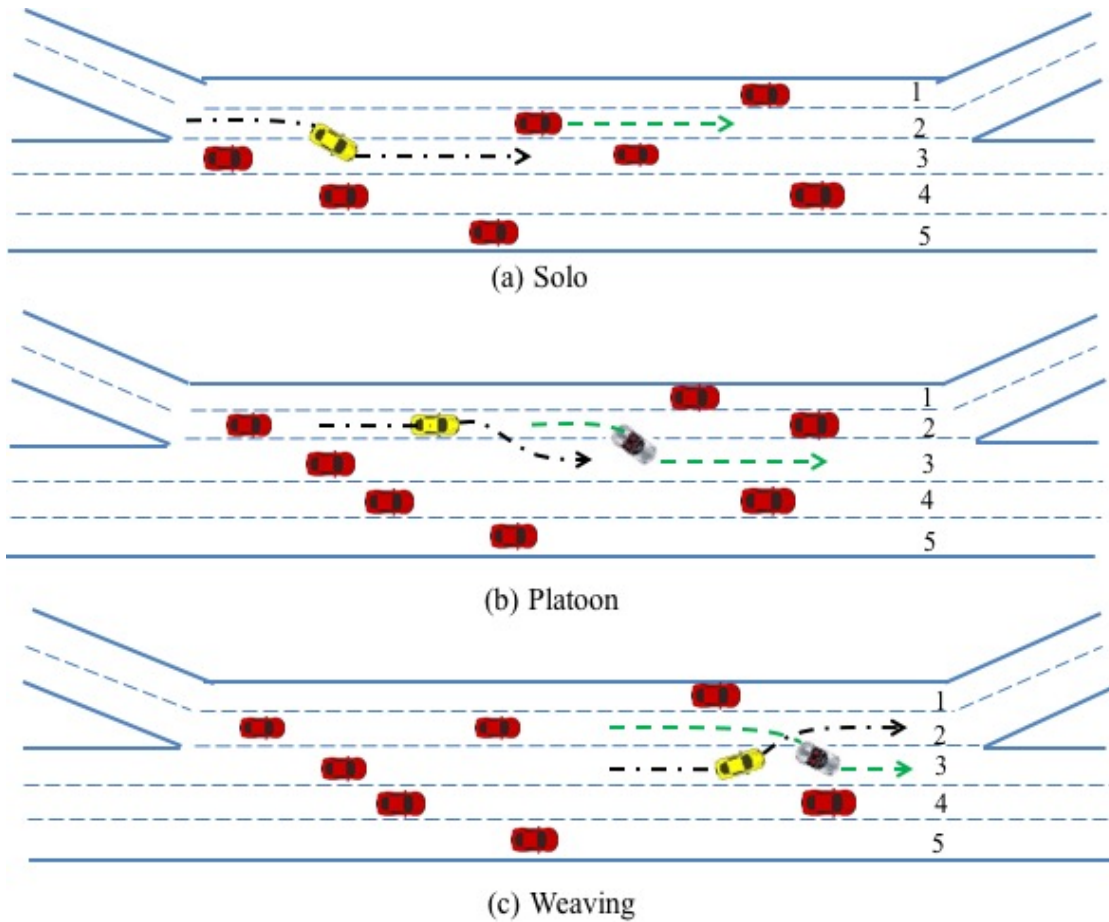
(b) Platoon

(c) Weaving

Figure 4.1 Schematic diagram of lane-changing mechanisms

4.2.1 Solo lane changing mechanism

Solo (s) lane changing involves no group behaviour (i.e. no platoon or weaving lane-changing manoeuvres) (see **Figure 4.1** a). The lane-changing vehicle moves individually toward the target lane while the front and lead vehicle maintain at their lane. This type of mechanism has relatively less complexity compared to the other two lane change mechanisms. In fact, the subject vehicle moves individually while both target lane lead and current lane front vehicles maintain to drive at their lane.

4.2.2 Platoon lane changing mechanism

Platoon (p) lane changing is a situation whereby the subject and the preceding vehicle from the same traffic stream change lanes together one after another. As shown in **Figure 4.1** (b), the subject vehicle at lane 2 moves together with the front vehicle towards lane 3 in order to merge with the main traffic. In this case, the complexity of

platoon lane change movement is less compared to solo lane-changing mechanism. Instead of triggering an interaction with target lane traffic, the subject vehicle in this mechanism follows the front vehicle movement in safely manner. This movement, therefore, perceives less impact on driver aggressiveness.

4.2.3   Weaving lane changing mechanism

Weaving (w) lane changing occurs if the subject vehicle and a lead vehicle from traffic stream on the left/right, cross each other at the same period. In other words, the subject vehicle and the adjacent vehicle swap their lanes to follow their preferred path. The adjacent vehicle initiating the weaving is termed as *lead vehicle* in this thesis. **Figure 4.1** (c) illustrates an example of lane changing with weaving mechanisms. Both subject vehicle at lane 3 and lead vehicle at lane 2 swap their lane between each other. Indeed, weaving lane change mechanism is more difficult and requires higher level of driver aggressiveness corresponding with the movement complexity compared to the platoon movement. In addition, the vehicle has to adjust their lane without assistance of traffic control device in relatively short period of time to avoid a delay in the downstream traffic.

The three different lane changing mechanisms yield differing sensitivities towards the positions and speeds of the front/lead vehicles in the current and target lanes and lead to variations in the acceptable gaps for the lane change. It may be noted that, in very congested conditions, drivers in the mainline often slow down to assist the vehicles entering/exiting from/to the ramps. This research deals with driving behaviour in moderately congested situations and hence the cooperative merging is beyond the scope of the research.

4.3 Lane Changing Modelling Framework

This section discusses the structure of the lane-changing model by incorporating different types of lane changing mechanism. A wide range of factors affect the lane-changing decision i.e. speed, lane occupancy, relative speed, travelling time at the current lane, number of lane-changing required, and the involvement of front/lead vehicle type of movement.

The proposed model structure is thus an extension of the freeway lane changing model proposed by Toledo et al. (2005) where the decision framework consists of choices of target lanes and gap acceptance but there is no explicit consideration of the lane changing mechanisms.

Given the choices of the target lanes and the lane changing mechanisms, the subject driver will accept/reject the available gaps. The acceptable gap can vary depending on the lane changing mechanisms. The acceptable gap is, however, (latent) unobserved in the data and only the final decision of the driver (Change Left, Change Right or No Change) is observed. The observed plans/decisions are shown in rectangles and the unobserved (latent) ones are shown in ovals in Figure 4.2.
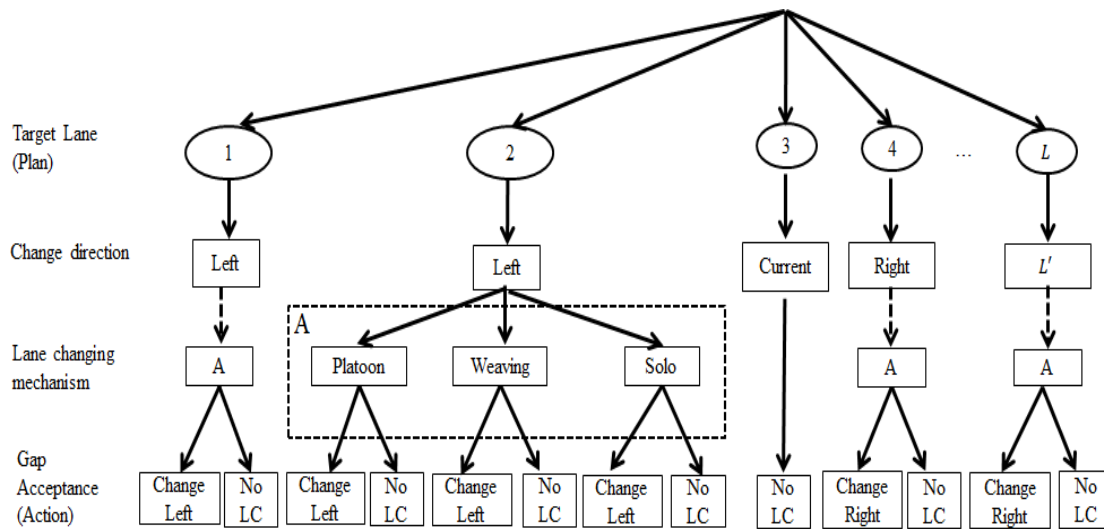
Figure 4.2 An example of the lane-changing framework for individual driver n in lane 3 of a 5-lane weaving section

An example of lane changing structure for a subject driver in lane 3 is shown in **Figure 4.2**. The driver first selects a target lane, which is the most preferred lane considering the traffic conditions and his/her path plan. The choice of the target lane indicates the preferred direction of lane change. For example, for a subject driver in lane 3 (as shown in **Figure 4.2**), lanes 2 and 1 are at the left hand side and lanes 4 and 5 are on the right hand side. If the target lane is the same as the current lane, the lane changing is not required (the observed action is 'No LC'). If the target lane is 1 or 2, the driver looks for suitable gaps on the left. If the target lane is lane 4 or 5, the driver seeks suitable gaps on the right. A lane change is observed when the driver finds an acceptable gap in the desired direction and moves to that lane. Otherwise, he/she stays in the current lane. It may be noted that the choice of target lane is unobserved in the trajectory data since the driver may or may not be successful in moving to the target lane.

The driver seeks for suitable gaps in the adjacent lane in the direction of the target lane and executes a lane change if he/she finds an acceptable gap. The acceptable gap can be different depending on the lane-changing mechanism (namely: solo, platoon or weaving). The observed actions of the front vehicle and lead vehicle in the current and

target lanes respectively (see **Figure 4.2**) define the selected lane-changing mechanism. If the front vehicle is also changing lanes in the same direction, the subject driver has the option to execute (or not execute) a platoon lane change; whereas if the front vehicle in the current lane is not changing lanes in the same direction but an adjacent vehicle in the target lane is making a change to the current lane, the subject driver has the option to execute (or not execute) a weaving lane change. The lane-changing mechanism is therefore observed in the data.

The different lane-changing mechanisms yield differing sensitivities towards the positions and speeds of the front/lead vehicles in the current and target lanes and lead to variations in the acceptable gaps (lead and lag) for the lane changing. It may be noted that, in very congested conditions, the drivers in the mainline often cooperate with the vehicles entering/exiting from/to the ramps. This research, however, deals with driving behaviour in moderately congested situations and hence the cooperative merging is beyond the scope of the research

The next section will discuss the detailed specification of both levels of decision-making process in the lane-changing model: (1) target lane model and (2) gap acceptance model.

4.3.1   Target lane modelling

The previous discussion demonstrates that the driver prefers the lane with highest utility value. In the proposed lane changing model, this study adopts the target lane choice model which was proposed by Toledo (2003). Presuming that all the observed drivers have same set of available lanes over the road stretch, the utility function of the driver n for choosing lane l at specific time (t) is written as follows:

$$U_n^l(t) = \widehat{U}_n^l(t) + \varepsilon_n^l(t) \tag{4.1}$$

Where:

$U_n^l(t)$: Target lane l of driver n at time t

$\widehat{U}_n^l(t)$: Systematic part of the utility of target lane l of driver n at time t

$\varepsilon_n^l(t)$: Random term associated with the utility of the target lane l of driver n at time t

The target lane choice is implied on the subject driver's preference for moving to the specific lane. The driver has to decide either to stay at the current lane or change the lane with respect to perceived better driving environment. In terms of the target lane

model, the lane changing decision is represented as a target lane utility function. Note that the driver prefers moving toward the target lane that provides the highest utility value compared to all set of available lanes. Moreover, several attributes may affect the systematic part of target lane utility $\left(\widehat{U}_n^l\right)$:

- Traffic attributes

  Several factors can be included as traffic attributes i.e. traffic density, speed, average lane speed, etc. In this case, the traffic tends to move towards a lane with less traffic to avoid delays or travel at higher speed. An increased of lane traffic density affects the target lane utility negatively. While both speed and lane average have a positive impact on the target lane utility.

- Vehicles attributes

  This attribute captures both vehicle characteristics and interaction with neighbouring traffic, which affects the target lane utility i.e. speed, gap/headway, relative speed between the subject and neighbouring traffic, and type of vehicle. Facing a slow moving front vehicle triggers the subject vehicle for changing lane to move at the desired speed and perform the overtaking manoeuvre. Also, the interaction between the neighbourhood vehicle and subject vehicle can be represented as relative speed as well.

  Many cases demonstrate that small subject vehicles tend to avoid tailgating with heavy vehicles as front vehicle due to a safety issue. Heavy vehicles tend to move slower and obscure the subject vehicle capturing the downstream traffic condition. This situation results in a negative impact on the target lane utility function.

- Path-plan

  This attribute represents the chosen path of the driver in order to arrive at the desired target lane. The path plan in the current research consists of two components: (1) remaining distance of the subject vehicle towards the mandatory lane changing, (2) number of lane change required from the current lane through the desired target lane. In this case, the target lane utility decreased significantly if the driver requires a large number of lane change while he/she reaches the end point of a mandatory lane change.

- Driver characteristics

  The driver characteristics (e.g. age, experiences, stress level, aggressiveness, etc.) have a significant impact on the lane changing behaviour. The current study considers the driver characteristics due to the relative target lane location from the current lane (left or right). The driver characteristics are however generally latent in the video recordings and represented by statistical distributions (i.e. Choudhury, 2007; Toledo et al., 2005)

Incorporating the attributes into the target lane utility of choosing target lane l of driver n at time t can therefore be written as follows:

$$U_n^l(t) = \beta^l X_n^l(t) + \alpha^l \vartheta_n + \varepsilon_n^l(t) \qquad l \in \{1, 2, 3, \ldots, L\} \qquad (4.2)$$

Where;

$X_n^l(t)$: Vector of explanatory variables associaed with driver n for lane l at time t

β^l : Vector of estimated parameters associated with target lane l

ϑ_n : Individual specific random error term to account for unobserved driver characteristics, assumed to follow normal distribution $\vartheta_n \sim N(0,1)$

α^l : Estimated parameters of individual specific random term ϑ_n for lane l

$\varepsilon_n^l(t)$: Random error term associated with target lane l of driver n at time t

L : Total number of available lanes in the section

The choice modelling presumes the random error term ε_n^l is independently and identically distributed (IID). This assumption of random error term leads the target lane choice as MNL, which is the simplest specification of discrete choice modelling. The structure of random error terms will be discussed in Appendix-A . The probability of lane choice l conditional on individual specific random term ϑ_n , therefore, can be written as:

$$P(l_n(t)|\vartheta_n) = \frac{exp\big(\widehat{U}_n^l(t)|\vartheta_n\big)}{\sum_l exp\big(\widehat{U}_n^l(t)|\vartheta_n\big)} \qquad l \in \{1, 2, 3, \ldots, L\} \qquad (4.3)$$

Where;

$P(l_n(t)|\vartheta_n)$: Probability of individual n is choosing the specific target lane l at time t

The target lane l choice constitutes the lane changing direction of the individual driver whether changing to left or right. There is no lane changing required if the driver is satisfied with the current lane condition. In this case, the driver maintains his/her vehicle in the current lane. As shown in **Figure 4.2**, the vehicle at lane 3 requires one lane change to the left (kerb-side) toward lane 2. If such vehicle chooses lane 3 as its target lane, then no lane change is required. If lane 4 is the target lane, it requires one lane change to right lane (far-side) of the road section.

4.3.2 Gap acceptance

Gap acceptance is the second level of lane-changing decision-making process as seen in **Figure 4.2**. The lane-changing driver evaluates both lead and lag gaps at the adjacent lane that corresponds with the direction of desired target lane and lane-changing tactical whether the action can be taken or not. Note that this action takes place if the driver accepts both gaps simultaneously.

This study represents the gap as time-based, which is a function of distance gap toward the object vehicle and subject vehicle speed. In this case, the distance gap is the clear spacing between the rear edge of the lead vehicle and the front edge of the following vehicle. Therefore, the lead gap is defined as a function of the clear spacing between the target lane lead vehicle rear edge and the observed vehicle front edge. Meanwhile, the lag gap is defined as a function of clear spacing between the rear edge of the subject vehicle and the front edge of target lane lag vehicle, and the subject vehicle speed. The detail of gap measurement is shown in **Figure 4.3**.
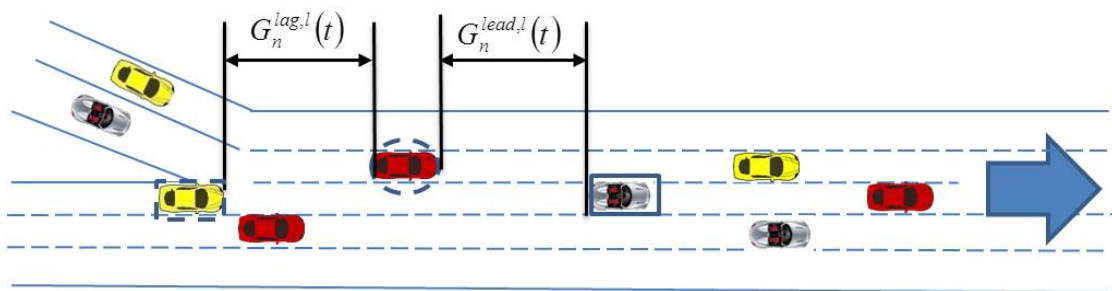
Figure 4.3 Lead and lag gaps definition

Where:

   : Subject vehicle n

   : Lead vehicle $n - 1$ at the target lane

   : Lag vehicle $n + 1$ at the target lane

$G_n^{lead\ l}(t)$: Gap of vehicle n to the leading vehicle at the target lane, at time (t) sec.

$G_n^{lag\ l}(t)$: Gap of vehicle n to the lag vehicle at the target lane, at time (t) sec.

This thesis adopts the gap-acceptance modelling framework which was developed by Ahmed (1999). The model presumes that the lane-changing driver considers only lead and lag gaps at the chosen target lane and omit the other gaps around them. The driver in this situation compares both lead and lag gaps with specific gaps threshold, which is known as critical gaps (G^{cr}). That is to say, the lane changing of individual n at time t is executed if both gaps are slightly greater than the critical gaps. Therefore, the gap acceptance can be expressed as follows: $G_n^{lead}(t) \geq G_n^{cr}(t)$ and $G_n^{lag}(t) \geq G_n^{cr}(t)$. Meanwhile, the driver delays the movement and maintain at the current lane if one of the gaps fails to meet the criteria.

Critical gaps are expressed as a random variable where their means are a function of explanatory variables. In the state-of-the-art models (e.g. Ahmed et al., 1996; Choudhury, 2007; Toledo and Katz, 2009; Toledo et al., 2005; etc.), they assume the critical gaps follow a lognormal distribution. This assumption ensures the critical gaps to be always non-negative values. The driver critical gaps are correlated and not constant or static rather they vary across observations associated with the surrounding traffic condition. Those listed models include the individual-specific error term to explain the correlations among the critical gap decisions of each individual driver. However, those existing gap acceptance models do not address the effect of lane changing mechanisms in the critical gap values.

Incorporating the lane-changing mechanisms, this PhD thesis formulates the critical gap model as follows:

$$G_n^{cr,j,l,m}(t) = \exp\left(X_n^{j,l,m}(t)\beta^{j,l,m} + \alpha^{j,m}\vartheta_n + \varepsilon_n^{j,l,m}(t)\right)$$

$$j \in \{lead, lag\}, m \in \{s, p, w\} \quad (4.4)$$

Where;

$G_n^{cr,j,l,m}(t)$: Critical gap j at the direction of target lane l of individual n at time t for lane changing mechanism m

$X_n^{j,l,m}(t)$: Vector of explanatory variables associated with driver n at time t for critical gap j, target lane l and lane changing mechanism m

$\beta^{j,m}$: Vector of estimated parameters for critical gap j and lane changing mechanism m

$\alpha^{j,m}$: Estimated parameters of individual specific random effect ϑ_n for critical gap j and lane changing mechanism m

$\varepsilon_n^{j,l,m}(t)$: Random error term associated with critical gap j and lane changing mechanism m for driver n at time t, ($\varepsilon_n^{j,l,m}$)$\sim N(0, \sigma^{j,m^2})$

m : Lane changing mechanism, solo (s), platoon (p) or weaving (w)

Lane change at time t occurs if the driver accepts both corresponding lead and lag gaps. The probability of accepting available gaps at the direction of lane l at time $(lc_n(t) = 1)$, which is relative to individual specific random term ϑ_n, can be expressed as follows:

$$P(lc_n(t) = 1|l_n(t), m_n(t), \vartheta_n)$$

$$= [P(accept\ lead\ gap|l_n(t), m_n(t), \vartheta_n)]\ [P(accept\ lag\ gap|l_n(t), m_n(t), \vartheta_n)]$$

$$= \left[P\left(G_n^{lead,l,m}(t) \geq G_n^{cr,lead,l,m}(t)|l_n(t), m_n(t), \vartheta_n\right)\right] *$$

$$\left[P\left(G_n^{lag,l,m}(t) \geq G_n^{cr,lag,l,m}(t)|l(t), m_n(t), \vartheta_n\right)\right] \tag{4.5}$$

Where;

$G_n^{lead,l,m}, G_n^{lag,l,m}$: Available lead and lag gaps at target lane l with mechanism m forn driver n

As discussed earlier, the critical gap follows the lognormal distribution. The conditional probabilities of accepting the available gap can be written as follows:

$$P\left(G_n^{j,l,m}(t) \geq G_n^{cr,j,l,m}(t)|l_n(t), m_n(t), \vartheta_n\right)$$

$$= P\left[ln\left(G_n^{j,l,m}(t) \geq G_n^{cr,j,l,m}(t)|l_n(t), m_n(t), \vartheta_n\right)\right]$$

$$= \Phi\left[\frac{ln\left(G_n^{j,l,m}(t)\right) - \left(X_n^{j,l,m}(t)\beta^{j,l,m} + \alpha^{j,m}\vartheta_n\right)}{\sigma^{j,m}}\right] \tag{4.6}$$

Where;

$\Phi[.]$: Cumulative standard normal distribution

Deriving Equation 4.5 and 4.6, the probability of lane changing at the rejected gaps ($lc_n(t) = 0$) is written as;

$$P(lc_n(t) = 0|l_n(t), m_n(t), \vartheta_n) = 1 - P(lc_n(t) = 1|l_n(t), m_n(t), \vartheta_n)$$

$$= 1 - \Phi\left[\frac{ln\left(G_n^{j,l,m}(t)\right) - \left(X_n^{j,l,m}(t)\beta^{j,l,m} + \alpha^{j,m}\vartheta_n\right)}{\sigma^{j,m}}\right] \qquad (4.7)$$

Gap acceptance is a result of the interaction between the subject vehicle and the traffic in the adjacent lane in the direction of the target lane. Such interaction can be represented by variables like relative speed between the subject vehicle and lead and/or lag vehicle on the target lane, types of vehicle, distance to exit, etc. The discussion on the estimation of gap acceptance modelling parameter will be conducted in Section 7.1.4.

4.4 Likelihood Function

The likelihood function is applied to estimate the parameters for the lane-changing modelling. As discussed earlier, the lane-changing behaviour is a result of two level decisions making process namely (1) target lane choice model and (2) gap acceptance model. The likelihood function of observing a lane change at time t, therefore, is a joint probability of choosing target lane l and accepting the available gap at the direction of lane l with conditional on individual specific (ϑ), and lane changing mechanisms (m). As discussed earlier, the individual specific (ϑ) is assumed to follow normal distribution $\left(\vartheta_n \sim N(0,1)\right)$. The likelihood function can be expressed as follows:

$$P\left(LC_n^{l'}{}_n(t)|\vartheta_n\right) = \sum_{l \in l'}\sum_m [P(l_n(t)|\vartheta_n)]\,[P(lc_n(t)|l_n(t), m_n(t), \vartheta_n)]$$

$$l' \in \{left, right, current\}, l \in \{1,2,...,5\}, m\{s,p,w\} \quad (4.8)$$

Where;

$P\left(LC_n^{l'}(t)\right)$: The probability of lane change in direction l' at time t with conditional on driver characteristics ϑ

Both $P(l(t)|.)$ and $P(lc_n(t)|.)$ are given by Equations 4.3 and 4.5 respectively. The trajectory data consist of observations sequence of the same driver over the study area.

Assuming that the observations from different drivers are independent over time, the joint probability of the sequence observations can be specified as follows:

$$\left[P\left(LC_n^{l'}(1)|\vartheta_n\right)\right]\left[P\left(LC_n^{l'}(2)|\vartheta_n\right)\right]\left[P\left(LC_n^{l'}(3)|\vartheta_n\right)\right] \ldots \left[P\left(LC_n^{l'}(T_n)|\vartheta_n\right)\right]$$

$$= \prod_{n=1}^{T_n}\sum_l\sum_m \left[P(l_n(t)|\vartheta_n)\right]\left[P(lc_n(t)|l_n(t),m_n(t),\vartheta_n)\right] \tag{4.9}$$

Where;

T_n : Number of observed time period for driver n (1, 2, 3, ….., T_n)

Integrating Equation 4.9, unconditional likelihood function (L_n) of the observed lane changing behaviour over the distributions can be written as follows:

$$LC_n = \int_v \prod_{n=1}^{T_n}\sum_l\sum_m \left[P(l_n(t)|\vartheta_n)\right]\left[P(lc_n(t)|l_n(t),m_n(t),\vartheta_n)\right] f(\vartheta)\, d\vartheta \tag{4.10}$$

Note that $f(\vartheta)$ is a standard normal probability density function. Following the IID distribution of the error terms, the log-likelihood function for all N individual observation is given by;

$$L = \sum_{n=1}^{N}\ln LC_n \tag{4.11}$$

The maximum likelihood estimations of the model parameters are found by maximizing this function. The Broyden-Fletcher-Goldfarb-Shanno (BFGS) optimisation algorithm is used for the maximization. More details of BFGS algorithm can be seen in Appendix-C.

4.5 Summary

This chapter presents the development of the modelling framework and estimation procedure of the proposed lane-changing model in a weaving section. The current study extends the state-of-the-art latent plant lane changing models to explicitly account the difference in behaviour under different lane changing mechanisms with respect to the

type of leader vehicle movement. In this case, there are three types of lane changing mechanism:

- Platoon   : if the front vehicle is at the current lane changes lane

- Weaving   : if the leader vehicle is at target lane changes lane

- Individual/solo: if both front and leader vehicle do not change lane.

Driver's decision in the lower level of lane changing decision-making process depends on those on the upper-level decisions. The observed lane changing direction is implied in the driver's latent target lane choice, while gap acceptance model incorporates the lane changing mechanisms. Both target lane choice and gap acceptance model parameters are jointly estimated based on vehicle trajectory data collected using Maximum Likelihood Estimation technique. The developed models can have a significant impact on improving the fidelity of the microsimulation results of the weaving sections. However, this modelling framework is based on a moderate traffic flow where such cooperation lane-changing behaviour is less significant. The estimation result of the proposed modelling framework is presented in Section 7.1.

Chapter 5   Acceleration Model

This chapter discusses the acceleration model framework in weaving section. The proposed acceleration model has four modelling components: (1) car-following regime, (2) free-flow, (3) gap threshold distribution, and (4) driver reaction time. This study extends the state-of-art of acceleration model framework which relaxes the condition for individual driver response. The flexibility of the proposed modelling framework allows this study capturing the drivers' car-following behaviour which is different from the stimulus condition. Both gap threshold and reaction time distribution capture the individual driver heterogeneity.

This chapter presents a discussion according to the following sequences: Section 5.1 discussed the background of the acceleration model in brief. The acceleration modelling framework is presented in section 5.2. Furthermore, this section discusses the modelling specification of the car-following regime, the free-flow regime, gap threshold distribution, and driver reaction time distribution in more details. Section 5.3 presents the likelihood algorithm for all parameters in the acceleration model, which are estimated jointly. A summary of acceleration model is presented in Section 5.4.

5.1 Background

Car-following behaviour is one of important aspects of the motorway traffic operation and driving in safe condition (Yousif and Al-Obaedi, 2011b). In this case, the vehicle in a particular road section interacts with the neighbouring traffic to maintain a safety distance towards the front vehicle. The driver, therefore, has to adjust his/her speed whether increasing (acceleration) or decreasing (deceleration) the current speed as the response of driver sensitivity and the stimulus from the neighbourhood. **Figure 5.1** illustrates a schematic of the car-following movement.
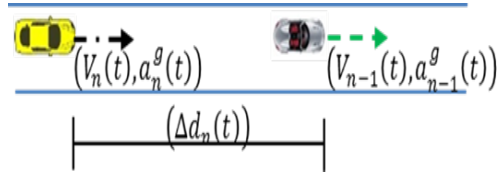
Figure 5.1 Schematic car-following movement

Where;

 : Subject vehicle n

 : Object vehicle $n-1$

$V_n(t)$: Speed of the subject vehicle at time t (m/sec)

$V_{n-1}(t)$: Speed of the object vehicle at time t (m/sec)

$a_n^g(t)$: Acceleration of vehicle n at time t (m/sec^2)

$a_{n-1}^g(t)$: Acceleration of vehicle $n-1$ at time t (m/sec^2)

$\Delta d_n(t)$: Space gap between the subject and front vehicle at time t (m)

g : "acc" ($acceleration \geq 0 \ m/sec^2$) or "dec" ($deceleration < 0 \ m/sec^2$)

Similar to lane changing movement, car-following movement in weaving section is a complicated situation where the vehicle has to response the stimulus in a relatively short of period and length of the road section. Sarvi et al. (2011) reported that the proportion of weaving and non-weaving traffic affects the car-following behaviour and the traffic performance on the weaving section significantly.

A large number of car-following models have been developed since the first appearance of GM's model by Pipes (1953). In fact, the GM's modelling specification has a limitation in capturing the interaction between the subject vehicle and the neighbouring traffic (i.e. object vehicle movement). Gipps (1981) has accordingly defined an acceleration modelling framework that incorporated various properties to resemble the traffic interaction during the car-following movement process. Yang and Koutsopoulos (1996) proposed three car-following regimes: car-following, free-flow, and emergency regime. Ahmed (1999) presented a rigorous improvement in acceleration model by specifying both stimulus and sensitivity component as a function of explanatory variables. This modelling structure has the flexibility to represent the traffic interaction during the acceleration decision-making process. Due to the time gap threshold, this study classified the car-following movement into two regimes:

- Car-following: if the available gap with the front vehicle is less than the gap threshold. The subject vehicle is likely to perceive a stimulus based on the interaction between his/her vehicle with the front vehicle.

- Free-flow : if the available gap with the front vehicle is greater than the gap threshold. In this case, the driver in car-following situation faces a relatively large gap with less traffic interaction compared to the car-following regime. The stimulus for the free-flow regime is a function of desired speed and current vehicle speed.

Furthermore, Ahmed (1999) included the driver reaction, which is a time lag between the appearance of stimulus and driver response, as conditional specification into acceleration model. Later, Toledo (2003) and Toledo et al. (2007) integrated the acceleration model as part of driving behaviour modelling behaviour together with the lane-changing model. The acceleration model in those models is developed under be continuous approach which provides a flexibility in capturing car-following behaviour in various traffic condition. As discussed in the literature, further development of car-following model has been carried out with various specifications i.e. including the traffic flow characteristics (Wang et al., 2005b), time-gap based (i.e. Tordeux et al., 2010; Zhang and Kim, 2005), and latent plan (Koutsopoulos and Farah, 2012).

A brief discussion of the existing acceleration model reveals limitation in capturing the car-following behaviour in different stimulus condition. In fact, the current models presume that the acceleration or deceleration decision corresponds with a specific relative speed condition. The assumption neglects several car-following scenarios such as: fast approaching vehicle (a vehicle which intends to join a downstream traffic), courtesy movement (creating a safe gap for the neighbouring traffic to merge on the current lane). The present study extends the state-of-the-art acceleration model which allows flexibility in capturing various car-following behaviours in each stimulus condition, particularly in the car-following regime. Thus, the car-following regime consists of four sub-models: (1) acceleration with positive relative speed, (2) acceleration with negative relative speed, (3) deceleration with positive relative speed, and (3) deceleration with negative relative speed. More details of the modelling specification will be discussed later in this chapter.

5.2 Acceleration Modelling Framework

This section presents the structures of the proposed acceleration model structure, which consists of two regimes: (1) car-following (cf) and (2) free-flow (ff) regimes. Instead of gap threshold, this study uses the gap threshold distribution G_n^* to classify the

acceleration condition. It is intuitively more sensible for the driver measuring the gap (front edge of subject to rear edge of the front/lead vehicle) and consistent with the gap acceptance model in the lane-changing model. Therefore, the condition for acceleration regime can be written as follows:

$$a_n(t) = \begin{cases} a_n^{cf}(t) & if\ G_n(t - \tau_n) < G_n^* \\ a_n^{ff}(t) & otherwise \end{cases} \tag{5.1}$$

Where;

$a_n(t)$: Acceleration of vehicle n at time t (m/sec^2)

$a_n^{cf}(t)$: Acceleration of vehicle n under car-following regime at time t (m/sec^2)

$a_n^{ff}(t)$: Acceleration of vehicle n under free-flow regime at time t (m/sec^2)

$G_n(t - \tau_n)$: Available gap event for vehicle n at the observed time $(t - \tau_n)$ (sec)

G_n^* : The threshold value of the available gaps at time t (sec)

τ_n : Reaction time of vehicle n (sec)

Based on the criteria, the subject vehicle falls into the car-following regime if the available gap at time $(t - \tau_n)$ is smaller than the gap threshold. Meanwhile, the vehicle drives in the free-flow regime, if the gap is greater than the threshold. The vehicle in the car-following regime has to make a decision correspond to the neighbouring traffic condition. Meanwhile, the free-flow regime allows the vehicle moving along with his/her desired speed. Mathematically, those situations are represented as a function of the stimulus and driver sensitivity.

The reaction time captures the time length for the driver to response the stimulus. As mentioned earlier, this attribute incorporates both the interpretation time and foot movement. In fact, this unique variable cannot be captured directly from the observed vehicle trajectory data. The reaction time in this study, therefore, is presented as a random number, which follows a specific distribution. The detailed of reaction time distribution is elaborated in Section 5.2.4.

Following sections will discuss the modelling specification of the car-following regime, free flow regime, the distribution of gap and reaction in more details.

5.2.1 Car following regime

Adopting the acceleration modelling framework by Ahmed (1999), this acceleration behaviour in the car-following regimes is represented as a function of both the stimulus-sensitivity, and random error components. Thus, the car-following (cf) regime form in the proposed acceleration model is given as follows:

$$a_n^{cf,g}(t) = S\left[X_n^{cf,g}(t)\right]\left[\Delta V_n(t - \tau_n)\right] + \varepsilon_n^{cf} \tag{5.2}$$

Where;

$a_n^{cf,g}(t)$: Acceleration g under car-following regime of driver n at time t

$S[.]$: Function of sensitivity

$X_n^{cf,g}(t)$: Vector of explanatory car-following g variables associated with driver n at time t

$\left[\Delta V_n(t - \tau_n)\right]$: Stimulus, a function of relative speed $\Delta V_n(t - \tau_n)$

$\varepsilon_n^{cf,g}$: Random error term associated with acceleration g for driver n at time t

The acceleration is a response of the stimulus-sensitivity components whether the driver's response would be accelerate (acc) or decelerate (dec) due to the neighbouring traffic condition (stimulus). An acceleration condition appears when the vehicle n speed increases during the specific time period. If the vehicle n speed is decreased during the specific time period, the vehicle will move under the deceleration regime. This condition can be expressed as follows:

$$g = \begin{cases} acc &, V_n(t) \geq V_n(t - \Delta t) \\ dec &, otherwise \end{cases} \tag{5.3}$$

Where;

g : Driver's response$\{accelerate(acc), decelerate(dec)\}$

$V_n(t)$: Vehicle n speed at time t

$V_n(t - \Delta t)$: Vehicle n speed at time $t - \Delta t$

Δt : Observation time step (i.e. 1 sec)

Meanwhile, the stimulus is represented as the function of relative speed between the object vehicle and subject vehicle at time $(t - \tau_n)$. The stimulus condition is given by:

$$st = \begin{cases} + &, \ \Delta V(t - \tau_n) \geq 0 \\ - &, \ otherwise \end{cases} \tag{5.4}$$

Where;

st : The condition of stimulus

The proposed acceleration model allows different of response (acceleration or deceleration) from each stimulus condition, which is a function of relative speed (positive or negative). This extension relaxes the limitation on the existing acceleration model car-following regime assumptions where the car-following behaviour is strictly based on the specific relative speed condition. This study defines that vehicle involves in acceleration when the object vehicle moves faster while the vehicle decelerates if the object vehicle is slower than his/her vehicle. It is worth noting that the proposed acceleration model in this thesis classifies the zero difference in speed as acceleration with positive relative speed. The proposed, therefore, car-following regime condition is written as follows:

$$a_n^{cf,g,st}(t) = \begin{cases} a_n^{cf,acc,+}(t), & if \ a_n^{cf,g}(t) \geq 0 \ and \ \Delta V(t - \tau_n) \geq 0 \\ a_n^{cf,acc,-}(t), & if \ a_n^{cf,g}(t) \geq 0 \ and \ \Delta V(t - \tau_n) < 0 \\ a_n^{cf,dec,+}(t), & if \ a_n^{cf,g}(t) < 0 \ and \ \Delta V(t - \tau_n) \geq 0 \\ a_n^{cf,dec,-}(t), & Otherwise \end{cases}$$

$$g\epsilon\{acc, dec\}; st\epsilon\{+, -\} \tag{5.5}$$

Where;

$a_n^{cf,g,st}(t)$: Car-following g of vehicle n associated with stimulus(st) at time t

$a_n^{cf,acc,+}(t)$: Car-following acceleration of vehicle n associated with positive st at time t

$a_n^{cf,acc,-}(t)$: Car-following acceleration of vehicle n associated with negative st at time t

$a_n^{cf,dec,+}(t)$: Car-following deceleration of vehicle n associated with positive st at time t

$a_n^{cf,dec,-}(t)$: Car-following deceleration of vehicle n associated with negative st at time t

The driver sensitivity component in the proposed acceleration model can be explained by several attributes, such as: vehicle speed, traffic density, remaining distance to exit, and type of vehicle (small or heavy vehicle). A fast moving vehicle is very sensitive if the neighbouring traffic is changed dramatically. For example, the vehicle in faster speed has to decelerate more compared to slow moving vehicle if an incident appears at the downstream. Small vehicles tend to decelerate and increase the gap while facing a heavy vehicle in front. As discussed earlier, a high proportion of traffic in a multilane facility such as weaving section adjusts their lane and performs a pre-emptive lane changing at the beginning of the section. The vehicle has to decelerate and adjust the speed to unify with or prepare for a lane-changing movement.

Integrating the condition of car-following behaviour (Equations 5.2) and stimulus condition (Equation 5.3), the car-following regime model can be modelled as follows:

$$a_n^{cf,g,st}(t) = S[X_n^{cf,g}(t)] [\Delta V_n^{st}(t - \tau_n)] + \varepsilon_n^{cf,g,st}$$

$$g \in \{acc, dec\}, st \in \{+, -\} \quad (5.6)$$

Where;

$a_n^{cf,g,st}(t)$: Car-following g of driver n under car-following regime associated with stimulus st at time t (m/sec^2)

$S[.]$: Function of sensitivity car-following acceleration at time t

$X_n^{cf,g}(t)$: Vector of explanatory car-following g variables associated with the sensitivity of driver n at time t

$[\Delta V_n^{st}(t - \tau_n)]$: Stimulus, a function of relative speed between the subject and object vehicle at time $(t - \tau_n)$. (m/sec)

$\varepsilon_n^{cf,g,st}$: Random error term of car-following g associated with conditional st for driver n at time t.

All random error terms $\left(\varepsilon_n^{cf,acc,+}, \varepsilon_n^{cf,acc,-}, \varepsilon_n^{cf,dec,+}, \varepsilon_n^{cf,dec,-}\right)$ represent the unobservable components on both car-following acceleration and deceleration with respect to variation of relative speed. This acceleration model presumes that the error term is normally distributed and independent of each condition of car-following regime and driver overtime period ($\varepsilon_n^{cf,g,st}) \sim N(0, \sigma^{cf,g,st^2}$). The detailed of the error term

structure will be discussed in Appendix-A . Furthermore, both reaction time and gap distributions in this modelling framework capture the correlation between the car-following behaviour of individual driver n.

Considering the assumption on the error function, the general form of car-following regime distribution for the car-following acceleration and deceleration with respect to relative speed conditional on reaction time is written by:

$$f\left(a_n^{cf,g,st}(t)|\tau_n\right)$$

$$= \frac{1}{\sigma^{cf,g,st}}\phi\left[\frac{a_n^{cf,g,st}(t) - \left(S\left[X_n^{cf,g}(t)\right]\left[\Delta V_n^{st}(t-\tau_n)\right]\right)}{\sigma^{cf,g,st}}\right] \tag{5.7}$$

Where;

$f\left(a_n^{cf,g,st}(t)|\tau_n\right)$: Function car-following distribution g of driver n associated with stimulus st and reaction time τ at time t

$\sigma^{cf,g,st}$, σ^{cf,g,st^2} : Standard deviation and variance of car-following distribution g of vehicle n associated with stimulus st

$\phi[.]$: Probability distribution functions of a standard normal distribution random variable

Then, the distribution for all those four car-following regime conditions is given by:

$$f\left(a_n^{cf,g,st}(t)|\tau_n\right)$$

$$= \left[f\left(a_n^{cf,acc,+}(t)|\tau_n\right)^{\delta[g_n(t)]*\delta\left[\Delta V_n^{st}(t-\tau_n)\right]}\right] *$$

$$\left[f\left(a_n^{cf,acc,-}(t)|\tau_n\right)^{\delta[g_n(t)]*\left(1-\delta\left[\Delta V_n^{st}(t-\tau_n)\right]\right)}\right] *$$

$$\left[f\left(a_n^{cf,dec,+}|\tau_n\right)^{\left(1-\delta[g_n(t)]\right)*\delta\left[\Delta V_n^{st}(t-\tau_n)\right]}\right] *$$

$$\left[f\left(a_n^{cf,dec,-}|\tau_n\right)^{\left(1-\delta[g_n(t)]\right)*\left(1-\delta\left[\Delta V_n^{st}(t-\tau_n)\right]\right)}\right] \tag{5.8}$$

Where;

$\delta[g_n(t)]$: 1 if the driver accelerates; 0 otherwise.

$\delta[\Delta V_n^{st}(t - \tau_n)]$: 1 if the relative speed is positive, 0 otherwise.

5.2.2   Free flow regime

The free-flow is a condition when a vehicle has more freedom to drive through the observation area. The current research defines that this regime shows that one of the following vehicles faces a larger gap than gap threshold. Consequently, the free-flow model is written as:

$$a_n^{ff}(t) = \beta^{ff}[V_n^{DS}(t - \tau_n) - V_n(t - \tau_n)] + \varepsilon_n^{ff}(t) \qquad (5.9)$$

Where;

$a_n^{ff}(t)$: Acceleration of vehicle n under free-flow condition at time t

β^{ff} : Estimated constant free sensitivity

$V_n^{DS}(t - \tau_n)$: Desired speed of driver n at time $(t - \tau_n)$

$[V_n^{DS}(t - \tau_n) - V_n(t - \tau_n)]$: Function of stimulus driver n at time $(t - \tau_n)$

$\varepsilon_n^{ff}(t)$: Random error term associated with the free flow car-following regime for driver n at time t

The free-flow modelling structure implies that the stimuli for the driver under this regime decision is a function of the difference between the vehicle desired speed and the actual vehicle speed at time $(t - \tau)$. The sensitivity is presumed to be constant. Similar to car-following regime, several explanatory variables explain the driver decision in free-flow regime i.e. speed limit, type of vehicle, speed, road geometry, and etc. The function of desired speed is give as follows:

$$V_n^{DS}(t - \tau_n) = \beta^{DS} X_n^{DS}(t - \tau_n) \qquad (5.10)$$

Where;

β^{DS} : Estimated constant desired speed

$X_n^{DS}(t - \tau_n)$: Vector of explanatory variables of desired speed of driver n driver at time $t - \tau_n$

A substitution of the vehicle desired speed V_n^{DS} component in Equation 5.9 with 5.10 derives the free-flow car-following model as follows:

$$a_n^{ff}(t) = \beta^{ff}[\beta^{DS}X_n^{DS}(t - \tau_n) - V_n(t - \tau_n)] + \varepsilon_n^{ff}(t) \qquad (5.11)$$

The free-flow modelling structure expects that the vehicle in a free flow regime will accelerate when the desired speed is higher than the actual speed. The vehicle decelerates when the actual vehicle speed is higher than the desired speed.

Similar to the car-following modelling, the random error term in the free-flow model $\left(\varepsilon_n^{ff}(t)\right)$ represents the unobservable variables during the vehicle movement in a free-flow regime. It is assumed to be normally distributed and independent for each different driver over a specific time period $\varepsilon_n^{ff}(t) \sim N\left(0, \sigma^{ff^2}\right)$. Moreover, both the reaction time and the gap threshold distribution in this model capture the correlation of each driver decision over the observation period. As discussed above, the structure of error term is presented in Appendix-A .

Considering the assumption of error term, the free-flow acceleration distribution with conditional on reaction time is written as follows:

$$f\left(a_n^{ff}(t)|\tau_n\right) = \frac{1}{\sigma^{ff}} \phi\left[\frac{a_n^{ff}(t) - (\beta^{ff}[\beta^{DS}X_n^{DS}(t - \tau_n) - V_n(t - \tau_n)])}{\sigma^{ff}}\right] \qquad (5.12)$$

Where;

$f\left(a_n^{ff}(t)|\tau_n\right)$: Function of free-flow car-following regime of vehicle n at time t is depending on reaction time τ

$\sigma^{ff}, \sigma^{ff^2}$: Standard deviation and variance of free-flow car-following regime of vehicle n

$\phi[.]$: Functions of a standard normal distribution's random variable

5.2.3 Gap threshold distribution

The time gap threshold assists to classify the car-following condition into two groups; (1) car-following regime or (2) free-flow regime. As mentioned earlier, the vehicle moves under the car-following regime if the gap toward the front vehicle is less than a specific gap threshold. The vehicle involves in the free-flow regime when the available gap is greater than the threshold. The gap threshold varies depend on the driver's aggressiveness, vehicle characteristics, road geometric and neighbouring traffic

condition. Those factors are captured in the time gap threshold that is distributed over the driver population.

Instead of using normal distribution as suggested by Ahmed (1999), this thesis presumes the gap threshold distribution follows the lognormal distribution as a high proportion prefers a short gap. The vehicle traffic trajectory in the current study demonstrates that the gap is skewed to the left-hand side, where a large proportion of traffic moves in smaller gap. More details of the observed gap distribution toward the front vehicle are shown in **Figure 6.12**. In addition, Yin et al. (2009) studied the vehicle trajectory saying that the lognormal distribution fits adequately with the vehicle trajectory in low-moderate traffic. Furthermore, the use of both side truncations ensures the gap to be positive and finite number.

Giving this description, the truncated lognormal distribution of gap acceptance is expressed as follows:

$$f(G_n^*) = \begin{cases} \dfrac{\dfrac{1}{G_n^* . \sigma_G} \phi\left(\dfrac{\ln (G_n^*) - \mu_G}{\sigma_G}\right)}{\Phi\left(\dfrac{\ln(G^{*,max}) - \mu_G}{\sigma_G}\right) - \Phi\left(\dfrac{\ln(G^{*,min}) - \mu_G}{\sigma_G}\right)} & if \ G^{*,min} \leq G_n^* \leq G^{*,max} \\ \\ 0 & Otherwise \end{cases} \tag{5.13}$$

Where;

$f(G_n^*)$: Function of time gap threshold distribution

G_n^* : The threshold value of the available gap (sec)

$G^{*,min}, G^{*,max}$: Minimum and maximum value of the gap threshold (sec) respectively

μ_G, σ_G : The mean and standard deviation of the truncated gap distribution

$\phi[.]$: Probability distribution functions of a standard normal distribution random variable

$\Phi[.]$: Cumulative distribution functions of a standard normal distribution random variable

As derived from Equation 5.13, the probability of the driver in the car-following regime can be expressed as follows:

$$P_n(car - following\ at\ time\ t) = P(G_n(t) \le G_n^*)$$

$$= \begin{cases} 1 - \dfrac{\Phi\left(\dfrac{ln\big(G_n(t)\big) - \mu_G}{\sigma_G}\right) - \Phi\left(\dfrac{ln\big(G^{*,min}\big) - \mu_G}{\sigma_h}\right)}{\Phi\left(\dfrac{ln(G^{*,max}) - \mu_G}{\sigma_G}\right) - \Phi\left(\dfrac{ln(G^{*,min}) - \mu_G}{\sigma_G}\right)} & G^{*,min} \le G_n^* \le G^{*,max} \\ \\ 0 & Otherswise \end{cases} \qquad (5.14)$$

The mean, variance and median of the gap threshold distribution are given by;

$$mean = \exp\left(\mu_G + 0.5\sigma_G{}^2\right)\frac{\Phi\left(\dfrac{ln(G^{max}) - \mu_G}{\sigma_G} - \sigma_G\right)}{\Phi\left(\dfrac{ln(G^{max}) - \mu_G}{\sigma_G}\right) - \Phi\left(\dfrac{ln(G^{min}) - \mu_G}{\sigma_G}\right)} \qquad (5.15)$$

$$median = \exp\left(\mu_G + \left(\sigma_G \Phi^{-1}\left[0.5\left(\Phi\left(\dfrac{ln(G^{max}) - \mu_G}{\sigma_G}\right) - \Phi\left(\dfrac{ln(G^{min}) - \mu_G}{\sigma_G}\right)\right)\right]\right)\right) \qquad (5.16)$$

$$variance = \exp^{2\mu_G + \sigma_G}\left(\exp^{\sigma_G{}^2} - 1\right)\frac{\Phi\left(\dfrac{ln(G^{max}) - \mu_G}{\sigma_G} - 2\sigma_\tau\right)}{\Phi\left(\dfrac{ln(G^{max}) - \mu_G}{\sigma_G}\right) - \Phi\left(\dfrac{ln(G^{min}) - \mu_G}{\sigma_G}\right)} \qquad (5.17)$$

5.2.4 Driver reaction time

Similar to the previous researches (i.e Ahmed, 1999; Subramanian, 1996; Toledo, 2003), the current study presumes the driver reaction time as a random variable that follows the truncated lognormal distribution. In this case, high proportion of driver requires a short reaction time while fewer drivers require large reaction time. The reaction time distribution is truncated due to avoid finiteness reaction time. Therefore, the probability density function of reaction time is written as follows:

$$f(\tau_n) = \begin{cases} \dfrac{\dfrac{1}{\tau_n \sigma_\tau}\phi\left(\dfrac{ln(\tau_n) - \mu_\tau}{\sigma_\tau}\right)}{\Phi\left(\dfrac{ln(\tau^{max}) - \mu_h}{\sigma_h}\right) - \Phi\left(\dfrac{ln(\tau^{min}) - \mu_h}{\sigma_h}\right)} & if\ \tau^{min} < \tau_n \le \tau^{max} \\ \\ 0 & Otherswise \end{cases} \qquad (5.18)$$

Where;

τ_n : Driver n reaction time

μ_τ, σ_τ : Mean and standard deviation of distribution $ln(\tau_n)$ respectively

τ^{min} : Lower bound of the reaction time distribution

τ^{max} : Upper bound of the reaction time distribution

Then the mean, variance and median of the driver reaction time distribution can be expressed as follows:

$$mean == = \exp\left(\mu_\tau + 0.5\sigma_\tau{}^2\right)\frac{\Phi\left(\frac{ln(\tau^{max}) - \mu_\tau}{\sigma_\tau} - \sigma_\tau\right)}{\Phi\left(\frac{ln(\tau^{max}) - \mu_\tau}{\sigma_\tau}\right) - \Phi\left(\frac{ln(\tau^{min}) - \mu_\tau}{\sigma_h}\right)} \tag{5.19}$$

$$median = \exp\left(\mu_\tau + \left(\sigma_\tau \Phi^{-1}\left[0.5\left(\Phi\left(\frac{ln(\tau^{max}) - \mu_\tau}{\sigma_\tau}\right) - \Phi\left(\frac{ln(\tau^{min}) - \mu_\tau}{\sigma_\tau}\right)\right)\right]\right)\right) \tag{5.20}$$

$$variance = \exp^{2\mu_\tau + \sigma_\tau}\left(\exp^{\sigma_\tau{}^2} - 1\right)\frac{\Phi\left(\frac{ln(\tau^{max}) - \mu_\tau}{\sigma_\tau} - 2\sigma_\tau\right)}{\Phi\left(\frac{ln(\tau^{max}) - \mu_\tau}{\sigma_\tau}\right) - \Phi\left(\frac{ln(\tau^{min}) - \mu_\tau}{\sigma_\tau}\right)} \tag{5.21}$$

Note that the mean value of the reaction time distribution μ_τ represents as a function of the explanatory variables. Then, the function is written:

$$\mu_\tau = X_i^\tau . \beta_i^\tau \tag{5.22}$$

Where;

X_i^τ : Explanatory variables of the reaction time distribution

β_i^τ : Specific constant parameter of reaction time

As discussed earlier, driver reaction time captures the time length between the appearance of stimulus and the driver response. The X_i^τ represents the affecting factors of the driver reaction time, which has been mentioned earlier in this section. In fact, each driver has different reaction time for each traffic condition. The reaction time may consist of three components: driver perception, foot movement and vehicle responses. Driver perception represents the time length, which the driver requires for interpreting the neighbouring traffic condition. The driver reacts based on the traffic condition by

moving his/her foot in order to accelerate or decelerate. This relates with the driver's foot movement time. The vehicle respond relates with the vehicle mechanical system reaction on the drive' inputs namely throttle, break, and gear shifting.

Several factors affect the driver reaction time such as: traffic condition (congested/uncongested), driver physical condition (i.e. age, gender, level of tiredness), driving time (daytime/night), and weather condition (dry, rainy or snowy). Driving in congested traffic condition stimulates the drivers to increase their alert and reduce their reaction, whilst the moderately congested one can relax and delay their response as regards these stimuli. In terms of the driver ages, older people need longer reaction time compared to the younger ones. Elder drivers may maintain large gap in this case. Lack of visibility during the bad weather and nigh time increases the driver alert level that requires a short driver reaction time compared to the normal daytime driving.

5.3 Likelihood Function

The likelihood procedure assists the estimation procedure for all parameters in acceleration model that include the car-following, free-flow, gap distribution and reaction time distribution. Given Equation 5.7 and 5.15, the distribution of acceleration of individual driver n at time t conditional on gap threshold (G^*) and reaction time (τ) is written by:

$$f(a_n(t)|G_n^*, \tau_n) = \left[f\left(a_n^{cf,g,st}(t)|\tau_n\right)^{\delta[G_n(t-\tau_n)]} \right] \left[f\left(a_n^{ff}(t)|\tau_n\right)^{1-\delta[G_n(t-\tau_n)]} \right] \quad (5.23)$$

Where;

$$\delta[G_n(t-\tau_n)] = \begin{cases} 1, & \text{if the } G_n(t-\tau_n) \leq G_n^* \\ 0, & Otherwise \end{cases} \quad (5.24)$$

The density functions of the car-following and free-flow regimes are presented in Equation 5.8 and 5.12 respectively. It is worth noting that the driver n acceleration behaviour is independent, while the gap threshold (G_n^*) and the reaction time (τ_n) capture the heterogeneity of the driver n acceleration behaviour over time T period. Then, the dependant joint density of the driver n acceleration decisions $\left(a_n(1), a_n(2), a_n(3), \dots, a_n(T)\right)$ is given by:

$$[f(a_n(1)|G_n^*,\tau_n)][f(a_n(2)|G_n^*,\tau_n)][f(a_n(3)|G_n^*,\tau_n)] \dots [f(a_n(T_n)|G_n^*,\tau_n)]$$

$$= \prod_{n=1}^{T_n} f(a_n(t)|G_n^*,\tau_n) \tag{5.25}$$

Deriving from the Equation 5.26, the unconditional distribution of driver n acceleration behaviour during the observation period is given by:

$$f\big(a_n(1),a_n(2),a_n(3),\dots,a_n(T_n)\big)$$

$$= \int_{\tau_{min}}^{\tau_{max}} \int_{G^{*,min}}^{G^{*,max}} \prod_{n=1}^{T_n} f(a_n(t)|G_n^*,\tau_n)\; f(G^*)\, f(\tau)\; d(G^*)\, d(\tau) \tag{5.26}$$

With an assumption that all drivers in the population are independent, the log-likelihood (LL) function for driver n is written as follows:

$$LL = \sum_{n=1}^{N} \ln\big[f\big(a_n(1),a_n(2),a_n(3),\dots,a_n(T_n)\big)\big] \tag{5.27}$$

Then, the application of Maximum Likelihood Estimation (MLE) method expresses the estimated parameters that maximise the mean acceleration value. Similar to lane-changing model, the likelihood estimation process in the acceleration model follows the Broyden-Flecther-Goldfarb-Shanno (BFGS) optimisation algorithm. The detailed of BFGS is discussed in Appendix-C .

5.4 Summary

This chapter presents a modelling specification and the likelihood estimation procedure of the proposed acceleration model, which consists of four components: the car-following regime, the free-flow regime, the gap distribution and the reaction time distribution. A gap threshold distribution in the proposed model defines whether the car-following event is in the car-following regime or free-flow regime.

This research extends the state-of-the-art relationship between car-following behaviour and stimulus condition during car-following regime. This modelling relaxes the assumption on the previous acceleration model that specifies the car-following behaviour that is corresponded with a specific stimulus condition. The driver

accelerates or decelerates due to the stimulus from the neighbouring traffic. In this case, the stimulus is represented by the relative speed between the subject and front/lead vehicle. Consequently, the car-following regime in the proposed model has four sub-model components: acceleration with positive relative speed $\left(a_n^{cf,acc,+}\right)$, acceleration with negative relative speed $\left(a_n^{cf,acc,-}\right)$, deceleration with positive relative speed $\left(a_n^{cf,dec,+}\right)$, and deceleration with negative relative speed $\left(a_n^{cf,dec,-}\right)$. The reaction time in this model represents the level of driver's aggressiveness. An aggressive driver requires a smaller reaction time while a conservative driver requires a longer reaction. All modelling components are estimated jointly by the likelihood estimation procedure. The estimation procedures and results of the proposed acceleration model are presented in Section 7.2.

Chapter 6 Empirical Traffic Data

This chapter presents the site characteristics, data collection, data extraction process, and data analysis. This work uses two types of traffic surveillance data sources, namely MIDAS (Motorway Incident Detection and Automatic Signalling) and the traffic video observation.

The observation was taken on the M1 between Junction (J) 41-43, which is part of motorway network in the north-south UK stretches between Wakefield and Leeds on Thursday, 16th May 2013 during the time period of 16:30-18:30. The afternoon and early evening period traffic flow at this section of the motorway is moderately congested (as shown by the MIDAS data in Section 6.2). Traffic through this section is mixed between long distance and local commuting traffic. J42 is an interchange for M1 and M62, whilst J43 links the M1 and M621 motorway toward to Leeds. Note that, the road is under good condition without any road works, improvements and side frictions during the observation period. Due to the site condition and the video recording's capability and its availability of the video recording tool, the study emphases the traffic video recording only for the first 320 metres of the weaving section between J42-43.

This chapter is presented as follows; Section 6.1 describes an overview of the observation site. Section 6.2 will discuss the MIDAS loop detector data, following by the extraction and data management. The detailed of traffic video recording process, vehicle trajectory extraction and management of trajectory dataset are presented in Section 6.3. Section 6.4 presents the overview of the traffic characteristics in weaving section including the traffic flow, speed analysis, characteristics of the observed vehicle and the relationship with the neighbouring traffic. The detailed of lane changing characteristics will be discussed in Section 6.5. This section classifies the weaving section in associated with the types, location, gap acceptance and group behaviour. Meanwhile, Section 6.6 summarises the findings of the data analysis.

6.1 Site Description

The observation site selection is important phase in order to gather a clear view of the driving behaviour in the weaving section. Moreover, there are several site requirements applied during the site selection. The site should have less obstacles such as road works, road geometric, and clear sight distance for traffic video recording.

Figure 6.1 Road alignment and loop detectors location (source: Google Earth)

The observation covers the section of M1 between junctions 41 and 43. The section between J41-42 is a three-lanes dual carriageway. The section between J42-43 is a five-lanes dual carriageway that consists of three lanes for through traffic (lane 3, 4, and 5) and two auxiliary lanes (lane 1 and 2) that can be seen in **Figure 6.2** . The distance of the weaving section between J41-42 and J42-43 are 1,250m and 1,265m respectively, which are slightly shorter than the 2,000m distance defined by (DMRB, 2006).

Most of the motorway networks in England are equipped with loop detectors located at ~500m apart and on each lane of the main carriageway as well as on-/off-ramps. They are part of the Management Incident Data Analysis (MIDAS) system (DMRB, 1994). The MIDAS system provides one-minute average traffic flow, speed, occupancy and types of vehicle. There are 15 MIDAS loop detectors over the site; their locations are marked in **Figure 6.1** and **Figure 6.2** .

The video recording was made from an over-bridge located 620 metres downstream from J42, and was made facing the traffic from J42. It was able to record all five lanes of traffic, for the first ~320m from the merge at J42 (between points *M* and *N* in **Figure 6.2**.

However, the speed and flow information available in the MIDAS data with larger spatial and temporal coverage have only limited details. Contrarily, the trajectory data extracted from the video recordings is enormously detailed that captured the traffic characteristics but then with limited spatial and temporal coverage. These data sources are complement accordingly.

6.2 MIDAS Loop Detector

MIDAS data provides traffic characteristics based on traffic censors, mainly the loop detectors in order to inform the Regional Control Centre (RCC). MIDAS (DMRB, 1994) loop detectors provide basic traffic data such as traffic volume, spot speed, level of occupancy, and headway for each lane. The Highway Agency (HA) has installed this system almost in all UK's main road network (i.e. M1, M6, M25) to improve the road traffic performance. Furthermore, MIDAS data have been widely used to capture the traffic characteristic and driving behaviour on a specific motorway network (Al-Jameel, 2011; Wang, 2006). Both researchers utilised MIDAS as validation instrument and preliminary indicator of the traffic at the observed location.

MIDAS aggregates the data for a period on basis of 1 minute period and stores them in binary format at the website www.midas-data.org.uk (Mott MacDonald, 2013). In terms of the data management, the system stores the data based on the regional control centre, where the loop detector is located, and the observation day. In fact, the observed section is under the North East Regional Control Centre. All the data can be accessed and is downloadable with permission from HALOGEN (Highway Agency Logging Environment) support system.

Figure 6.2 The observation area (distance are in metres)
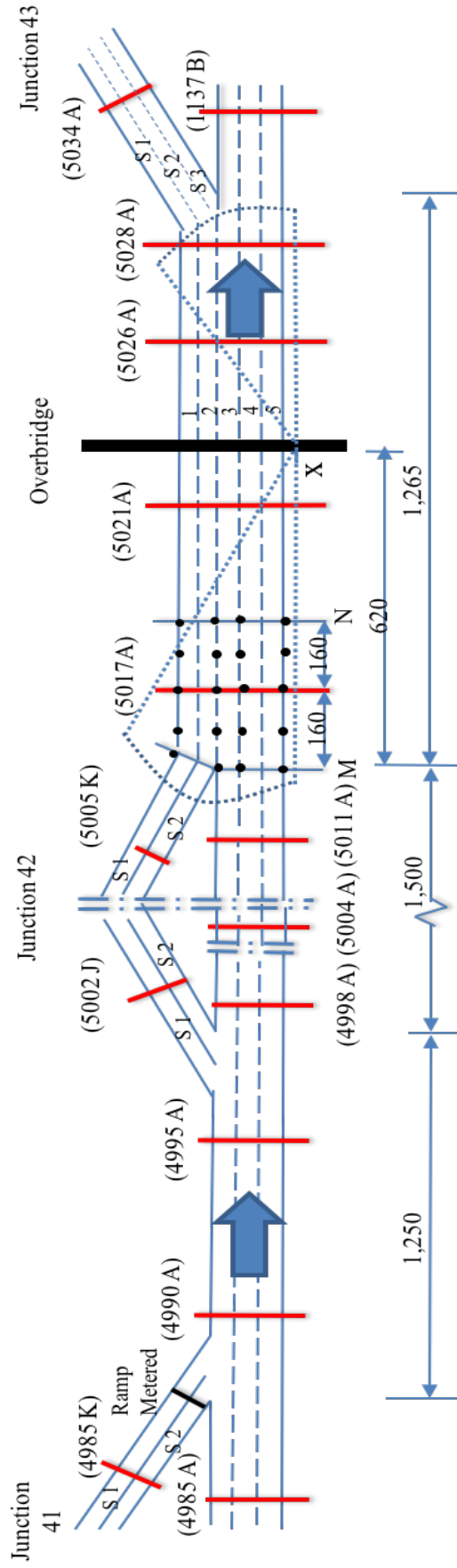
Legends:

― ( ) : MIDAS loop detector location and (loop detector ID)

▬ : The over bridge where the video recording at J 42 was made at X point

: The reference points

● 1,2 : The Auxiliary lane 1 and Auxiliary lane 2

3,4,5 : The main lanes traffic

S1, S2, S3 : The entry slip or exit slip road lane 1, 2 and 3.

6.2.1 Identifying the loop detector location

The loop detector ID (xxxxy) in the form of a unique number indicates the approximate loop detector location. The "xxxx" consists of four digit numbers that indicates the loop detector position relative to the road chainage, while 'y' is a character, indicating the carriageway as it is seen in **Table 6.1**.

Table 6.1 Road carriageway information in associated with loop detector ID

Approaches	Type	Observing Traffic
	A	Main / Through
Northbound	J	Exit slip road
	K	Entry slip road
	B	Main / Through
Southbound	L	Exit slip road
	M	Entry slip road

Table 6.2 shows all loops detector together with the lane-coverage over the observation area between J 41-42 while **Table 6.3** shows all loop detectors in J 42-43.

Table 6.2 Loop detector location and lane coverage at J 41-42

Section	Loop Detector ID	Lane Coverage
	4985 A	3, 4, and 5
	4985 K	S1, and S2
	4990 A	3, 4, and 5
J41 - J42	4995 A	3, 4, and 5
	4998 A	3, 4, and 5
	5002 J	S1, and S2
	5004 A	3, 4, and 5

Table 6.3 Loop detector location and lane coverage at J 42-43

Section	Loop Detector ID	Lane Coverage
	5005 K	S1
	5011 A	3, 4, and 5
	5017 A	1, 2, 3, 4, and 5
	5021 A	1, 2, 3, 4, and 5
J42 – J43	5026 A	1, 2, 3, 4, and 5
	5028 A	1, 2, 3, 4, and 5
	5034 A	3,4,5
	1133 B	3,4,5

For example, the distance between two loop detectors 5021A and 5017A, the estimation, initially, divides the 'xxxx' element of the loop detector ID with 10 (default number) in order to define the loop detector relative location. The relative location of 5021 A and 5017 A) are thus 502.1 km (5021/10) and 501.7 km (5017/10). Note that the chainage of M1 section refers to London as the benchmark. The distance between those two loop detectors is thus 502.1-501.7=0.4 km or 400 m.

6.2.2   Managing MIDAS loop detector data

The downloaded binary-format files of MIDAS loop detector are required to be reformatted into CSV files. MIDAS provides the conversion application namely 'TCD to CSV GUI'. This application is can be downloaded freely from www.midasinfo.co.uk. The application aids the extraction and filters the loop detector information based on the road network, carriageway and the loop detector ID's.
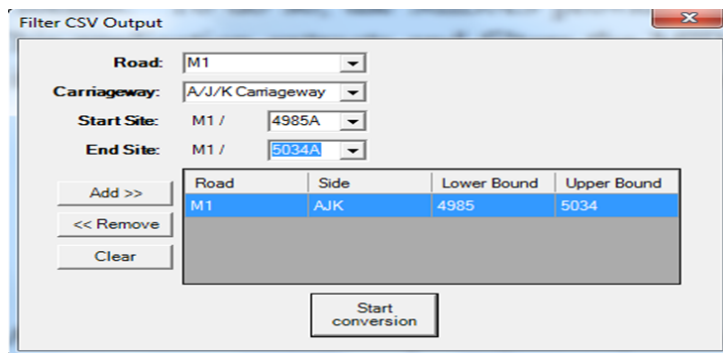
Figure 6.3 TCD to CSV GUI interface

Figure 6.3 shows the interfaces of TCD to CSV GUI. It shows the example of loop detectors conversion at the observed section (J41 to J43).

The converted MIDAS output files consists of several information namely the loop detector ID, observation time and date, flow category, mean spot speed (km/h), total flow (number of vehicles), average occupancy (%), and average headway/gap (sec). In addition, all MIDAS data are aggregated into one-minute data for each observed lane. Following list presents the detail information of MIDAS loop detector data;

- MIDAS defines the traffic flow category as the total vehicle that passes the loop detector within one-minute period of time. Moreover, there are five vehicle categories in MIDAS in terms of the length of vehicle as shown in **Table 6.4**.

Table 6.4 Vehicle categories in MIDAS

Vehicle Categories	Length of Vehicle (metres)
1	0 – 5.2
2	5.2 – 6.6
3	6.6 – 11.6
4	>11. 6

- The speed (km/h) is the average speed for all vehicles for one-minute period on each lane.
- Total flow (veh/h) is the total of vehicles that passing the loop detector during one-minute period. MIDAS records the flow in the lane basis.
- The average occupancy level is defined as a percentage of time that the detector considered as vehicle presence during one-minute period. The occupancy level will vary from 0 – 100 %.
- The headway is defined as the average time between successive vehicles that passed the counting site during the observation time. The units of the headway are $1/10^{ths}$ of a second. MIDAS loop detector is able to record and measure the headway among the vehicle, if it is between 0.0 to 25.4 sec. In this case, the loop detector uses maximum default value (25.4 sec) for the aggregated one-minute period headway analysis, if the recorded headway is larger than 25.4 sec.

MIDAS data have a significant role in the validation process of the traffic video dataset and illustrates the traffic characteristic at the observation location. This PhD research utilises MIDAS data to capture the ambient of the downstream traffic that it might affect

the driving behaviour in the weaving section. Several previous studies used MIDAS data as their based line dataset in the validation processes, for example; Al-Jameel (2011), and Wang (2006).

6.3 Vehicle Trajectory Data

Traffic surveillance is a method to capture the driving behaviour at the observation location. This research classified the traffic surveillance method based on their data extraction approach. In general, there are two well-known systems, namely automatic and manual systems.

The automatic system is somewhat an advanced image processing where the video contains the metadata of the vehicle characteristics, for example; NGSIM. This method needs extensive methodology and it is a large scale project. NGSIM is widely used in the USA, where many of researches utilise the NGSIM data to develop driving behaviour modelling (i.e. Koutsopoulos and Farah, 2012; Toledo et al., 2007b, 2005)

The manual traffic surveillance camera is relatively modest and demands less operational cost when compared to the automatic traffic surveillance systems. Standard recording devices (i.e. video camera, memory stick and tripod) and installation procedures simplified the data collection process. This approach is commonly used for investigating the driving behaviour especially in i.e. Al-Jameel (2011), Kusuma and Koutsopoulos (2011), Wang (2006), Yousif and Al-Obaedi (2011). However, this approach requires an extensive effort on the data extraction and data management processes.

6.3.1   Traffic video recording

The traffic video recording in this research assists the researcher in capturing the vehicle characteristics and movements in the observation area. This study should obtain permission previously from the Highways Agency for utilising their CCTV on the observed location, with the purpose for gathering high quality and clear image of the traffic movement. Unfortunately, the request was declined due to the data protection regulation. The research is consequently decided to observe and record the traffic with a standard video camera.

Figure 6.4 Traffic video camera recording (main camera)

Figure 6.4 illustrates the traffic video recording process. The video recording was made from an overbridge located at Sharp lane, 620m downstream from J42. This study uses two different cameras to record both upstream and downstream traffic movement. The main camera (Canon MVX200) faced the upstream traffic at J42 and recorded all of five traffic lanes. Second camera (Kodak Zi8) faced the J43 and recorded the traffic between the overbridge and the exit ramp. The trajectory data was extracted using a semi-automated vehicle trajectory extractor application by Lee et al. (2008). Due to the software limitation, the detailed trajectory data are only available for the first 320 m from J42 (between points M and N in **Figure 6.2**). The rest of the data have been exclusively used for creation of local origin-destination analysis and number of lane changes. In addition, the speed and flow information from MIDAS database has been used to validate the trajectory data. As mentioned previously, the video recording was taken on Thursday 16th June 2013. More details of the video recording location can be seen in **Figure 6.2**.

6.3.2 Vehicle trajectory extraction process

This research applies the Trajectory Extractor software (Lee et al., 2008) to identify and record the positions of individual vehicles over the observed weaving section. The software is specifically designed for video recordings of traffic moving along the sight (longitudinally). Meanwhile, NGSIM (FHWA, 2006) is operated for recordings of traffic moving horizontally across the frame.
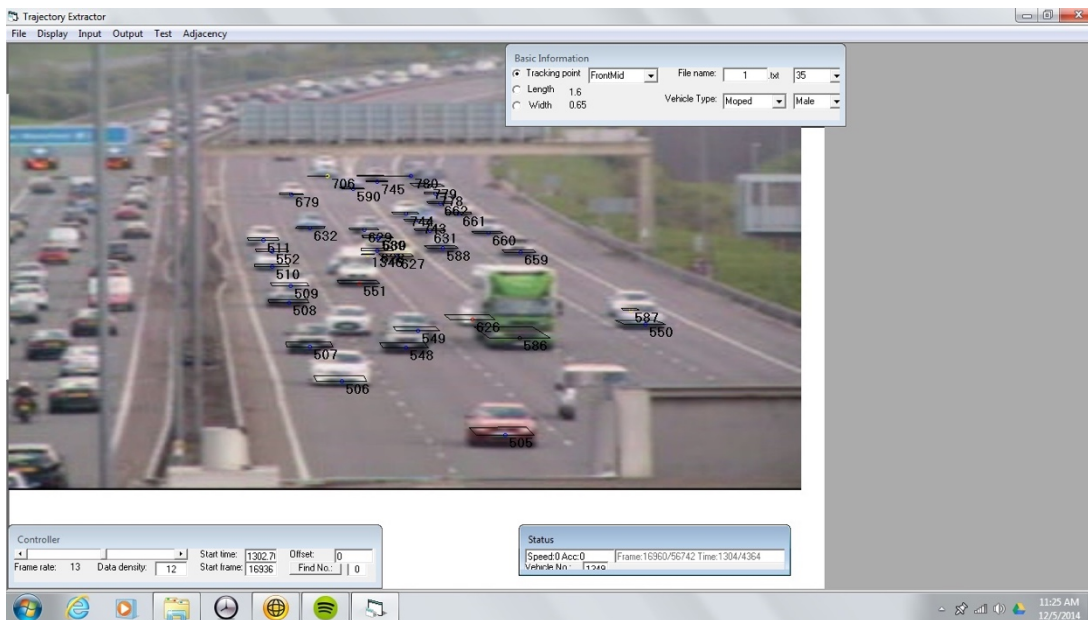
Figure 6.5 The interface of trajectory extraction software (Lee et al., 2008)

Moreover, the Traffic Extractor software provides the information including the type and the (x, y) coordinates of the observed vehicles for each time frame. This software classifies the vehicle type based on the vehicle length, and in our study they are grouped into:

- Small vehicles (average length 4.3m)

- Van (5m)

- Heavy vehicles (11m)

The data extraction process is a semi-automatic vehicle trajectory extractor application. Briefly, the extraction process follows the following process:

1. Define the type vehicles and the observed vehicle ID, once the subject vehicle enters the observation area.
2. The observer requires to direct the cursor toward the middle section of the vehicle front rear.
3. Clicking the cursor, the application records the observed vehicle type, location (x, y coordinates) and time frame into a vehicle trajectory database (csv format). Then, the video will move forward at specific time step. The study setup the time step to be 1 sec as suggested in the previous study.
4. Follow the step 2 and 3 to record the observed vehicle trajectory at the observation area.

5. Once the vehicle passes the observation, the observer may continue with the following observed vehicle by followed the step 1.

Identifying the specific object location (x, y coordinates) at the observation area is critical phase in the vehicle trajectory extraction process. This phase is aimed to ensure that the video footage presents the observed location in the real world. Hence, a high quality aerial map is used as the baseline map. This phase needs to be done before the extraction process.

The object location identification process in this research has been done for two times which are Google Maps and Google Earth. The first validation process used the Google maps. However, there is a difficulty in identifying the geographical of co-ordinate and performing the distance measurement due to unavailability of the features in a google maps. The current work, therefore, uses the Google Earth which is a free open source and provides flexibility for the user to mark and identify the geographical co-ordinate of the interested point. This application is the extension of Google Maps which is equipped with spatial measurement features.

The vehicle trajectory extractor (Lee et al., 2008) adopts the photogrammetry approach for transforming the pixel of the video footage to the geographical coordinate (real world) or vice versa (Mikhail et al., 2001). Briefly, an eight-parameters transformation method for each (x,y) coordinates is adopted in the transformation process. The estimation requires at least four references points in the real-world condition which correspond with a specific point in the video footage. Note that, the current research proposes 20 references points (see **Figure 6.2**), where the minimum reference point is four. A large number of reference points assists to increase the accuracy level of the transformation process. The references points in the x-axis are located for every 80m (x-axis) over the observation area.

The extraction process takes a significant role in order to ensure the data quality. This phase is time consuming, and requires high concentration during the extraction processes. This study acknowledged several factors which affect the data quality: the video footage quality, playback control and obscuring view from the leading vehicle. High variations of speed and acceleration profiles in the raw trajectory dataset indicate the appearance of measurement error during the extraction process. Hence, this research uses the locally weighted regression method to smoothing the vehicle trajectory profile.

6.3.3 Locally weighted regression

Locally weighted regression is a method to estimate a regression surface through a multivariate smoothing procedure. Cleveland (1979) introduced this method by adapting the iterated weighted least squares technique in order to minimise the deviation points that distort the smoothed data. Furthermore, Cleveland et al. (1988) extended the discussion regarding the concept, properties and the estimation algorithm of the locally weighted regression. Their research applied the algorithm in numerous applications such as explanation of graphical analysis explanation, fitting the field data distribution due to the objective function, and the simulation results. Moreover, they found as well that the locally weighted regression is involved while the dependent variables are a function of the independent variable.

This approach has been widely used in microscopic behaviour modelling for smoothing the vehicle trajectory in order to gather less variation in both speed and acceleration of the observed vehicle (e.g. Punzo et al., 2011; Toledo et al., 2007a). Assuming that the vehicle trajectory is a function of time (t):

$$f(t, \beta^{loc}) = loc(t) + \varepsilon(t) \tag{6.1}$$

Where;

$f(t, \beta^{loc})$: Function of the observed vehicle fitted location at the time (t) by the local regression

$loc(t)$: Observed vehicle location at the observed time

β^{loc} : Vector parameters of the estimated curve, and $\varepsilon(t)$ a normally distributed error term.

The fitting process is estimated locally by using the weighted neighbourhood points with their distance to the observed point. The proportion of neighbourhood points in the estimation depends on the span size or degree of smoothing (θ) that varies between 0 and. ∞. A larger span size leads the fitting result into a linear form. On the other hand, small span size is less neighbourhood points in order to try fitting the observation in a curve forms.

The estimated function $f(t, \beta^{loc})$ follows the weighted least-square estimation with the N observation of each vehicle inside the defined time (t) window. Moreover, the objective function of the locally weighted regression is aimed to minimise the deviation

between the observed vehicle trajectory and the global polynomial curve. The Equation is written as;

$$\min_{\beta}[LOC - f(t, \beta^{loc})]' \dot{W}[LOC - f(t, \beta^{loc})] \tag{6.2}$$

Where;

LOC : Column vector of the N position observations used to estimate a trajectory function,

$\dot{W}$: [NxN] matrix with elements corresponding to weight of observations used for local regression.

The computation process of locally weighted regression involves three elements namely;

- The locally weighted objective function.

- The span size which is the parameter that control the Degree of Smoothing (θ).

- The weight assignment for each observed vehicle location within the local regression span.

Several weight conditions $(\dot{w}(u))$ have been applied in order to represent the time function (u) between the observed location and the interested point. Cleveland et al., (1988) defined that the smooth weight shall produce smoother estimates. Higher weights to the observed data will be more fit to the point of the interest and satisfy the below condition:

$$\dot{w}(u) \geq 0 \tag{6.3}$$

$$\dot{w}(u) = 0 \text{ for } u \geq 1 \tag{6.4}$$

$$\dot{w}(u) \text{ is non-increasing for } u \geq 0 \tag{6.5}$$

Moreover, Cleveland et al. (1988) found that a tricube weight function is decent option to capture the optimum results. The tricube function is written:

$$\dot{w}(t_0, t) = (1 - u(t_0, t)^3)^3 \tag{6.6}$$

while,

$$u(t_0, t) = \frac{|t - t_0|}{d_0} \tag{6.7}$$

Where;

$\dot{w}(t_0, t)$: Weight assigned to the observation at time t in fitting a curve centred at t_0

$u(t_0, t)$: Normalised measure of the time difference between t_0 and t

d_0 : Distance from t_0 to the nearest point outside the span of N points to be considered in fitting the curve

The weight assignment and the span size affect significantly the bias and the variance of the fitted locations in opposite direction (Cleveland et al., 1988). Additionally, the bias has linear relationship with the span size or degree of smoothing (θ) , which varies between 0 and ∞. A large span size leads the fitting result into a linear form. A small span size on the other hand focuses on the neighbourhood points and tries to fit a higher order polynomial curve.

This PhD thesis has tried several span sizes value 0.8, 0.9, and 1 with second polynomial order when fitting the trajectory. Note that, the acceleration is the second derivative of the vehicle trajectory. The estimation is performed by using "R" programming package, which known as LOESS. Moreover, the Mean Absolute Error (MAE) assists to evaluate the goodness-of-fit between the observed vehicle trajectory data and the fitted vehicle trajectory corresponding with those observed span size. MAE is written as follows:

$$MAE = \frac{\sum_{t=1}^{T} |loc(t) - \widehat{loc(t)}|}{T} \tag{6.8}$$

Where;

$loc(t)$: The observed vehicle location

$\widehat{loc(t)}$: The estimated vehicle location

t, T : Observation time period for each vehicle

Figure 6.6 illustrates the distribution of goodness of fit from the observed span size. The Mean Absolute Error (MAE) distribution of observed individual vehicles is skewed to the left with mean values of 0.089m, 0.12m, 0.125m due to various span size 0.8, 0.9 and 1, respectively. A relatively small average MAE indicates that the measurement provides a reliable trajectory data. By analysing both Mean Absolute Errors (MAE) and the vehicle profiles, a span size 0.8 has been selected (MAE ±0.089m). The 0.8 span size provides optimum computational iteration result and relatively smooth profile of

the estimated vehicle trajectory, speed and acceleration in comparison to the other tested span sizes. It is worth noting that the result of MAE does not represent the average measurement error of the trajectory dataset. The value represents the deviation between the observed and the fitted trajectory dataset.

Overall, the loop detector data captures and identifies the aggregated traffic characteristics over the specific section of the road, whilst the vehicle trajectory data assists in disaggregated traffic with level of details. Additionally, the second-by-second individual vehicle trajectory data were extracted for the first 320m of the weaving section and across all five lanes (including two auxiliary lanes**).**
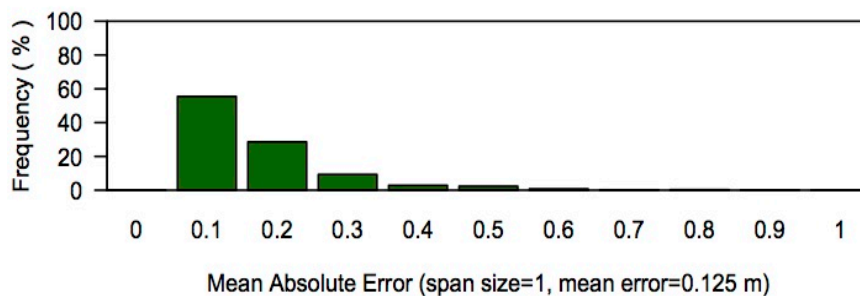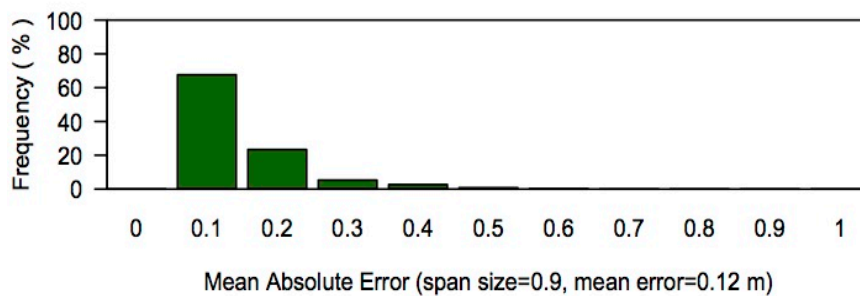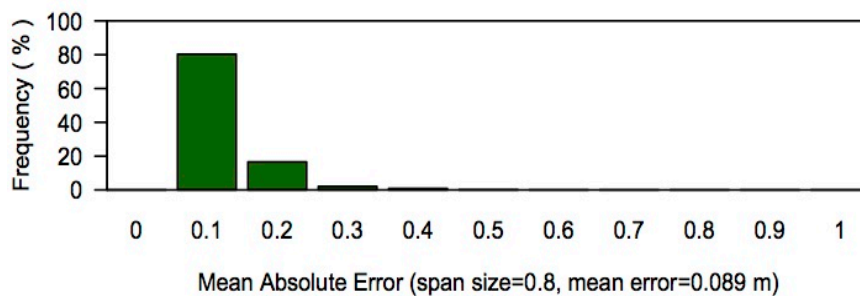
Figure 6.6 Distribution of goodness of fit between the observed vehicle trajectory data and the fitted different span sizes (a) 0.8, (b) 0.9 and (c) 1
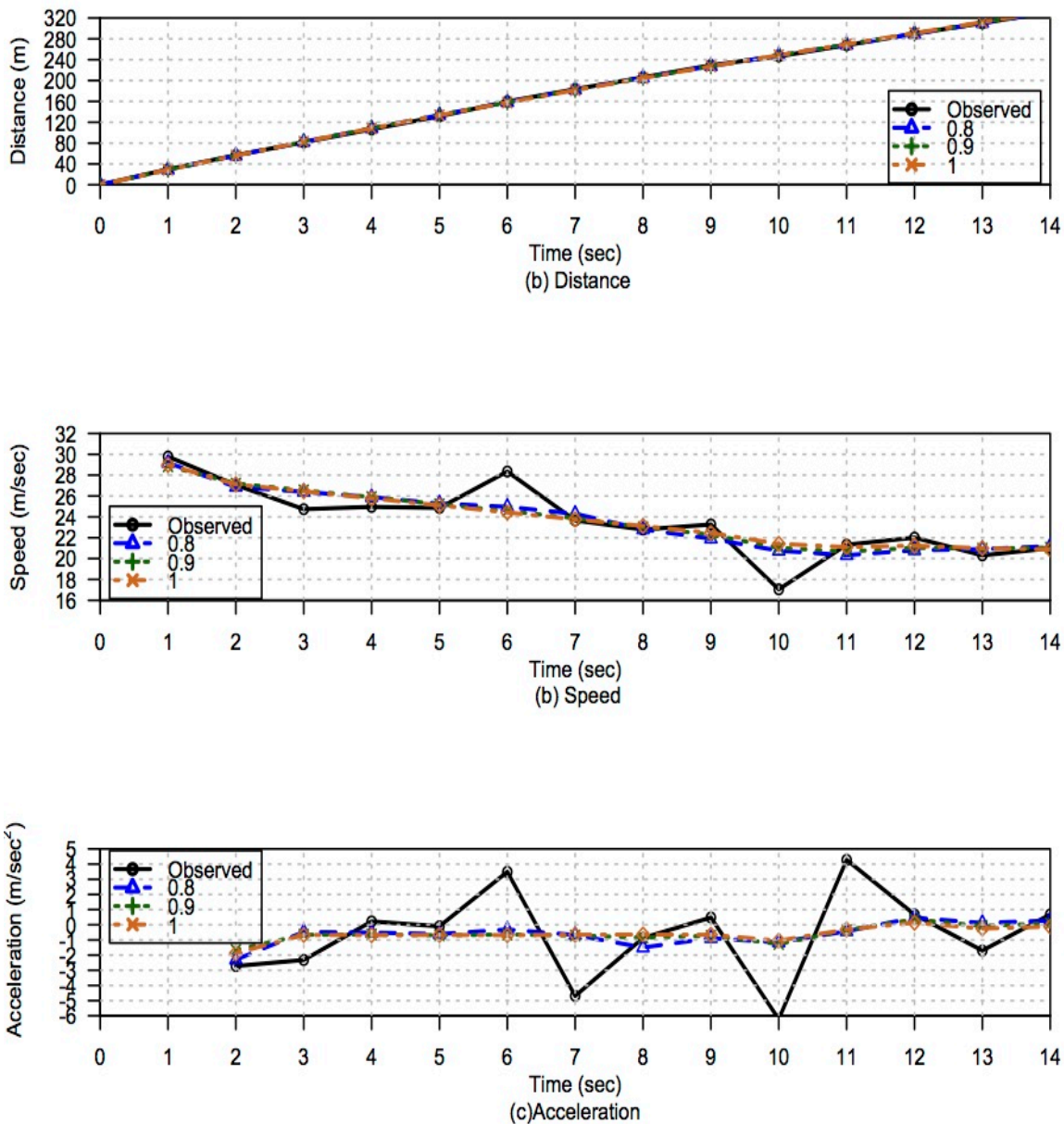
Figure 6.7 An example of locally weighted regression estimation with different span
size

6.4 Traffic Analysis

MIDAS loop detector located 160m downstream from the merge nose of J42 (**Figure 6.2**) showed that the evening peak occurs between the 16:45-17:45, with the total flow 5,646 veh/h. MIDAS data analyse under HCM 2010 algorithm implies that the weaving section is in a moderate traffic flow with Level of Service (LOS) C. Detail weaving section capacity analysis is presented in Appendix-A

However, this study faces a limitation in extracting all vehicles trajectory during the one-hour evening peak period due to the limitation of software and human resources. As mentioned earlier, the extraction process is performed semi-automatically where the researcher has to follow individual vehicle with specific time step. In this case, the trajectory is extracted with 1-sec time step. Consequently, the current work focuses only on the highest 15 min of the one-hour evening period, between 17:15-17:30.

6.4.1   Traffic flow variation

During 17:15-17:30, MIDAS loop detector (5017A) data recorded 1,453 vehicles. The traffic flow variations denote that the main lanes traffic (lane 1, 2, 3) take 59.1% of the total traffic during the auxiliary lane, that is around 40.9% in average during the 15 min period. Also, most of the traffics prefer to move in lane 3 and 4. Contrarily, less traffics move on lane 5 (far-side) which is designated for the fast moving traffic.

Detailed analysis of the MIDAS loop detector data has been performed to investigate the variations of flow patterns in the weaving section. **Figure 6.8** shows the propagation of one hour aggregated traffic flow and speed respectively between J 41-J42 (Detectors 4985A- 4998A) and J42-J43 (Detectors 5011A-5028A) respectively over the afternoon peak period. Noted that, detector 5004 is located between the two weaving sections

40% of the traffic observed between J41-J42 took the exit at J42 towards M62 or leave the motorway network. Even higher traffic flow entered the motorway using the on-ramp at J42, which ultimately resulted in an increased in total flow in between J42-J43 compared to that between J41-J42. Exact proportion of the on-ramp traffic is unavailable due to malfunctioning loop detectors located at J42.

The speed propagation analysis (see **Figure 6.8**) shows that there is a speed drop at Detectors 4990A and 5017A, located at the start of the two weaving sections (J41-J42 and J42-J43). This could be due to increased lane-changing activities. The average speeds are in the range of 105-112km/h at the J41-J42 (4985A–4998A), and 109-112km/h at the J42-J43 section (5011A-5028A), which is around the speed limit (112km/h). The presence of auxiliary lanes in J42-43 provides additional capacity and could contribute to discharge the delay and isolate the slow moving merging and diverging traffic from the mainline

Figure 6.8 illustrates that both weaving sections reach the peak traffic flows between 16:45:00-17:45:00. It is worth pointing out that the significant different in total traffic flow between those sections are due to the difference in number of lanes (**Figure 6.2**). A low traffic condition is shown from Detectors 4998A to 5011A, the section between off- and on-ramps at J42.
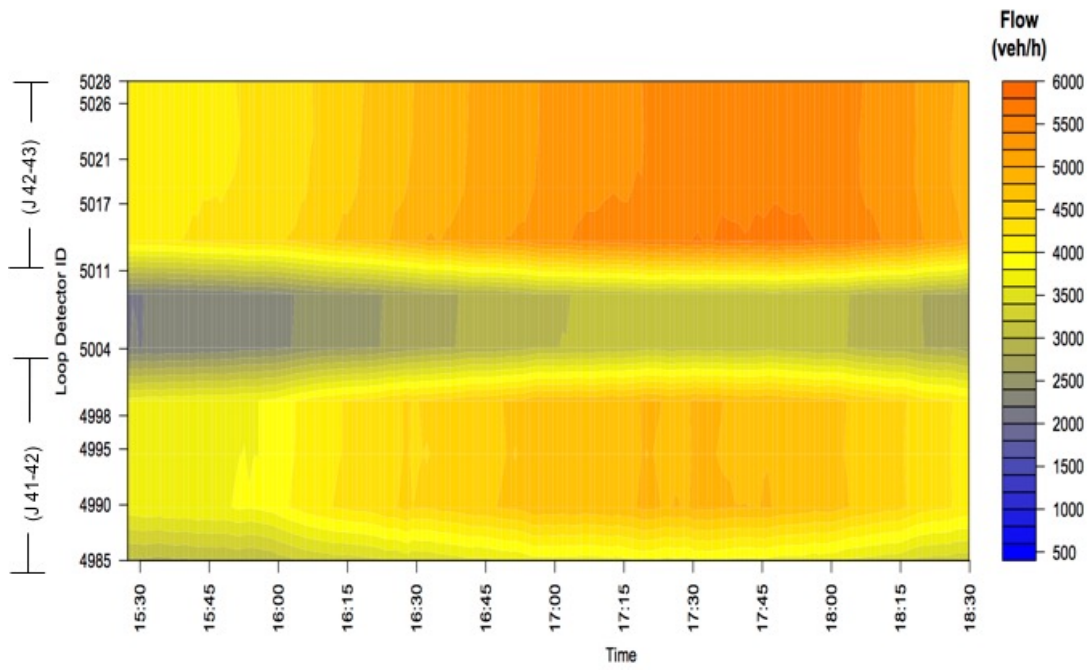
(a) Traffic flow propagation
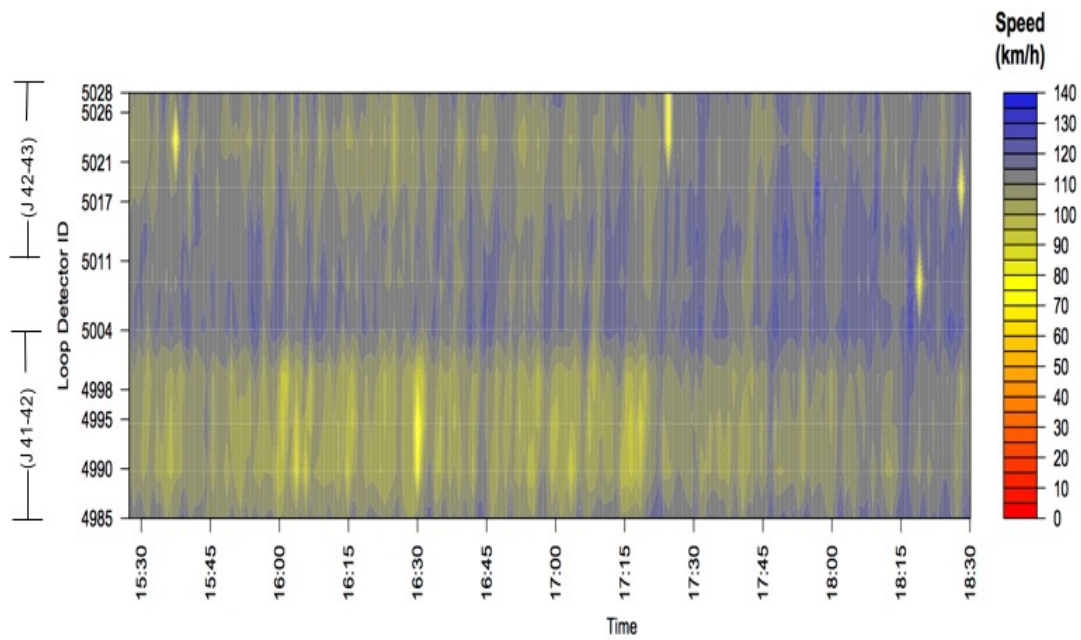
(b) Speed propagation

Figure 6.8 Aggregated traffic flow (a) and speed (b) at the weaving section

From the video recording, we extracted 17,981 trajectory data points from 1,386 vehicles observed during the period. From the vehicle trajectories, we can trace their origin and destination movements over the section between J42 – J43. As shown in **Figure 6.9**, the observed weaving section has two origin nodes (A and B) and two destination nodes (C and D). The observed OD traffic volumes are shown in parenthesis in **Figure 6.9**.
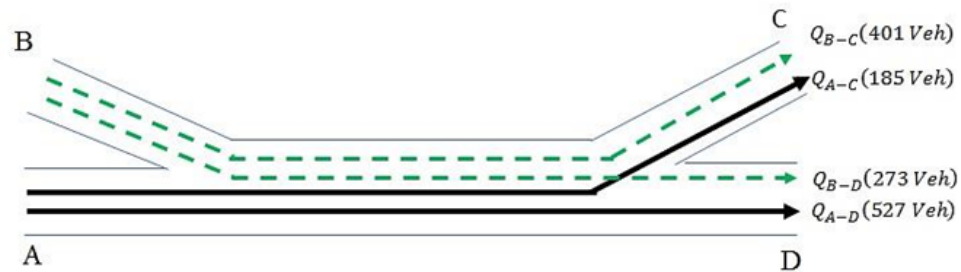
Figure 6.9 Schematic of origin-destination in the weaving section (based on traffic video recording)

Analysing both video cameras recording during the highest 15 minutes period (17:15-17:30), several key findings of the observation are listed below:

- 731 (52.7 %) of the traffic observed in the video data made lane changes during the observation period.

- 458 vehicles $(Q_{A-C} + Q_{B-D})$ required a mandatory lane-changing movement whether to exit from the motorway through lane 1 and 2 or merged into the main traffic on lane 3, 4, and 5. This type of lane changing is approximately 62.7% of the total lane-changing traffic.

- Around 95.0% of the total lane-changing traffic took place in the upstream section while a small proportion (5%) of lane-changing traffic resulted after the overbridge.

- Most vehicles made a single lane change (73.8% of total lane-changing traffic) while the rest made multiple changes.

- The maximum number of lane changes caused by vehicles was 3. This situation typically took place for vehicles that merged or diverged from the main traffic.

- The traffic composition (of the 1,386 vehicles from the video recordings) were as follows: Small vehicles (84.9%), Vans (10.6%), and Bus and heavy vehicles: (4.5%).

Furthermore, the detailed of origin destination on the observed weaving section (**Figure 6.9**) is presented in **Table 6.5**. The analysis is based on the fitted trajectory second-by-

second trajectory data and incorporates the lane-changing movement over the observation area. The vehicle trajectory dataset assists in identifying the subject vehicle characteristics (i.e. speed and acceleration). Meanwhile, 662 out of 731 lane changing vehicles (95%) involves in the lane-changing movement in the first 320m of the weaving section. Giving this proportion of the movement lets the study to focus on the upstream movement as less traffic (5%) change lane on the part of the weaving section. It is worth noting that the extracted traffic flow is slightly slower than the MIDAS as it recorded 1,453 vehicles resulting in 4.61% difference between the two measurements.

The potential spatial inaccuracies in the data have been a concern in this case and in spite of best efforts, the data are likely to have errors due to the limitations of the video recording tool, pixel resolution, frame rate, camera vibration, camera synchronization and longitudinal and lateral angles. The locally weighted regression (Cleveland and Devlin, 1988) has been consequently used to smooth the observed trajectories and to minimise the errors as shown in **Figure 6.7**.

Table 6.5 Proportion of traffic movement origin and destination in the first 320 m

Origin	Destination									
	1		2		3		4		5	
	No.	%	No.	%	No.	%	No.	%	No.	%
1	251	18.1%	55	4.0%	3	0.2%	0	-	0	-
2	26	1.9%	90	6.5%	119	8.6%	49	3.5%	10	0.7%
3	57	4.1%	157	11.3%	74	5.3%	10	0.7%	-	-
4	4	0.3%	25	1.8%	78	5.6%	185	13.3%	14	1.0%
5	0	-	9	0.6%	15	1.1%	31	2.2%	124	8.9%
Total	338	24.4%	336	24.2%	289	20.9%	275	19.8%	148	10.7%

Table 6.5 demonstrates that the traffic proportion of main lanes (lane 3, 4, and 5) and auxiliary lane traffic (lane 1 and 2) have a relatively similar proportion. Note that the traffic proportions are 51.37% and 48.63% respectively. In terms of the vehicle movements, a significant vehicle proportion on lane 1(18.1%), 4(13.3%), and 5(8.9%)

prefers to maintain their lane through the end observation area. While the situation on lane 2 and 3 is slightly different, most of the traffic on those two lanes involve in the lane changing traffic. Most of the traffic (8.6%) on lane 2 changes lane through lane 3. On the other hand, there is a significant proportion of traffic (11.3%) on lane 3 which moves through lane 2. More details of lane changing movement will be discussed in Section 6.5.

6.4.2 Speed analysis

This section compares the space-mean mean speeds (SMS) obtained from the fitted trajectory data and the time-mean speed (TMS) from the MIDAS data. The MIDAS data of 1min time resolution, collected from the loop detector 5017A (located 160m from the on-ramp nose at J42 and within the video recording section) is used in this aspect.

For the trajectory data, the SMS are initially calculated by using the fitted vehicle trajectory data. These are converted to TMS using the following relationship:

$$\bar{V}_{TMS} = \bar{V}_{SMS} + \frac{\sigma_{SMS}^2}{\bar{V}_{SMS}} \tag{6.9}$$

Where;

$\bar{V}_{TMS}$: The aggregated time-mean speed

$\overline{\bar{V}_{SMS}}$: The aggregated space-mean speed

Table 6.6 shows all lanes with 1min aggregate of the traffic flow, the mean speed of vehicle trajectory data and the loop detector data. The result shows that 15min average TMS is lower than the loop detector data (see the Δ in **Table 6.6**). The average Δ is relatively low which varies between 2.37% (lane 2) and 5.81% (lane 5) during the 15min period. As the result, trajectory extraction process performed appropriately and the data are reliable. However, there are situations when the vehicle trajectory mean speeds are slightly higher than the average speeds i.e. lane 1 at 17:28-17:29 (-0.05%); lane 2 at 17:21-17:22, 17:26-17:27, and 17:29-17:30 (-0.13%, -3.28%, and -1.44%) ; lane 3 at 17:28-17:29 (-1.68%); lane 3 at 17:16-17:17 (-0.43%). The speed difference between the trajectory and loop detector dataset are relatively small which vary between -0.13% and -3.28%. This error may occur due to the video quality, obscured views and/or measurement errors in controlling time steps.

Table 6.6 MIDAS loop detector vs traffic video surveillance average mean speed data (km/h)

(a) Lane 1, 2 and 3

Time	Lane 1					Lane 2					Lane 3				
	No.of Vehicle	Detector	Speed (km/h) Trajector Mean	s.d	Δ	No.of Vehicle	Detector	Speed (km/h) Trajector Mean	s.d	Δ	No.of Vehicle	Detector	Speed (km/h) Trajector Mean	s.d	Δ
	(Σ=300)	(μ=95.00)	(μ=91.11)		(μ=4.07%)	(Σ=334)	(μ=103.20)	(μ=100.74)		(μ=2.37%)	(Σ=328)	(μ=101.47)	(μ=98.39)		(μ=3.07%)
17:15-17:16	15	90	88.78	5.31	1.36%	20	104	103.42	7.96	0.56%	15	106	105.16	6.31	0.79%
17:16-17:17	24	95	88.76	8.30	6.57%	20	109	104.72	9.96	3.92%	15	102	101.86	11.90	0.14%
17:17-17:18	24	96	92.16	10.51	4.00%	13	98	95.63	10.95	2.42%	27	99	93.31	13.18	5.75%
17:18-17:19	21	99	97.07	11.12	1.95%	27	100	97.33	13.74	2.67%	21	95	89.89	12.07	5.38%
17:19-17:20	20	93	91.19	8.53	1.94%	31	103	101.15	10.26	1.80%	19	98	93.31	9.15	4.79%
17:20-17:21	19	99	96.66	12.49	2.37%	25	102	100.32	8.77	1.65%	30	96	93.84	14.64	2.25%
17:21-17:22	18	96	87.30	13.45	9.06%	20	100	100.13	14.12	-0.13%	24	100	89.95	13.21	10.05%
17:22-17:23	17	90	84.47	10.22	6.14%	24	99	91.59	9.87	7.49%	16	100	95.36	9.17	4.64%
17:23-17:24	20	94	91.80	4.40	2.34%	25	103	101.69	10.33	1.27%	26	100	96.27	10.55	3.73%
17:24-17:25	27	94	90.28	11.00	3.96%	18	108	100.82	12.41	6.64%	25	102	102.43	10.79	-0.42%
17:25-17:26	19	97	89.59	9.01	7.64%	19	109	103.55	7.53	5.00%	19	107	102.12	10.79	4.56%
17:26-17:27	16	98	96.38	8.46	1.66%	23	103	106.38	12.59	-3.28%	30	104	103.27	13.27	0.70%
17:27-17:28	19	98	89.02	13.13	9.17%	21	104	101.83	14.03	2.09%	22	106	103.39	10.42	2.46%
17:28-17:29	17	90	90.05	12.18	-0.05%	26	102	97.05	14.84	4.86%	22	102	103.71	13.85	-1.68%
17:29-17:30	24	96	93.13	13.56	2.99%	22	104	105.50	8.40	-1.44%	17	105	101.96	9.07	2.89%
Average		95.00	91.11		4.07%	334	103.20	100.74		2.37%	328	101.47	98.39		3.07%

(b) Lane 4, and 5

Time	Lane 4					Lane 5				
	No.of Vehicle	Detector	Speed (km/h)			No.of Vehicle	Detector	Speed (km/h)		
			Trajectory Mean	s.d	Δ			Trajectory Mean	s.d	Δ
	(Σ=333)	(μ=113.6)	(μ=109.02)		(μ=4.00%)	(Σ=158)	(μ=126.2)	(μ=118.79)		(μ=5.81%)
17:15-17:16	21	119	113.08	6.33	4.97%	8	127	120.41	9.66	5.19%
17:16-17:17	17	114	114.48	10.03	-0.43%	10	136	127.87	11.44	5.98%
17:17-17:18	28	114	106.38	9.93	6.69%	22	125	115.30	5.97	7.76%
17:18-17:19	22	111	107.21	12.58	3.41%	13	125	113.51	7.01	9.19%
17:19-17:20	25	116	109.45	11.70	5.65%	13	127	117.80	6.51	7.25%
17:20-17:21	22	110	107.64	9.80	2.14%	15	123	121.65	7.13	1.10%
17:21-17:22	24	107	104.69	8.64	2.16%	15	118	110.86	9.15	6.05%
17:22-17:23	19	113	108.54	8.02	3.95%	11	125	116.68	5.36	6.66%
17:23-17:24	22	111	105.25	5.17	5.18%	8	125	121.99	9.47	2.40%
17:24-17:25	22	117	113.47	10.48	3.02%	1	126	122.44	2.46	2.83%
17:25-17:26	15	115	110.35	7.53	4.04%	3	123	122.44	2.46	0.46%
17:26-17:27	26	111	107.74	8.08	2.94%	6	126	116.34	6.25	7.67%
17:27-17:28	19	116	104.68	10.01	9.76%	15	134	118.34	13.44	11.69%
17:28-17:29	28	111	110.69	10.01	0.28%	13	122	121.75	13.47	0.21%
17:29-17:30	23	119	111.62	13.14	6.20%	5	131	114.40	7.74	12.67%
Average	333	113.60	109.02		4.00%	158	126.20	118.79		5.81%

Where; Δ: the relative difference between the mean of the trajectory data and the detector data (5017A), Σ: the total of the vehicle, and μ: the mean value of the observed vehicle.

6.4.3 Characteristics of subject vehicle

The characteristics of subject vehicle including the speed and acceleration are analysed based on the fitted trajectory data. **Figure 6.10** illustrates the interactions between subject and neighbouring traffic including current lane front vehicle, and both target lane lead and lag vehicles.
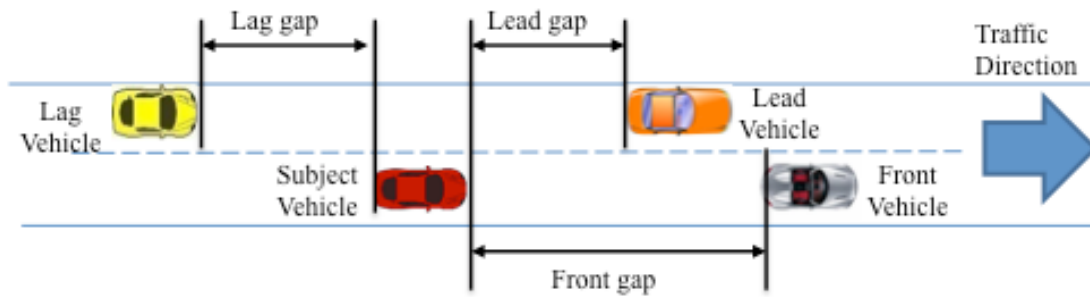
Figure 6.10 Interaction between subject and neighbouring traffic (front, lead and lag vehicles)

Table 6.7 describes the descriptive statistics of speed and acceleration of subject vehicle characteristics, which are based on the fitted trajectory dataset of 1,386 vehicles (17,981 observation). The analysis shows that the speed in the observation varies between 18.76 m/sec (67.52 km/h) and 37.87 m/sec (136.34 km/h) with mean value 26.75. 19.5% of the traffic moves over the speed limit in corresponds with the UK traffic rule. Note that the speed limit on the UK' motorways is 31.11 m/sec (112 km/h or 70 mi/h).

Table 6.7 Descriptive statistics of subject vehicle characteristics

Variable	Mean	Std Dev	Median	Minimum	Maximum
Speed (m/sec)	26.75	4.51	25.96	18.76	37.87
Acceleration (m/sec^2)	-0.96	1.27	-1.03	-4.36	5.04
Positive (m/sec^2)	1.07	1.29	0.47	0.00	5.04
Negative (m^2/sec)	-1.32	0.85	-1.23	-4.36	0.00

Furthermore, the acceleration in the area varies between -4.36 and 5.04 m/sec^2 with the mean value is -0.96 m/sec^2. The mean value implies that most of the traffic (84.9%) tends to decelerate in the upstream traffic. This finding is similar with the speed propagation profile between loop 5011 A and 5017A in **Figure 6.8** (b). It demonstrates that the traffic speed is decreased in the upstream traffic as the traffic requires adjustment of their lane or creating a safest distance for the lane-changing vehicle mer-

ging into their lane. Note that the distribution of both speed and acceleration of the observed vehicles (1,386 veh ≈ 17,981 observations) are presented in **Figure 6.11**.

(a) Speed (m/sec)

(b) Acceleration (m/sec^2)
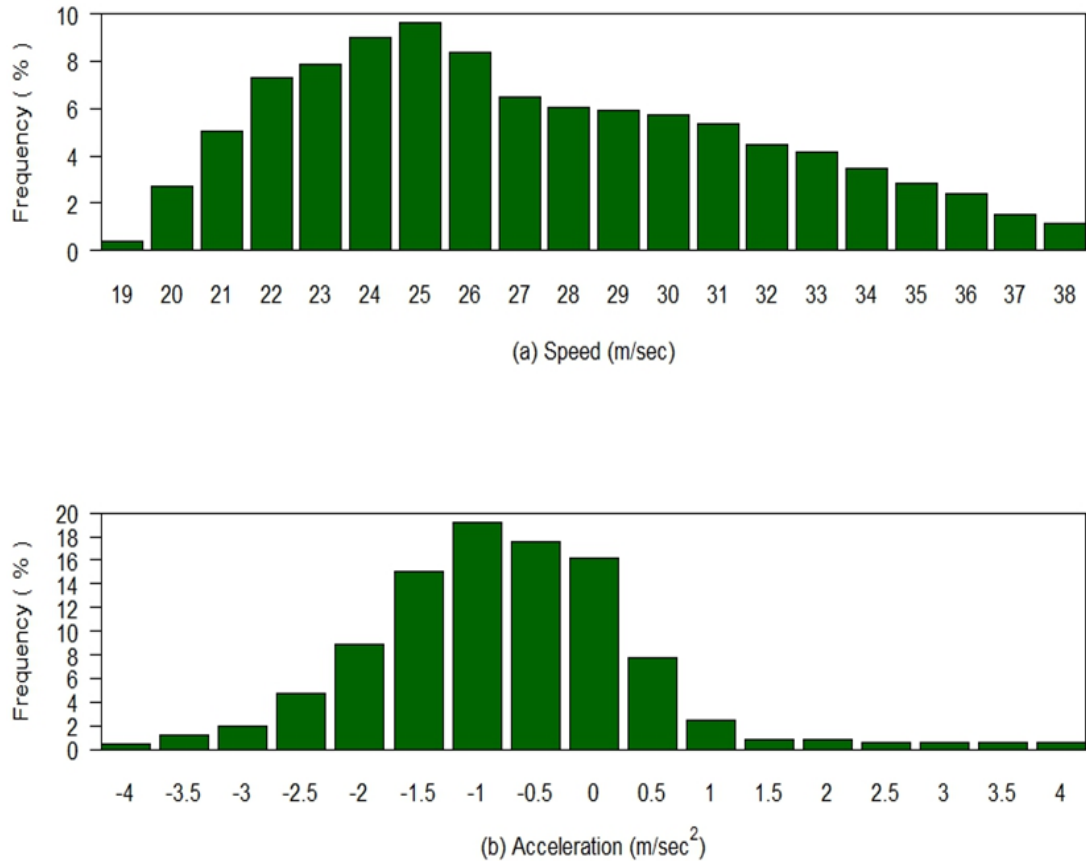
Figure 6.11 Distribution of subject vehicle speed and acceleration

6.4.4 Characteristics of relationship between the subject and neighbouring traffic

Driving behaviour on the motorway is significantly affected by the relationship between subject and neighbourhood vehicles, which are the front vehicle at a current lane, and both lead and lag vehicles at target lane.

As shown in **Figure 6.10**, this thesis represents the interaction between the subject and neighbouring traffic as gaps. There are three types of gap namely; front gap, lead gap and lag gap. This study measures those three gaps as follows:

- Front gap : a time distance between the subject vehicle front rear and the object vehicle back rear at the current lane.
- Lead gap : a time distance between the subject vehicle front rear and the object vehicle back rear at the adjacent / target lane.
- Lag gap : a time distance between the subject vehicle back rear and the object vehicle front rear at the adjacent / target lane.

The time distance gap is a space distance between the subject vehicle front rear and object back rear or vice versa divided by the subject vehicle speed. It is worth noting that the gap measurement is based on fitted trajectory dataset.

Table 6.8 summarises the descriptive statistic of those variables related to the subject vehicle characteristics. It is worth to note that the descriptive statistic of the relationship between the subject vehicle and target lane traffic reflect only the value of both accepted lead and lag gaps. Meanwhile, the descriptive statistic of the relation with the current lane front vehicle is estimated based on the entire data set.

Table 6.8 Descriptive statistics of related characteristics to subject vehicle

Variable	Mean	Std.Dev	Median	Minimum	Maximum
Relation with the front vehicle at the current lane					
Relative Speed[*] (m/sec)	-0.76	4.92	-0.51	-13.49	11.17
Gap (sec)	3.65	2.51	2.95	0.60	12.37
Relation with the lead vehicle at the target lane					
Relative Speed [*](m/sec)	-1.91	4.38	-1.71	-12.78	11.11
Gap (sec)	3.27	2.48	2.71	0.04	10.98
Relation with the lag vehicle at the target lane					
Relative Speed[**](m/sec)	1.35	5.94	1.00	-10.80	16.32
Lag (sec)	5.24	3.48	4.15	0.59	14.16

$*)$ *lead or front veh. speed − subject veh. speed;* $**)$ *lag veh. speed − subject veh. speed*

Figure 6.12 illustrates the distribution of relative speed and accepted gaps between the subject, and neighbouring traffic including the front, lead and lag vehicles. The relative speed mean values between the subject and the current lane front vehicle and target

lane's lead and lag vehicles are -0.76, -1.91 and 1.35 m/sec respectively. This value illustrated that most of the subject vehicle faced a slower front and lead vehicle while the lag traffic tended to be faster than the subject vehicle. This finding confirms repeatedly our previous discussion that the traffic tended to decelerate in the upstream traffic, even though the traffic flow is relatively moderate.
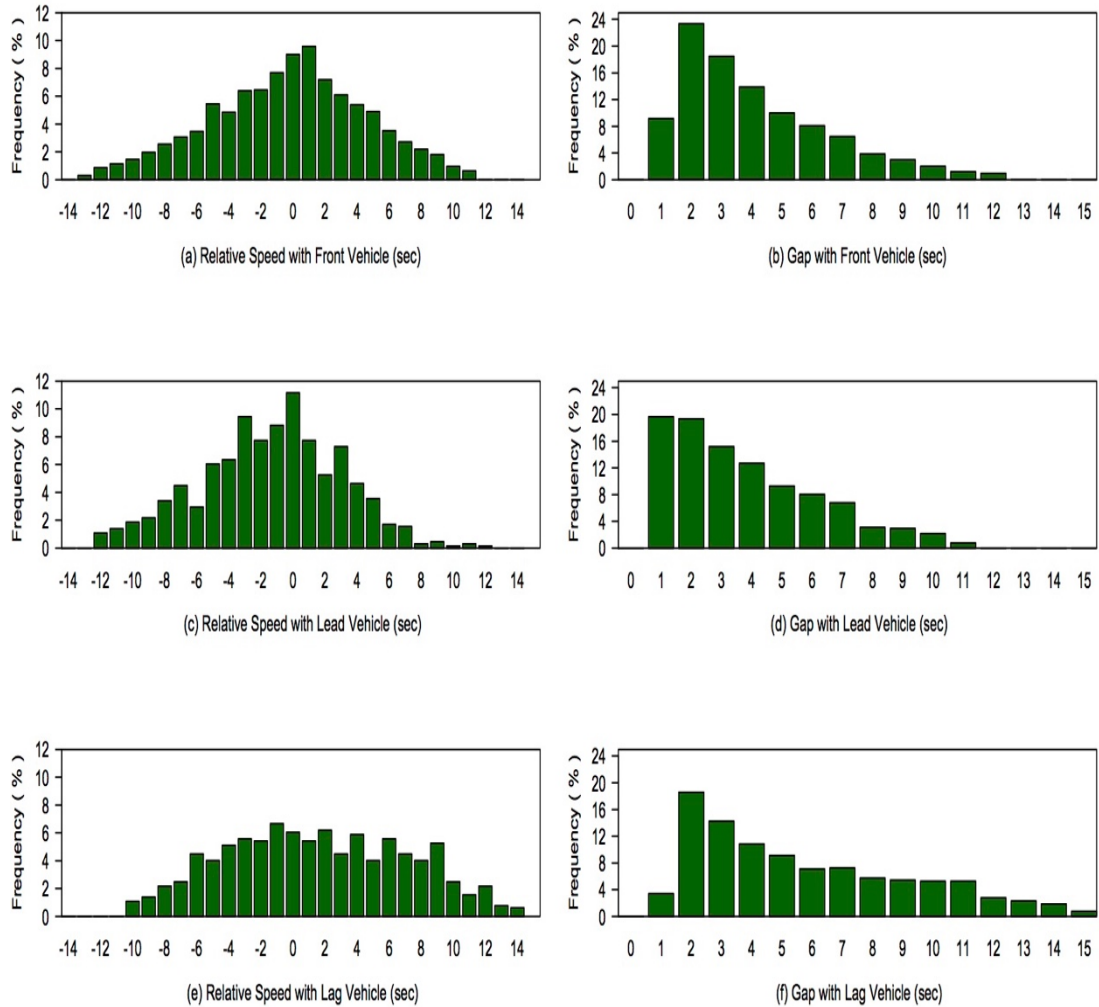
Figure 6.12 Relative speed and gap acceptance between the subject and front vehicle
(a, and b), lead vehicle (c, and d)* and lag vehicle (e, and f)* at target lane

Based on observations associated with execution of lane changes only

In terms of gap acceptance, the accepted gap at target lane varies between 0.04 sec and 10.98 sec with mean value of 3.27 sec and median value 2.71 sec, while the accepted lag is distributed between 0.59 sec and 14.16 sec with mean value of 5.23 sec and median value of 4.15 sec. The values denote that large proportion of traffic accepts smaller gaps rather than a large gap. Moreover, the distribution profiles of gaps fit with

lognormal distribution as they skew to the left hand side. This finding confirms our assumption in the proposed gap-acceptance model in Chapter 4.
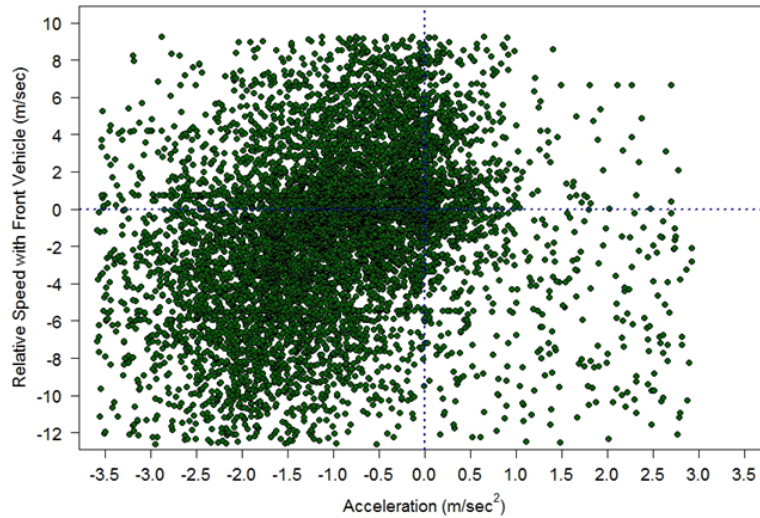
Figure 6.13 Acceleration vs relative speed of front vehicle

Figure 6.13 illustrates the relationship between the acceleration and relative speed with front vehicle. 82% of weaving section traffic involves in deceleration while 43.5% and 38.5% of the deceleration events fall in positive and negative relative speed. In fact, the rest of vehicle trajectory data are acceleration events (18%). Furthermore, this finding is confirmed as well by the speed propagation profile between loop detectors 5011-5017 (see **Figure 6.8**) where the speed tends to decrease from 120 km/h to 80 km/h.

The relationship between acceleration vs relative speed of front vehicle supports the acceleration model hypothesis saying that the traffic moves under decelerating regime over the beginning of weaving section. Although the front vehicle moves faster, the subject vehicle at the beginning of weaving section tends to accelerate in corresponds to anticipate or pre-emptive lane changing movement. Therefore, it is necessary to omit the relationship between stimulus and response conditions to capture the acceleration behaviours in weaving section due to the high proportion of lane changing.

6.4.5 Lane occupancy

As mentioned earlier, the lane occupancy defines as a percentage of time that the detector records the presence of a vehicle on basis of one-minute period. An increased percentage of lane occupancy implies that the higher possibility of congestion appears at the specifically observed lane.
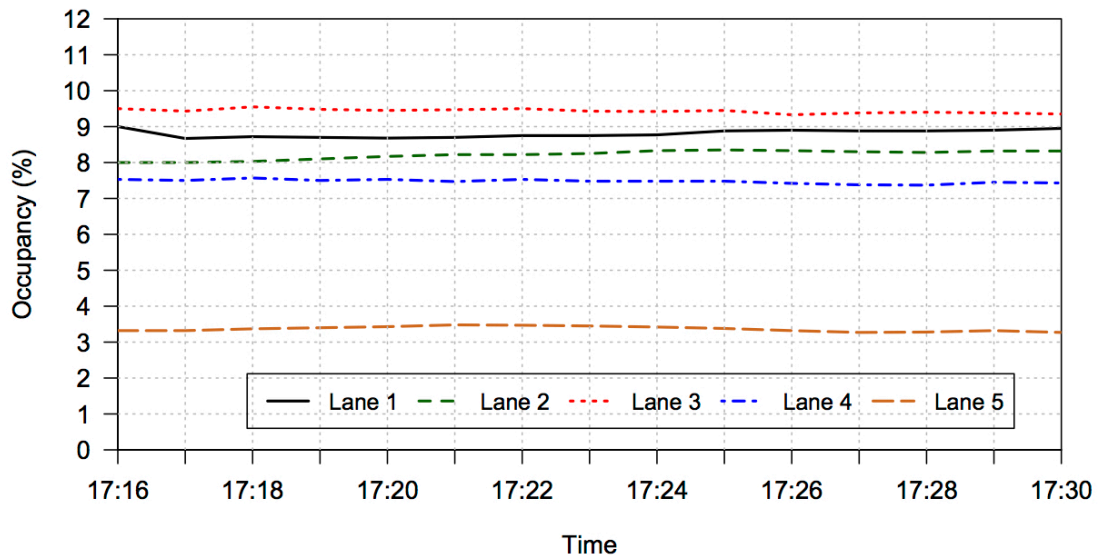
Figure 6.14 Variation of lane occupancy during the observation period

Figure 6.14 represents the occupancy during the observation period showing that lane 3 has the highest occupancy with average of 9.44%. It means that the loop detector in lane 1 is utilised as much as 9.44% in average over one-minute period. Meanwhile, the average occupancy for the other lanes as follows; lane 1 (8.81%), lane 2 (8.21%), lane 4 (7.48%), and lane 5 (3.37%). These findings illustrate that the lane 3 is relatively more congested and preferable. Note that it is relatively more accessible (i.e. exit from- and merging toward the through traffic) compared to the other lanes in the observation area.

This variable in the modelling specification is considered as explanatory variables that affect the target lane choice negatively. In that sense, the parameters of the occupancy variable in the model is expected to be negative.

6.5 Lane Changing Characteristics

In this section, the study classifies the lane changing in terms of: the vehicle's origin lane (before lane-changing), the direction, and the number of lane-changed. From these basic characteristics, this study identifies the vehicles' lane-changing mechanisms including the platoon effect in lane-changing and the involvement in weaving movement.

6.5.1 Lane changing types and strategies

In terms of number of lane-changing performed in the observation area, this study classifies lane changes types into two groups; (1) single lane-changing (SLC) is a vehicle with one lane change over the observation area; (2) compound lane-changing (CLC) is a vehicle with more than one lane-change within the observation area. Moreover, the study postulates two CLC strategies:

Staggered : if the CLC driver has to drive at the intermediate lane and prepare for the following lane-changing to reach its ultimate target lane.

Direct : if the CLC driver moves directly to the target lane.
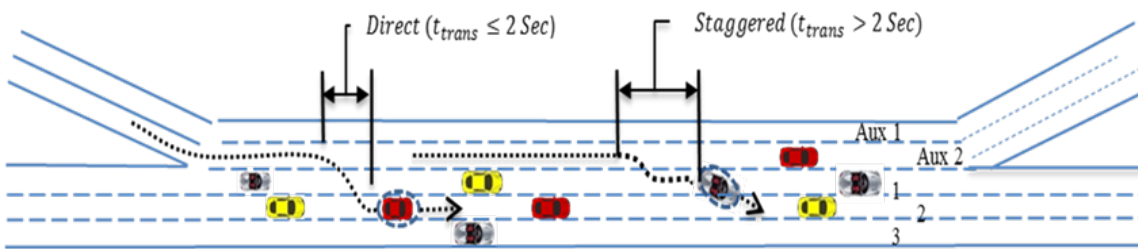
Figure 6.15 Schematic illustrations of lane changing strategies associated with transit time length

The transit time (t_{trans}) is the preferred time length of the lane-changing vehicle, who involves in CLC, to stay and wait at the intermediate lane before performing the following lane-changing. By analysing the fitted trajectory dataset, the transit time (t_{trans}) threshold in this study is 2 sec whether the observed vehicle involves in staggered or direct CLC. With 2 sec transit time threshold, 14% of the CLC are direct CLC where the observed vehicle moves directly to the ultimate target lane. Among the 86% of the staggered CLC, 21% of staggered LC took 3sec transit time and the other 20% took 4sec.

This research structures the relative movement ID (A[BCD]) that consists of unique sign and number that relates to each characteristic type.

A : Origin lane (lane numbers as per. **Figure 6.2**)

B : LC direction left (-) and right (+)

C : Number of lane-changing 1, 2, or 3.

D   : The type of strategies (0) Direct SLC, (1) Staggered CLC, (2) Direct CLC, and (3) Staggered-Staggered CLC, (4) Direct-Direct CLC, (5) Staggered-Direct CLC, and (6) Direct-Staggered CLC.

For example, 2[+10] indicates a relative movement for SLC from lane 2 to the right direction with 1 lane changing required and none of lane changing strategies are required. Meanwhile, 4[-21] indicates a relative movement for the vehicles at lane four who moves to left with 2 lane changing required and direct lane changing strategy.

The video trajectory result shows that 662 vehicles (48.2% of the observed traffic) involves in lane-changing movement during the observation period. In addition, 483 vehicles (35.5%) perform SLC and 179 vehicles (12.6%) perform multiple lane change (CLC). More details of the types of lane changing are presented in **Figure 6.16** as follows:

- Most of the lane changes are SLC (73.8%) while the rest are CLC.
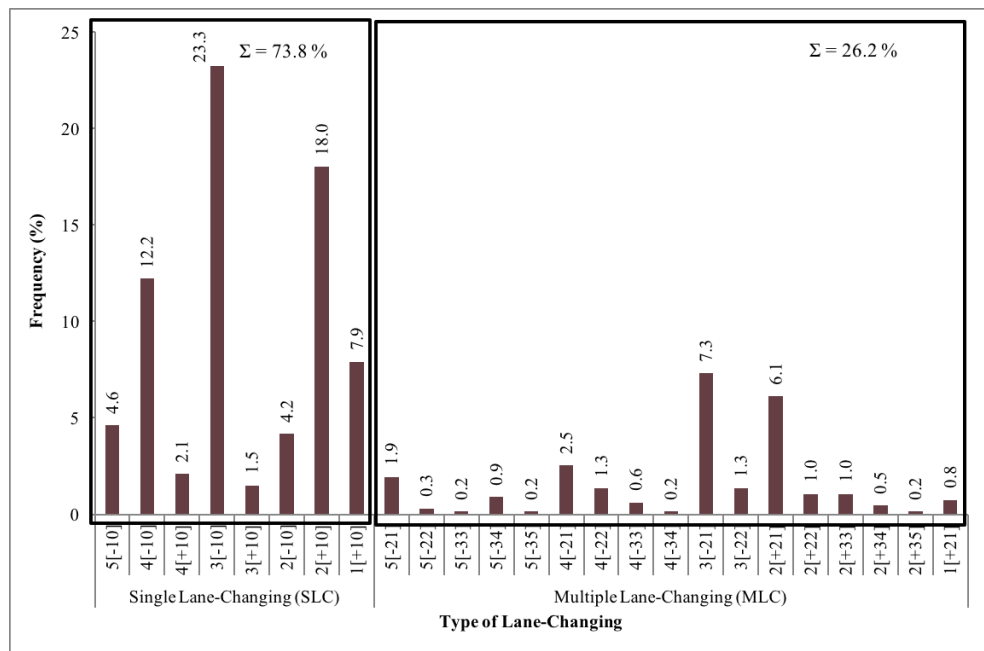
Figure 6.16 Types of lane-changing based on number of lane-changing and strategies

- The maximum number of lane changes made by vehicles is 3. This situation typically occurs for vehicles merging or diverging from the main traffic.

- Most of the SLC appears between lane 3 and lane 2 and vice versa. The most frequently observed type of lane change is an SLC from lane 3 to lane 2 on the left (3[-10]) (23.3%), which consists of traffic diverging from the mainline. This is followed by SLC from lane 2 to lane 3 on the right (2[+10], 18.0%) and SLC from lane 4 to lane 3 on the left (4[-10], 12.2%) respectively.

- A majority of the CLC prefers staggered LC strategy (18.6%) rather than direct one. Performing a direct CLC in a fast moving traffic may be difficult. The CLC drivers prefer to observe and wait for the safest headway to perform multiple lane changes. Such high level of direct CLC is unexpected, as the highway regulations stipulate staggered LC for safety concerns. CLC from lane 3 to lane 1 (3[-21]), which involves two lane changes on the left, has the largest share in the CLC traffic (7.3%).

6.5.2 Lane changing location

The lane-changing locations for each vehicle involved in lane changing is analysed using the fitted trajectory dataset. Note that the distance measurement is referred to the observation starting point *M* (see **Figure 6.2**). **Figure 6.17** illustrates that the lane-changing vehicle tends to pre-position their lane relatively at the beginning of weaving section. The first 50.0-100.0m is preferable range for performing the first lane-changing with 19.3% of the total lane-changing traffic. This finding is in the range of previous studies such as Wang et al. (1993), and Bham (2008)

Moreover, an intensive lane changing in the beginning of weaving section may create a delay towards the upstream traffic. In comparison to the previous research, Al-Jameel (2011) found that the lane-changing movement created a bottle neck situation. It was built around the first 70.0m and enforced the driver to delay the lane changing towards the approximately 150.0m from the beginning weaving section.
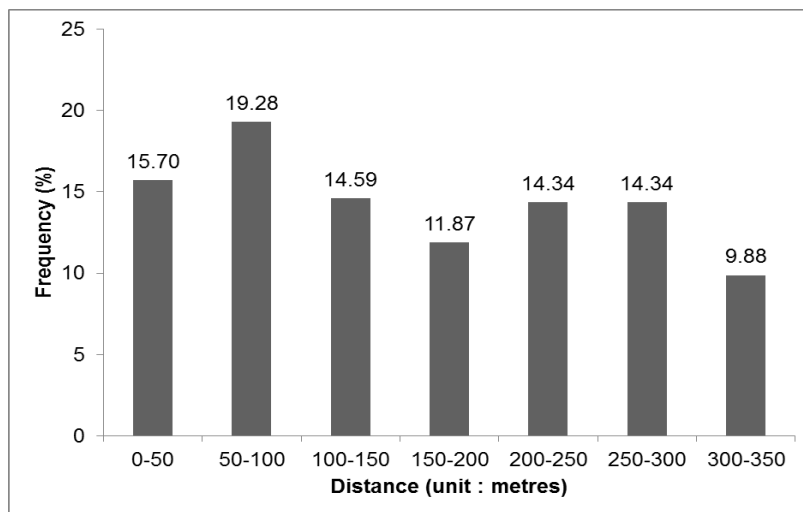
Figure 6.17 Proportion of lane-changing location

The mean value of lane-changing location in the current study is 175.8m, where the SLC location occurs at 170.0m in average. Meanwhile, the location for the first, second, and third movement of CLC are 106.3m, 245.7m, 298.5m respectively. Those average

values indicate that SLC vehicles tend to delay the lane changing towards the downstream, considering that target lane is next to their current lane. On the other hand, the CLC vehicles tend to plan ahead and perform the first lane change rather earlier since they have to travel one or more transit lanes before reaching the target lane.

6.5.3 Lane changing gap acceptance

Performing the lane changing, each driver evaluates the lead and lag gaps at the target lane at the time (t). The details of lead and lag gaps measurement are discussed in Section 6.4.4.

The accepted gap is a condition when the observed vehicle initiates (start to change the direction) the lane-changing process. Furthermore, the lane-changing driver expects that the gap at the target lane is increased during the lane-changing process.

Table 6.9 Lane-changing accepted gap associated with types and strategies (unit: sec)

Direction	Type of Gap	SLC		CLC					
				1st		2nd		3rd	
		Min	Mean	Min	Mean	Min	Mean	Min	Mean
Left	Lead	0.04	3.33	0.06	1.96	0.06	1.01	0.06	0.54
	Lag	0.09	5.27	0.04	2.36	0.04	1.2	0.05	0.63
Right	Lead	0.06	3.87	0.62	2.47	0.04	3.44	1.2	5.42
	Lag	0.04	4.68	0.62	2.4	0.55	4.94	3.44	9.6

Table 6.9 shows the minimum and the average accepted headways for both directions of the SLC and CLC. Compared to the SLC traffic, the CLC drivers are relatively more aggressive when they tend to accept smaller headway at the 1st CLC manoeuvre. This situation occurs since the CLC drivers are making pre-emptive lane changes at the beginning of the section, as they are required to make multiple mandatory lane changes closer while reaching their target lane or exit.

In fact, the left lane-changing vehicles are more aggressive compared to the right lane-changing vehicles as they accept smaller gap. The right lane-changing drivers consider initiating the lane nearly after the leading vehicle at the target lane just passed them. They prefer to have large lag in order to merge with the fast lane traffic. Moreover, the

left CLC vehicles tend to accept smaller gap while gap acceptance tends to increase at the right CLC. Given the descriptive statistic, this study draws several hypotheses for the lane-changing movement as follows; (1) moving toward to the right lane is more difficult and challenging compared to the left lane-changing as the driver merge towards a fast moving traffic, (2) the left lane-changing movement perceive higher priority due to UK driving rule. In that sense, the driver tends to accept smaller gap compared to right lane-changing movement, (3) the lane-changing drivers seek for lager lag gap rather lead gap in order to merge safely toward the target lane.

6.5.4   Group behaviours

The group behaviour in lane changing movement is a situation when both current lane front vehicle and target lane vehicle are involved in the lane-changing movement as well. The video recording showed that the lane vehicles often tend to change lanes in groups (i.e. platoon, weaving, etc.). A platoon lane-changing situation occurs when two or more vehicles from the same origin lanes move to the same target lane simultaneously or exactly after each other. Meanwhile, the weaving movement occurs when two vehicles interchange lanes simultaneously or exactly after each other. In some cases, two vehicles merge into the same lane from two different directions sequentially exactly after each other and in another cases exactly after a vehicle makes a lane change, his/her following vehicle makes a lane change in the opposite direction. There is indeed a slightly different characteristic between the isolated/solo and group lane-changing behaviours including platoon and weaving.

The group lane changing actions have a substantial effect on the capacity of the weaving section. As discussed earlier, the lane-changing vehicle will be involved in platoon lane changing when the subject and front vehicle changes lane relatively at the same time while the weaving lane-changing movement appears when subject and target lane vehicle swap their lane relatively at the same time period. Moreover, both type of leader movement in the current study has different consequence on lane changing behaviour compared to solo lane-changing movement.

The trajectory data have been analysed to explore potential platoon effects, weaving lane-changing mechanism as part of group behaviours in the weaving sections. This study classifies the lane changes in terms of presence or absence and type of group behaviour into three categories, as follows:

- No platoon or weaving / Solo (76.6%)

- Platoon (10.7%)

- Weaving (12.7%)

23.4% of the lane-changing traffic involves in the group behaviour where the majority (12.7%) performs the weaving manoeuvre. Lane 3 and 2 traffic take the largest share of weaving traffic compared to the other lanes. The data illustrates that 3.6 % of the lane-changing traffic involve weaving lane-changing mechanisms when changing lane from lane 3 toward lane 2 (diverging from with the main traffic). Similarly, most of platoon lane changing appears to change lane from lane 3 toward lane 2 which is 3.5% of the lane-changing traffic.

The group behaviour has significant share on the lane-changing traffic. For the in-depth study, this finding is significant input and consideration on the proposed lane-changing modelling framework with different lane changing mechanisms (platoon, weaving, and solo) and the traffic simulation as well.

6.6 Summary

This section offers an insight and presents an empirical observation of the lane-changing characteristics at the particular weaving section traffic during moderate traffic flow using both disaggregated individual vehicle trajectory and aggregated loop detector data. In fact, working with the microscopic data is a massive work and requires high concentration during the data collection, extraction and managing processes. Adopting the same data extraction process and analysis in different traffic condition and weaving section types may result in different driving characteristics. As the consequence, the empirical result of this study is required to be revalidated for different traffic and weaving sections.

This section offers insight and presents a general framework of empirical observation of the driving characteristics at the weaving section using both disaggregated individual vehicle trajectory and aggregated loop detector data. In fact, working with the microscopic data is a massive work and requires high concentration during the data collection, extraction and managing processes. It is worth that the observation focuses on moderate traffic flow. Adopting the framework of data extraction process and analysis in different traffic condition and weaving section types may result from different driving characteristics. As the consequences, the empirical outcome of this study requires being revalidated for different traffic and weaving sections.

This PhD study uses a traditional video camera to record all the traffic characteristics and movements over the observation area. In fact, there is a limitation in capturing the traffic movements for the whole area of weaving section due to the availability and capacity of the video camera recording. As the consequence, this study exclusively focuses on the beginning of the weaving sections area (320m). Note that, there is only

5% of traffic that performs the lane changing after the observation area. Several factors should be addressed during the video traffic recording to ensure the data quality i.e. the recording tool, coverage area, and site condition. A good quality of aerial map (i.e. Google Earth) is required to transforms the video footage pixel with the real world coordinate using the photogrammetry algorithm. In the next step, the trajectory extractor application extracts the vehicle trajectory which requires an intensive work and focuses to identify the precise location of the observed vehicle at the specific time period. Several factors may affect the vehicle trajectory data quality such as: the video footage quality, playback control and obscuring view from the leading vehicle. The measurement error issues raise when there are high variations in both speed and acceleration profiles. A fitting algorithm, therefore, is applied in the managing data process minimising the extreme variation of the speed and acceleration profile due to measurement errors.

Meanwhile, MIDAS loop detector assists to mimic the traffic in macroscopic level. They provide the traffic flow, occupancy, and speed at 1-minute aggregate level. The current study uses MIDAS in the data validation process as the baseline data. In addition, the validation process in this study is applied for two variables; traffic flow and speed.

Overall, the data finds that the weaving section traffic was not highly congested over the observation period. This gives more opportunity to capture a lane changing under free-flow traffic. In fact, high proportion (82%) at the beginning of weaving section decelerates in order to cooperate with the merging and diverging traffic (average acceleration -1.2m/sec^2). A significant proportion (48.2%) is involved in lane-changing at the first 320m of weaving section in order to pre-emptive the, many of which are part of compound lane-changing for the upcoming traffic or pre-condition their target. Compared to the SLC drivers (35.5%), the CLC drivers (12.7%) for both directions at the first manoeuvre are more aggressive by accepting smaller gaps. In terms lane-changing direction, the left lane-changing vehicles accept smaller gap compared to the right lane-changing vehicles. This condition appears due to several lane-changing characteristics; (1) moving toward to the right lane is more difficult and challenging compared to the left lane-changing as the driver merge towards a fast moving traffic, (2) the left lane-changing movement perceive higher priority due to UK driving rule. In that sense, the driver tends to accept smaller gap compared to right lane-changing movement, (3) the lane-changing drivers seek for lager lag gap rather lead gap in order to merge safely toward the target lane.

Chapter 7 Estimation Process and Results

This chapter presents the estimation process and result of the lane-changing and acceleration models using the vehicle trajectory dataset in Chapter 6. The statistical assessment and interpretation of the parameters are presented as well in this chapter. All the modelling components and attributes in each model are jointly under the likelihood approaches, which were presented in the previous Chapter 4 and Chapter 5.

The structure of this chapter is represented as follows; Section 7.1 presents the estimation for lane changing model along with the description of modelling setup, result and discussion of the lane changing model components including the target lane choice and gap acceptance models. Similar structure is used to describes the proposed of acceleration model in Section 7.2. Section 7.3 summarises the estimation and findings of both proposed models.

7.1 Estimation of Lane Changing Model

The proposed lane-changing model consists of two components, namely target lane choice model and gap acceptance model. Those components capture the decision-making process on the lane-changing behaviour. Note that, the target lane choice is the upper level while the gap acceptance is the lower level of the lane changing decision-making process. As discussed in Chapter 4, the proposed lane-changing model hypotheses that the driver has a different lane-changing characteristic as a response to the front and lead vehicle movement at the current and target lane vehicle. In this case, there are three types of lane-changing movement: solo, platoon and weaving. The current modelling framework incorporates this situation as an action plan that is represented in the gap acceptance model.

7.1.1 Lane changing modelling setup

This process estimates all beta parameters in both level models using the maximum likelihood approach simultaneously. The estimation corresponds with the conditional individual latent variables (ϑ).

Details below illustrate the estimation algorithm of lane-changing model:

1. Identify the variables that correspond to each level of the lane changing decision process models. It is mentioned earlier in Chapter 4; there are two levels of decision process during the lane changing movement namely (1) target lane and (2) gap acceptance. Further details of the potential variables were discussed already in Chapter 6.

2. Setup the reasonable ranges of individual latent variables (ϑ) which is assumed to be normally distributed $\vartheta_n \sim N(0,1)$.

3. Based on the observed variables at step 1 and the conditional individual latent variable, the beta parameters are estimated using the maximum likelihood method (Equation 4.10).

4. The iteration process provides the beta parameters that correspond with a specific conditional individual latent variable that maximise the log-likelihood value.

5. Follow step 1 to 4 for the different boundary of individual latent variable and modelling specification until the maximum log-likelihood value is obtained.

This study examines several modelling specifications with different ranges of the conditional individual latent variable accordingly, which is any discrete value between -5 (lower bound) and 5 (upper bound). The estimation demonstrates that the optimum range of conditional individual latent is between -3 and 3 compared to the other conditional individual latent variable. It may be noted that this field provides higher log-likelihood in comparison to other conditional individual latent variable range.

The application of Maximum Likelihood package (Henningsen and Toomet, 2010) in "R" programming assists the iteration procedure to find the optimum beta parameters that maximise the likelihood function. Furthermore, the iteration process is performed under Broyden-Fletcher-Goldfarb-Shanno (BFGS) algorithm which is a relatively more efficient algorithm compared to other method i.e. Newton-Raphson (NR) algorithm. The detailed of BFGS algorithm is presented in Appendix-C

7.1.2 Lane changing model estimation result

Table 7.1 Lane-changing model estimation results

Modelling Variables	Parameter	Std error	t-value
Target Lane Model			
Lane 2 constant	0.800	0.067	11.92
Lane 3 constant	1.049	0.067	15.60
Lane 4 constant	0.070	0.079	0.89
Lane 5 constant	-1.290	0.144	-8.99
Average speed (m/sec)	0.0174	0.004	4.70
Occupancy (%)	-0.00185	0.012	-0.16
Relative speed to the front veh (m/sec)*	0.0487	0.006	8.80
No of lane changing required	-10.223	0.525	-19.48
Exponent component of distance to exit (km)	-0.135	1.356	-1.47
α left direction	0.0644	0.142	0.45
α right direction	-0.0667	0.133	-0.50
Critical Gap Solo			
Gap constant ($\beta^{cr,lead,s}$)	-0.864	0.172	-5.01
Relative speed with lead veh at target lane (m/sec)*	-0.0204	0.006	-3.52
Relative speed with front veh at current lane (m/sec)*	-0.00730	0.009	-0.81
α gap	-1.440	0.282	-5.10
σ gap	0.150	0.039	3.85
Critical Gap Platoon			
Gap constant ($\beta^{cr,lead,p}$)	-2.360	0.422	-5.59
Relative speed with lead veh at current lane (m/sec)*	-0.263	0.020	-13.03
α gap	-1.200	0.793	-1.51
σ gap	1.692	0.423	4.00
Critical Gap Weaving			
Gap constant ($\beta^{cr,lead,w}$)	-0.539	0.143	-3.76
Relative speed with lead veh at target lane (m/sec)*	-0.127	0.034	-3.70
α gap	-1.680	0.377	-4.46
σ gap	0.410	0.091	4.50
Critical Lag for All Types			
Lag Constant ($\beta^{cr,lag}$)	0.421	0.103	4.09
Relative speed with lag veh at target lane (m/sec)**	0.0146	0.0051	2.84
α lag	-2.420	0.560	-4.32
σ lag	0.872	0.207	4.21
Number of observation	17,891		
Number of driver	1,386		
Number of parameters	28		
Final Log-Likelihood	-6512.663		
Adjusted Rho-Bar Square	0.342		

$* \; lead \; or \; front \; veh. speed - subject \; veh. speed; ** \; lag \; veh. speed - subject \; veh. speed$

The estimation result is based on the highest 15 min traffic flow (17:15-17:30) during the afternoon peak hour period between 16:45-17:45. During the observation period there are 1,386 vehicles where 48.2% are involved in lane-changing movement.

The proposed model (unrestricted) is compared with a reduced form (restricted) model that ignores the effect of lane changing mechanisms in the model structure. Such reduced form model assumes same critical gap functions disregard the lane changing mechanism (e.g. Toledo et al., 2005; Choudhury, 2007). Note that the unrestricted model (28 parameters) incorporates various type of lane-changing mechanism with respect to leader movement characteristic while the restricted model consists of 20 parameters. Both restricted and unrestricted models are estimated with the same trajectory data. The detail of restricted lane-changing model is illustrated in **Figure 7.1**.
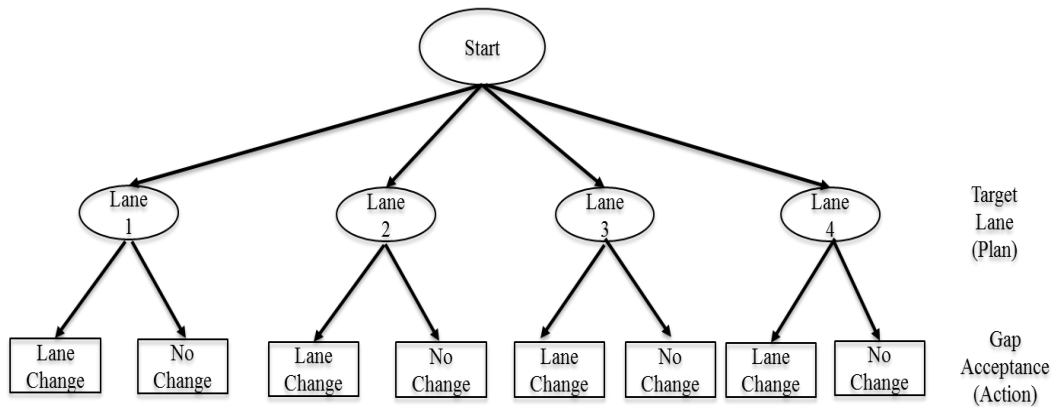
Figure 7.1 Lane-changing modelling framework (Choudhury, 2007; Toledo et al., 2005)

Table 7.2 Lane-changing modelling comparison

Statistics	Restricted	Unrestricted
Number of observations	17,981	
Number of drivers	1,386	
Initial likelihood value $(L(0))$	-9935.222	
Final likelihood value $(L(\beta^*))$	-6544.203	-6512.663
Number of parameters (no par)	20	28
Chi-square test value (χ^2)	63.080 (15.51)	
Adjusted rho-bar $(\bar{\rho}^2)$	0.339	0.342
Akaike Information Criterion (AIC)	-6564.203	-6540.663

Pearson (1900) introduced a Chi-square test (χ^2), which is commonly used in a likelihood ratio test. This statistical test analyses the improvement of goodness-of-fit between two models with a large number of the dataset (Wilks, 1938). This study compares a particular case of lane-changing model (unrestricted model), which incorporates the lane-changing mechanism, and a conventional lane-changing model (restricted model).

Based on the estimated likelihood value, Chi-square test can be formulated as follows:

$$\chi^2_{df} = -2 * \left(-L(\beta^{*,res}) - L(\beta^{*,unres}) \right)$$

$$= 63.080 > \chi^2_8(15.51) \tag{7.1}$$

Where;

χ^2_{df} : Chi-square test value on a specific degree of freedom

$L(\beta^{*,res})$: Final likelihood value of restricted model

$L(\beta^{*,unres})$: Final likelihood value of unrestricted model

By applying Equation 7.1, the chi-square test value (χ^2) is 63.080, significantly larger than the critical value of χ^2 Distribution with 8 degrees of freedom at 5% level of confidence (15.51). Note that the degree of freedom is the difference between the number of parameters of unrestricted and restricted models ($no.par.unrestricted - no.par.restricted; 28 - 20 = 8$). The result of chi-square test confirms that the inclusion of the lane changing mechanisms in the decision framework results in an improved goodness-of-fit even after discounting for the increase in the number of parameters.

Adjusted Rho-bar ($\bar{\rho}^2$) measures a fraction of between the final and initial likelihood value by incorporating the modelling complexity (number of the parameters). Note that the value of $\bar{\rho}^2$ is between 0 and 1. Therefore, it can be formulated as follows:

$$\bar{\rho}^2 = 1 - \frac{L(\beta^*) - No.par}{L(0)} \tag{7.2}$$

Where;

$\bar{\rho}^2$: Adjusted rho-bar

$L(\beta^*)$: Final likelihood value

L(0) : Initial likelihood value

No.par: Number of parameters

Akaike (1973, 1974, 1981) developed a statistical analysis tool that is known as Akaike Information Criterion (AIC) which measures the relative quality of various statistical models for the given dataset. This approach provides information to choose an optimum model from several alternatives of modelling specification. AIC penalises the final likelihood value with the number of the parameter to incorporate the modelling complexity. Thus, this statistical analysis is expressed by:

$$AIC = L(\beta^*) - no.\,par \tag{7.3}$$

Given the values in **Table 7.1**, Adjusted Rho-bar $(\bar{\rho}^2)$ for the unrestricted model (0.342) is slightly greater than restricted model (0.339). Meanwhile, AIC analysis reports that the unrestricted model (-6512.663) has higher AIC value compared to the restricted model (-6544.203). Indeed, the model with higher $\bar{\rho}^2$ and AIC is chosen (see. Ben-Akiva and Lerman, 1985).

An asymptotic t-test aims to observe the difference in the coefficient. In this case, this studies paper aims to test whether the parameter in particular lane-changing mechanism differ from the other mechanisms. Based on the information of the estimation result and covariance matrix, the t-test for the null hypothesis $\beta^{cr,lead,p} = \beta^{cr,lead,s}$ is expressed by:

$$\frac{\beta^{cr,lead,p} - \beta^{cr,lead,s}}{\left(var(\beta^{cr,lead,p}) + var(\beta^{cr,lead,s})\right)^{1/2}} = \frac{-1.496}{0.456} = -3.281 \tag{7.4}$$

Then, the t-test result for the null hypothesis $\beta^{cr,lead,p} = \beta^{cr,lead,w}$ equals -4.086. Both results reject the null hypotheses at the 5% level of significance, as they are greater than the critical value (1.703). This finding provides a noteworthy support that the differences between the platoon lane-changing mechanism and the other mechanisms are significant. While the other attributes remain equal, the platoon lane changing movement is more aggressive as this type of movement accepts smaller gap in comparison to the other mechanisms.

All those statistical analysis including the Chi-square test, Adjusted Rho-bar, and AIC confirm that inclusion of the lane changing mechanisms in the decision framework results in a statistically significant improvement in the goodness-of-fit even after discounting for the increase in the number of parameters. These findings are in line with

the Asymptotic t-test results, which denote that the parameters for platoon and weaving are statistically different from those of solo lane changes. Following sections discuss the estimation result of both target lane choice and gap-acceptance models, which are estimated jointly, in more details.

7.1.3 Target lane choice model

A linear utility function in the current study measures the target lane choice modelling by presuming that all drivers perceive same set of lane choice and move towards the target lane with the highest utility value. Furthermore, the lane change appears if the driver moves towards the neighbourhood lane that provides the best driving environment. The estimation result in **Table 7.1** demonstrates several attributes, which affect the target lane choice of the driver such as relative speed, average speed, occupancy, and path-plan impact. Though, the estimation result specifies that some variables cannot be included in the modelling due to statistically insignificant or unexpected signs issue.

The modelling specification on lane specific constant variable is relative to lane 1. The lane specific constants denote that, with the other characteristics being equal, the traffic prefers to move on the lane 3 and 2 respectively as both two lanes provide flexibility in terms of merging or diverging from the main traffic beyond the study area. A slight difference of lane specific constant constitutes a tough completion between lane 3 and 2 In contrast, all else being equal, the driver tends to avoid lane 5 (fast lane traffic) which is further away from the entry and exit ramps and is the fastest lane.

As expected, both target lane average speed and current lane front vehicle relative speed have positive signs. This sign denotes that both affect the specific target lane utility positively. The average lane speed variable captures average vehicle speed on a particular lane at certain period. In the meantime, the relative speed represents speed difference between current lane front vehicle and subject vehicle.

Occupancy variable in target lane choice model explains the traffic density on each particular lane during the observation period. This variable represents the percentage of time length when the observation range occupies a loop detector in the observation area. Note that loop detector records the occupancy at one-minute aggregated period. This current study presumes that the occupancy remains the same over 1 minute aggregated time. This current study presumes that the occupancy remains the same over one-minute aggregated time. The target lane model expects that the increased of lane occupancy affects negatively the driver preference on a specific lane as shown in the estimation result **Table 7.1**. This finding implies that the increased of lane occupancy affects

negatively the target lane choice. In the other words, the target lane choice is less preferable as the occupancy is increased.

The required number of lane changing and the exponent of remaining distance to the mandatory lane-changing point (exit) explain the path plan impact on individual driver lane choice. The iteration results show that the parameters for both variables are negative (see **Table 7.1**). In this case, the target lane utility is decreased together with the increased of number of lane changing required toward the particular target lane to maintain the path. Furthermore, the magnitude diminishes as the vehicle approaches the mandatory lane-changing point (off-ramp). This effect is represented by the negative exponent of remaining distance to exit $\left(\delta^{dist.exit} = -0.135 \right)$
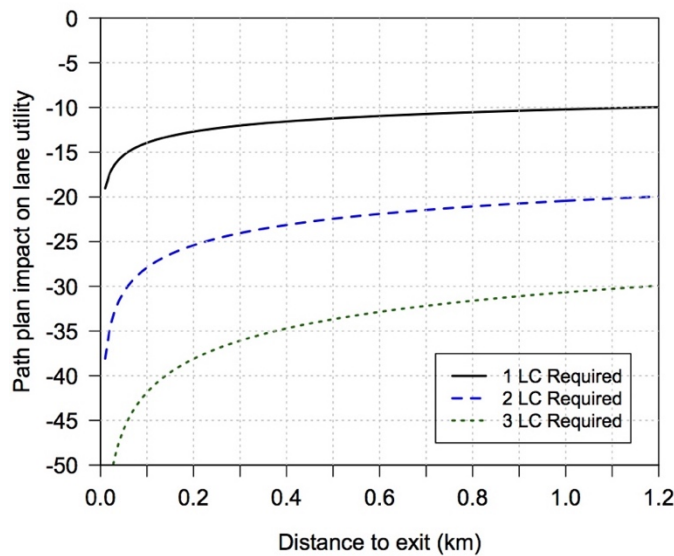
Figure 7.2 Impact of path plan lane changes on lane utility

For example, if a driver needs to take the exit, at 0.2 km away from the off-ramp, Lane 3 has an additional disutility of $10.2*(0.2^{-0.135})$ units, while lane 4 has an additional disutility of $20.4*(0.2^{-0.135})$ units, etc. At 0.1 km away from the off-ramp, the disutilities are $10.2*(0.1^{-0.135})$ units and $20.4*(0.1^{-0.135})$ units, respectively. This is shown schematically in **Figure 7.2**, where the disutility of being on the incorrect lane amplifies significantly as he/she approaches the end of weaving section. In terms of probabilities, this translates to the fact that the drivers have substantially high probabilities of making pre-emptive lane changes if they are multiple lanes away from the 'correct' lane.

Individual specific term captures the driver aggressiveness with respect to the target lane location either left or right of the current lane location. A positive sign on the left lane changing direction implies that the aggressive drivers are more likely moving to

the left lane rather than a right lane during moderately congested traffic. It is worth noting that the UK driving rule mandates provision of precedence to the approaching traffic from the right lane. On the other hand, moving toward the right/far-side lane requires more cautious as the driver merges toward the higher speed lane. It is important for the driver to ensure and change in a safe manner and minimises the accident risk for both subject vehicle and neighbouring traffic. The parameters are statistically insignificant though. However, they have been retained as they capture the correlation between the lane choice and the gap acceptance decisions of the same driver.

Giving the estimation result in **Table 7.1**, the target lane utility can be written as follows:

$$U_n^l(t) = \beta^l + 0.0174\,\overline{V}_n^l(t) - 0.00185\,\text{occ}_n^l(t) + 0.0487\,\Delta V_n^l(t)$$
$$\left(\left(d_n^{exit}(t)\right)^{-0.135} \left(-10.224\,No.\,LC(t)\right)\right) + \alpha^{l'}\vartheta_n + \varepsilon_n^l(t) \qquad (7.5)$$

Where;

β^l : Lane l specific constant

$\overline{V}_n^l(t)$: Average speed at lane l of driver n at time (t) (m/sec)

$\text{Occ}_n^l(t)$: Lane l occupancy level of driver n at time (t) (percentage (%))

$\Delta V_n^l(t)$: Relative speed between driver n and the leading vehicle at lane l at time (t)

$d_n^{exit}(t)$: Remaining distance to the mandatory lane changing point of the driver n at time t, ∞ if no mandatory lane changing is required.

$No.\,LC(t)$: Number of lane changing required toward the target lane at time t

$\alpha^{l'}$: Estimated parameters of individual specific random effect ϑ_n for direction l'

l' $\in \{left, right\}$ depends on the orientation of target lane l with respect to the current lane.

The choice of the target lane indicates the direction of lane-change (e.g. stay in the current lane, look for gaps in the right, look for gaps in the left) and the driver looks for acceptable gaps in that direction.

(a) avg.speed =30 m/sec; occ =8%;relative speed=-1m/sec
;remaining distance to exit =1.2km

(b)avg.speed= 30m/sec; occ=8%;relative speed=-1m/sec
remaining distance to exit = 0.6km

(c) avg.speed = 30m/sec; occ = 8%; relative speed=-1m/sec;
remaining distance to exit= 0.1km
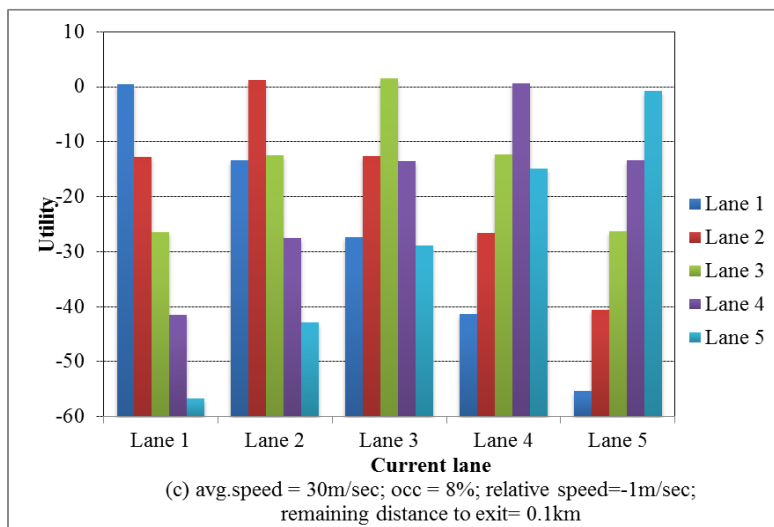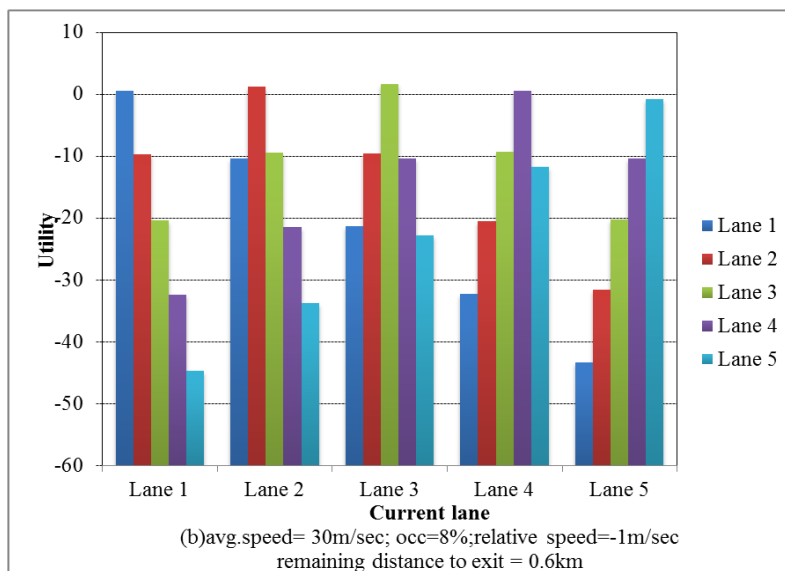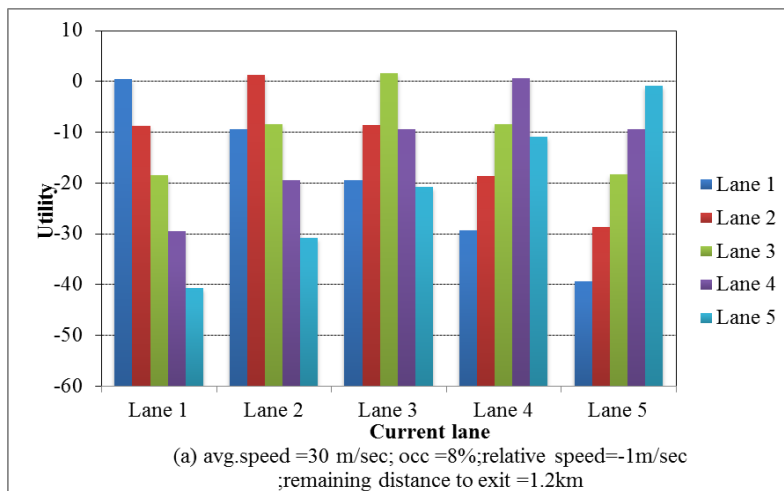
Figure 7.3 Variation of target lane utilities at remaining distance to exit (a) 1.2km, (b) 0.6km, (c) 0.1km

Figure 7.3 illustrates the variation of the target lane utility for various path plan and lane location of the observed vehicle. As discussed earlier, the path plan incorporates number of lane changing required and the subject vehicle remaining distance toward the exit. The analysis observes the target lane utility value for three various remaining distance values; 1.2km, 0.6km, and 0.1km. Meanwhile, the other variables in target lane choice are default values; avg.speed (30m/sec), occupancy (8%), and relative speed between the subject and observe vehicle (-1m/sec).

The analysis illustrates that target lanes utility varies significantly correspond with the driver's current lane and the path plan variable, which has an adverse impact on the target lane choice behaviour. The target lane utility decreases significantly due to the increased number of lane changing towards the target lane and if the vehicle approaches the mandatory lane changing location (exit slip road), as shown in **Figure 7.2**. The variation of target lane utility confirms that the driver prefers to perform a pre-emptive lane changing movement at relative early weaving section rather than delaying until the mandatory lane-changing point.

7.1.4 Gap acceptance model

The gap acceptance is second level of lane change decision-making process. Note that the subject vehicle has to accept both gap and lag at the target lane at the particular time(t). As discussed earlier, three different mechanisms of lane changes have been considered here: solo, platoon and weaving.

Solo critical gap

The estimation of solo gap acceptance model defines that both relative speed to the lead vehicles at current lane and target lane are applied as explanatory variables. More details on the estimation result are presented in **Table 7.1**.

Estimation result indicates that the relative speed between the subject and lead vehicles has stronger impact in solo gap acceptance decision-making process rather than the relative speed with current lane front vehicle. As expected, both relative speed parameters have negative signs. The signs imply that the critical gap increases slightly with the relative speeds (gap opening). A lane change vehicle under this situation tends to minimise the accident risk by accepting a large of the critical gap while performing the lane change.

Given the estimation result in **Table 7.1**, the critical gap model for solo lane-changing mechanism can be expressed as follows:

$$G_n^{cr,lead,l,s}(t) = \exp\left(-0.864 - 0.0204\,\Delta V_n^l(t) - 0.00730\,\Delta V_n^{cl}(t) \right.$$
$$\left. - 1.440\,\vartheta_n^{lead,s}(t) + \varepsilon_n^{lead,s}(t)\right) \qquad (7.6)$$

Where;

$G_n^{cr,lead,l,s}(t)$: Solo lead critical gap at target lane l of driver n at time t

$\Delta V_n^l(t)$: Relative speed between driver n and the lead vehicle in the direction of the target lane l at time t

$\Delta V_n^{cl}(t)$: Relative speed between driver n and the front vehicle at current lane l at time t

$\varepsilon_n^{lead,s}(t) \sim N(0, 0.150^2)$

Platoon critical gap

Estimation result in **Table 7.1** demonstrates that the critical gap in platoon lane-changing mechanism is significantly affected by the relative speed at the current lane. This finding is intuitive as for the platoon mechanisms; the front vehicle in the current lane has a more dominant role rather the target lane lead vehicle. As expected, the relative speeds in all lane-changing mechanisms have a negative sign indicating that the critical gaps of the lane-changing vehicle are decreased along with the increased of relative speed.

The critical gap acceptance model with platoon mechanism can be written as follows:

$$G_n^{cr,lead,l,p}(t) = \exp\left(-2.360 - 0.263\,\Delta V_n^{cl}(t) - 1.200\,\vartheta_n^{lead,p} + \varepsilon_n^{lead,p}(t)\right) \quad (7.7)$$

Where;

$G_n^{cr,lead,l,p}(t)$: Platoon lead critical gap at target lane l of driver n at time t

$\varepsilon_n^{lead,p}(t) \sim N(0, 1.692^2)$

Weaving critical gap

The critical gap acceptance in a weaving mechanism is significantly affected by the relative speed of the target lane lead vehicle as shown in **Table 7.1** As expected, the relative speed has a negative sign. The lane change vehicle in weaving mechanism accepts shorter gap if the target lane lead vehicle moves faster than the subject vehicle.

In contrast, a lane change vehicle that faces slow moving lead traffic prefers a large gap to minimise the accident risk while performing the weaving movement.

The weaving critical gap was formulated as follows;

$$G_n^{cr,lead,l,w}(t) = \exp\left(-0.539 - 0.127\Delta V_n^l(t) - 1.680\,\vartheta_n^{lead,w} + \varepsilon_n^{lead,w}(t)\right) \quad (7.8)$$

Where;

$G_n^{cr,lead,l,w}(t)$: Weaving lead critical gap at target lane l of driver n at time t

$\varepsilon_n^{lead,w}(t) \sim N(0, 0.410^2)$

The estimated constants for the critical gaps are found to be statistically different from each other mechanism showing that the platoon lane-changing driver accepts the smallest critical gap compared to the solo and weaving mechanisms. In this case, the driver decision in a platoon lane-changing mechanism is affected significantly by the relative speed with the current lane front vehicles, which change lane relatively at the same time. Meanwhile, the relative speed with the target lane lead vehicle affects individual driver decision in solo and weaving mechanism. The relative speeds in all lane-changing mechanisms are negative denoting that the observed vehicle prefers for a smaller gap if the current lane front vehicle or the target lane lead vehicle moves faster than the subject vehicle (i.e. gap opening up).

An aggressive driver is defined as the one who requires a smaller critical gap all else being equal. The estimation results indicate that levels of aggressiveness has various effects on the critical gaps depending on the lane changing mechanism. This attribute has a negative sign for all critical gap models where the effect of aggressiveness is most (i.e. reduction in critical gap is the largest) on weaving manouevres and least on platoon lane changes. The complexity of the weaving mechanism requires the drivers to be more alert and respond quickly due to the change of traffic situation during the lane-changing movement. Indeed, This characteristic raises a safety issue as stated in Golob et al. (2004) where a significant proportion of accident in the weaving section is a swideswipe collusion. In contrast, the platoon lane changing requires less level of aggressiveness. The driver in this mechanism is relatively relaxes and follow the movement of front vehicle, who takes the role to initiate an interaction for creating space with the target lane traffic.

Figure 7.4 shows the variation of lead critical gap median value with the different lane-changing mechanism as a function of relative speed. The critical gap in all mechanisms is increased with the relative speed. In all lane-changing mechanism, the analysis of critical gaps confirms that the critical gap is slightly increased with relative speed between the subject and both current lane front vehicle and target lane lead vehicles. The platoon lane-changing mechanism, which tends to be the simplest lane-changing movement, has the lowest critical gap compared to solo and weaving lane-changing mechanisms. Meanwhile, the weaving mechanism has the largest critical gap among those three mechanisms due to the complexity of the weaving lane-changing mechanism. Furthermore, the variation of the weaving lane-changing critical gap is significantly sensitive to the relative speed changes compared to the other mechanisms.
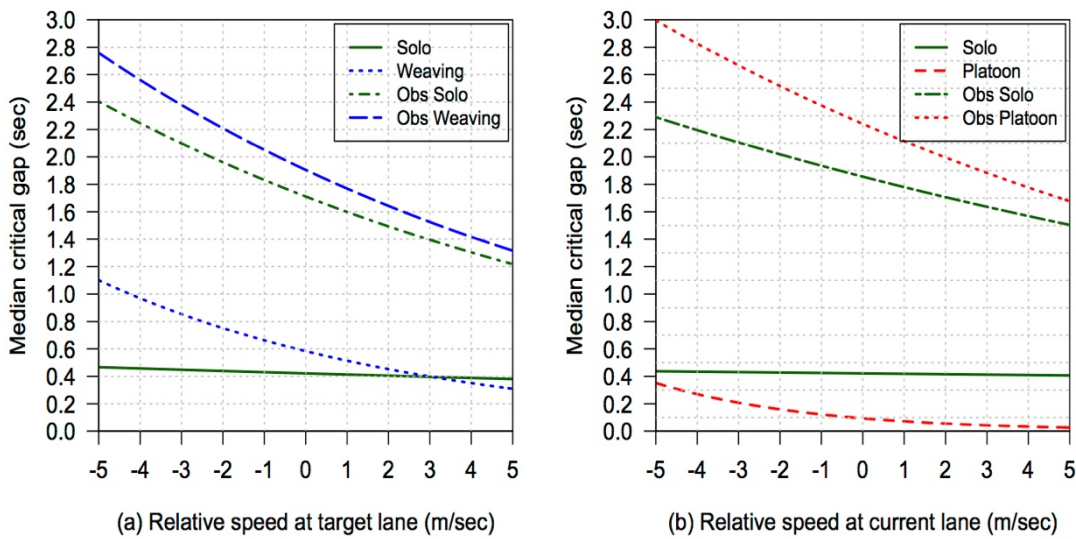
Figure 7.4 Variation of median critical lead gaps and observed accepted gaps in different lane-changing mechanism as a function of relative speed

Furthermore, **Figure 7.4** compares the estimated critical gap with the observed accepted gap for those three lane-changing mechanisms as a function of relative speed. This process aims to validate the variation of estimated critical gap with the observed critical gap. Thus, this study represents nonlinear regression to capture the relationship between the observed accepted gap (dependent variable) and relative speed (explanatory variable) for given fitted trajectory vehicle dataset. Similar to the critical gap, the regression results show that the observed accepted gap is increased with the relative speed between the subject vehicle and front/lead vehicles. The analysis confirms that the estimated critical gaps in all lane changing mechanisms are slightly smaller compared to the observed accepted gaps as expected. The significant differences

between those values denote that individual driver tends to relax and finds of a large gap for changing lane in a safe manner.

Critical lag gap

The difference in critical lag gap specification is depending on the lane changing mechanism that revealed statistically insignificant differences. A common critical lag gap model has been retained accordingly, which is intuitively acceptable due to several issues i.e. less upstream traffic, movement priority, and courtesy movement of the lag vehicle at the target lane. The dataset analysis illustrates that more than 50% of the lane changing appears when the lag is larger than 3 sec. Moreover, the lag distribution has a longer tail (larger standard deviation) compared to both acceptable gaps with current lane's front vehicle and target lane's lead vehicle (see **Figure 6.12**). **Table 7.1** shows that the critical lag gap is affected by the relative speed with respect to target lane lag vehicle. A positive sign of this attribute implies indicating that the critical lag gap of the lane-changing vehicle is larger if the lag vehicle in the target lane is moving faster (i.e. gap closing). Similar to the critical lead gaps, the critical gaps are found to be smaller for aggressive drivers. Given the estimation result in **Table 7.1**, the lag critical gap is written as follows;

$$G_n^{cr,lag,l}(t) = \exp\left(0.421 + 0.015\,\Delta Vlag_n^l(t) - 2.418\,\vartheta_n^{lag} + \varepsilon_n^{lag}(t)\right) \qquad (7.9)$$

Where;

$G_n^{cr,lag,l}(t)$: Lag critical gap at target lane l of driver n at time t

$\Delta V.lag_n^l(t)$: Relative speed between the driver n and the lag vehicle in the direction of the target lane l at time t

$\varepsilon_n^{lag}(t) \sim N(0, 0.863^2)$

The specific individual constant of lag gap model is slightly larger compared to all critical gap mechanisms. This finding implies that the lane-changing driver is more alert when accepting the lag due to the difficulty in interpreting the lag vehicle behaviour (i.e. observe through the mirror) rather than the downstream traffic movement. This is in agreement with the findings of Bham (2008) for uncongested situations.
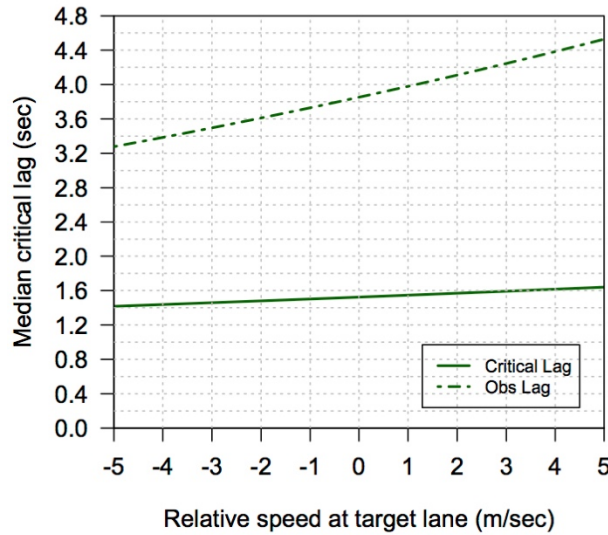
Figure 7.5 Variation of median critical lag gap and observed accepted lag gap in different lane-changing mechanism as a function of relative speed

Figure 7.5 shows the variation of median and descriptive statistic of the lag gap as function of relative speed. As expected, the median value of critical lag is slightly smaller compared observed lag acceptance as expected.

7.2 Estimation of Acceleration Model

The proposed acceleration model consists four components: car-following regime model, free-flow regime model, gap threshold distribution and reaction time distribution. As discussed earlier in Chapter 5, the model extends the car-following regime condition by relaxing the relationship between car-following behaviour and stimulus condition. In this case, the study specifies four different sub-models in the car-following regime; acceleration with positive relative speed, acceleration with negative relative speed, deceleration with positive relative speed, and deceleration with negative relative speed.

7.2.1   Acceleration modelling setup

The proposed acceleration model estimation follows the maximum likelihood approach with a conditional on gap threshold distribution (G^*) and the driver reaction time(τ) as discussed in Section 5.3. Briefly, these are the procedures of acceleration model:

1.   Define the reasonable value for upper and lower bound of both truncated gap threshold distribution (G^*) and reaction time distribution(τ). The current model

presumes that the lower boundaries of both distributions are the minimum value of the observable gap towards the front vehicle. This assumption simplifies the modelling estimation procedure.

2. Specify the explanatory variables on both car-following regime and free-flow regime. The proposed model considers several explanatory variables i.e. speed, gap/headway to front vehicle, distance to exit, no. of front vehicle at the current lane, occupancy, relative speed between subject and object vehicles, and relative speed between the subject vehicle and the speed limit

3. Perform the estimation for all beta parameters with maximum likelihood method condition on headway threshold and driver reaction time. The likelihood function of acceleration model can be seen in Section 5.3.

4. Follow step 1 to 3 for different values of (G^{max} and τ^{max}) and the modelling specification until the maximum log-likelihood is obtained.

Same with the lane-changing model, the iteration process is performed in R programming under Maximum Likelihood package (Henningsen and Toomet, 2010) with Broyden-Fletcher-Goldfarb-Shanno (BFGS) algorithm.

7.2.2   Acceleration model estimation result

By applying the same dataset with lane changing modelling estimation, all beta parameters in the acceleration model are estimated jointly using the likelihood method conditional on gap threshold and reaction time distributions. As mentioned earlier, the study presumes that the lower bound of the reaction time and gap threshold distributions equal minimum observed gap, which is 0.6 sec (see **Table 6.8**). This assumption simplifies the number of combinations of both distributions in the estimation process. In that case, the estimation process requires only setup the upper bound of both gap threshold and reaction time distribution.

Several modelling specifications with different upper boundary values of both attributes have been tested in the estimation process (stage 3) to identify the optimum acceleration model. **Table 7.3** shows the estimated maximum likelihood values from different combination of both gap threshold and reaction time distribution. Note that the lower boundaries of both distributions are 0.6 sec as discussed earlier. The iteration results imply that the acceleration model likelihood function reach the maximum for condition $\tau^{max} = 4$ sec, G^{max} = 11 sec, while the lower boundaries of both distributions $\tau^{min} = G^{min} = 0.6$ sec. The estimation results of the proposed acceleration model are presented in **Table 7.4**.

Table 7.3 Estimated likelihood value for different upper boundaries of gap threshold and reaction time distribution

Reaction Time (sec)	Gap Threshold (sec)	
	10	11
3	-24268.39	-23816.35
4	-24355.86	-23810.51
5	-24462.64	-24500.95

All parameters in all modelling components have expected signs and significant t-value, expect the parameters for the gap threshold distribution. Although both constant and standard deviation of the reaction time distribution have expected sign, the t-value indicates that the parameters are less significant. This condition may appear as there is none of vehicle trajectory dataset which are appropriate to explain the driver reaction time. However, we need to retain those parameters representing the reaction time, which is critical component in acceleration model.

Similar to the lane changing model, the application of asymptotic t-test is used to capture the difference among the constant on the car-following regime models. Given the estimated parameters and covariance matrix, the tested null hypothesis $\beta^{cf,acc,-} = \beta^{cf,acc,+}$ of t-test is expressed by:

$$\frac{\beta^{cf,acc,-} - \beta^{cf,acc,+}}{\left(var(\beta^{cf,acc,-}) + var(\beta^{cf,acc,+})\right)^{1/2}} = \frac{-0.0311}{0.00115} = -26.992 \tag{7.10}$$

Then, the t-test result for the null hypothesis $\beta^{cf,dec,+} = \beta^{cf,dec,-}$ equals 6.221. Given the results, it is possible to reject the null hypothesis at 5% level of significance as they are greater than the critical value (1.711). Those values imply that individual driver acceleration and deceleration behaviour are significantly different in each type of stimulus (positive relative speed or relative negative speed).

The following sections will present and discuss estimation result of acceleration model: car-following regime, free-flow, gap threshold distribution and reaction time distribution.

Table 7.4 Acceleration model estimation results

Modelling Variables	Parameters	Std. error	t-value
Car-following regime			
Acceleration with ΔV (+)			
Constant	0.0312	0.00115	27.10
Relative speed (m/sec)	0.890	0.089	9.96
Space gap (m)	0.505	0.049	10.32
$\sigma^{cf,acc,+}$	1.086	0.026	41.843
Acceleration with ΔV (-)			
Constant	0.000119	0.000002	50.150
Relative speed (m/sec)	-0.0762	0.0142	-5.359
Space gap (m)	0.0697	0.0265	2.627
Speed (m/sec)	-2.592	0.032	-84.339
$\sigma^{cf,acc,-}$	1.601	0.016	52.744
Deceleration with ΔV (+)			
Constant	-0.876	0.016	-54.340
Relative speed (m/sec)	-0.0670	0.0074	-9.020
Distance to exit (km)	4.822	0.096	50.375
$\sigma^{cf,dec,+}$	0.826	0.009	87.738
Deceleration with ΔV (-)			
Constant	-1.136	0.039	-29.436
Relative speed (m/sec)	0.396	0.010	40.745
Space gap (m)	-0.0496	0.0015	-32.919
$\sigma^{cf,dec,-}$	0.911	0.007	123.271
Free-flow regime			
Constant	0.0773	0.0043	18.163
Desired speed constant	14.444	0.734	19.675
No. of front vehicles	-0.817	0.106	-7.723
σ^{ff}	0.795	0.009	92.415
Gap threshold distribution (0.6 sec < G^* < 11 sec)			
Constant	0.799	0.177	4.519
σ^{G^*}	0.998	0.655	1.523
Reaction time distribution (0.6 sec < τ < 4 sec)			
Constant	0.859	0.524	1.639
σ^{τ}	0.100	0.371	0.271
Number of observation	17,891		
Number of driver	1,386		
Number of parameters	25		
Initial Log-Likelihood	-41682.34		
Final Log-Likelihood	-23810.51		
Adjusted Rho-Bar Square	0.429		

$*)\ lead\ or\ front\ veh.\ speed - subject\ veh.\ speed$

7.2.3 Car following regime

The proposed acceleration modelling framework specifies the driver's car-following behaviour or response as a function of stimulus and sensitivity component. As discussed in earlier there are four sub-models in the car-following regime; acceleration with positive relative speed, acceleration with negative relative speed, deceleration with positive relative speed, and deceleration negative relative speed.

The stimulus component is a function of relative speed between the object vehicle and subject vehicle at the same traffic streams. In fact, the term of stimulus is slightly different when the subject vehicle faces a merging movement of the adjacent lead vehicle. This movement governs the subject vehicle to consider and response the stimulus from the merging vehicle rather than the front vehicle at his/her current lane. In the estimation, a dummy notation is introduced to identify the resources of stimulus; (1) if the adjacent lane lead vehicle tends to merge and (0) if no merging effect.

Several explanatory variables explain individual acceleration and deceleration behaviour in the car-following regimes including space gap, speed, and remaining distance toward the exit (off-ramp of weaving section).

The space gap explains individual driver sensitivity in three car-following conditions: acceleration with positive relative speed, acceleration with negative relative speed, and deceleration with negative relative speed. This variable fits well in the acceleration model instead of time gap which is used in the lane-changing model. In this case, the distance gap is a clear distance between front edge of subject vehicle and rear edge of the object vehicle in the same traffic stream. Note that, the modelling specification using time gap provides an unexpected result and sign in the overall model. Incorporating the gap with merging adjacent vehicle as explanatory variable results a similar problem as well. This study therefore considers only the space gap with the current lane front vehicle as one of the sensitivity component. Intuitively, this condition is acceptable as the driver consider to maintain the safe gap toward the front vehicle and leave gap the for the neighbouring traffic to merge safely into his/her current lane.

More detailed analysis and discussions on estimation result of car-following regime model are presented below.

Acceleration with positive relative speed

Estimation result defines both the positive relative speed and space gap to explain the car-following acceleration during positive relative speed. The relative speed represents

the stimulus component of the car-following regime model while the gap captures the driver's sensitivity in corresponding to the appearance of the stimulus.

As shown in **Table 7.4**, both the relative speed and gap have positive sign. The positive sign in the relative speed denotes that the vehicle acceleration increases correspond to the increment of the relative speed between the subject and object vehicle. Furthermore, the increased positive relative speed leads the gap between those vehicles to become larger. This condition allows the vehicle to accelerate faster compared to situation where subject vehicle faces smaller relative speed and gap.

The acceleration with positive relative speed model is given by:

$$a_n^{cf,acc,+}(t) = 0.0312\,(G_n(t)^{0.505})\,|\Delta V^+(t - \tau_n)|^{0.890} + \varepsilon_n^{cf,acc,+}(t) \qquad (7.11)$$

Where;

$a_n^{cf,acc,+}(t)$: Car-following acceleration of driver n, conditional on positive ΔV at time t

$G_n(t)$: Available space gap towards the front vehicle at the observed time (t)

$|\Delta V^+(t - \tau_n)|$: The absolute value of the relatively positive speed between the speed of the object vehicle (V_{n-1}) and subject vehicle (V_n) at time$(t - \tau_n)$.

τ_n : Reaction time of vehicle n (sec)

$\varepsilon_n^{cf,acc,+}(t) \sim N(0, 1.086^2)$

Acceleration with negative relative speed

This modelling specification captures a situation where the subject vehicle tends to approach the object vehicle. The negative relative speed represents the stimulus of the car-following while both space gap and speed explain the driver's sensitivity component of the acceleration model.

Table 7.4 summarises the result of the car-following acceleration with negative relative speed. The negative sign in the relative speed implies that the vehicle acceleration decreases with the increased of the subject vehicle speed. As expected, the space gap in the sensitivity component has positive sign. The speed, which is the denominator of the sensitivity, has a negative sign. The vehicles under this stimulus condition accelerate faster when the gap is relatively large while they accelerate less as the gap toward front

vehicle become small. The parameters explain that the subject vehicle prefers to join the downstream traffic in a convenience movement during the short period.

The car-following acceleration with negative relative speed can be expressed by:

$$a_n^{cf,acc,-}(t) = 0.000119 * \left(\frac{\Delta d_n(t)^{0.0670}}{V_n(t)^{-2.592}}\right) * |\Delta V^-(t - \tau_n)|^{-0.0762} + \varepsilon_n^{cf,acc,-}(t) \quad (7.12)$$

Where;

$a_n^{cf,acc,-}(t)$: Car-following acceleration of driver n, conditional on negative ΔV at time t

$\Delta d_n(t)$: The distance between the subject vehicle n and the object vehicle $n-1$ in front at time t (m)

$|\Delta V^-(t - \tau_n)|$: The absolute value of the negative relative speed between the speed of the object vehicle (V_{n-1}) and subject vehicle (V_n) at time ($t - \tau_n$).

$\varepsilon_n^{cf,acc,-}(t) \sim N(0, 1.601^2)$

Deceleration with positive relative speed

This modelling specification represents the situation when the subject vehicle decelerates in order to providing a safe gap for the neighbourhood lead vehicle that is about to merge into current lane or preparing for lane-changing movement. Similar to the previous car-following modelling regime, relative speed represents the stimulus for the car-following regime. Meanwhile, the remaining distance to exit explains the driver sensitivity during the car-following deceleration with positive relative speed.

As expected, the positive relative speed in this modelling specification has a negative sign. This sign implies that the deceleration is slightly decreased correspond to the relative speed increment. The vehicle deceleration in this condition is relatively more relax compared to the vehicle which faces negative relative speed. A positive sign for the remaining distance implies that the subject vehicle decelerates more aggressive when it gets closer to the exit in order to leave a large gap for the neighbourhood to merge safely.

Therefore, the deceleration with positive relative speed is given by:

$$a_n^{cf,dec,+}(t) = -0.876 * \left(d_n^{exit}(t)^{4.822}\right) * |\Delta V^+(t - \tau_n)|^{-0.0670} + \varepsilon_n^{cf,dec,+}(t) \quad (7.13)$$

Where;

$a_n^{cf,dec,+}(t)$: Car-following deceleration of vehicle n, conditional on positive ΔV at time t

$d_n^{exit}(t)$: Remaining distance to the mandatory lane changing point of the nth driver at time (t).

$\varepsilon_n^{cf,dec,+}(t) \sim N(0, 0.826^2)$

Deceleration with negative relative speed

Estimation result defines that both relative speed and gap affect the deceleration behaviour while facing a negative relative speed. It is worth noting that the relative speed captures the stimulus component of car-following regime decision. In the meantime, the space gap represents the driver's sensitivity that affects his/her response.

As shown in **Table 7.4** a positive sign of negative relative speed implies that the subject vehicle deceleration is increased of the negative relative speed. Note that the negative relative speed indicates that the subject vehicle is significantly faster than the object vehicle. The subject vehicle reduces slightly the deceleration with the decreased of negative relative speed. Meanwhile the gap has negative signs as well. This finding confirms that the vehicle deceleration tendency is more aggressive in correspond with the decreased of gap between the subject and object vehicles.

The car-following deceleration with negative relative speed is written as follows:

$$a_n^{cf,dec,-}(t) = -1.136 * (G_n(t)^{-0.0496}) * |\Delta V^-(t - \tau_n)|^{0.396} + \varepsilon_n^{cf,dec,-}(t) \qquad (7.14)$$

Where;

$a_n^{cf,dec,-}(t)$: Car-following deceleration of vehicle n, depending on negative ΔV at time t

$\varepsilon_n^{cf,dec,-}(t) \sim N(0, 0.911^2)$

Sensitivity analysis

The sensitivity analysis in this study presents the impact of various variables in car-following regime behaviour. Unless the observed explanatory variables are varied, the other variables in the sensitivity analysis are constant at the mean value as summarised in **Table 7.5**.

Table 7.5 Variables default value for sensitivity analysis

Variables	Value
Space gap (m)	80 m
Speed (V)	25 (m/sec)
Remaining distance (d^{exit})	1 km
Positive Relative Speed (ΔV^+)	3 m/sec
Negative Relative Speed (ΔV^-)	-3 (m/sec)
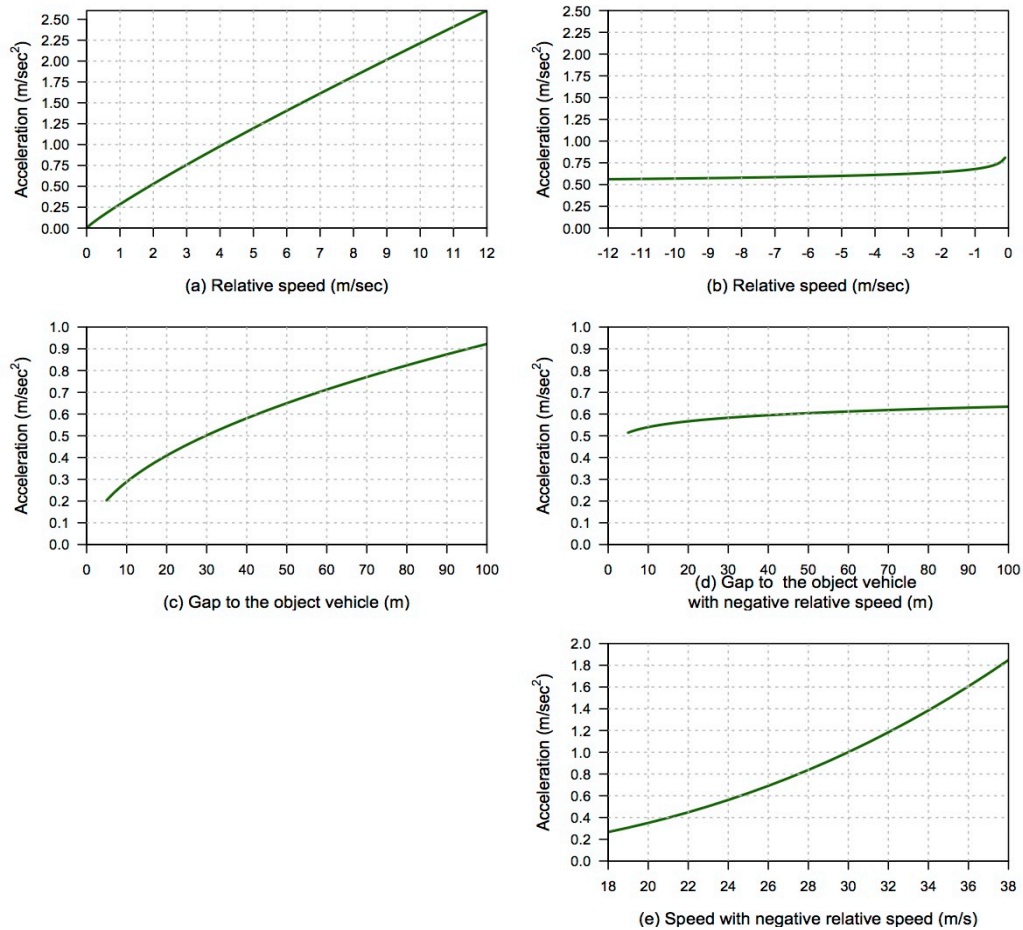
Figure 7.6 Car-following acceleration sensitivity with various factors and depending on relative speed condition: positive relative speed (a and c), and negative relative speed (b, d and e)

Figure 7.6 illustrates the variation of mean acceleration value depending on relative speed. Note that all figures on the left side (a, and c) relates to positive relative speed while the right side (b, d, and e) relate to negative relative speed

In terms of relative speed, the slope of acceleration with positive relative speed is decreased in correspond with the increased relative speed. This finding implies that the vehicle acceleration is significantly affected by the drive aggressiveness and vehicle capability to respond the stimulus appearance. Meanwhile, the slope of acceleration with negative relative speed is decreased gradually as the subject vehicle becomes faster than the object vehicle due to safety issue.
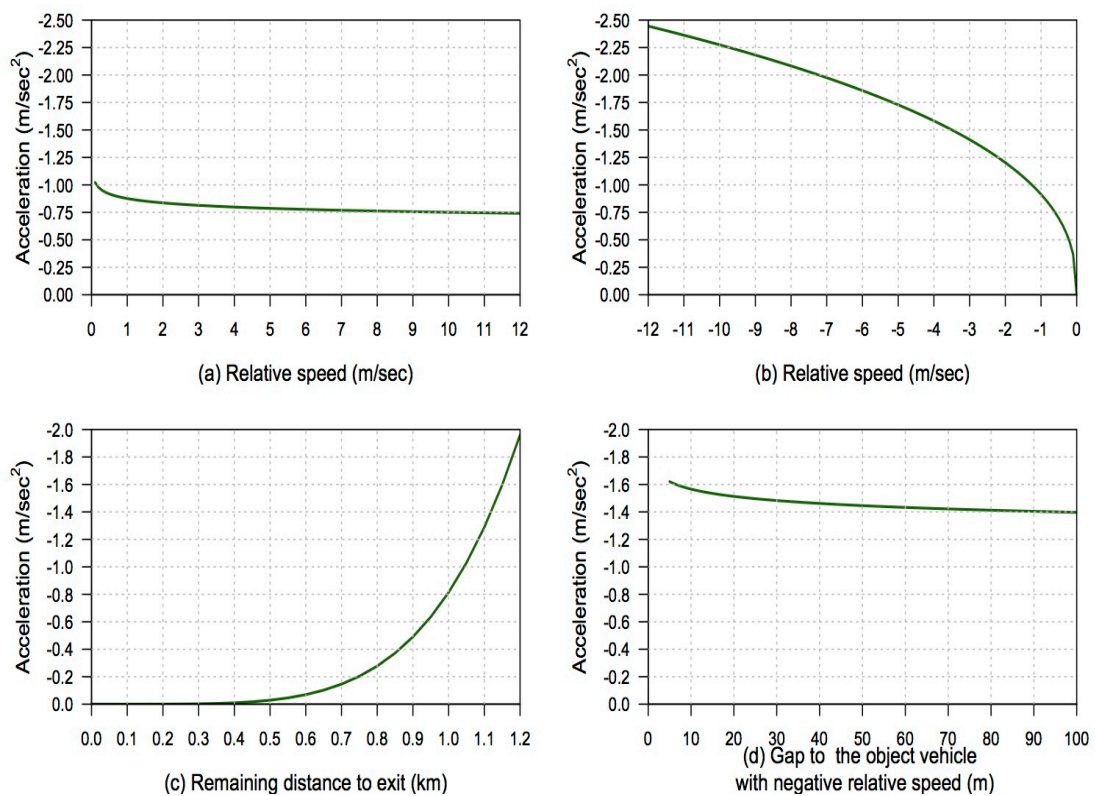
Figure 7.7 Car-following deceleration sensitivity with various factors and relative speed condition dependent: positive relative speed (a and b) and negative relative speed (c and d)

Figure 7.7 shows the mean value of deceleration behaviour with relative speed in different explanatory variables. Both figures on the left side (a, and c) relate with the deceleration with positive relative speed while the right side represents the variation of negative relative speed (b, and d)

The slope of the deceleration with positive relative speed decreases correspond with the increased of relative speed. This finding is intuitively acceptable, as the driver requires

less effort to decelerate and provide a safe gap for the neighbourhood vehicle to merge toward the current subject lane. If the positive relative speed is small, the subject vehicle requires slightly higher deceleration in this regard.

In the negative relative speed, the deceleration is increased significantly with respect to increasing relative speed (a negative value). The variation mean value demonstrates that the vehicle in this condition is more sensitive to the change of negative relative speed between 0 and -2 m/sec. Then, the slope of deceleration decreases corresponds with the increased of negative speed. This finding confirms that the limitation in vehicle mechanism and driver's aggressiveness have a significant impact on the deceleration capacity.

As discussed earlier, the remaining distance component has a significant effect on the deceleration with positive relative speed. The slope of deceleration is decreased significantly at the beginning of weaving section. This finding confirms that the traffic tends to decelerate at the beginning of weaving section to pre-emptive the neighbouring traffic movement and their plan to move safely over the weaving section.

7.2.4   Free flow regime

Similar to the car-following regime, the driver's response to a free flow regime is a function of the stimulus and driver's sensitivity. The stimulus component in a free-flow regime modelling specification is a function of the desired speed (V_n^{DS}), which is an explanatory function variable and observed speed at the time $(t - \tau)$. The estimation result defines the number of lead vehicles as an explanatory of desired speed. Meanwhile, the sensitivity constant represents the driver's sensitivity during the free-flow movement. The free-flow regime modelling specification is performed under linear form instead.

The acceleration behaviour in free-flow traffic regime is affected by the number of current lane front vehicles (see **Table 7.4**) . The number of the lead vehicle in a free-flow regime model has a negative sign. The negative sign implies that the vehicles decelerate more aggressive due to the increased number of the front vehicle during the free-flow regime. Equation 7.15 expresses the estimated free-flow regime model:

$$a_n^{ff}(t) = 0.0733 * [(14.444 - 0.817 * k_n(t)) - V_n(t - \tau_n)] + \varepsilon_n^{ff}(t) \quad (7.15)$$

Where:

$a_n^{ff}(t)$: Acceleration of vehicle n under free-flow regime at time t

$k_n(\text{t})$: Number of vehicle in front of vehicle n at time t

$V_n(t - \tau_n)$: Vehicle n speed at time $t - \tau_n$

$\varepsilon_n^{ff}(t) \sim N(0, 0.801^2)$

The sensitivity analysis represents the impact of the number of front vehicle variable in the free-flow movement behaviour. A linear function of the free-flow regime indicates that the vehicle decelerates aggressively with respect to the increased traffic on the downstream. This analysis confirms that the traffic tends to decelerate at the beginning of weaving section, though the vehicle moves under a free-flow regime as shown in **Figure 7.8**.
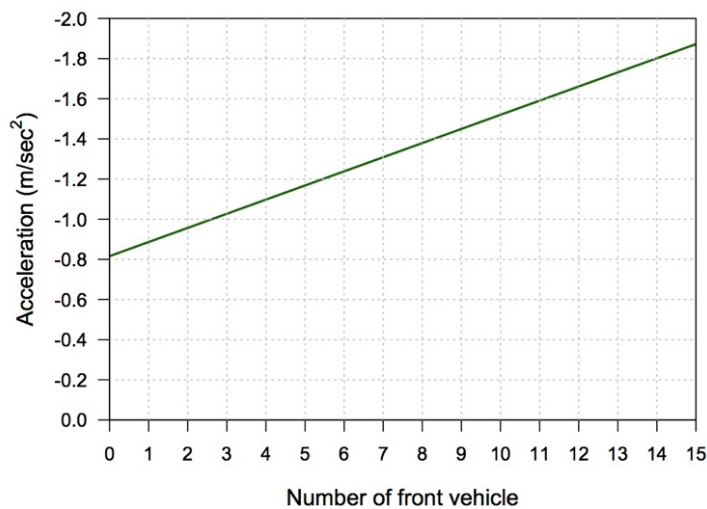
Figure 7.8 Free-flow sensitivity with respect to the number of vehicles

7.2.5   Gap threshold distribution

The gap threshold (sec) distribution assists to classify a regime of each car-following event whether it falls into a car-following or free-flow regime. The current study describes the distance toward the front vehicle as the gap (distance between the front vehicle back-edge and the subject vehicle front-edge). As discussed in Section 5.2.3, the current study presumes that the gap threshold distribution follows a lognormal distribution which is truncated in both sides (lower and upper boundaries).

The truncated lognormal distribution in the proposed model fits with the profiles of the gap acceptance between the subject and front vehicle distribution where a high proportion of traffic prefers a small headway during their movement as seen in **Figure 6.12** (b). Furthermore, the proposed acceleration model suggests that the lower boundary of the truncated lognormal distribution equals to the minimum observable gap

between the subject and the front vehicle. Assuming that none of the observed vehicle accepts gap that is smaller than 0.6 sec in order to maintain the safest gap between them. This assumption simplifies the estimation process.

The application of truncated lognormal distribution is certainly avoiding the negative value and finiteness of gap that never occurs in the real traffic. The proposed acceleration model incorporates the gap threshold distribution as a conditional specification of the car-following behaviour joint density.

Given Equation 5.13, the gap threshold distribution can be expressed as follows:

$$f(G_n^*) = \begin{cases} \dfrac{1}{G_n^*.\,2.506}\phi\left(\dfrac{\ln\,(G_n^*) - 0.799}{0.998}\right) & if\ 0.6 \leq G_n^* \leq 11 \\ 0 & Otherwise \end{cases} \qquad (7.16)$$

The joint estimation defines that the gap is distributed between 0.6 and 11 sec. The proposed acceleration model suggests that the minimum gap threshold equals to the minimum observable gap between the subject and the front vehicle. Note that no vehicle accepts gap that is smaller than 0.6 sec in order to maintain the safest gap between them. This assumption simplifies the estimation process.

Several possible values between 10, 11, and 12 sec were observed as the maximum gap threshold value. However, the estimation result suggests that the gap threshold maximum value equals 11 sec. The dataset shows that approximately 2% of the traffic facing headway larger is than 11 sec.

Further, the probability of the vehicle n on a car-following regime at time t is formulated as follows:

$$P_n(car - following\ at\ time\ t) = P(G_n(t) \leq G_n^*)$$

$$= \begin{cases} 1 - \dfrac{\Phi\left(\dfrac{\ln(G_n(t)) - 0.799}{0.997}\right) - \Phi\left(\dfrac{\ln(G^{*,min}) - 0.799}{0.997}\right)}{\Phi\left(\dfrac{\ln(G^{*,max}) - 0.799}{0.997}\right) - \Phi\left(\dfrac{\ln(G^{*,min}) - 0.799}{0.997}\right)} & 0.6 \leq G_n^* \leq 11 \\ 0 & Otherwise \end{cases} \qquad (7.17)$$

Figure 7.9 presents both gap threshold distribution and probability of car-following based on the given Equation 7.16 and 7.17 respectively. The median, mean and standard

deviation of the gap distribution threshold are 2.07, 2.66 and 2.82 sec. The descriptive statistic values are estimated based on Equations 5.15, 5.16 and 5.17.
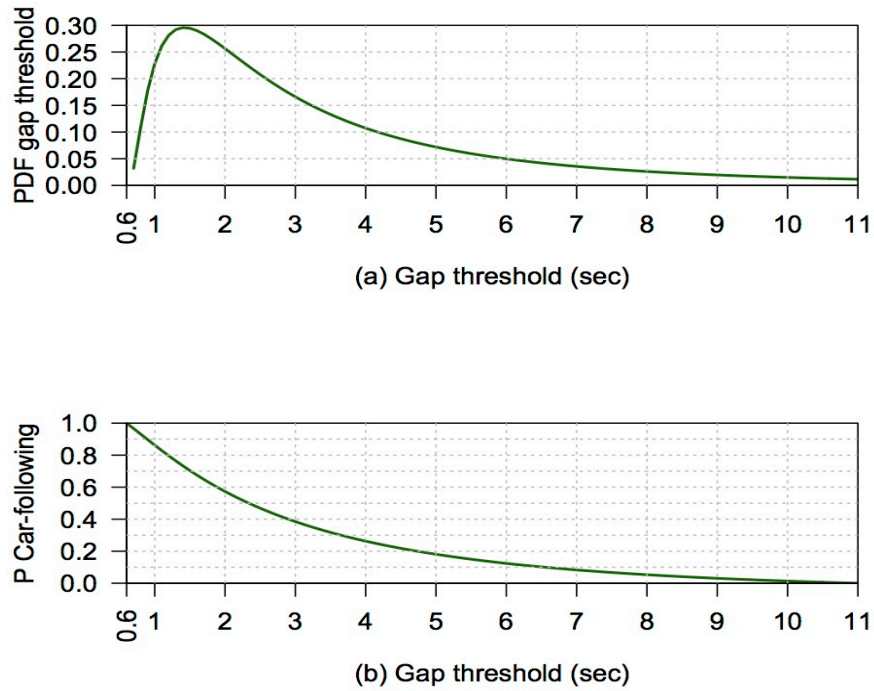
Figure 7.9 Gap threshold distribution and probability of car-following regime as a function of the time gap
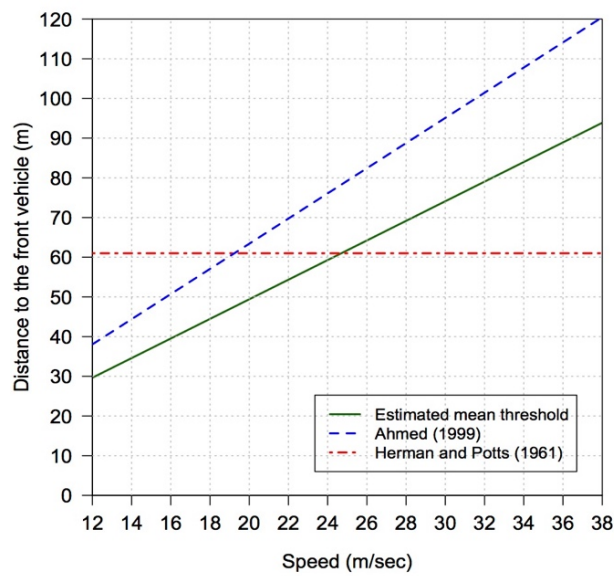
Figure 7.10 Comparison of mean gap threshold distribution between the estimated result, Ahmed (1999) and Herman and Potts (1961)

Figure 7.10 measured the distance between subject and front vehicle as headway (distance between the front vehicle front-rear and the subject vehicle front-rear). The mean value of headway threshold distribution in Ahmed (1999) equals to 3.17 sec. Although the current model has the lower average value slightly, the estimated gap threshold has the similar pattern with Ahmed's study. Both studies show that the gap/headway is increased correspond to the increased speed mean value. Herman and Potts (1961) defined the headway threshold as a constant at 61m (200 ft) for all variation of speed. This assumption leads to being an unrealistic result as the traffic in the real-world need larger gap due to the increased of the speed and maintains a safety distance toward the front vehicle.

7.2.6   Reaction time distribution

Similar to gap threshold distribution, the reaction time distribution follows a lognormal distribution with a truncation on both sides. This assumption implies that a high proportion of driver prefers a short reaction time while less proportion of driver requires a large reaction time distribution. Moreover, both side truncated lognormal distribution ensures that the population reaction time shows a positive and finite value. The proposed acceleration model specifies the reaction time distribution as conditional form of the acceleration model joint density function together with the gap threshold distribution.

Based on Equation 5.15 and estimation result, the probability density function of reaction time can be expressed as follows:

$$f(\tau_n) = \begin{cases} \dfrac{1}{\tau_n 0.010} \phi \left(\dfrac{ln(\tau_n) - 0.859}{0.100} \right) & if\ 0.6 < \tau_n \leq 4 \\ 0 & otherwise \end{cases} \quad (7.18)$$

The estimation result defines that the driver's reaction time is between 0.6 and 4 sec. In this case, the proposed car-following model presumes that minimum value of reaction time distribution equals to the gap threshold distribution lower bound. This assumption suggests that none of the subject vehicles prefers a reaction time that is less than 0.6 sec to maintain the safest headway/gap towards the front vehicle.
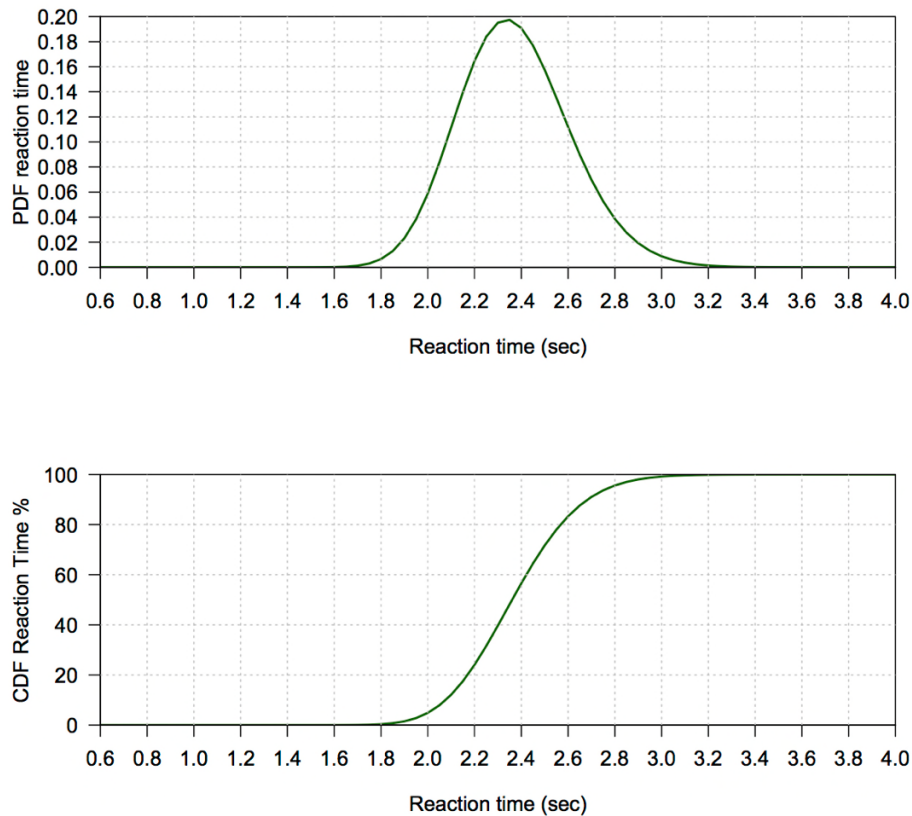
Figure 7.11 Probability Density Distribution Function (PDF) and Cumulative Distribution Function (CDF) of driver reaction time

Figure 7.11 illustrates both probability density function and cumulative distribution function of reaction time. By applying Equations 5.18, 5.20, and 5.21 The reaction time distribution median, mean and standard deviation values are 2.36, 2.37 sec and 0.06.

As described in Section 5.2.4, the model included several explanatory variables that affect the driver's reaction time such as types of vehicle, traffic density/occupancy, the front vehicle speed. However, incorporating those explanatory variables provides an unexpected result including smaller likelihood value, insignificant t-statistic value and sign of explanatory variables. Consequently, the current study includes the specific constant only that represents the mean value of driver's reaction time.

Furthermore, this study compares the estimated reaction time distribution with the previous studies comprising Ahmed (1999), Toledo (2003) studies as shown in **Table 7.6**. Note that current study and both previous studies presume the relative speed between subject and front vehicle as the stimulus component of the car-following behaviour

Table 7.6 Variation of reaction time distribution parameters from different studies

Studies	Reaction time threshold		Sample Size (veh)	Median (sec)	Mean (sec)	Std. dev. (sec)
	Lower	Upper				
This study	0.6	4	1,386	2.36	2.37	0.25
Toledo (2003)	0	6	442	0.85	1.1	1
Ahmed (1999)	0	3	402	1.31	1.34	0.31

The estimated median, mean of reaction time distribution in this study are slightly larger compared to the previous works. Meanwhile, the standard deviation is slightly smaller compared to Ahmed (1999) and Toledo (2003). The difference in the estimated parameters of reaction time distribution appears because of several factors such as characteristics of site location, the traffic condition, the length of observation period, the modelling framework and the estimation procedure. Note that the current study focuses on the weaving section with a moderate traffic condition where the traffic tends to relax during their movement in the observation area.

This research covers a significant large of dataset compared to both previous studies. Having a real knowledge of the road network and traffic condition affects the awareness of the drivers when moving on a particular stretch of road. The driver tends to relax in this condition and prefers longer reaction time. In general, the estimated mean, median and standard deviation are within the range of acceptable reaction time value.

Overall, extending the acceleration model framework particularly in the car-following regime model allows variation of stimulus conditions in both car-following behaviours. This proposed model provides a new horizon and flexibility in capturing various car-following behaviours as the responses of stimulus and driver's sensitivity. The extension of acceleration model in this study allows four different car-following behaviours: acceleration with positive relative speed, acceleration with negative relative speed, deceleration with positive relative speed, and deceleration with negative relative speed. The sensitivity term in both car-following and free-flow regime models represents the unobservable variable. This study presumes that both gap threshold and reaction time distribution follow lognormal distribution as a conditional form of the likelihood estimation. Note that the model faces same issues with the previous acceleration to incorporate the driver sensitivity and socio demographic data to explain individual driver reaction time due to the inevitability of information in the current dataset. Having the socio demographic data (i.e. gender, and age) assist to improve the accuracy in predicting the driver reaction time.

7.3 Summary

The lane changing model in the current research captures two levels of the decision-making process during the lane-changing movement: target lane choice and gap acceptance. The proposed model incorporates various lane-changing mechanisms, which corresponds with the lead/front vehicle movement during the lane changing process. The study observes three different lane-changing mechanisms: solo, platoon and weaving. Those lane-changing tactics are part of the gap acceptance behaviour. Furthermore, the model includes the heterogeneity component capturing the variation of driver preference during the lane changing process which is identic with the level of driver's aggressiveness.

Parameters in both target lane choice and gap acceptance model were estimated jointly with likelihood estimation procedure with conditional on the heterogeneity. The target lane is a function of several explanatory variables including the average speed, occupancy, relative speed of the current lane front vehicle and target lane lead vehicle, path plan and heterogeneity. The estimation result indicates that most of traffic prefers lane 3 while they avoid moving on the far-side lane (lane 5). The path plan variable confirms that the driver prefers performing a pre-emptive lane changing at the beginning of weaving section. Interpreting the heterogeneity variable, it is more likely that the aggressive driver in the moderate traffic flow prefer left lane rather than right lane.

Various lane-changing mechanisms have a significant effect on the critical gap acceptance. The solo gap acceptance is a function of both relative speeds towards the front and the lead vehicle respectively. The platoon lane changing is significantly affected by the relative speed between the subject and front vehicle at the current lane, which changes lane. Meanwhile, the weaving lane changing is affected by the relative speed of target lane lead vehicle. All the relative speeds in critical lead gap are negative denoting that the subject vehicle requires a smaller gap if the current lane front vehicle and target lane lead vehicle move faster than his/her speed. The aggressive driver is an individual who accepts smaller critical gap all else being equal. The driver aggressiveness varies associated with the lane-changing mechanisms. The weaving lane-changing mechanism, which tends to face a largest reduction critical gap, is the most aggressive driver compared to the other lane-changing mechanisms.

The difference of specification in critical lag gap associated with lane-changing mechanism is insignificant. The current study, therefore, retain the common critical lag gap model. A positive sign of relative speed between target lane lag and subject vehicles explains that the critical lag gap is increased as the lag vehicle moves faster than the

subject vehicle (i.e. gap closing). Individual-specific constant of critical lag gap is sligtly larger compared to the critical lead gaps of all lane-changing mechanisms. This finding denotes that individual driver is more vigilant with accepting available lag due to difficulty intepreting the lag vehicle behaviour rather than the current lane front vehicle and the target lane lead vehicle.

The proposed lane-changing framework shows interesting result and practical implication in the weaving section design process. For example, parameter values indicate that (a) all else being equal, platooned lane-changing involves smaller gap (b) for aggressive drivers, the critical gaps of weaving lane changes are significantly smaller (c) platoon and weaving drivers are more sensitive to relative speed changes and increase their critical gaps significantly with negative relative speed, and (d) lane-changing is more likely to occur at the beginning of a weaving area, particularly if multiple lane changes are required to follow the path. The implications of (a) and (b) can be considered from a safety point of view: platoon and weaving lane-changing mechanisms are potentially unsafe and should, therefore, be discouraged. An intervention on the traffic management may require maintaining a large gap among the traffic, equalises the vehicle speed and critical gap among those lane-changing mechanism resulting on the improvement of lane-changing efficiency according to (c) condition. Spreading the merging and diverging traffic across the weaving section would minimise the conflict intensity at the beginning of weaving section according (d). Indeed, this can improve the safety aspect of weaving section.

This section compares the estimated of both critical gaps and lag, with the observed accepted gaps and lag as a function of relative speed. This phase is part of validation process. In this case, the study represents the observed accepted gap as non-linear regression. The analysis illustrates that the median of critical gaps is relatively smaller compare to the regression of the observed accepted gaps for all variation of relative speed. Similar condition appears in the critical lag. The differences between those values denote that individual driver tends be conservative by finding large gap and lag for changing lane in a safe manner.

Meanwhile, the proposed acceleration model defines the car-following behaviour as a function of the stimulus and driver's sensitivity components. In this case, the stimulus is a relative speed's linear function of an absolute value while the sensitivity is a function of explanatory variables as regards particular observation period. Furthermore, the application of gap threshold distribution in this study classifies the car-following condition into two regimes: car-following regime and the free-flow regime. The extension on the car-following behaviour and relative speed assumptions lessen the

limitation in capturing various stimulus (relative speed between the subject and object vehicles) condition impacts over the decision in the car-following regime. In this case, there are four types of decision in the car-following regime: acceleration with positive relative speed, acceleration with negative relative speed, deceleration with positive relative speed, and deceleration with relative negative speed.

All parameters in the acceleration model were estimated jointly using the likelihood estimation procedure conditional on gap threshold and reaction time distributions. The estimation result shows that the sensitivity term in acceleration with positive relative speed is a function of space gap, while the acceleration with negative relative speed is a function of space space gap and speed. The sensitivity component in deceleration with positive relative speed is a function of remaining distance toward the mandatory lane changing location. Meanwhile, the deceleration with negative relative speed sensitivity component is a function of gap. In the free-flow regime, the model indicates that the vehicle tends to decelerate in correspond with the increased number of vehicle. Both the gap threshold and reaction time distribution is presumed to follow a truncated lognormal distribution with the lower boundary equals 0.6 sec. This assumption is based on minimum gap acceptance toward the front vehicle in the vehicle trajectory dataset. Note that, no vehicle accepts smaller gap than 0.6 sec toward the front vehicle. Meanwhile, the upper boundaries for the gap threshold and reaction time are 4 sec and 11 sec respectively. Given the estimation result, the mean and standard deviation of the gap threshold distribution are 2.66 and 2.82 sec, while for the values for reaction time distribution are 2.36 and 0.06 sec respectively.

As a final point of this section, both estimation results of the lane-changing model and car-following model were estimated based on a same dataset that consists of 1,386 vehicles and 17,981 events. The dataset was gathered from the traffic video trajectory data during the highest 15 minutes period of a particular motorway weaving sections. The fact is that the appearance of auxiliary lanes and short distance between the entry point (beginning of weaving section) and mandatory lane changing location (beginning of weaving section) has significant impact on the estimation result. However, even in its current form, the developed models have a strong potential to improve the fidelity of microsimulation tools in the context of improved simulation of weaving sections in moderate congestion levels.

Chapter 8   Conclusion

This chapter summarises the research and highlights the main contributions of this Ph.D. thesis. Directions for the further research are discussed at the end.

8.1 Research Summary

Driving in a weaving section is a unique condition and complex, where the driver requires adjusting his/her path and maintains the safe space toward the front/lead vehicle in a relatively short length of the road. In this case, the lane-changing and acceleration behaviours are critical which affect the traffic performance in weaving section.

Lane changing in a weaving section is challenging where the driver requires deciding lane choice and available gap simultaneously during his/her movement in a weaving section. In the real traffic, the lane-changing vehicle in weaving section may move with different strategies (mechanisms) due to the complexity of weaving section traffic condition. The similar condition appears in acceleration behaviour, where the driver may response differently with the stimulus condition. Those conditions have significant impact on the driver behaviour models, which is omitted by the previous studies. These limitations of the previous models challenge this Ph.D. study to develop new modelling frameworks for both driving behaviours in weaving section particularly in moderate traffic flow condition.

Lane-changing model

This current research extends the state-of-the-art random utility-based lane-changing model to explicitly incorporate the effect of lane changing mechanism (platoon, weaving and solo) in the modelling framework as an intermediate plan. Thus, it changes the structure of the hierarchical of lane-changing process slightly as follows target lane choice, lane-changing mechanisms, and gap acceptance. The lane choice is latent (unobserved) while it is only the executed lane-changing movement (action) that can be observed. The driver requires accepting both gaps correspond with the lane changing

mechanisms (solo, platoon, and weaving) to change the lane. Otherwise, the driver stays in the current lane. The plans and actions of the driver conditional on individual-specific are presumed to be independent over a period. Individual-specific latent variable of level aggressiveness captures the interdependencies among the decisions plan (target lane) choice and action of the same driver. The level of aggressiveness in the target lane choice in the proposed model is related to the relative location of the target lane. Meanwhile, individual aggressiveness in the action level is associated with the gap acceptances and lane changing mechanisms. Therefore, the estimated lane-changing latent plan can be structured as shown in **Figure 8.1** (L denotes the number of available lane choice while L' denotes the lane-changing direction associated with current lane)
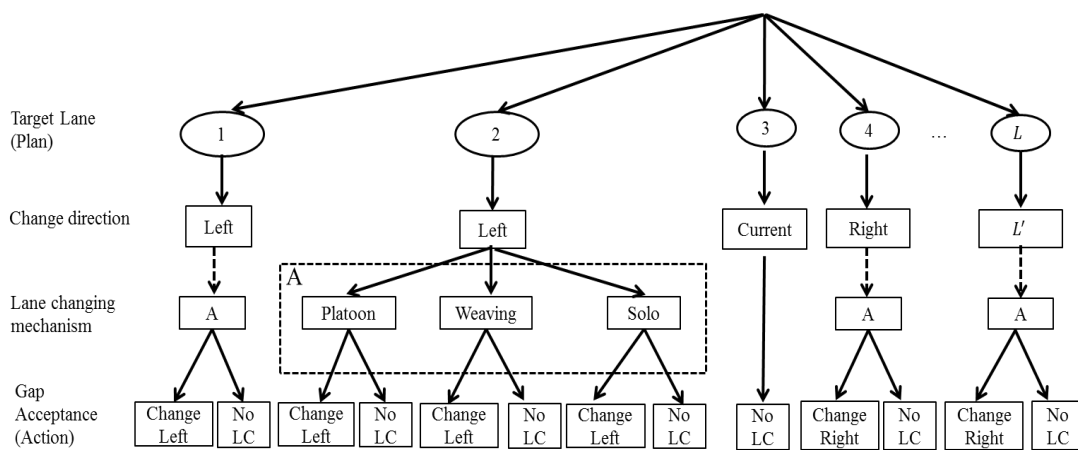
Figure 8.1 Estimated modelling framework for lane-changing decision making processes

All the parameters in the proposed lane-changing model were estimated jointly with likelihood estimation procedure. The target lane is a function of several explanatory variables including the average speed, occupancy, the relative speed of the front vehicle, path plan and individual-specific constant. In general, the estimation results on the lane constant indicate that most of the traffic prefers to move on the middle lane and curbside lane. Moving on the fast lane (far-side lane) is less preferable during the less congested traffic condition. The path-plan captures the disutility of driving in the wrong lane. The magnitude increased significantly when approaching the mandatory lane-changing point. In additions, this finding indicates that the driver is most likely perform a pre-emptive lane changing if the final target lane is multiple away from the current lane. Individual-specific constant in the target lane choice model captures the driver aggressiveness with respect to the target lane location either left or right of the current lane location. A positive sign on the left lane changing direction implies that aggressive drivers are more likely to choose a left lane over a right lane.

The estimation results indicate significant differences in parameters as well as influencing variables among the three types of lane changing mechanisms. This is supported by statistically significant improvements in the goodness-of-fit results as well as asymptotic t-tests. Furthermore, both of critical lead and lag gaps are significantly affected by the relative speed. The solo lane-changing mechanism is explained by the relative speed between the subject vehicle and both current lane front and target lane lead vehicles. Meanwhile, the platoon and weaving are affected by the relative speed between the subject vehicle and the current lane front vehicle, the relative speed between the subject vehicle and the target lane lead vehicle respectively. All the relative speeds has negative signs indicating that the subject vehicle accepts smaller gap if the current lane front vehicle and target lane lead vehicle move faster than the subject vehicle.

Individual-specific constant captures the level of aggressiveness that varies depends on the lane-changing mechanisms. In comparison among those three mechanisms, the aggressiveness affects significantly the weaving movement which receives the largest critical gap reduction due to the movement complexity while least impact on the platoon lane-changing mechanism. Changing lane in a weaving mechanism, therefore, requires higher level of aggressiveness, as the driver needs to be more alert and responds swiftly due to the change of traffic situation during the lane-changing movement. Meanwhile, the driver in platoon mechanism is relatively relaxed as this type of movement receive less effect of aggresiveness compared to the other mechanism. The lane-changing traffic in platoon mechanism needs only to follow the front vehicle movement, who trigers the interaction for creating a space at the target lane.

This study retains the critical lag gap model to be same for all type lane-changing mechanisms. Differentiating the critical lag is statistically insignificant difference. The relative speed in the critical lag gap model has positive sign implying that the critical lag gap is increased with the relative speed (i.e. lag gap closing). Individual-specific constant of critical lag gap is sligtly larger compared to the critical lead gaps of all lane-changing mechanisms. This finding denotes that individual driver is more vigilant with accepting available lag due to difficulty intepreting the lag vehicle behaviour rather than the current lane front vehicle and the target lane lead vehicle.

The median, median and standard deviation of the estimated critical lead gaps of all lane-changing mechanisms are; solo: 0.42, 0.43, and 0.05 sec; platoon: 0.10, 0.29, and 0.89 sec; weaving: 0.68, 0.93, and 1.03 sec.

The parameter values in the proposed lane changing model estimation results imply several key findings:

(a) All else being equal, platooned lane-changing involves smaller gap.

(b) For aggressive drivers, the critical gaps of weaving lane changes are significantly smaller.

(c) Platoon and weaving drivers are more sensitive to relative speed changes and increase their critical gaps significantly with negative relative speed.

(d) Lane-changing is more likely to occur at the beginning of a weaving area, particularly if multiple lane changes are required to follow the path.

Further, those four key findings imply the weaving section design in various aspects such as;

1. The implication of findings (a) and (b) can be considered from a safety point of view: platoon and weaving lane-changing mechanisms are potentially unsafe and should, therefore, be discouraged.

2. An engineering intervention in the weaving section could include advice on keeping a safer headway. Advice/intervention (such as; the variable speed limit, ramp metering) to equalise vehicle according to findings (c), reduce the critical gap and therefore improve lane-changing efficiency

3. For finding (d), an improvement on weaving section geometric or lane-marking to separate lane changing for merging from lane-changing for diverging would minimise the intensity of lane-changing at the beginning of weaving area and spread lane-changing across the whole weaving area. This can improve safety as well as the traffic performance of the weaving section.

Though, this study provided the opportunity to observe higher shares of platoon and weaving mechanisms, it lacked observations on other mechanisms (e.g. courtesy and forced lane changings). The results therefore may not be directly applicable to congested or over saturated situations.

Acceleration model

Acceleration model is a function of the stimulus and the driver sensitivity attributes. The stimulus is represented by the relative speed between the front vehicle and lead vehicle. The proposed model classifies the acceleration behaviour in two conditions: car-following regime and a free-flow regime. This classification depends on the gap threshold. Similarly with the driver reaction time, this study presumes that gap threshold is assumed to be a random variable that is independent between individuals

and follows the lognormal distribution with truncation in both sides. This assumption is identical with the distribution of the observed gap between the observed vehicle and the front vehicle (see **Figure 6.12**). Meanwhile, the lognormal assumption in the reaction time implies that a high proportion driver prefers small reaction time.

Focusing on the car-following regime, this study relaxes the assumption on the previous studies allowing each car-following behaviour (acceleration or deceleration) relate to both relative speed conditions (positive and negative). Therefore, there are four types of car-following behaviours: acceleration with positive relative speed, acceleration with relative negative speed, deceleration with relative positive, and deceleration with relative negative speed. This proposed structure provides flexibility in capturing some traffic, which acts differently from the stimulus. Although perceiving a positive stimulus, a high proportion of traffic prefers decelerates at the beginning of weaving section due to several reasons i.e. maintain the safest distance with the front vehicle, leave a safe space for the neighbourhood vehicle to merge at the same lane, and prepare for lane-changing movement.

Estimating with the same dataset with lane-changing model, all the parameters in the proposed acceleration model is estimated jointly under the likelihood estimation procedure. The estimation results show several key findings on the acceleration behaviours as follows:

- The driver sensitivity of the car-following acceleration with positive relative speed condition is a function of space gap while the car-following acceleration with negative speed is a function of space gap and speed.
- The car-following deceleration with positive relative speed sensitivity is a function of remaining distance towards the exit. The parameters in this stimulus condition indicates that the observed vehicle tends to decelerate higher in the beginning of weaving section compared to the end of weaving section.
- The sensitivity of car-following deceleration with relative negative speed is a function of headway.
- The free-flow acceleration is a function of number of vehicle on the current lane. In fact, the vehicle tends to decelerate higher as the number vehicle is increased.

The median, mean and standard deviation of the gap threshold distribution are 2.07, 2.66 and 2.82 sec. Then, the median, mean and standard deviation of reaction time distribution are 2.36, 2.37 and 0.06 sec.

The research however has several limitations. First of all, the data used for the research includes trajectory data extracted from video recordings, which though widely used,

have known limitations such as the possibilities of spatial measurement errors, capability of the recording tools, and absence of driver characteristics and information about indicators. The used of semi-automatic vehicle trajectory extractor for a large observation area may contribute to the measurement error. Indeed, the quality of dataset affects the estimation results. This study, therefore, requires a proven algorithm to transfer the pixel into coordinate and fitted the trajectory vehicle. The quality of the models would certainly be improved with better data.

Secondly, the proposed models are estimated using data collected from moderately congested traffic conditions. Though this provided the opportunity to observe higher shares of platoon and weaving mechanisms, it lacked observations on other mechanisms, as such courtesy and forced lane changings. The results therefore may not be directly applicable to congested or over saturated situations (as modelled by Choudhury, 2007; Hidas, 2005; Wan et al., 2014; Wang, 2006).

However, even in its current form, the developed models have a strong potential to improve the fidelity of microsimulation tools in the context of improved simulation of weaving sections in moderate congestion levels. The current models are yet to be validated in any microsimulation tool. Moreover, it will be interesting to test the transferability of the modelling framework in other weaving sections and other congestion levels. Another potential direction of extension can be to investigate the effect of the lane changing mechanism on acceleration behaviour.

8.2 Contributions

This thesis contributes to improve state-of-the-art of lane-changing and acceleration models in following aspects:

- This study offers an insight of driving characteristics and general modelling framework for lane changing and acceleration behaviours at particular weaving section with moderate traffic. The lane-changing mechanisms have significant impact on lane-changing characteristics. Meanwhile, relaxing the relationship of sensitivity and stimulus condition allows to capture various acceleration phenomena which does not considers in the previous study.

- An extended of latent plan lane-changing modelling framework is proposed. This framework incorporates the various lane-changing strategies (i.e. individual/solo, platoon and weaving), correspond with the front/lead vehicle movement. The lane changing strategies become critical in a weaving section, where the vehicle has to adjust the lane in a relative short length of the road The empirical traffic data constitute that significant traffic proportion (23.4%) involves in a group behaviour

where 12.7% performs a weaving manoeuvre and 10.7% in platoon lane-changing mechanism. The flexibility of the latent plan modelling framework allows integrating that strategies/mechanism as an intermediate plan.

- The proposed acceleration model relaxes the condition of stimulus in the car-following regime. This approach relates each car-following behaviour with both stimulus conditions whether positive or negative. In this case, the stimulus condition is a function of the relative speed between the subject and object vehicle. This framework provides an opportunity to capture the variation of car-following behaviours, especially in the weaving section where some of the traffic may act differently with the stimulus due to maintaining the safe space in order to anticipate the lane-changing movement of neighbourhood vehicle or preparing for pre-emptive lane-changing movement. The vehicle trajectory analysis implies that 43.5% of the traffic falls in deceleration with positive relative speed while 38.5% involves in deceleration with negative relative speed. Giving the traffic condition, it confirms that most of the traffic in the beginning of weaving section decelerates and tends to response differently from the stimulus condition.

- For each of the lane-changing and acceleration models, all the parameters are estimated jointly using a likelihood estimation procedure. Both models are estimated based on the same set of vehicle trajectory data. Each model is estimated separately. In comparison with the previous studies, the estimation result goodness-of-fit implies that incorporating various lane-changing mechanisms in the proposed latent plan lane-changing model and relaxing the relationship between the stimulus and individual driver respond in the acceleration model produce better understanding on the driving characteristic in the weaving section particularly. Moreover, the developed of the proposed lane-changing and acceleration models have a strong potential to improve the fidelity of microsimulation tools in the context of improved simulation of weaving sections in moderate congestion levels.

- The estimation results of lane changing model imply that lane-changing mechanisms are critical in the lane-changing decision-making process particularly in a moderate traffic flow. The use of path impact captures the disutility of being on the wrong lane which increases significantly as the traffic approach the mandatory lane-changing point (off-ramp). In this case, the traffic prefers to perform a pre-emptive lane changing at the beginning of weaving section. Individual-specific constant represents the driver heterogeneity in terms of the level of aggressiveness when choosing a specific target lane choice and critical gap in various lane-changing mechanisms Interpreting the heterogeneity variable, it is

more likely that the aggressive driver in the moderate traffic flow prefer left lane rather than right lane. Meanwhile, in critical gap model, the driver aggressiveness is most in weaving mechanism and least on platoon mechanism. Identifying various lane-changing mechanism characteristics assists the researchers and engineers to address the conflict (i.e. spreading the merging and diverging traffic due to high lane-changing intensity in upstream traffic) by intervening the traffic with optimum solutions (i.e. improvement of marking and signing, the installation of ramp metering and road geometry improvement).

- The result indicates that relaxing the stimulus condition in acceleration provides better interpretation of the car-following behaviour in the weaving section. The remaining distance toward the mandatory lane changing location affects the decision on the deceleration with positive stimulus. A positive sign of remaining distance implies that the vehicle tend to decelerate higher at the beginning of weaving section to provide a safe space towards the front vehicle and preperation to adjust their lane. Assuming that the minimum gap threshold and reaction time are equal, it simplies the estimation procedure and is intuitively acceptable as the aggressive driver may maintain the gap at the minimum reaction time. The gap term is more realistic in representing the distance between the subject and front vehicle rather than the headway, as it is more difficult for the driver to measure in the real traffic.

8.3 Direction for Further Research

A large number of studies have been carried out on the lane-changing behaviour and car-following behaviour. The proposed lane-changing latent plan modelling framework and acceleration model provide a significant enhancement in capturing various lane-changing and acceleration behaviours respectively. In fact, these modelling frameworks retain the opportunities for further development. Some of further research direction is discussed as follows:

- This thesis presents the extension of latent plan modelling framework for lane-changing behaviour in the weaving sections. The framework incorporates explicitly various lane-changing mechanisms associated with the front/lead vehicle movement as the intermediate plan. The application of this framework for different traffic characteristics and other multilane facilities offers a benefit for the modelling development.

- Incorporating the state-dependence condition in the lane-changing modelling allows capturing the impact of the interdependencies and causalities relationship

among the lane-changing decision. Thus, it is a need to find or develop an algorithm and estimation procedure which able to integrate this component.

- An integration of the proposed lane-changing and acceleration models is an advance development. This integration provides enormous benefits in understanding the nature of driving behaviour as holistic approach and fits properly with driving behaviour in the real traffic as shown in **Figure 8.2**. However, the increased of modelling complexity requires an advance estimation procedure and tools.
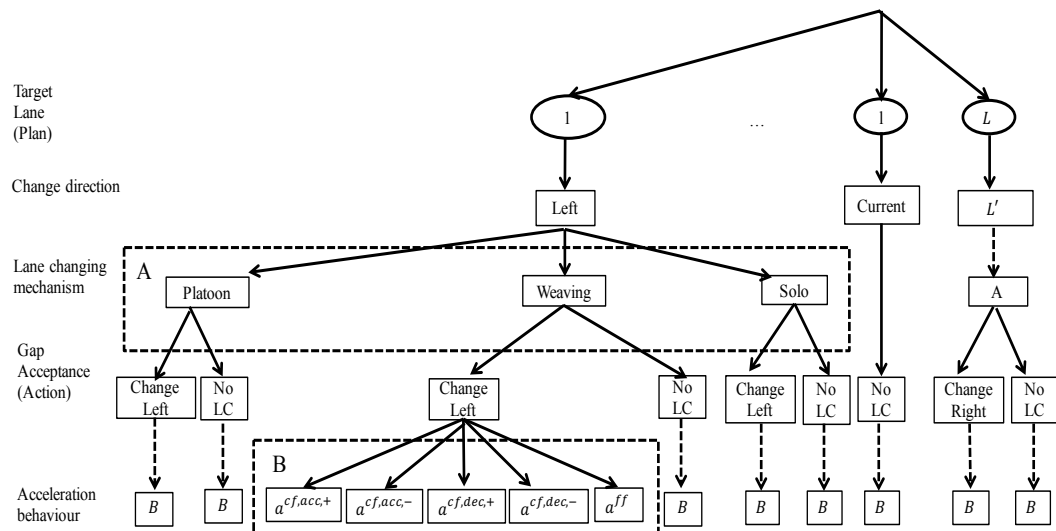
Figure 8.2 The proposed integrated driving behaviour

- In terms of driver heterogeneity and reaction time, this study finds difficulty to generate a related attribute for those components from the video trajectory dataset. The study, therefore, suggests to combines individual trajectory data set with the socio-demographic data (i.e. gender and age).

- Data collection, extraction and management process play one of the key roles in ensuring the quality of modelling result. A low quality of dataset will provide an inaccurate result and misleading interpretation on the model. Several factors affect this quality such as, the traffic recording quality, the location of camera, recording angle. This stage is challenging and time consuming, as the current available trajectory extraction requires us to follow and track the observed vehicle semi-automatically. It requires a high concentration from the extractor. An obscuring from the lead vehicle increased the difficulty on having an accurate dataset. Indeed, a video application with ability on detection moving object helps to solve the issues and provide more accurate vehicle trajectory dataset. It is also suggested to use an

advance video recording tools (i.e. HD quality), which provide a good and clean video recording.

- This result presents interesting practical implications, which may improve the fidelity of microscopic traffic simulation tools, particularly in the context of weaving section traffic analysis. Note that the current models are yet to be validated in the microsimulation tools. Moreover, it will be interesting to test the transferability of the modelling frameworks in other weaving sections and variations of traffic flow condition.

References

Ahmed, K., 1999. *Modeling Drivers' Acceleration and Lane Changing Behavior*. PhD Thesis. Massachusette Institute of Technology, USA. Massachusette Institute of Technology, USA.

Ahmed, K., Ben-Akiva, M., Koutsopoulos, H., and Mishalani, R.G., 1996. Models of freeway lane changing and gap acceptance behavior. In: Lesort, J.-B. (Ed.), Proceedings of the 13th International Symposium on the Theory of Traffic Flow and Transportation. Oxford, UK, pp. 501–515.

Ajzen, I., 1991. The theory of planned behavior. Organizational Behavior and Human Decision Processes 50 (2), 179–211.

Akaike, H., 1973. Information theory and an extension of the maximum likelihood principle. In: Petrov, B.., Caski, F. (Eds.), Proceeding of the Second International Symposium on Information Theory. Budapest, pp. 267–281.

Akaike, H., 1974. A new look at the statistical model identification. IEEE Transactions on Automatic Control 19 (6), 716–723.

Akaike, H., 1981. Likelihood of a model and information criteria. Journal of Econometrics 16 (1), 3–14.

Al-Jameel, H., 2011. *Developing a Simulation Model to Evaluate the Capacity of Weaving Section*. PhD Thesis. University of Salford, UK.

Al-Jameel, H., 2013. Characteristics of the driver behaviour in weaving sections: empirical study. International Journal of Engineering Research and Technology 2 (11), 1430–1446.

Al-Kaisy, A.F., Stewart, J.A., and Aerde, M. Van, 1999. Microscopic simulation of lane changing behaviour at freeway weaving sections. Canadian Journal of Civil Engineering 26 (6), 840–851.

Al-Obaedi, J., and Yousif, S., 2009. The use of visual angle in car following traffic microsimulation models. In: International Built and Human Environment Research Week (IRW).

Ashworth, R., 1970. The analysis and interpretation of gap acceptance data. Transportation Science 4 (3), 270–280.

Awad, W.H., 2004. Estimating traffic capacity for weaving segments using neural networks technique. Applied Soft Computing Journal 4 (4), 395–404.

Ben-Akiva, M., and Lerman, S.R., 1985. *Discrete Choice Analysis: Theory and Application to Travel Demand*. MIT Press, Cambridge, Massachusetts, USA.

Bertoli, P., Cimatti, A., Roveri, M., and Traverso, P., 2006. Strong planning under partial observability. Artificial Intelligence 170 (4), 337–384.

Bham, G.H., 2006. Intensity of lane changing at freeway weave section. In: Wang, K.C.P., Smith, B.L., Uzarski, D.R., Wong, S.C. (Eds.), 9th International Conference on Applications of Advance Technology in Transportation. American Institute of Physics, Chicago, Illinois, USA, pp. 310–318.

Bham, G.H., 2008. Analyzing microscopic behavior: driver mandatory lane change behaviour on a multilane freeway. Missiouri S&T, Center for Infrastructure Engineering Studies. UTC R157.

Bloomberg, P.E.L., 2011. A preliminary assessment of the 2010 HCM weaving methodology. In: Procedia - Social and Behavioral Sciences 16. pp. 131–138.

Blythe, J., 1999. Desicion-theoretic planning. AI Magazine 20 (2), 37–54.

Boutilier, C., Dearden, R., and Goldszmidt, M., 2000. Stochastic dynamic programming with factored representations. Artificial Intelligence 121 (1), 49–107.

Brackstone, M., Sultan, B., and McDonald, M., 2002. Motorway driver behaviour: studies on car following. Transportation Research Part F: Traffic Psychology and Behaviour 5 (1), 31–46.

CALTRANS, 2007. California Highway Design Manual, 6th Edition. California Department of Transportation.

Cassidy, M., 1990. A proposed analytical technique for the design and analysis of major freeway weaving sections. Institute of Transportation Studies, University of California at Berkeley.

Cassidy, M., Skabardonis, A., and May, A.D., 1989. Operation of major freeway weaving sections: recent empricial evidence. Transportation Research Record: Journal of the Transportation Research Board 1225, 61–72.

Chandler, R.E., Herman, R., and Montroll, E.W., 1958. Traffic dynamics: studies in car following. Operation Research 6 (2), 165–184.

Chang, M.-S., Messer, C.J., and Santiago, A.J., 1985. Timing traffic signal change intervals based on driver behavior. Transportation Research Record: Journal of the Transportation Research Board 1027, 20–30.

Choudhury, C., 2007. *Modeling Driving Decisions with Latent Plans*. PhD Thesis. Massachusetts Institute of Technology, USA.

Choudhury, C., and Ben-Akiva, M., 2013. Modelling driving decisions: a latent plan approach. Transportmetrica A : Transport Science 9 (6), 546–566.

Choudhury, C., Ben-Akiva, M., and Abou-Zeid, M., 2010. Dynamic latent plan models. Journal of Choice Modelling 3 (2), 50–70.

Choudhury, C., Ben-Akiva, M., Toledo, T., Rao, A., and Lee, G., 2007. Modeling statedependence in lane-changing behavior. In: Allsop, R.E., Benjamin, G.H., Bell, M.G.H. (Eds.), 17th International Symposium on Transportation and Traffic Theory,. London, UK.

Chu, T.D., Miwa, T., and Morikawa, T., 2015. Gap acceptance on urban expressway merging sections: an application of inverse time to collision. In: TRB 94th Annual Meeting Compedium of Papers.

Cleveland, W., 1979. Robust locally and smoothing weighted regression scatterplots. Journal of the American Statistical Association 74 (368), 829–836.

Cleveland, W., and Devlin, S., 1988. Locally weighted regression : An approach to regression analysis by local fitting. Journal of the American Statistical Association 83 (403), 596–610.

Cleveland, W., Devlin, S., and Grosse, E., 1988. Regression by local fitting. Journal of Econometrics 37 (1), 87–114.

Daganzo, C.F., 1981. Estimation of gap acceptance parameters within and across the population from direct roadside observation. Transportation Research Part B: Methodological 15 (1), 1–15.

Dean, T., and Givan, R., 1997. Model minimization in Markov decision processes. In: Proceedings of the Fourteenth National Conference on Artificial Intelligence and Ninth Conference on Innovative Applications of Artificial Intelligence. pp. 106–111.

Dean, T., Kaelbling, L., Kirman, J., and Nicholson, A., 1993. Planning with deadlines in stochastic domains. Proceedings of the National Conference on Artificial Intelligence (AAAI) 93, 574–579.

Dearden, R., and Boutilier, C., 1997. Abstraction and approximate decision-theoretic planning. Artificial Intelligence 89 (1), 219–283.

Dijker, T., Bovy, P., and Vermijs, R., 1998. Car-following under congested conditions: empirical findings. Transportation Research Record: Journal of the Transportation Research Board 1644, 20–28.

DMRB, 1994. Motorway Incident Detection and Automatic Signalling (MIDAS). Highway Agency, UK.

DMRB, 2006. Design Manual for Roads and Bridges. Highway Agency, UK.

Domencich, T., and McFadden, D., 1975. *Urban travel demand: a behavioural analysis*. North-Holland Publishing, Co.

Drew, D.R., LaMotte, L.R., Wattleworth, J.A., and Buhr, J.H., 1967. Gap acceptance in the freeway merging process. Highway Research Record 208.

Eddy, S.R., 1996. Hidden Markov models. Current opinion in structural biology 6 (3), 361–365.

Farah, H., Bekhor, S., Polus, A., and Toledo, T., 2009. A passing gap acceptance model for two-lane rural highways. Transportmetrica 5 (3), 159–172.

Feldman, J.A., and Sproull, R.F., 1977. Decision theory and artificial Intelligence II: the hungry monkey. Cognitive Science: A Multidisciplinary Journal 1 (2), 158–192.

FHWA, 2006. Next Generation SIMulation (NGSIM). Federal Highway Administration. FHWA-HRT-06-135.

Gazis, D., Herman, R., and Maradudin, A., 1960. The problem of the amber signal light in traffic flow. Operations Research 8 (1), 112–132.

Gazis, D., Herman, R., and Potts, R., 1959. Car-following theory of steady-state traffic flow. Operations Research 7 (4), 499–505.

Gazis, D., Herman, R., and Rothery, R., 1961. Nonlinear follow-the-leader models of traffic flow. Operations Research 9 (4), 545–567.

Gipps, P.G., 1981. A behavioural car-following model for computer simulation. Transportation Research Part B: Methodological 15 (2), 105–111.

Gipps, P.G., 1986. A model for the structure of lane-changing decisions. Transportation Research Part B: Methodological 20 (5), 403–414.

Golob, T.F., Recker, W.W., and Alvarez, V.M., 2004. Safety aspects of freeway weaving sections. Transportation Research Part A: Policy and Practice. 38 (1), 35–51.

Greene, W.H., and Hensher, D.A., 2003. A latent class model for discrete choice analysis: contrasts with mixed logit. Transportation Research Part B: Methodological 37 (8), 681–698.

HCM, 1985. Highway Capacity Manual 1985. Transportation Research Board, USA.

HCM, 1994. Highway Capacity Manual 1994. Transportation Research Board, USA.

HCM, 1997. Highway Capacity Manual 1997. Transportation Research Board, USA.

HCM, 2000. Highway Capacity Manual 2000. Transportation Research Board, USA.

HCM, 2010. Highway Capacity Manual 2010. Transportation Research Board, USA.

Henningsen, A., and Toomet, O., 2010. maxLik: A package for maximum likelihood estimation in R. Computational Statistics.

Herman, R., and Potts, R., 1961. Single lane traffic theory and experiment. In: Herman, R. (Ed.), Symposium on Theory of Traffic Flow. Elsevier, p. 120.

Herman, R., and Weiss, G., 1961. Comments on the highway-crossing problem. Operation Research 9 (6), 828–840.

Hess, S., and Ben-Akiva, M., 2011. Advantages of latent class over continuous mixture of logit models, Institute for Transportation Studies. University of Leeds. Working Paper. Leeds, UK.

Hidas, P., 2002. Modelling lane changing and merging in microscopic traffic simulation. Transportation Research Part C: Emerging Technologies 10 (5), 351–371.

Hidas, P., 2005. Modelling vehicle interactions in microscopic simulation of merging and weaving. Transportation Research Part C: Emerging Technologies 13 (1), 37–62.

Hoffmann, E.R., and Mortimer, R.G., 1994. Drivers' estimates of time to collision. Accident Analysis and Prevention 26 (4), 511–520.

Horvitz, E.J., Breese, J.S., and Henrion, M., 1988. Decision theory in expert systems and artificial intelligence. International Journal of Approximate Reasoning 2 (3), 247–302.

Hwang, S.Y., and Park, C.H., 2005. Modeling of the gap acceptance behavior at a merging section of urban freeway. Proceedings of the Eastern Asia Society for Tansportation Studies 5, 1641 – 1656.

Jin, W.-L., 2010. Macroscopic characteristics of lane-changing traffic. Transportation Research Record: Journal of the Transportation Research Board 2188, 55–63.

Kesting, A., Treiber, M., and Helbing, D., 2007. General lane-changing model MOBIL for car-following models. Transportation Research Record: Journal of the Transportation Research Board 1999, 86–94.

Kita, H., 1999. A merging–giveway interaction model of cars in a merging section: a game theoretic analysis. Transportation Research Part A: Policy and Practice 33 (3), 305–312.

Knoop, V.L., Hoogendoorn, S.P., Shiomi, Y., and Buisson, C., 2012. Quantifying the number of lane changes in traffic. Transportation Research Record: Journal of the Transportation Research Board 2278, 31–41.

Koshi, M., Kuwahara, M., and Akahane, H., 1992. Capacity of sags and tunnels on Japanese motorways. ITE Journal 62 (5), 17–22.

Koutsopoulos, H., and Farah, H., 2012. Latent class model for car following behavior. Transportation Research Part B: Methodological 46 (5), 563–578.

Kusuma, A., and Koutsopoulos, H., 2011. Critical gap analysis of dual lane roundabouts. In: Procedia - Social and Behavioral Sciences 16. Elsevier, pp. 709–717.

Lee, G., 1966. A generalization of linear car-following theory. Operations Research 14 (4), 595–606.

Lee, T., Polak, J.W., and Bell, M.G.H., 2008. Trajectory Extractor Version 1.0. Centre for Transport Studies. Imperial College, London, UK.

Leisch, J.E., and Leisch, J.P., 1984. Procedure for analysis and design of weaving sections. Federal Highway Administration.FHWA-RD-073.

Lertworawanich, P., and Elefteriadou, L., 2001. Capacity estimations for type B weaving areas based on gap acceptance. Transportation Research Record: Journal of the Transportation Research Board 1776, 24–34.

Lertworawanich, P., and Elefteriadou, L., 2003. A methodology for estimating capacity at ramp weaves based on gap acceptance and linear optimization. Transportation Research Part B: Methodological 37 (5), 459–483.

Lertworawanich, P., and Elefteriadou, L., 2007. Generalized capacity estimation model for weaving areas. Journal of Transportation Engineering 133 (3), 166–179.

Lewis, A., and Overton, M., 2009. Nonsmooth optimization via BFGS. Submitted to SIAM J. Optimiz 1–35.

Liu, H.X., Xin, W., Adam, Z., and Ban, J., 2007. A game theoretical approach for modelling merging and yielding behaviour at freeway on-ramp sections. Elsevier, London 197–211.

Liu, R., 2010. Traffic simulation with DRACULA. In: Barceló, J. (Ed.), Fundamentals of Traffic Simulation, Chapter 8, International Series in Operations Research and Management Science. Springer New York, pp. 295–322.

Liu, R., and Hyman, G., 2012. Modelling motorway merge: The current practice in the UK and towards establishing general principles. Transport Policy 24, 199–210.

Liu, R., Van Vliet, D., and Watling, D., 1995. DRACULA: Dynamic Route Assignment Combining User Learning and Microsimulation. In: Proceedings of the 23rd European Transport Forum (PTRC). pp. 143–152.

Luce, R., and Suppes, P., 1965. Preference, utility and subjective probability. In: Luce, R.D., Bush, R.R., Galanter, E. (Eds.), Handbook of Mathematical Psycology, Vol.3. John Wiley & Sons, Ltd, pp. 249–240.

Mahmassani, H., and Sheffi, Y., 1981. Using gap sequences to estimate gap acceptance functions. Transportation Research Part B: Methodological 15 (3), 143–148.

McFadden, D., 1978. Modelling the choice of residential location, Spatial Interaction Theory and Planning Models 477, 75-96. Institute for Transportation Studies, University of California.

Mikhail, E.M., Bethel, J.S., and McGlone, J.C., 2001. *Introduction to Modern Photogrammetry*. John Wiley & Sons, Inc, New York.

Mott MacDonald, 2013. MIDAS data traffic count data and logs. URL www.midas-data.org.uk

Nocedal, J., and Wright, S., 2006. *Numerical Optimization*, 2nd ed. Springer Verlag.

O'Flaherty, C.A., 1986. *Highways : Traffic planning and engineering*, Vol 1, 3rd. ed. Edward Arnold, London, UK.

Ortúzar, J. de D., and Willumsen, L.G., 2007. *Modelling Transport*, 3rd ed. John Wiley & Sons, Ltd.

Papola, A., 2004. Some developments on the cross-nested logit model. Transportation Research Part B: Methodological 38 (9), 833–851.

Pearson, K., 1900. On the criterion that a given system of deviations from the probable in the case of a correlated system of variables is such that it can be reasonably supposed to have arisen from random sampling. The London, Edinburgh, and Dublin Philosophical Magazine and Journal of Science 50 (302), 157–175.

Pipes, L.A., 1953. An operational analysis of traffic dynamics. Journal of Applied Physics 24 (3), 274.

Precup, D., Sutton, R., and Singh, S., 1998. Theoretical results on reinforcement learning with temporally abstract options. Machine Learning: ECML-98. Springer Berlin Heidelberg 382–393.

Punzo, V., Borzacchiello, M., and Ciuffo, B., 2011. On the assessment of vehicle trajectory data accuracy and application to the Next Generation SIMulation (NGSIM) program data. Transportation Research Part C: Emerging Technologies 19 (6), 1243–1262.

Rabiner, L.R., 1989. A tutorial on hidden Markov models and selected applications in speech recognition. Proceedings of the IEEE 77 (2), 257–286.

Rabiner, L.R., and Juang, B.H., 1986. An introduction to hidden Markov models. IEEE ASSP Magazine 3 (1), 257–286.

Roess, R., and Ulerio, J., 2000. Weaving area analysis in year 2000 Highway Capacity Manual. Transportation Research Record: Journal of the Transportation Research Board 1710, 145–153.

Roess, R., and Ulerio, J., 2009. Level of service analysis of freeway weaving segments. Transportation Research Record: Journal of Transportation Research 2130, 25–33.

Roess, R., Ulerio, J., and Prassas, E., 2008. Analysis of freeway weaving sections. National Research Council. NCHRP 3-75.

Rust, J., 1994. Structural estimation of markov decision processes. Handbook of Econometrics 4 (4), 3081–3143.

Sarvi, M., Ejtemai, O., and Zavabeti, A., 2011. Modelling freeway weaving manoeuvre. In: 34th Australian Transport Research Forum, 28-30 Sept. Adelaide, Australia.

Shafer, G., 1987. Probability judgment in artificial intelligence and expert systems. Statistical Science 2 (1), 3–16.

Shoraka, M., and Puan, O.C., 2010. Review of evaluating existing capacity of weaving segments. International Journal of Civil and Structural Engineering 1 (3), 683–694.

Sivak, M., Olson, P., and Farmer, K., 1982. Radar-measured reaction times of unalerted drivers to brake signals. Perceptual and Motor Skills 55 (2), 594.

Skabardonis, A., 2002. Simulation of freeway weaving areas. Transportation Research Record: Journal of the Transportation Research Board 1802, 115–124.

Skabardonis, A., and Kim, A., 2010. Weaving analysis, evaluation and refinement (UCB-ITS-PRR-2010-19). Institute for Transportation Studies, University of California at Berkeley, USA.

Skabardonis, A., and Mauch, M., 2015. Freeway Ramp Weave Performance Analysis. In: TRB 94th Annual Meeting Compedium of Papers. Washington, DC, USA.

Smets, P., and Kennes, R., 1994. The transferable belief model. Artificial Intelligence 66 (2), 191–234.

Son, T.C., and Baral, C., 2001. Formalizing sensing actions— A transition function based approach. Artificial Intelligence 125 (1), 19–91.

Stewart, J., Baker, M., and Van Aerde, M., 1996. Evaluating weaving section designs using INTEGRATION. Transportation Research Record: Journal of the Transportation Research Board 1555, 33–41.

Subramanian, H., 1996. *Estimation of Car-Following Models*. PhD Thesis. Massachusetts Institute of Technology, USA.

Taoka, G.T., 1989. Brake reaction times of unalerted drivers. ITE Journal 59 (3), 19–21.

Toledo, T., 2003. *Integrated Driving Behavior Modeling*. PhD Thesis. Massachusttes Insitute of Technology, USA.

Toledo, T., Choudhury, C., and Ben-Akiva, M., 2005. Lane-changing model with explicit target lane choice. Transportation Research Record: Journal of the Transportation Research Board 1934, 157–165.

Toledo, T., and Katz, R., 2009. State dependence in lane-changing models. Transportation Research Record: Journal of the Transportation Research Board 2124, 81–88.

Toledo, T., Koutsopoulos, H., and Ahmed, K., 2007a. Estimation of vehicle trajectories with locally weighted regression. Transportation Research Record: Journal of the Transportation Research Board 1999, 161–169.

Toledo, T., Koutsopoulos, H., and Ben-Akiva, M., 2007b. Integrated driving behavior modeling. Transportation Research Part C: Emerging Technologies 15 (2), 96–112.

Tordeux, A., Lassarre, S., and Roussignol, M., 2010. An adaptive time gap car-following model. Transportation Research Part B: Methodological 44 (8), 1115–1131.

Train, K., 2009. *Discrete Choice Methods with Simulation*, 2nd ed. Cambridge University Press.

Treiber, M., Hennecke, A., and Helbing, D., 2000. Congested traffic states in empirical observations and microscopic simulations. Physical Review E 62 (2), 1805–1824.

Van Aerde, M., 1994. INTEGRATION: A model for simulating integrated traffic networks user's guide for model version 1.5g. Van Aerde and Associates, Ltd: Transportation Systems Research Group, Queen's University, Kingston, Canada.

Vovsha, P., and Bekhor, S., 1998. Link-nested logit model of route choice: overcoming route overlapping problem. Transportation Research Record: Journal of the Transportation Research Board 1645, 133–142.

Wan, X., Jin, P.J., Yang, F., and Ran, B., 2014. Modeling vehicle interactions during freeway ramp merging in congested weaving section. Transportation Research Record: Journal of the Transportation Research Board 2421, 83–92.

Wang, J., 2006. *A Merging Model for Motorway Traffic*. PhD Thesis. University of Leeds, UK.

Wang, J., Liu, R., and Montgomery, F., 2005a. A simulation model for motorway merging behaviour. In: Mahmassani, H. (Ed.), Transportation and Traffic Theory: Flow, Dynamics and Human Interaction (ISTTT). Elsevier Ltd, pp. 281–302.

Wang, J., Liu, R., and Montgomery, F., 2005b. Car-following model for motorway traffic. Transportation Research Record: Journal of the Transportation Research Board 1934, 33–42.

Wang, M., Cassidy, M., Chan, P., and May, A., 1993. Evaluating the capacity of freeway weaving sections. Journal of Transportation Engineering 119 (3), 360–384.

Wang, X., Luo, Y., Qiu, T.Z., and Yan, X., 2014. Capacity estimation for weaving segments using a lane changing model. Transportation Research Record: Journal of the Transportation Research Board 2461, 94–102.

Wei, H., Lee, J., Li, Q., and Li, C., 2000. Observation-based lane-vehicle assignment hierarchy: Microscopic simulation on urban street network. Transportation Research Record: Journal of the Transportation Research Board 1710, 96–103.

White, C.C., and White, D.J., 1989. Markov decision processes. European Journal of Operational Research 39 (1), 1–16.

Wilks, S.S., 1938. The large-sample distribution of the likelihood ratio for testing composite hypotheses. The Annals of Mathematical Statistics 9 (1), 60–62.

Wortman, R.H., and Matthias, J.S., 1983. Evaluation of driver behavior at signalized intersections. Transportation Research Record: Journal of the Transportation Research Board 904, 10–30.

Yang, L., Widjaja, B.K., and Prasad, R., 1995. Application of hidden Markov models for signature verification. Pattern Recognition 28 (2), 161–170.

Yang, Q., and Koutsopoulos, H., 1996. A microscopic traffic simulator for evaluation of dynamic traffic management systems. Transportation Research Part C: Emerging Technologies 4 (3), 113–129.

Yin, S., Li, Z., Zhang, Y., Yao, D., Su, Y., and Li, L., 2009. Headway distribution modeling with regard to traffic status. In: Intelligent Vehicles Symposium, IEEE. pp. 1057–1062.

Yousif, S., and Al-Obaedi, J., 2011a. Close following behavior: Testing visual angle car following models using various sets of data. Transportation Research Part F: Traffic Psychology and Behaviour 14 (2), 96–110.

Yousif, S., and Al-Obaedi, J., 2011b. Modeling factors influencing the capacity of motorway merge actions controlled by ramp metering. In: Procedia - Social and Behavioral Sciences 16. pp. 172–183.

Yousif, S., Al-Obaedi, J., and Henson, R., 2013. Drivers ' lane utilization for United Kingdom motorways. Journal of Transportation Engineering 139 (5), 441–447.

Zhang, H.M., and Kim, T., 2005. A car-following theory for multiphase vehicular traffic flow. Transportation Research Part B: Methodological 39 (5), 385–399.

Zhang, L., and Levinson, D., 2004. Optimal freeway ramp control without origin–destination information. Transportation Research Part B: Methodological 38 (10), 869–887.

Zhang, Y., Owen, L., and Clark, J., 1998. Multiregime approach for microscopic traffic simulation. Transportation Research Record: Journal of the Transportation Research Board 1644, 103–114.

Appendix-A Discrete Choice Model

General Framework of Discrete Choice Model

The discrete choice modelling framework is developed based on the random utility approach which originally hypotheses that:

- Each individual is a part of homogenous population that act rationally and have perfect information. It assumes that the individuals accept the choice (i.e. lane choice, available gaps) that maximizes their utility.
- The observed objects faces the same set alternatives $l = \{1, 2, 3 \dots L\}$ and set of measured vectors of measured attributes of the individuals and their alternatives. l given individual n is endowed with a set of attributes x ϵ X and in general will face a choice set $l(n) \epsilon l$.
- Each option $l \epsilon L$ is related with a net utility function (U). However, the researcher cannot receive complete information about all the elements considered by the individual making a choice. We, therefore, presumes that the utility of individual n of choosing alternative l can be represented by two components:

  - Schematic part $\widehat{U}_n^l$: function of the measured attributes

  - Random term ε_n^l : the idiosyncrasies and each individual specific tastes together with any observation or measurement errors which is created by the researcher.

Hence, this the discrete choice model can be expressed as follows;

$$U_n^l = \widehat{U}_n^l + \varepsilon_n^l \qquad (A.1)$$

Assuming that, all individuals share the same set of alternatives and face the same constraints from a point of view (Ortúzar and Willumsen, 2007). According to Equation A.1 above shows that the $\widehat{U}$ represent subscript n, it means that a function of the attributes x and this may differ from one individual to the other individual

and assumes that the residual ε are random variable with mean 0 and the probability distribution to be specified;

$$\widehat{U}_n^l = \beta^l X_n^l \tag{A.2}$$

Where;

β^l : Vector of estimated parameters associated with choice l

X_n^l : Vector of explanatory variables associaed with individual n for choosing l

Note that the estimated parameters are constant for all individual n (fixed-coefficient-model) which varies across the alternative

- Each individual (driver) choose the maximum utility alternative, that the individual chooses l if only if;

$$U_n^l \geq U_n^L, f \, l \in L \tag{A.3}$$

Where L denotes available alternatives for individual n. That is the equation can be transformed into;

$$\widehat{U}_n^l - \widehat{U}_n^L \geq \varepsilon_n^l - \varepsilon_n^L \tag{A.4}$$

As it is difficult to observed the $(\varepsilon_n^l - \varepsilon_n^L)$ can be observed with the certitude if holds. Thus the probability of choosing one set of alternative l is written by;

$$P_n^l = Prob\left\{\varepsilon_n^L \leq \varepsilon_n^l + \left(\widehat{U}_n^l - \widehat{U}_n^L\right), rl \in L\right\} \tag{A.5}$$

However, the distribution of the error term is undefined hence is not possible to derive an analytical expression for this model. The only thing that the researcher can assumes that the residuals are random variable that follows with a certain distribution. We can denote the function of error term is $f(\varepsilon) = f(\varepsilon_1, \varepsilon_2, f, \varepsilon_n)$. Let the probability of utility function in Equation A.5 is transform to;

$$P_n^l = \int_{RN} f(\varepsilon) d\varepsilon \tag{A.6}$$

Where;

$$RN = \begin{cases} \varepsilon_n^L \leq \varepsilon_n^l + \left(\widehat{U}_n^l - \widehat{U}_n^L\right), \forall \, l \in L \\ \widehat{U}_n^l + \varepsilon_n^l > 0 \end{cases} \tag{A.7}$$

It is necessary to classify of random utility models that produce by the utility function with independent and identically distributed (IID) residuals across the plan choices, time, and individuals. Therefore, the $f(\varepsilon)$ can be moldered into;

$$f\left(\varepsilon_1, \varepsilon_2, \ldots \varepsilon_N\right) = \prod_n^N g\left(\varepsilon_n\right) \tag{A.8}$$

Note that, the error structure is given by

$$cov\left(\varepsilon_n^l, \varepsilon_{n'}^{l'}\right) = \begin{cases} \sigma^{l^2} & if\ t = t', n = n'\ and\ l = l' \\ 0 & Otherwise \end{cases} \tag{A.9}$$

$$cov(\varepsilon_n^l, v_{n'}) = 0\ \forall\ t, l, n, n'$$

$$cov\left(U_n^l, U_{n'}^{l'}\right) = \begin{cases} (\alpha^l)^2 + \sigma^{l^2} & if\ l = l', n = n'\ and\ t = t' \\ (\alpha^l)^2 & if\ l = l', n = n'\ and\ t \neq t' \\ \alpha^l \alpha^{l'} & if\ l \neq l', n = n'\ and, \forall t \\ 0 & Otherwise \end{cases} \tag{A.10}$$

where σ^{l^2} is the standard deviation of error random terms (ε_n^l). Moreover, the different on ε_n^l distribution assumptions indicates to different discrete choice model approaches (i.e. probit or logit).

The utility distribution represent by $g(\varepsilon_n)$ that associated with option then the general expression reduces into;

$$P_l = \int_{-\infty}^{\infty} g(\varepsilon^l) d(\varepsilon^l) \prod_{L \neq l} \int_{-\infty}^{\widehat{U}^l - \widehat{U}^L + \varepsilon^l} g(\varepsilon^L) d\varepsilon^L \tag{A.9}$$

The formula A.9 above can extended in fact that a two dimensional geometric together with extensions to the more general case of correlation and unequal variances, hence the Equation A.9 can be expressed as;

$$P_l = \int_{-\infty}^{\infty} g\left(\varepsilon^l\right) d(\varepsilon^l) \prod_{i \neq j} G\left(\varepsilon^l + \widehat{U}^l - \widehat{U}^L\right) \tag{A.10}$$

Where;

$$G(x) = \int_{-\infty}^{X} g(x)dx \qquad (A.11)$$

The assumption of IID constitutes that the alternative is independent while a combination or correlation between alternatives will usually violate in this condition

Multinomial Logit Model (MNL)

MNL is a simplest and practical of discrete choice model where the random residual is distributed IID Gumble (Domencich and McFadden, 1975). The general framework of MNL can be expressed as follows:

$$P_n^l = \frac{exp\left(\beta^l \, \widehat{U}_n^l\right)}{\sum_{l \in L} exp\left(\beta^L \, \widehat{U}_n^L\right)} \qquad (A.12)$$

The utility function is commonly is represented as linear function where the estimated parameters (β) of the alternatives relate with a standard deviation of Gumbel variation as written by:

$$\beta^2 = \pi^2 / 6\sigma^2 \qquad (A.13)$$

The MNL follows the principle of Independence Irrelevant Alternative (IIA) saying that: where any two alternatives having a non-zero probability of being chosen, the ratio of choices probability over the other alternatives remains unchanged by the presence of any additional alternative in the choice set (Luce and Suppes, 1965).

Appendix-B HCM 2010 Weaving Section Analysis

Volume adjustment

All demands in the analysis shall be converted into to their ideal equivalent condition using this expression:

$$q_i = \frac{Q_i}{PHF \cdot f_{HV} \cdot f_p}$$

(B.1)

Where;

q_i : Flow rate for traffic flow i in ideal condition (pc/h)

Q_i : Hourly traffic volume for flow i in prevailing condition (veh/h)

PHF : Peak hour factor $(Q_{1-hour}/4 * Q_{15-min})$

f_{HV} : Proportion of heavy vehicle traffic

f_p : Proportion of driver factor

i : F-F (freeway-to-freeway), F-R (freeway-to-ramp), R-F (ramp-to-freeway), R-R (ramp-to-ramp), w (weaving), nw (non-weaving)

Critical lane-changing movement

The minimum hourly rate of lane-changing movement in one-sided weaving section can be expressed as follows:

$$LC_{min} = (q_{R-F} \cdot LC_{R-F}) + (q_{F-R} \cdot LC_{F-R})$$

(B.2)

Meanwhile, the formula for two-sided weaving section is written by

$$LC_{in} = (q_{R-R}.LC_{R-R})$$

(B.3)

Where;

LC_{min} : Minimum number of lane-changing required by all weaving vehicles to execute the movement in hourly rate, lc/h

LC_{R-F} : Minimum number of lane-changing required for each vehicle in the ramp-to-freeway flow

LC_{F-R} : Minimum number of lane-changing required for each vehicle in the freeway-to-ramp

LC_{R-R} : Minimum number of lane-changing required for each vehicle in the ramp-to-ramp

Maximum length of weaving section

The section length in HCM is based on the traffic volume ratio between weaving and non-weaving, and number of available lanes for lane-changing. Giving the L_s parameter, the maximum length (L_{max}) of weaving section is written as follows:

$$L_{max} = [5728(1 + VR)^{1.6}] - [1566N_{wl}]$$

(B.4)

Where;

L_{max} : The maximum length of weaving section (based on the short length definition) (ft)

VR : Volume ratio (Volume of weaving/Total traffic in the segment)

N_{wl} : Number of lanes for weaving manoeuvre.

L_{max} and L_s justify whether the observed location is analysed as a weaving section or two separate junctions. There are two conditions in this regard, if the value of L_s is less than the L_{max} value ($L_s < L_{max}$). And then, if the L_s is greater than or equal to the maximum ($L_s \geq L_{max}$) than the observed location is analysed as a separate two junctions.

Weaving section capacity

HCM (2010) defines two methods for determining the weaving section capacity which are by the density or demand traffic flow. Note that the smallest value of those results is taken into consideration for determining the weaving section V/C ratio. The weaving section capacity associated with density is given by:

$$C_w = C_{Dwl} \cdot N \cdot f_{HV} \cdot f_p \tag{B.5}$$

While, the formulation for weaving section associated with demand traffic flow is expressed as follows:

$$C_w = C_{qwl} \cdot N \cdot f_{HV} \cdot f_p \tag{B.6}$$

Where;

C_w : Total weaving section capacity (veh/h)

C_{Dwl} : Capacity per lane of weaving section under ideal condition associated with density (pc/h/ln)

C_{qwl} : Capacity per lane of weaving section under ideal condition associated with demand traffic flow (pc/h/ln)

Then, the following step is to compare the total weaving section capacity (C_w) from those two equations (B.5 and B.6). Giving the smallest value of C_w, the volume and capacity (v/c) ratio can be written mathematically:

$$v/c = \frac{(q \cdot f_{HV} \cdot f_p)}{C_w} \tag{B.7}$$

If the v/c ratio is greater than 1.00, the section fails to perform a smooth traffic movement and result a Level of Service F. The analysis is ended in this case. Meanwhile, the analysis will be continued if the v/c ratio is less than 1.00.

Lane-changing rate

The lane-changing rate is affected by two components including the weaving vehicle and non-weaving vehicle. Both components are estimated separately with different formula. The total lane-changing rate for weaving vehicles can be expressed as follows:

$$LC_w = LC_{min} + 0.39[(L_s - 300)^{0.5}.N^2.(1 + ID)^2]$$

(B.8)

Where;

LC_w : Lane changing hourly rate of weaving vehicle over the weaving section (lc/h)

LC_{min} : Minimum equivalent hourly rate of weaving vehicle lane changing within the weaving section (lc/h)

L_s : Length of weaving section associated with short length definition (ft) (see. Figure 2.2)

N : Number of available lanes in weaving section

ID : Interchange density

Meanwhile, the lane-changing rate for non-weaving vehicles which firstly initiates by estimating the non-vehicle index:

$$I_{nw} = \frac{L_s.ID.q_{nw}}{10000}$$

(B.9)

Note that two models are applied to estimate the lane-changing rate of non-weaving vehicle in weaving section:

$$LC_{nw1} = (0.206.q_{nw}) + (0.542.L_s) - (192.6.N)$$

(B.10)

And,

$$LC_{nw1} = 2135 + 0.223(q_{nw} - 2000)$$

(B.11)

Following condition is used to define the final lane-changing rate of weaving section;

$$if\ I_{nw}\ \leq 1300:$$
$$LC_{nw} = LC_{nw1}$$

(B.12)

$$if\ I_{nw}\ \geq 1950:$$
$$LC_{nw} = LC_{nw2}$$

(B.13)

$$if\ 1300 < I_{nw} < 1950$$

$$LC_{nw} = LC_{nw1} + (LC_{nw2} - LC_{nw1}).\left(\frac{I_{nw} - 1300}{650}\right) \tag{B.14}$$

Then, the total lane-changing rate of all vehicles (LC_{all}) is estimated by :

$$LC_{all} = LC_w + LC_{nw} \tag{B.15}$$

Weaving section speed

The space-mean speeds of both weaving and non-weaving traffic are the critical input in the weaving section analysis. They are estimated separately as shown in equation

$$V_w = V_{min} + \left[\frac{V_{max} - V_{min}}{1 + \left(0.226\left(\frac{LC_{all}}{L_s}\right)^{0769}\right)}\right] \tag{B.16}$$

And

$$V_{nw} = V_{max} - (0.0072.LC_{min}) - \left(0.0048.\frac{q}{N}\right) \tag{B.17}$$

Then, the average speed of all vehicles in weaving section can be written as follows:

$$V = \frac{q_w + q_{nw}}{\left(\frac{q_w}{V_w}\right) + \left(\frac{q_{nw}}{V_{Nw}}\right)} \tag{B.18}$$

Where;

V_w : Average speed of weaving vehicle in the weaving section (mi/h)

V_{nw} : Average speed of non-weaving vehicle in the weaving section (mi/h)

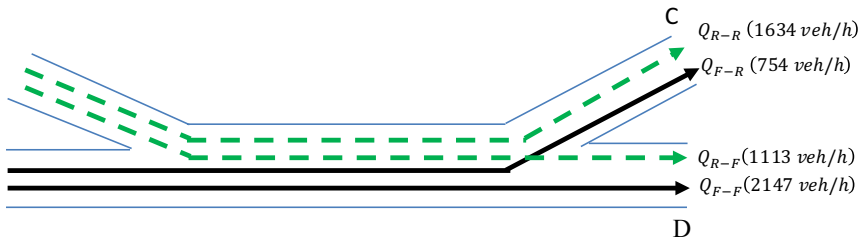V_{max} : Maximum predicted speed (mi/h)

V_{min} : Minimum predicted speed (15 mi/h)

VR : Volume ratio (Volume of weaving/Total traffic in the segment)

q_w : Total traffic flow per hour of weaving traffic (pc/h)

q_{nw} : Total traffic flow per hour of non-weaving traffic (pc/h).

An estimation of Level of Service (LOS) of the observed weaving section

Phase	Calculation
Specifying input data	PHF = 0.971 ; Heavy vehicles (P_T) = 7% $(E_T = 1.5)$; Recreational vehicles = 0%; Driver population = regular commuters $(f_p = 1)$; FFS= 70 mi/h ; C_{Dwl}= 1200 pc/h/ln for FFS =70 mi/h; Interchange Density (ID) = 0.49, Terrain = level.

Volume adjustment	$$f_{HV} = \frac{1}{1+P_T(E_T-1)+P_T(E_T-1)} = \frac{1}{1+0.07(1.5-1)} = 0.967$$ Using Equation B.1 the flow rate for all four traffic flow in ideal condition (pc/h) is given; q_{F-F} =2288 pc/hr; q_{F-R} =804 pc/hr ; q_{R-F} =1186 pc/hr ; q_{R-R} =1741 pc/hr Then the flow for weaving and non-weaving traffic is expressed ; q_w = 804 + 1186 = 1990 pc/hr; q_{nw} = 2288 + 1741 = 4029 pc/hr; =$VR = \frac{1990}{6019}$= 0.33
Configuration characteristics	For one-sided weaving section; $LC_{R-F} = 1$; LC_{F-R}=1 ; N_{wl}=2 By Applying Equation B.2, the critical lane-changing movement equals; $LC_{min} = 1990\ lc/h$

Maximum weaving length	The maximum weaving section length is estimated based on Equation B.4 which is L_{max}= 5934.68 ft > 4149.2 ft $\approx$ 1265 $m(L_s)$

Capacity of the weaving section	Capacity controlled by density:
	$$C_{Dwl} = C_{Dfl}\left[438.2(1 + VR)^{1.6} + [0.0765L_s]\right] + [119.8N_{wl}]$$
	$= 1317$ pc/h/ln
	Based on Equation B.5, the estimated capacity controlled by density equals, 6363 veh/ln
	Capacity controlled by maximum weaving flow rate:
	$$C_{qwl} = {3500}/{VR} = 10586 \text{ pc/h}$$
	Based on Equation B.6, the estimated capacity controlled by density equals, 10227 veh/h
	Controlling value of weaving section capacity is C_w =6363 veh/h
	The estimated v/c ratio is 0.91 (Equation B.7) (Less than 1, Not LOS F)

Lane-changing rates	For weaving vehicles, $LC_w = 2823$ lc/h (Equation B.8)
	For non-weaving vehicle ;
	I_{nw} = 819 < 1300 (Equation B.8)
	LC_{nw}= 2116 lc/h
	Total lane-changing rate: $LC_{all} = LC_w + LC_{nw}$= 4939 lc/h

Speeds	Average speed of weaving vehicle;
	$V_w = 68.41$ mi/h (Equation B.16)
	Average speed of non-weaving vehicle
	$V_{nw} = 49.90$ mi/h (Equation B.17)
	Average speed of all vehicles;
	$V = 54.80$ mi/h (Equation B.18)

Density and Level of Service	$D = \dfrac{q/N}{V} = \dfrac{6019/5}{54.8} = 22$ pc/mi/ln
	Level of service C (Exihibit 24-9, HCM (2010))

Appendix-C Broyden-Fletcher-Goldfarb-Shanno Algorithm

Broyden-Fletcher-Goldfarb-Shanno (BFGS) is a quasi-Newton, a class of hill-climbing technique that estimates the parameters in non-linear optimisation problem. The quasi-Newton algorithm assists the iteration process to constraint the optimum solution of the secant function (S_{k-1}) in defining the displacement of vector. Moreover, BFGS is the most effective compared to the other algorithms in solving non-linear optimisation problem (Nocedal and Wright, 2006; Lewis and Overton, 2009).

The iteration in a quasi-Newton uses an approximation value of Hessian matrix, which is based on the difference in gradient (y_{k-1}) between iteration process, rather than the true value of Hessian matrix. It is worth noting that estimating the true Hessian value is computationally expensive. BFGS uses the inverse of Hessian matrix to define the direction $(\bar{p})$ during the iteration process. Instead of solving a linear system, the search direction in BFGS is a multiplication of a matrix/vector, which can be expressed as follows:

$$\bar{p} = -H_k \nabla f_k \qquad (C.1)$$

In this case, the use of inverse Hessian (H_k) chanBFGSges the secant equation as follows:

$$H_k y_{k-1} = s_{k-1} \qquad (C.2)$$

Therefore, the optimisation process is given by:

$$minimise \|H - H_{k-1}\|_W, subject\ to\ H = H^T, H_k y_{k-1} = s_{k-1} \qquad (C.3)$$

where the unique solution

$$H_k = (I - \rho_{k-1} s_{k-1} y_{k-1}^T) H_{k-1} (I - \rho_{k-1} y_{k-1}) + s_{k-1} \rho_{k-1} s_{k-1}^T \qquad \text{(C.4)}$$

Defining the initial value is a critical phase which affect the efficiency of the iteration process. In practice, the optimum initial value is a scalar multiple of the identity matrix where the scaling factor is the true Hessian Eigen values.